Functional analysis of the microtubule-end binding protein CLASP2

Printing of the thesis was partially supported by the J.E. Jurriaanse Stichting

The work presented in this thesis was performed at the Department of Cell Biology at the Erasmus University Medical Center Rotterdam, The Netherlands. The department is part of the Medisch Genetich Centrum Zuid-West Nederland.
Research performed in this thesis was supported by the Nederlandse Organisatie voor Wetenschappelijk Onderzoek (NWO-MW and NWO-ALW).
Cover design: Dubi&Xenia
Cover photography: Ruud Koppenol
Thesis layout: Xenia

Printed in PrintPartners Ipskamp
ISBN 9090200630

Functional analysis of the microtubule-end binding protein CLASP2

Functionele analyse van CLASP2 een eiwit dat aan microtubuli bindt

Proefschrift

ter verkrijging van de graad van doctor
aan de Erasmus Universiteit Rotterdam
op gezag van de Rector Magnificus
Prof.dr. S. W. J. Lamberts
en volgens besluit van het College voor Promoties

De openbare verdediging zal plaatsvinden op
woensdag 26 oktober 2005 om 11.45 uur

door

Ksenija Drabek

geboren te Belgrado
(Joegoslavië)

Promotiecommissie

Promotor:	Prof.dr. F. Grosveld
Overige leden:	Prof.dr. E. A. Dzierzak Prof.dr. R. Fodde Dr. J. N. J. Philipsen
Copromoter:	Dr.ir. N. Galjart

mami i tati

Contents

Scope of the thesis 9

Chapter 1 **Introduction**
1. Cytoskeleton 13
General introduction 14
1.1. Actin filaments 14
1.2. Intermediate filaments 19
1.3. Microtubules 22
1.3.1. Structure and assembly 22
1.3.2. Microtubule dynamics 24
1.4. Microtubule associated proteins 25
1.4.1. Tubulin binding proteins 25
Stathmin
Collapsin response mediator protein-2
1.4.2. Microtubule binding proteins 27
1.4.2.1. Classical microtubule associated proteins 27
1.4.2.2. Motor proteins 29
1.4.2.3. Microtubule plus-end tracking proteins (+TIPs) 31
CLIPs
The EB1 family
Adenomatous polyposis coli
Lissencephaly 1
CLIP-Associated proteins
1.5. Cell polarity 36

2. Hematopoiesis 49
General introduction 50
2.1. Megakaryocytes 51
Endomitosis
Cytoplasmic differentiation
2.2. Megakaryocytopoiesis 54
2.2.1. Cytokine regulation of megakaryocytopoiesis and TPO signaling 56
2.2.2. Molecular regulation of megakaryocytopoiesis 57
2.3. Thrombocytopenias 57

Chapter 2 **CLASPS are CLIP-115 and –170 associating proteins involved in the regional regulation of microtubule dynamics in motile fibroblasts** 67

Chapter 3 **CLASP2 targets to focal adhesions and regulates cell polarity in fibroblasts in response to fibronectin signalling** 83

Chapter 4 **Murine CLASP2 regulates microtubule levels in vivo and is essential for gametogenesis and hematopoiesis** 109

Chapter 5 **Differential roles of microtubule assembly and sliding in proplatelet formation by megakaryocytes** 131

Discussion 153

Appendix **Generation and characterisation of the CLASP2 specific llama derived single domain antibody** 159

Summary 168

Samenvatting 170

Curriculum vitae 172

Dankwoord 174

Scope of the thesis

Microtubules play an important role in many essential cell functions, such as maintenance of cell shape, intracellular transport, positioning of cell organelles and formation of the mitotic spindle during cell division. Microtubules perform many of their cellular tasks by changing their organization and stability in response to the needs of the cell. These processes are highly regulated, mainly by heterologous protein interactions between microtubules and specific regulatory proteins. Microtubule associated proteins (MAPs) play an essential role in controlling the dynamic instability of microtubules, thus controlling the state of their assembly and organization in cells. Particularly interesting is the group of MAPs that bind specifically to the plus ends of microtubules, where they can influence microtubule behavior and microtubule connections with other cellular structures. The best examples of such proteins are cytoplasmic linker proteins (CLIPs), as well as CLIP-associated proteins, or CLASPs. The aim of this thesis was to investigate role of CLASPs on microtubule behavior, in particular the involvement and in vivo function of CLASP 2.

Introduction describes the cytoskeleton. Three constitutive parts of the cytoskeleton are described (actin, intermediate filaments and microtubules). MAPs are described in more detail, especially plus end binding proteins (+TIPs). The involvement of microtubules and these proteins in the establishment of cell polarity is described. Since CLASP2 is involved in the structural changes that hematopoietic cells undergo during their differentiation, the process of hematopoiesis is shortly described. Particular focus is directed to a description of the process of megakaryocytopoiesis and thrombopoiesis.

Chapter 2 describes the isolation and characterization of a two novel CLIP-associated proteins, CLASP 1 and CLASP 2. It describes their cellular localization and possible function as observed through experiments allowing for their overexpression or inhibition, using motile fibroblasts as a model system. The regulation of CLASP binding to microtubules is also described.

Chapter 3 describes cellular function of CLASP 2 in fibroblasts, isolated from CLASP 2 knock-out (KO) mice.

Chapter 4 describes the generation of a CLASP 2 KO mouse. In this chapter the phenotypic characterization of the CLASP 2 KO mouse is described, as well as its possible role in the process of megakaryocytopoiesis and thrombopoiesis.

In chapter 5, the involvement of dynamic microtubules in the process of proplatelet and platelet formation is described. Studies on the dynamics of microtubules are followed up through the use of EB3-GFP fusion protein. Finally, in chapter 6 (Discussion) the results described in this thesis are discussed, as well as some future prospects. The Appendix describes the generation and characterization of the CLASP2-specific llama single domain antibody and the use of such antibodies in the study of CLASP2 function.

Chapter 1

Introduction

1. Cytoskeleton

General introduction

The cytoskeleton plays a central role in many cellular processes. It provides a structural framework for the cell, serving as a scaffold that determines cell shape and the general organization of the cytoplasm. In addition to this structural role, the cytoskeleton also mediates organelle transport and positioning, cell polarity, formation of cell extensions, cytokinesis, mitosis, secretion and maintenance of cell integrity. The cytoskeleton consists of three types of protein filaments: actin filaments (or microfilaments), intermediate filaments, and microtubules (Figure 1). They differ in their diameter, type of subunit, and subunit arrangement.

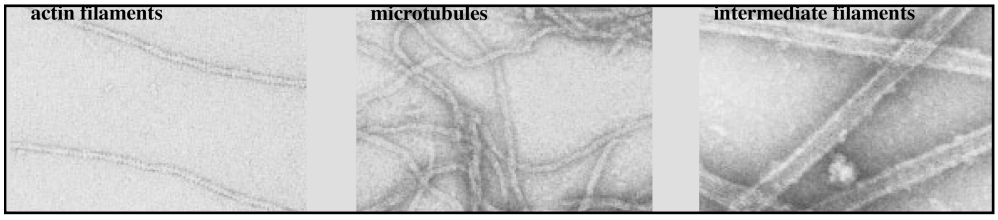

Figure 1. Eukaryotic cytoskeletal polymers. Panels are showing electron micrographs of actin filaments, microtubules and intermediate filaments.
Adapted from Thomas D. Pollard 2003

1.1. Actin filaments

The major cytoskeletal protein of most cells is actin. Actin polymerizes to form actin filaments – thin, flexible fibers approximately 7 nm in diameter and up to several micrometers in length. Within the cell, actin filaments (also called microfilaments) are organized into higher order structures, forming bundles or three–dimensional networks with the properties similar to that of semisolid gels. The assembly and disassembly of actin filaments (actin turnover) allows cells to respond to extracellular signals by moving, changing shape and translocating intracellular organelles. Such processes are critical to the normal development and function of a multicellular organism, but are also important in the disease state, for example for the ability of a tumor cell to become metastatic (Feldner and Brandt 2002).

First thought to be uniquely involved in muscle contraction, actin is now known to be an extremely abundant protein in all types of eukaryotic cells. Yeasts have only a single actin gene, but higher eukaryotes have several distinct types of actin, which are encoded by different members of the actin gene family. Mammals have at least six distinct actin genes. Four are expressed in different types of muscle tissue and two are expressed in non-muscle

cells. However, all of the actins are very similar at the amino acid level and have been highly conserved throughout the evolution of eukaryotes.

Actin exists in two principal forms, as globular monomeric (G) actin, and filamentous polymeric (F) actin, which is a linear chain of G-actin subunits (Figure 2). Each actin subunit binds to either adenosine triphosphate (ATP) or adenosine diphosphate (ADP). The assembly of G-actin into F-actin is accompanied by the hydrolysis of ATP to ADP and inorganic phosphate (Pi). ATP hydrolysis affects the kinetics of polymerization but is not necessary for initiation of polymerization (De La Cruz et al. 2000). All subunits in an actin filament point toward the same end of the filament. Consequently, a filament with two ends that differ from each other exhibits polarity. This polarity was first recognized by electron microscopy. Actin filaments decorated with one myosin attached to each actin subunit, appear in electron micrographs as a string of arrowheads repeating every 36 nm. One end of the filament is known as the barbed end (plus end) and the other as the pointed end (minus end). Polarity is important as the two ends differ in their affinities for and kinetics of association with actin monomers, and interaction with different proteins that regulate the assembly and architecture of actin filament networks.

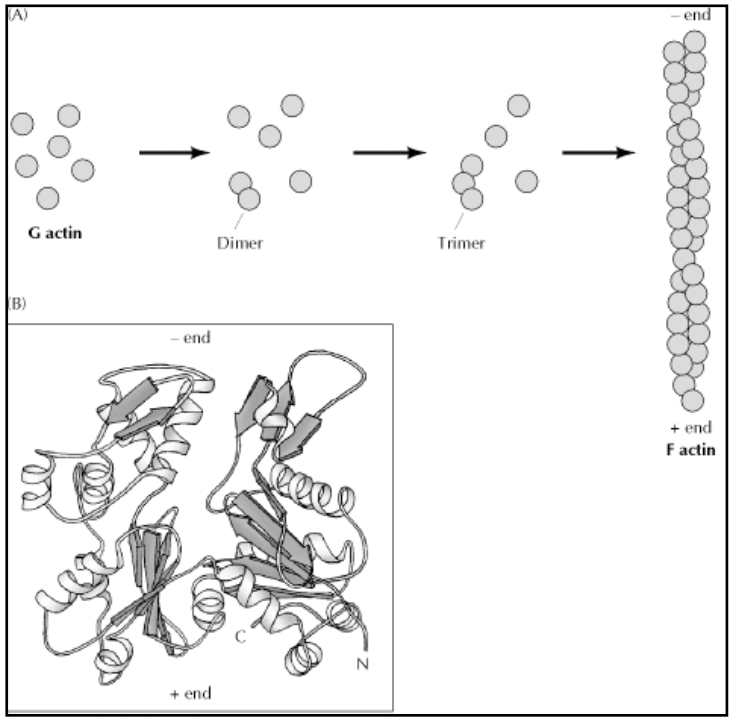

Figure 2. Assembly and structure of actin filaments. (A) Globular monomeric (G) actin is polymerizing through dimer and trimer forms in order to form filamentous (F) actin. **(B)** Structure of an actin monomer.
From Cooper, 2000

Polymerization of G-actin in vitro occurs in three phases. In the initial nucleation phase, ATP-G-actin monomers slowly form stable complexes. These nuclei are rapidly elongated in the second phase by the addition of subunits to both ends of the filament. Actin polymerization proceeds until only a small amount (~ 0.1μM) of unpolymerized actin (G-actin) remains. This 'critical concentration' is also the minimum concentration required to form F-actin filaments (Kasai et al. 1962). Because of ATP hydrolysis within filaments, polymerization proceeds to a steady state rather than a simple equilibrium (Wegner 1976). At the steady state, there is net assembly of ATP-bound actin at barbed ends and net disassembly of ADP-bound subunits at pointed ends. Subunits therefore flux from barbed to pointed ends in a process described as "treadmilling" (Figure 3) (Kirschner 1980). After disassembly, ADP-bound actin monomers are recharged with ATP to complete the actin cycle. Although the existence of treadmilling was predicted from calculations based on rate constants (Pollard 1986), it has been visualized on individual filaments only recently (Fujiwara et al. 2002). In the third phase, the ends of actin filaments are in a steady state with monomeric ATP-G-actin. After their incorporation into a filament, subunits slowly hydrolyze ATP and become stable ADP-F-actin.

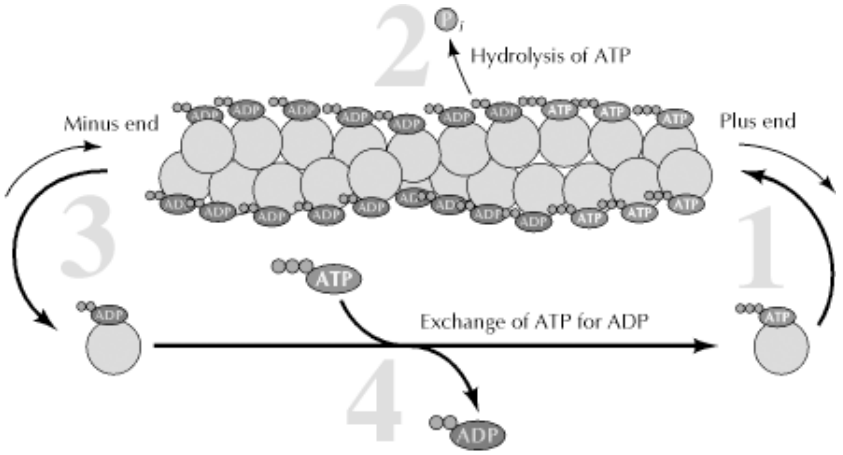

Figure 3. Treadmilling. 1. Actin bound to ATP associates with the plus end of the filament. **2.** ATP bound to actin is hydrolyzed to ADP. **3.** Actin bound to ADP dissociates from the minus end of the filament. **4.** Actin exchanges ADP for ATP. These steps repeat, causing the plus end of the filament to grow and the minus end to shrink. There is an actin monomer concentration below which actin will not polymerize. This value has been termed the critical concentration (CC). At monomer concentration above the CC, the actin will polymerize until the free monomer concentration is equal to the CC.
From Cooper 2000

In the cell, a dense 'meshwork' of F-actin is closely associated with the plasma membrane. This so-called actin cortex plays an important role in the maintenance of cell shape and as the focal point for the generation of forces associated with cell motility. For example, when a protrusion extends, it is presumed that the cytoskeleton provides the stiff framework against which the force is applied. In addition to cell shape changes, the actin cytoskeleton plays a critical role in local shape changes that lead to membrane protrusions associated with filopodium extension, macropinocytotic vesicle formation and phagocytosis (Gottlieb et al. 1993; Lamaze et al. 1997). Extensive work has focused on the mechanisms that determine where and when actin filaments polymerize. Initiation of new filaments seems to boil down to creating new barbed ends by uncapping, severing existing filaments or de novo nucleation of new filaments. Persuasive evidence indicates that all three mechanisms can be used by cells, but recent attention has focused on de novo creation of new ends (Figure 4). De novo nucleation of new filaments is unfavorable, owing to the extremely high dissociation rates of actin dimers and trimers, thus cells use regulated accessory proteins to generate new barbed ends. The cellular factor that nucleates actin filaments de novo was discovered some time ago. It is a complex of seven polypeptides including two actin related proteins, Arp2 and Arp3 (Machesky et al. 1994). This Arp2/3 complex was found to bind both at the side and at the pointed end of filaments. Molecular modeling indicates that Arp2 and Arp3 might form a dimer capable of barbed end elongation, but highly purified Arp2/3 complex was only a weak actin filament nucleator (Mullins et al. 1998; Zigmond 1998). This low intrinsic nucleation activity is important to avoid indiscriminate actin assembly and depletion of the monomer pool and to allow a tight regulation. The first recognized activator of nucleation by Arp2/3 complex was the protein ActA, expressed by the intracellular pathogen Listeria monocytogenes (Domann et al. 1992). ActA allows Listeria to 'pirate' the actin assembly machinery of the host cell and to create a comet tail of filaments that propels the bacterium through the cytoplasm of the host cell and from cell to cell. The first identified endogenous cellular activator of Arp2/3 was the WASp/Scar adaptor protein (Machesky et al. 1999). WASp is the product of the gene mutated in Wiskott-Aldrich syndrome (a human platelets and white blood cell disorder) (Derry et al. 1994). Like the Arp2/3 complex itself, WASp (and its more ubiquitously expressed homolog N-WASP) is intrinsically inactive, apparently due to auto-inhibition of the activation domain located at the protein's carboxyl terminus. Signaling pathways operating through Rho-family GTPases, particularly Cdc42 (Hall 1998), and via acidic phospholipids, such as phosphatidylinositol-4, 5-bisphosphate (PIP_2), overcome this auto-inhibition, allowing the activation of the Arp2/3 complex. The second endogenous activator of the Arp2/3 complex identified are actin filaments themselves. Binding of the Arp2/3 complex to the side of an existing filament enhances activation by WASp/Scar proteins. The Arp2/3 complex nucleates a new filament, which grows in the barbed direction at a 70^0 angle off the side of the 'mother' filament. This is known as the dendritic nucleation mechanism of actin assembly (Pollard et al. 2001) (see Figure 4).

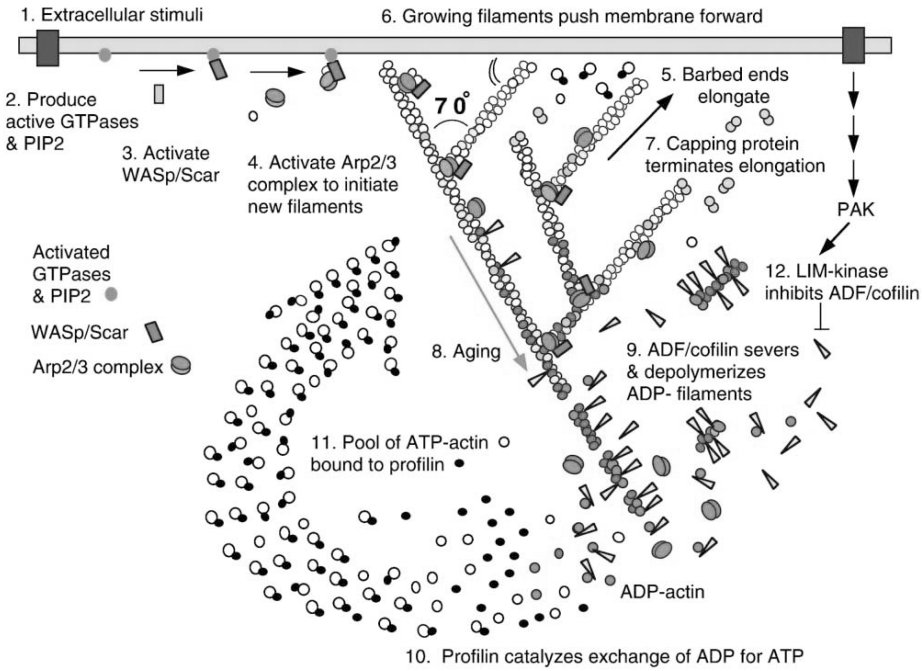

Figure 4. Dendritic Nucleation/Array Treadmilling Model for Protrusion of the Leading Edge. (1) Extracellular signals activate receptors. (2) The associated signal transduction pathways produce active Rho-family GTPases and PIP2 that (3) activate WASp/Scar proteins. (4) WASp/Scar proteins bring together Arp2/3 complex and an actin monomer on the side of a preexisting filament to form a branch. (5) Rapid growth at the barbed end of the new branch (6) pushes the membrane forward. (7) Capping protein terminates growth within a second or two. (8) Filaments age by hydrolysis of ATP bound to each actin subunit followed by dissociation of the γ phosphate. (9) ADF/cofilin promotes phosphate dissociation, severs ADP-actin filaments and promotes dissociation of ADP-actin from filament ends. (10) Profilin catalyzes the exchange of ADP for ATP, returning subunits to (11) the pool of ATP-actin bound to profilin, ready to elongate barbed ends as they become available. (12) Rho-family GTPases also activate PAK and LIM kinase, which phosphorylates ADF/cofilin. This tends to slow down the turnover of the filaments.
Adapted from Thomas D. Pollard 2003

There are two complementary mechanisms that allow a cell to maintain the pool of unpolymerized actin, in order to be ready for rapid assembly of new filaments when required. All eukaryotic cells have a small protein called profilin that binds actin monomers in a way that inhibits nucleation and elongation of pointed ends but not elongation of barbed ends (Pollard et al. 2000). Given some barbed ends, the actin-profilin pool would rapidly be depleted by growth of these ends unless cells cap the barbed ends of actin filaments with proteins such as heterodimeric capping protein and gelsolin family members. Together, pro-

filin and capping maintain the huge pool of polymerization-competent actin subunits that are poised to elongate barbed ends if they become available.

In addition to profilin, animal cells typically use another small protein, thymosin-β4, to sequester part of the actin monomer pool in a form incapable of polymerization (Huff et al. 2001). Profilin shuttles actin monomers from this sequestered pool to barbed ends when they become available. Capping of pointed ends is not essential, since neither actin-thymosin-β4 nor actin-profilin elongate pointed ends. Given sufficient quantities of these two proteins, the concentration of free actin monomers will be below the critical concentration at pointed ends, allowing them to slowly disassemble in cells.

In conclusion, in the dendritic nucleation mechanism, the actin-monomer-binding protein profilin (with help in vertebrate cells from thymosin β4), maintains a pool of unpolymerized ATP-actin subunits. Extracellular stimuli such as chemotactic factors bind to plasma membrane receptors, thus activating intracellular signaling molecules including Rho family GTPases. These GTPases bind and activate WASp/Scar family proteins by releasing them from autoinhibition. Active WASp/Scar proteins bring together an actin monomer and Arp2/3 complex. Arp2/3 complex then initiates the growth of a new actin filament as a branch on the side of an older actin filament. The branch grows rapidly at its barbed end by addition of actin-profilin complexes. As it grows, it pushes the plasma membrane forward. The new filament elongates until it is capped by capping protein (Figure 4).

1.2. Intermediate filaments

Intermediate filaments (IF) have a diameter of about 10 nm, thus being between the diameters of the other two main elements of the cytoskeleton, actin (7 nm) and microtubules (25 nm). In contrast to actin filaments and microtubules, the intermediate filaments are not directly involved in cell movements. Instead, they appear to play a structural role by providing mechanical strength to cells and tissues. These proteins are divided into six major classes (types) based on their sequences and tissue distribution (Steinert and Liem 1990) (Table 1).

Class	IF protein	Molecular weight (kDa)	Tissue distribution
Type I	Acidic keratins	40-64	Epithelia
Type II	Basic keratins	52-68	Epithelia
Type III	Vimentin Desmin GFAP Peripherin	55 53 51 54	Mesenchyme Muscle Astroglia Neurons
Type IV	NF-L NF-M NF-H α-internexin	68 110 130 66	Neurons Neurons Neurons Immature neurons
Type V	Lamin A Lamin B Lamin C	70 67 67	Nucleus Nucleus Nucleus
Type VI	Nestin	240	CNS stem cells

Table 1. The family of IF proteins in vertebrates.

Types I and II intermediate filaments consist of two groups of keratins, each made of about 15 different proteins, which are expressed in epithelial cells. Each type of epithelial cell synthesizes at least one keratin of type I (acidic), and one keratin of type II (basic), which co-polymerize to form filaments. Some of the type I and II keratins, called hard keratins, are used for production of structures such as hair, nails, and horns. The other types of I and II keratins, called soft keratins, are abundant in the cytoplasm of epithelial cells, with different keratins being expressed in various differentiated cell types.

The type III intermediate filaments are distributed in a number of cell types. They include vimentin in fibroblasts, endothelial cells and leukocytes, desmin in muscle, glial fibrillary acidic protein (GFAP) in astrocytes and other types of glia, and peripherin in peripheral nerve fibers. The type IV intermediate filament proteins include the three neurofilament (NF) proteins designated NF-L, NF-M, and NF-H (where L, M, and H stands for light, medium and heavy, respectively). These proteins form the major intermediate filaments of many types of mature neurons. Another type IV intermediate filament protein is α-internexin. It is expressed at an earlier stage of neuronal development.

Type V intermediate filaments are represented by the lamins which have nuclear signal sequences, allowing them to form a filamentous support inside the inner nuclear membrane. Lamins are vital to the re-formation of the nuclear envelope after cell division.

The single type VI intermediate filament protein is nestin. It is expressed very early during the development of neurons and in stem cells of the central nervous system. The various intermediate filament proteins share a common structural organization. As illustrated in Figure 5, intermediate filament monomer peptides are an elongated fibrous class of proteins with a central α-helical region capped with globular ends at both the amino and carboxylic acid termini (Steinert 1991). Two of the monomer units form a coiled-coil dimer, that self-associates in an anti-parallel arrangement to form a staggered tetramer, which is the analogous soluble subunit for the globular actin monomer and the tubulin heterodimer. Tetramer units pack together laterally to form a sheet of eight parallel protofilaments that are supercoiled into a tight bundle. Each tightly coiled intermediate filament cross section reveals 32 individual α-helical peptides, which renders the filament easy to bend but quite difficult to break, thus accounting for the extreme structural rigidity. Although previously thought to be rigid structures, it now has become clear that some classes are highly dynamic structures with a significant rate of turnover in many cell types (Yoon et al. 1998; Windoffer and Leube 1999). Live cell imaging techniques suggested that intermediate filaments can be as dynamic as microtubules and microfilaments (Yoon et al. 1998). The dynamics of vimentin filaments are probably the best characterized to date. Live imaging of cells expressing a GFP-vimentin fusion protein has revealed that the vimentin network is motile, with filaments constantly changing their shape (Yoon et al. 1998; Helfand et al. 2002). It has been shown that vimentin structures are moving along microtubules in both directions, and that both conventional kinesin and cytoplasmic dynein are involved in this movement (Prahlad et al. 1998; Helfand et al. 2002).

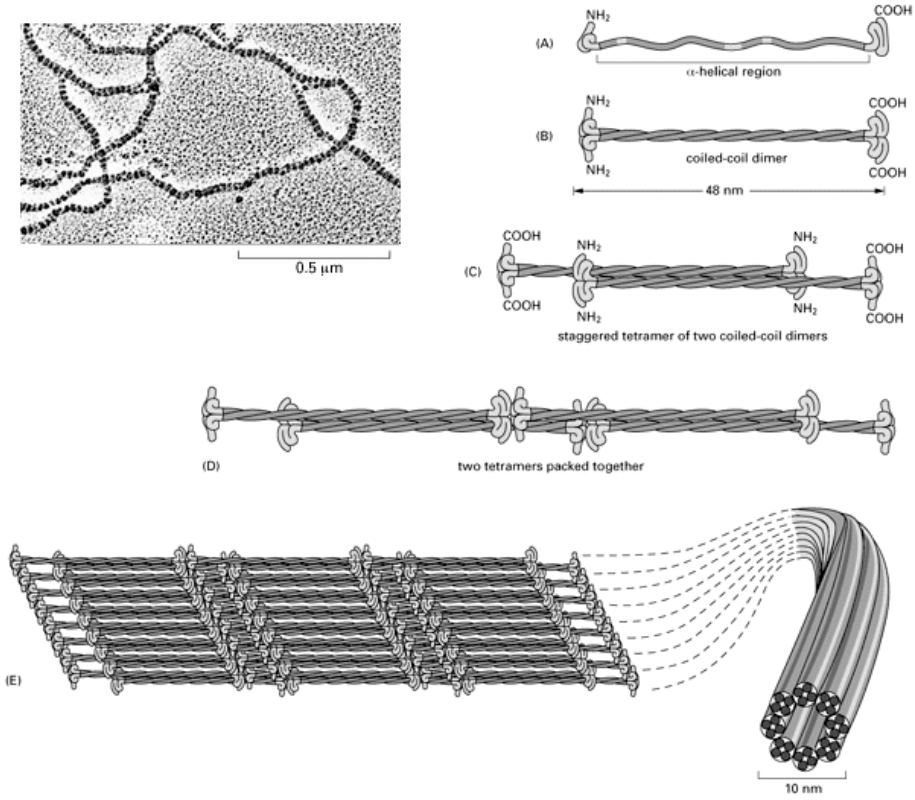

Figure 5. Assembly of intermediate filaments. The central rod domains of two polypeptides wind around each other in a coiled-coil structure to form dimers. Dimers then associate in a staggered antiparallel fashion to form tetramers. Tetramers associate end to end to form protofilaments and laterally to form filaments. Each filament contains approximately eight protofilaments wound around each other in a ropelike structure.
From Alberts 1994

Mutations in intermediate filament genes lead to a wide range of diseases. For example, defective keratins in skin tissue lead to a disorder known as epidermolysis bullosa simplex (Fuchs 1995), manifested by skin blisters produced with even a slight mechanical stress. Similar blistering diseases due to keratin mutations in other tissues affect the esophagus, eyes, and mouth. Several neurodegenerative diseases, such as amyotrophic lateral sclerosis (ALS or Lou Gehrig's Disease), are associated with malfunctions in the intermediate filament (neurofilament) network (Liu et al. 2004), while defects in desmin intermediate filaments produce muscle disorders.

1.3. Microtubules

Microtubules are hollow cylindrical tubulin polymers, present in the cytoplasm of eukaryotic cells, where they perform a wide variety of functions (Alberts 1994). They are vitally involved in cell motility and division, in organelle transport, and in cell morphogenesis and organization. This amazing variety of microtubule functions is paralleled by an equally remarkable flexibility in microtubule organization.

In most interphase cells, microtubule arrays are nucleated and organized by the centrosome from which the polymers radiate into the cell cytoplasm. Interphase microtubules are thought to be major organizers of the cell's interior. They are essential determinants of cell shape and motility, required for the assembly of essential cell structures such as the endoplasmic reticulum and the Golgi apparatus, and used as highways for organelle transport. During mitosis, microtubules rearrange to form the mitotic spindle. The mitotic spindle orients the plane of the cell cleavage and functions as a supramolecular motor to segregate the chromosomes to the cell poles during anaphase. Microtubule arrays in cells are generally dynamic, capable of assembly, disassembly and rearrangement on a time scale of seconds to minutes. Microtubule dynamics in vivo are based on intrinsic dynamic properties of the polymers themselves determined by the biochemical properties of the microtubule-structural unit.

1.3.1. Structure and assembly

The structural unit of a microtubule is the α-β tubulin heterodimer. Tubulin dimers connect head to tail to form protofilaments that associate laterally into a polar, 25 nm wide cylindrical structure (Figure 6). Both in vivo and (under some conditions) in vitro, most microtubules have 13 protofilaments, although this number can vary from 9 to 16 (Chretien and Wade 1991). Ultrastructural analysis of motor-decorated microtubules has showed that each protofilament is shifted slightly lengthwise by about 0.9 nm with respect to its neighbor, so that tubulin dimers form helices around the microtubule. This arrangement also leads to the observation of a seam, parallel to the long axis of the microtubule (Wade and Hyman 1997). The organization of α- and β-tubulin heterodimers in the microtubule lattice is polarized, and this feature results in structural and kinetic differences at the microtubule ends. The faster growing end (named the plus end) has the β-tubulin subunit of each heterodimer exposed, whereas the slower growing end (named the minus end) has the α-tubulin subunit exposed. The earliest structures formed during microtubule assembly are small sheets of protofilaments. Later, the sheet closes to form a microtubule. Once assembled, tubulin addition to and loss from existing microtubules occurs only at microtubule ends (Erickson and Stoffler 1996).

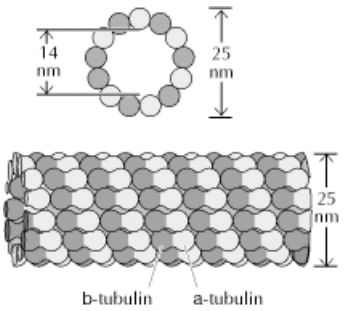

Figure 6. Structure of microtubules. Dimers of α- and β-tubulin polymerize to form microtubules, which are composed of 13 protofilaments assembled around a hollow core.
From Cooper, 2000

The tubulin superfamily consists of seven members, named α-, β-, γ-, δ-, ϵ-, ζ- and η-tubulin and a distantly related bacterial filamentous temperature sensitive protein (ftsZ) (Luduena 1998; Schiebel 2000). Expression of tubulin genes is developmentally regulated with synthesis of specific tubulins restricted to certain tissues or to discrete developmental occasions. Additionally, some cells have an autoregulatory mechanism in which an increase in the amount of non-polymerized tubulin leads to reduced β-tubulin mRNA stability and a subsequent decrease in tubulin synthesis (Theodorakis and Cleveland 1992).

Besides α- and β-tubulin, a third major isoform, γ-tubulin, has been discovered (Burns 1991; Stearns et al. 1991; Zheng et al. 1991). Although showing sequence homology to the α- and β-tubulins, γ-tubulin is not a structural protein of microtubules. γ-tubulin is rather a component of the centrosome, the major microtubule organizing center (MTOC) in many eukaryotic cells (Joshi 1994). Immunoelectron microscopy has localized γ-tubulin to ring structures within the centrosome, and in vitro studies have shown that γ-tubulin ring complexes nucleate microtubule assembly and cap the minus ends of microtubules (Zheng et al. 1995).

Much of the heterogeneity among tubulin isotypes is localized within the 50 amino acids of the carboxy-terminus. In particular, the last 15 residues of the extreme carboxy-terminus of β-tubulins and, to a lesser degree, α-tubulins, contain the greatest variation, and this region is termed isotype defining.

In the mouse there are six α-tubulin genes and six β-tubulin genes. Products of mα3 and mα7 are expressed only in testis, while mα1 amd mα2 genes are highly expressed in the brain. Six mouse β-tubulin genes are yielding six major isotype classes (Lopata and Cleveland 1987), and except for class VI, which is found only in hematopoietic cells, and class IVb, which is testis specific, all are expressed in neuronal tissues. Class II β-tubulin is the major brain β-tubulin, and class III is neuron specific in mammalian and avian brain (Lee et al. 1990).

1.3.2. Microtubule dynamics

Microtubules are intrinsically dynamic polymers. Soluble tubulin binds GTP reversibly at a site in the β subunit and the GTP becomes hydrolyzed to GDP and Pi at the same time as or shortly after the tubulin polymerizes onto a growing microtubule end. The irreversible hydrolysis of GTP during tubulin addition to the microtubule creates two unique dynamic behaviors. One such behavior, treadmilling (Hotani and Horio 1988; Margolis and Wilson 1998), characterized by net growth at the plus end of a microtubule and net shortening at the minus end, is caused by a difference in critical tubulin subunit concentrations at plus and minus ends. The second behavior, dynamic instability, is characterized by switching of relatively slow sustained growth with rapid shortening at the microtubule ends (Mitchison and Kirschner 1984; Walker et al. 1988). At or near the steady state, both behaviors can coexist in microtubule populations (Figure 7). The transition from growth to shrinkage is called catastrophe and the transition from shrinkage to growth is called rescue. These transitions are accompanied by complex chemical and structural changes at the microtubule ends (Hyman and Karsenti 1996).

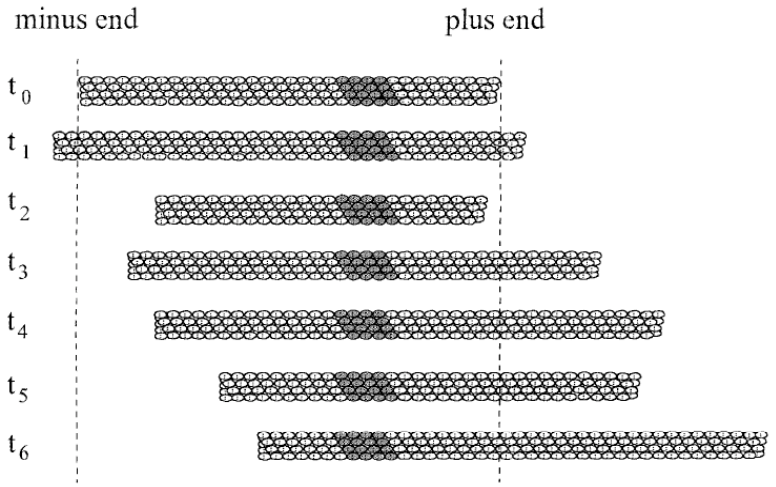

Figure 7. Simultaneous treadmilling and dynamic instability are producing a net flow of tubulin subunits from plus to minus ends. Shown are consecutive 'snapshots' of a microtubule exhibiting growth and shortening at plus and minus ends, with net growth at the plus end and net shortening at the minus end. The shaded subunits represent a marked segment. t_0- zero time, t_1 to t_6 represents arbitrary equal units of time.
From Wilson et al., 1999

Treadmilling and dynamic instability are crucial for many microtubule-dependent cell functions. Dynamic instability has long been considered to give microtubules the ability to search or sample the three-dimensional space of the cell for sites of interaction or attachment that contribute to the formation of specific arrays necessary for a particular cell function. In the selective stabilization hypothesis, Kirschner and Mitchison proposed that exter-

nal signals would locally activate cortical factors to stabilize dynamic microtubules that happened to encounter the activated cortical factors (Kirschner and Mitchison 1986). One essential aspect of this model, namely the need for dynamic microtubules, has been supported by abundant evidence that dynamic microtubules are necessary for cell division, cell migration and cell differentiation (Liao et al. 1995; Tanaka et al. 1995). However, evidence for signal-mediated changes in microtubules and the identity of cortical factors that mediate microtubule interactions with the cortex has been more difficult to obtain. Rapid microtubule dynamics is especially prominent in mitosis and is essential for proper spindle assembly and function. In interphase cells, microtubules exchange their tubulin with soluble tubulin in the cytoplasmic pool with half times of several minutes to several hours. However, with the onset of mitosis, a population of highly dynamic mitotic spindle microtubules replaces the interphase microtubules. These microtubules are 10 to 100 times more dynamic than microtubules in interphase cells (Belmont et al. 1990). The extremely rapid dynamics of mitotic spindle microtubules play a crucial role in the complex movements of the chromosomes. For example, extensive growth and shortening appear to be responsible for the initial attachment of the chromosomes at their kinetochores to the forming spindle. Rapid treadmilling of microtubules also occurs during metaphase and anaphase, where it may be involved in signaling from kinetochores to poles of the mitotic spindle (Mitchison and Salmon 1992).

1.4. Microtubule associated proteins

There are many different proteins that are influencing and regulating microtubule behavior in the cells. Microtubule associated proteins can stabilize or destabilize microtubules by interacting either with tubulin or microtubules themselves.

1.4.1. Tubulin binding proteins

Most of the proteins that regulate microtubule dynamics bind directly to microtubules. However, some tubulin-binding proteins bind preferentially to free tubulin dimers compared to polymerized tubulin. Some of those proteins, such as stathmin, MINUS and cofactor D, inhibit microtubule assembly.

Stathmin

Stathmin, also known as Op 18 (Hailat et al., 1990), is a ubiquitous phosphorylated protein thought to act as an intracellular relay for diverse regulatory pathways (Maucuer et al. 1990; Sobel 1991). Moreover, stathmin is overexpressed in many types of cancers (Melhem et al. 1991; Ghosh et al. 1993; Brattsand 2000), where these pathways are altered, an abnormality that may be exploited for new therapeutic approaches. Stathmin was subsequently found to have a microtubule destabilizing activity (Belmont and Mitchison 1996; Jourdain et al. 1997), that can be turned off in vivo by phosphorylation of its four serine

residues (Horwitz et al. 1997). Stathmin is a member of a family of well conserved phosphoproteins, which are the products of four distinct genes. The remaining three genes encode for SCG10, SCLIP, RB3 and its two splice variants RB3' and RB3" (Ozon et al. 1997). Whereas stathmin is expressed ubiquitously, but more abundantly in the nervous system, other members of the stathmin family are exclusively restricted to the nervous system. They are differentially regulated during neuronal differentiation and brain development, and differentially expressed and regulated in the adult brain (Beilharz et al. 1998; Ozon et al. 1998). Thus proteins of the stathmin family seem to play distinct, possibly complementary roles in relation to the control of proliferation, differentiation, and specific activities of cells of the nervous system. The neuronal proteins all contain a domain highly homologous to stathmin and also have additional sequences at their N termini that probably anchor them to membranes (Ozon et al. 1997). Each of those proteins is capable of destabilizing microtubules, but the exact mechanism is under debate. Based on in vitro microtubule assembly assays, evidence has been presented supporting conflicting destabilization models of either tubulin sequestration (Curmi et al. 1997; Jourdain et al. 1997) or promotion of microtubule catastrophes (Belmont and Mitchison 1996). Stathmin (S) interacts with two α/β tubulin heterodimers (T) in vitro to form a T_2S complex which sequesters free tubulin and therefore hinders microtubule formation (Steinmetz et al. 2000). Alternatively, it has also been proposed that stathmin could directly increase the frequency of microtubule catastrophes, an effect possibly triggered by an interaction with microtubule ends (Steinmetz et al. 2000). Since it is possible to separate tubulin sequestering and microtubule catastrophe promoting activities by truncating stathmin, one of the propositions is that stathmin has bifunctional properties. For example, deletion of the C terminus results in a protein that is no longer able to sequester tubulin dimers but can still stimulate catastrophes. In contrast, the N-terminal truncation is able to sequester tubulin but has lost catastrophe-promoting activity (Howell et al. 1999). Thus, stathmin has two functional regions: the N terminus, necessary for catastrophe promotion, and the C terminus, required for sequestering tubulin dimers.

Collapsin response mediator protein-2

Collapsin response mediator protein-2 (CRMP-2) is an example of a protein that binds preferentially to tubulin heterodimers, but it promotes microtubule assembly (Fukata et al. 2002b). CRMP-2 is expressed exclusively and highly in the developing nervous system. It has been shown that CRMP-2 is enriched in the growing axons of hippocampal neurons. Its overexpression induces the formation of multiple axons and elongation of the primary axon, while its mutant form, that lacks activity towards microtubule assembly, inhibits axon formation (Inagaki et al. 2001). Thus, CRMP-2 is crucial for axon outgrowth and determination of the fate of the axon and dendrites, and thereby in establishing and maintaining neuronal polarity.

CRMP-2 is phosporylated at Thr-514 by GSK-3β (Yoshimura et al. 2005), and this phosphorylation lowers its binding activity to tubulin. The Thr-514 phosporylated CRMP-2 is enriched in axonal shafts, but it is low in the growth cone of the axons, where non-phosphorylated CRMP-2 accumulates at high levels (Arimura et al. 2004). In shafts, the

phosphorylation of CRMP-2 may prevent the co-polymerization of CRMP-2 with tubulin dimers into microtubules until reaching the growth cone, or it may induce dissociation of CRMP-2 from microtubules. In the growth cone, non-phosphorylated CRMP-2 binds to tubulin heterodimers and promotes tubulin polymerization at the plus ends of microtubules, thereby contributing to the axonal growth (Arimura et al. 2000).

1.4.2. Microtubule binding proteins

Microtubule binding proteins preferentially bind to microtubules. They can bind along the whole length of microtubules, such as classical microtubule-associated proteins and motor proteins, or they can preferentially accumulate at the microtubule plus ends, where they are best positioned to influence microtubule dynamics and interactions with other cellular structures in their surrounding.

1.4.2.1. Classical microtubule associated proteins

Various proteins associate with microtubules and control their dynamics in vitro and in vivo. The term microtubule-associated proteins (MAPs) was originally used to describe a group of a high molecular weight proteins which bind to in vitro reconstituted microtubules. These proteins have been discovered by co-purification with microtubules in the original self-assembly procedures developed to purify microtubules from vertebrate brain homogenates (Borisy and Olmsted 1972). Additional experiments revealed that MAPs, isolated from brain tissue, stimulated the rate and extent of microtubule assembly in vitro by reducing the dissociation rate constant for tubulin (Sloboda and Rosenbaum 1979) and bound periodically along the length of the microtubule (Wiche et al. 1991; Chapin and Bulinski 1992). Those MAPs are known as classical, structural MAPs. A high molecular weight group of MAPs is represented most abundantly by MAP1A (340 kDa), MAP1B (320 kDa), two closely related MAP2 isoforms (MAP2A and MAP2B) of 280 kDa, and MAP4 (210kDa) (Aizawa et al. 1990; Olmsted 1991; Hirokawa 1994). The second group of lower molecular weight MAPs, designated Tau, consists of a set of four polypeptides migrating in SDS-PAGE between 55 kDa and 62 kDa. MAP1, MAP2 and Tau are neuronal MAPs expressed almost exclusively in the brain, while MAP4 is ubiquitously expressed. The finding that Tau proteins are the major structural components of the neurofibrillary tangles, the pathological hallmark of Alzheimer disease, has stimulated intense interest in their molecular and cellular role (Kosik 1993; Mandelkow and Mandelkow 1993). Tau is present only in axons, while MAP2 is expressed in dendrites and the cell bodies. MAP1A and MAP1B exist in both dendrites and axons. Due to their characteristic distribution pattern in nerve cells and presence in crossbridges between microtubules and other organelles in nerve cells, they are thought to be involved in neuronal morphogenesis (Matus 1991).

Classical MAPs are fibrous molecules, ranging from 50 nm to 185 nm, that form filamentous projections from the microtubule surface. Molecular cloning and sequencing of

MAPs cDNAs, revealed that MAP2, Tau and MAP4 are all composed of an amino-terminal projection domain and a carboxy-terminal microtubule-binding region. The microtubule-binding regions are well conserved among these three proteins, and are divided into three subdomains: a region rich in proline and basic residues (Pro-rich region), a region containing four repeats of an assembly-promoting sequence (AP sequence region), and a region rich in acidic and hydrophobic residues (Tail region) (Aizawa et al. 1989; Aizawa et al. 1990). Each subdomain plays a distinguishable role in tubulin polymerization and microtubule stabilization. Studies on MAP4 microtubule-binding region, using different truncated fragments of the region, has shown that the Pro-rich region promotes microtubule nucleation, that the AP-sequence region elongates microtubules, and that the tail region can not directly interact with microtubules (Katsuki et al. 1999). Since the AP sequences of MAP2, MAP4 and Tau are homologous, and the whole AP sequence region and the Pro-rich region of the three MAPs are similar, these regions likely interact with microtubules by a common mechanism.

MAP1A and MAP1B bind to the microtubule by an unrelated binding domain (Wiche et al. 1991). Those two structurally related MAPs exhibit different patterns of synthesis during neuronal development. MAP1B peaks early in the development and declines after maturation, while MAP1A appears later and persists in mature neurons (Schoenfeld et al. 1989). Phosphorylation of the microtubule-binding domain may regulate the binding of MAPs to the microtubule surface (Brugg and Matus 1991). Although the function of the projection domain is less clear, recent evidence demonstrates that the microtubule-microtubule spacing found in axons and dendrites of neuronal cells is determined by the projection domain (Chen et al. 1992). The projection domain may also be involved in linking microtubules to other organelles and/or microtubule-microtubule bundling.

The best-known function of MAPs is promotion of tubulin assembly and stabilization of microtubules (Hirokawa 1994; Maccioni and Cambiazo 1995; Mandelkow and Mandelkow 1995), but accumulating evidence suggests a much broader range of MAP functions. MAPs can form cross-bridges that appear to link neuronal microtubules (Lee and Brandt 1992) and suppress their dynamic properties (Dhamodharan and Wadsworth 1995). They may also link microtubules to actin filaments (Cross et al. 1993) and intermediate filaments (Capote and Maccioni 1998). Several strategies have been used to examine MAP function. For example, expression of Tau and MAP2 by transfection, or microinjection into cells that do not normally express these MAPs, results in increased microtubule stability and bundling, and outgrowth of axon-like processes. Tau and MAP2 antisense experimentes, showing inhibition of process outgrowth from neurons, also indicate the importance of these proteins in neuronal morphogenesis (Heidemann 1996). However, results from experiments with transgenic mice are more ambiguous. By immunostainings, the nervous system of mice lacking the Tau gene appears histologically normal, except for a decrease in microtubule stability and change in microtubule organization in some small-calibre axons. Interestingly, these mice exhibit increased amounts of MAP1A, perhaps compensating for the loss of Tau in the large-calibre axons (Harada et al. 1994). In another transgenic study, the presence of high quantities of embryonic MAP2 in adult brain had no obvious effect on the arrangement or morphology of neurons, suggesting that MAP2 does not function in regulation of neu-

ronal morphogenesis (Marsden et al. 1996). In contrast, MAP1B deficient mice generated by gene targeting methods have shown an abnormal brain architecture including reduced axon caliber, tract malformation, and layer disorganization (Edelmann et al. 1996; Gonzalez-Billault et al. 2000; Meixner et al. 2000). Simultaneous inhibition of MAP2 and MAP1B resulted in more severe phenotypes than those seen in single knockouts (Teng et al. 2001), showing synergistic effect of MAP2 and MAP1B in neuronal migration, dendritic outgrowth, and microtubule organization.

The most studied MAP is Tau. This protein is involved in paired helical filaments (PHFs) that form neurofibrillary tangles (NFTs) found in Alzheimer's disease. The protein forming these filaments is abnormally phosphorylated (Kosik et al. 1986). Alterations in Tau phosphorylation and function play a significant role in a variety of neurodegenerative diseases. Mutations in the Tau gene cause rare autosomal dominant neurodegenerative diseases, collectively known as frontotemporal dementia with Parkinsonism linked to chromosome 17 (FTDP-17). A number of sporadic neurodegenerative diseases are termed "tauopathies", since they are characterized by brain lesions which contain phosphorylated Tau (Abraha et al. 2000). In both Alzheimer's disease and in other Tau-related diseases, Tau phosphorylation is increased, which leads to abnormal Tau interactions and mis-localization, which are key events in the pathogenic processes that result in neuronal dysfunction and death. According to one model, in normal physiological conditions there is a balance between the phosphorylation and deposphorylation of Tau that regulates Tau's binding to microtubules and interactions with other specific binding partners (Abraha et al. 2000). It can be hypothesized that "initiating" phosphorylation events in the Tau pathogenic process would disrupt the normal localization of Tau, and its association with microtubules. Displacement of Tau from microtubules would result in pathological phosphorylation at fibrillogenic sites and/or cleveage by proteases (such as caspases). This results in a decrease in Tau's binding to its normal partners and increased Tau-Tau interactions, which might be the key pathological event. Subsequently, there is Tau filament formation and eventually aggregation into neurofibrillary tangles (NFTs). The mislocalization of Tau due to abnormal phosphorylation and/or cleavage is likely to have numerous pathological consequences. For example, changes in Tau could disrupt microtubule transport along the axons to the synapses, causing synaptic dysfunction. Synaptic dysfunction induced by aberrant posttranslational modifications of Tau could result in cognitive deficits, which would be intensified as affected neurons progress through dysfunction and death.

1.4.2.2. Motor proteins

Members of the kinesin (KIFs) and dynein superfamilies are microtubule-associated motor proteins. They bind to microtubules and transduce chemical energy, provided by ATP hydrolysis, into kinetic energy – in the form of the movement of the motors along the microtubules. Motors of the dynein family move along microtubules towards the minus end, whereas motors of the kinesin family usually move towards the plus end, with some exceptions that move in the opposite direction (Bloom and Endow 1995). There are at least 10 different families of kinesins, and 2 groups of dyneins, with up to several dozen

members each. The complement of motors varies widely between different organisms. Yeast, for example, functions with 6 kinesins, and 1 dynein, whereas mammals have genes for over 40 kinesins, and more than a dozen dyneins.

Kinesins are responsible for intracellular trafficking of vesicles and organelles along microtubules and for the dynamics of chromosomes and microtubules in mitosis and meiosis (Endow 1999; Sheetz 1999). Kinesin is a molecule of approximately 380 kDa, consisting of two heavy chains (120 kDa each) and two light chains (64 kDa each)(Figure 8). The heavy chains have long α-helical regions that wind around each other in a coiled-coil structure. The amino-terminal globular head domains of the heavy chains are the motor domains of the molecule. They bind to both microtubules and ATP. ATP hydrolysis provides the energy required for movement (Hirokawa et al. 1989). The globular tail, in partnership with the light chain, is thought to be involved in cargo specificity. The conventional kinesin, or kinesin I (Vale et al. 1985) was originally described as an axonal vesicle motor, but it also moves mitochondria and the endoplasmic reticulum (ER) and participates in the organization of the Golgi apparatus (Lane and Allan 1998).

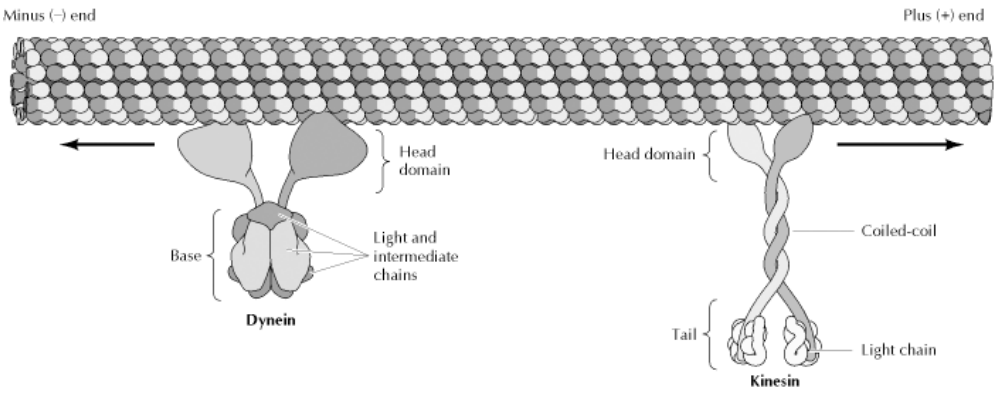

Figure 8. Microtubule motor proteins. Kinesin and dynein move in opposite directions along microtubules, toward the plus and minus ends, respectively. Kinesin consists of two heavy chains, wound around each other in a coiled-coil structure, and two light chains. The globular head domains of the heavy chains bind microtubules and are the motor domains of the molecule. Dynein consists of two or three heavy chains (two are shown here) in association with multiple light and intermediate chains. The globular head domains of the heavy chains are the motor domains.
From Cooper 2000

Dyneins are minus end-directed motor proteins. They were first studied in cilia and flagella. Like kinesins, dyneins generate movement along microtubules, using energy released from hydrolysis of ATP. However, dyneins are large multisubunit complexes structurally unrelated to kinesins. Dynein complexes play important roles in mitotic spindle

function, movement of cilia and flagella, and in vesicular trafficking in a variety of cell types.

Members of the cytoplasmic dynein family manifest their diverse functions quite differently from the kinesin superfamily. Instead of evolving various primary structure differences in their heavy chains, dyneins interact with distinct partners in order to be targeted and regulated properly. Cytoplasmic dynein is a protein complex of 1200 kDa, that has two large globular heads connected by thin stalks to a common base. The two dynein heavy chains contain active ATPase sites, one in each globular head, and generate force to move cargo. The role of dynein light chains (6 – 22 kDa), light intermediate chains (50 – 60 kDa) and intermediate chains (~74 kDa) may be to specify the cargo with which dynein interacts and/or to regulate the function of the heavy chains. Cytoplasmic dynein requires a second multi-subunit complex, dynactin, for full activity (Schroer et al. 1996; Vallee and Sheetz 1996).

Dynactin is a multiprotein complex that is necessary for the majority of dynein functions. Ultrastructural, molecular and biochemical analyses have provided clues into how dynactin may activate cytoplasmic dynein. One prominent feature of dynactin is a minifilament of the actin-related protein Arp1 (Schafer et al. 1994), which has the potential to bind isoforms of the actin-crosslinking protein spectrin that are found on the Golgi apparatus (Holleran et al. 1996).

1.4.2.3. Microtubule Plus-End Tracking Proteins (+ TIPs)

+TIPs are a highly diverse group of MAPs that specifically accumulate at the plus ends of microtubules (Carvalho et al. 2003; Howard and Hyman 2003). This new family of MAPs was discovered by observing the movements of cytoplasmic linker protein 170 (CLIP-170)-green fluorescent protein (GFP) in live cells. As microtubule grows in the presence of GFP-CLIP-170, bright patches or ‘comets’ can be seen at the growing end. These patches disappear when the microtubule stops growing (Perez et al. 1999). Thus, CLIP-170 binds to plus ends of microtubules and continue to ‘track’ with the plus ends as they elongate. Both GFP fusions of tip1p, the homologue of CLIP-170 in S. pombe, and Bik1, the homologue of CLIP-170 in S. cerevisiae, display a similar behavior (Brunner and Nurse 2000; Lin et al. 2001).

Since the discovery of CLIP-170, many more structurally unrelated plus-end tracking proteins have been identified, such as end binding proteins EB1, EB2 (RP1), and EB3, the dynactin large subunit p150glued, adenomatous polyposis coli (APC), CLIP-associating proteins (CLASPs) and lissencephaly 1 (Lis-1) (Schuyler and Pellman 2001; Carvalho et al. 2003; Galjart and Perez 2003; Akhmanova and Hoogenraad 2005).

There are currently two models of possible mechanisms of accumulation of +TIPs at microtubule plus ends (Figure 9). One mechanism is ‘treadmilling’ or ‘transient immobilization of proteins’ at the plus end of growing microtubule. +TIPs that treadmill, preferentially bind to the plus end of growing microtubule and are released a short time later as the plus end grows past (Figure 9, A). Treadmilling +TIPs do not translocate through the cytoplasm with the plus end but instead bind and release at the same point in space (Perez et al.

1999). Thus, the comet that appears to surf the plus end when GFP-tagged proteins are visualized in living cells is an illusion caused by the +TIPs hopping on and off the end as it grows and passes a region in the cell. Several factors can contribute to preferential end localization of treadmilling +TIPs, including copolymerization with tubulin dimers, high-affinity binding to microtubule ends, and selective release from the tubule walls (Schuyler and Pellman 2001; Carvalho et al. 2003). This mechanism was demonstrated for CLIP-170 and EB1 (Perez et al. 1999; Tirnauer et al. 2002). One of the explanations how GFP-CLIP-170 binds specifically to the growing microtubules, is that it recognizes a specific transient conformation of tubulin polymer found only at the growing end (Desai and Mitchison 1997), and/or CLIP-170 copolymerizes with tubulin, since the amino-terminal microtubule-binding domain of CLIP-170 is highly similar to sequences with cofactors B and E, proteins known to be involved in tubulin folding (Diamantopoulos et al. 1999; Perez et al. 1999).

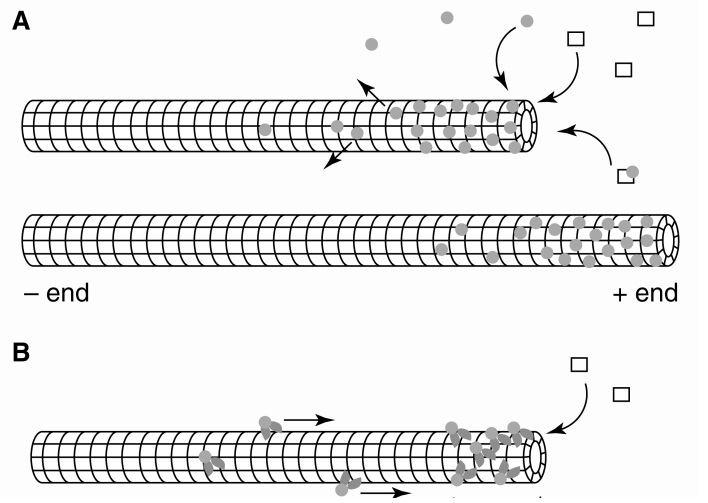

Figure 9. Models for the localization of microtubule plus end associated proteins (+TIPs). A. Treadmilling model. Tubulin (squares) and +TIP (grey dots) from cytoplasmic pools either coassemble or independently associate with growing microtubule ends. +TIP subsequently dissociates, producing a continous comet-tail on a growing microtubule as it elongates. Two different time points are shown. **B.** Sliding model. +TIPs (grey dots) associate with kinesins (black dots) and move towards plus ends.

The second proposed mechanism of +TIP accumulation at microtubule plus ends, is the 'sliding' or 'delivery of proteins' model (Figure 9, B). In this model +TIPs can associate with MTs along their length and they accumulate at the tips of both polymerizing and depolymerizing microtubules, by a motor-driven process.

Bik1p, the CLIP-170 homologue in budding yeast, and Tip1p, the CLIP-170 homologue in fission yeast, are using this mechanism of accumulation at growing microtubule plus ends (Brunner and Nurse 2000; Lin et al. 2001). They are accumulated to the mi-

crotubule plus ends by the action of kinesin motors Kip2p and Tea2p (Busch et al. 2004; Carvalho et al. 2004).

Finally, recent evidence indicates that plus end accumulation may be considerably more complicated. A +TIP may associate with plus ends using both treadmilling and sliding mechanisams, and different organisms may use distinct pathways to localize the same +TIP family member (Carvalho et al. 2003; Lee et al. 2003; Xiang 2003). Furthermore, many of the +TIPs interact with one another leading to speculation that there may be rafts of interacting proteins surfing on the plus ends of microtubules, where they regulate microtubule dynamics and capture (Coquelle et al. 2002; Galjart and Perez 2003). There is also a third possible mechanism of accumulation of +TIPs at the microtubule ends, called hitchhiking. Hitchhiking +TIPs bind the microtubule plus end indirectly through other proteins, thus appearing to surf the plus end, but are not transported through the cytoplasm with the growing microtubule (Carvalho et al. 2003).

CLIPs

CLIP-170 was the first protein shown to track the plus ends of microtubules, and is considered as the prototype +TIP (Rickard and Kreis 1990; Perez et al. 1999). CLIP family members have been identified in diverse phyla where they regulate microtubule dynamics and appear to link microtubules to intracellular sites (Pierre et al. 1992; Dujardin et al. 1998; Brunner and Nurse 2000; Lin et al. 2001).

Tip1, the homologue of CLIP-170 in the fission yeast (S. Pombe), is involved in guidance of microtubules to the cell ends, and is proposed to be a suppressor of microtubule catastrophes. Tip1p somehow distinguishes between the cell cortex in the middle regions of the cell and the cortex at cell ends (Brunner and Nurse 2000). This difference in cortical regions might be caused by the polarized distribution of yet other factors.

In mammalian cells, in addition to a possible role in organelle or membrane targeting, CLIPs function as rescue factors in microtubule dynamics (Komarova et al. 2002). CLIPs at growing microtubule plus ends interact with other +TIPs, and might be involved in regulatory activities in addition to serving as a rescue factor (Akhmanova et al. 2001; Coquelle et al. 2002; Tai et al. 2002). It has been shown that CLIPs interact with IQGAP1, possibly functioning as linkers between the plus ends of microtubules and the cortical actin meshwork downstream of Rac1 and Cdc42 (Fukata et al. 2002b), see next section). Thus, CLIPs are likely to be multifunctional proteins in which one domain modulates microtubule dynamics, whereas another domain serves a cross-talk function with the cell cortex. Although the overall sequence similarity is not high among CLIPs, the proteins all share conserved domains. The microtubule-binding region, located at the amino terminus, consists of one or more CAP-Gly domains; it is followed by a central coiled-coil and one or more putative metal-binding motifs at the carboxy terminus. A close relative of CLIP-170, CLIP-115, has been mainly localized in neurons (De Zeeuw et al. 1997), and a CLIP-170 homologue in Drosophila, CLIP-190, has been localized on Golgi membranes (Sisson et al. 2000).

CLIP-115 is the product of the CYLN2 gene that encodes a protein of 115 kDa. CLIP-115 is prominently expressed in various areas of the adult central nervous system such

as the hippocampus, amygdala and cerebellum (De Zeeuw et al. 1997; Hoogenraad et al. 2002). Knock-out (KO) mice lacking CLIP-115, mimic some of the neurological symptoms of Williams syndrome patients (Hoogenraad et al. 2002), thus linking cytoskeletal defect to a neurological disease.

The EB1 family

End binding 1 (EB1) proteins play important roles in diverse organisms, ranging from human to fungi. By regulating microtubule dynamics and mediating attachment of MT ends to subcellular sites, they are instrumental in assembling and aligning the mitotic spindle, guiding polarized cell growth, and facilitating chromosome capture by spindles (Schuyler and Pellman 2001; Carvalho et al. 2003). EB1 was originally identified as a protein that interacts with APC (Su et al. 1995). EB1 targets to microtubule plus ends independently of APC (Morrison et al. 1998), but APC targeting to microtubule plus ends requires EB1 (Askham et al. 2000; Mimori-Kiyosue et al. 2000). To date, EB1 has been found in every organism and nearly every cell type examined, including neuronal, lymphocytic, and epithelial cells (Renner et al. 1997). The budding yeast possesses a single EB1 homologue, called Bim1 (Schwartz et al. 1997). The fission yeast homologue mal3 was isolated in a screen for mutations that caused chromosome loss (Beinhauer et al. 1997). Caenorhabditis elegans has two EB1 related genes, and Drosophila melanogaster has at least three EB1 family members (Benson et al. 2000). The number of EB1 proteins in humans is unknown, but to date EB1, EB2, EB3, and EBF3 have been reported, along with the highly related RP1, RP2, and RP3 proteins (Su et al. 1995; Renner et al. 1997; Juwana et al. 1999; Nakagawa et al. 2000). All human EB1 family proteins are expressed ubiquitously, but most studies so far have focused on EB1. Recently, EB3 was shown to be neuronally expressed and to interact with a neuron-specific homologue of APC, APCL (Nakagawa et al. 2000). RP1 was identified by its induction upon T lymphocyte activation, and it shares APC binding and subcellular localization with EB1 (Renner et al. 1997). EB1 family proteins associate with microtubule plus ends and centrosomes when expressed at endogenous levels but associate with the entire microtubules when overexpressed. EB1 family proteins have been shown to regulate the assembly and functions of microtubules. Bim1 protein regulates microtubule dynamics in interphase S. cerevisiae cells and anchors microtubule plus ends at the bud cortex through the interaction with Kar9 protein (Tirnauer et al. 1999; Adames and Cooper 2000; Korinek et al. 2000). Inactivation of Drosophila EB1 affects the assembly, dynamics, and positioning of the mitotic spindle (Rogers et al. 2002). In mammalian cells overexpression of EB1 and EBF3 has been shown to induce bundling of microtubules (Bu and Su 2001).

Adenomatous polyposis coli

The adenomatous polyposis coli (APC) protein is the 312 kDa product of a tumor suppressor gene, which is mutated in familial adenomatous polyposis, a condition that predisposes carriers to the development of colorectal cancer. In addition to intestinal epithelial

cells, APC is expressed in a wide variety of tissues and is particularly abundant in the brain (Bhat et al. 1994). APC concentrates in growth cones of developing neurons (Brakeman et al. 1999). Another important function of APC is its involvement in the Wingless (Wnt) signaling pathway, in which APC forms complexes with cytoplasmic β-catenin, glycogen synthase kinase-3β (GSK-3β) and axin. APC binds to microtubules, promotes their assembly and induces their bundling in vitro and in transfected cells (Munemitsu et al. 1994). APC can form complexes with other +TIPs, e.g. the microtubule-end binding protein, EB1 (Berrueta et al. 1998; Morrison et al. 1998). EB1 appears to be required for APC to bind to plus ends. APC mutants that cannot bind to EB1 still associate with microtubules but are not targeted to plus ends (Askham et al. 2000), suggesting a requirement for EB1 in this localization process. The tubulin-binding domain of APC is located in the carboxy-terminal end of the protein, and most of the mutations linked to familial adenomatous polyposis are C-terminal deletions that result in the loss of both the β-catenin and the microtubule-binding domains.

Lissencephaly 1

Humans carrying mutations in the Lissencephaly 1 (LIS1) gene have a severe developmental brain deformity known as lissencephaly type 1. Lissencephaly is a human brain malformation characterized by a smooth cerebral surface and a disordered organization of the cortical layers resulting from a defect in neuronal migration (Reiner 2000). LIS1 proteins are conserved across large evolutionary distances and have been shown to form comet-like structures at the growing ends of microtubules. They regulate dynein activity and MT dynamics by mechanisms that are not well understood (Coquelle et al. 2002; Lee et al. 2003). The targeted knockout of the LIS1 gene created a mouse model for Lissencephaly. Homozygous null mice die early in embryogenesis whereas heterozygous mice survive, showing evidence of delayed neuronal migration (cortical, hippocampal, cerebellar and olfactory bulb disorganization) confirmed by in vitro and in vivo cell migration assays (Hirotsune et al. 1998).

CLIP-Associated proteins

CLIP-associated proteins, or CLASPs, are members of the +TIP family of proteins that are implicated in the regulation of microtubule stability (Akhmanova et al. 2001), and in axonal guidance (Lee et al. 2004). They are well conserved throughout evolution. The Drosophila homologue, Orbit/MAST, is essential for mitosis (Inoue et al. 2000; Lemos et al. 2000), as is cls-2, one of the three C. elegans homologues (Gonczy et al. 2000). Orbit/MAST is present at kinetochores, and its inactivation results in monopolar spindles with chromosomes buried in the interiour of the aster (Maiato et al. 2002). There are two mammalian CLASPs, CLASP-1 and CLASP-2, that share about 77% homology. As a result of alternative splicing, both CLASPs exist in several isoforms, that differ in their N-terminal part, with molecular mass of 170 kDa (α isoforms), and 140 kDa (β/γ isoforms). Both CLASPs bind to microtubules, and to CLIP-170 and CLIP-115, through their C-terminal

CLIP-interacting domain (Akhmanova et al. 2001). In motile fibroblasts, CLASPs are involved in the local stabilization of microtubules, at the leading edge of the cells (Akhmanova et al. 2001). Their asymmetric distribution is mediated by PI3-kinase and GSK-3β. Reduced levels of CLASPs leads to partial disassembly of the microtubule array and abnormal distribution of microtubule plus ends, which lose their ability to localize near the cell cortex (Mimori-Kiyosue et al. 2005).

+TIPs are positioned ideally for influencing microtubule behavior. They can regulate both microtubule dynamics and the structure/polarity of the microtubule array.

1.5. Cell polarity

All cell types polarize, at least transiently during division, or to generate specialized shapes and perform specific functions. This capacity extends from yeast to mammals, and it is now clear that many features of the molecular mechanisms controlling polarization are conserved in all eukaryotic cells. Polarity in living cells is created by reorganization of cytoskeletal components, in conjunction with directed intracellular transport and membrane compartmentalization. The whole process requires cooperation and coordinated reorganization of the actin cytoskeleton and microtubules (Goode et al. 2000).

Rho GTPases have emerged as a key regulators in cell polarization, as well as in actin organization. At the centre of the action is Cdc42, a small GTPase of the Rho family. Its activity is precisely controlled both temporally and spatially, and this can be achieved by a wide variety of extracellular cues in multicellular organisms (Etienne-Manneville 2004).

A very useful system for genetic studies of the process of cell polarization is provided by Schizosaccharomyces pombe, or fission yeast (Nurse 1994; Hirata et al. 1998; Brunner and Nurse 2000). Fission yeast are simple, rod-shaped cells that grow at cell tips in a regulated manner. After cell division, growth begins only at the old end of the cell (so-called unipolar growth). Then after some time, growth is initiated at the new ends (Mitchison and Nurse 1985), and it continues from both tips (so-called bipolar growth) (Figure 10). This transition in cell polarization, in which monopolar cell is initiating bipolar growth, is known as New End Take Off (NETO). Both actin (actin cables) and microtubule cytoskeletons are implicated in the regulation of this process (Chang 2001). It has been shown that microtubules and microtubular transport are important for generating positional information within the fission yeast cell, and in defining the site of growth extension (Mata and Nurse 1998).

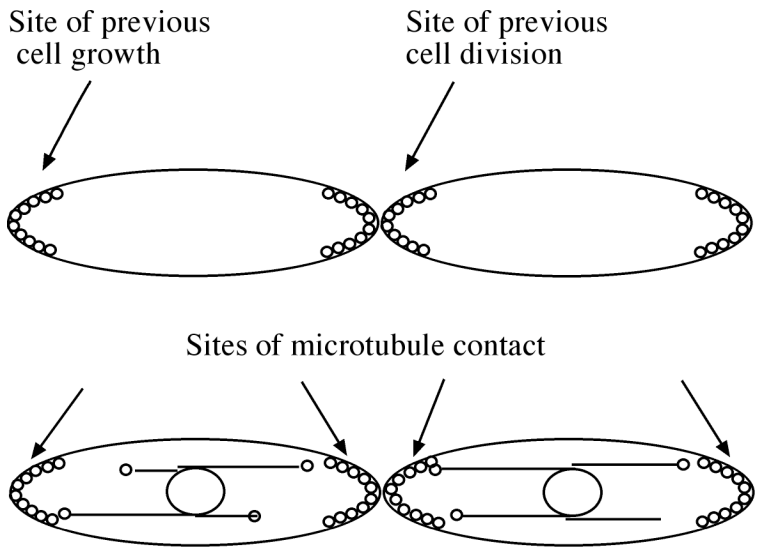

Figure 10. Polarized cell growth of fission yeast. Fission yeast first grows at previous sites of cell growth, and then begin to grow at the previous cell division sites. Microtubules, through deposition of an end-tip protein Tea1p (circles), regulate this process.
From Chang and Peter 2003.

Microtubules are organized in antiparallel bundles, and are oriented along the length of the cell. Depolarization of microtubules leads to the formation of branched cells (Radcliffe et al. 1998; Sawin and Nurse 1998), and different morphological mutants have abnormal arrays of cytoplasmic microtubules (Verde et al. 1995; Radcliffe et al. 1998).

Mutational analysis has discovered several factors that are involved in the regulation of NETO and establishment of cell polarity, such as kelch-repeat protein Tea1p, the kinesin-related protein Tea2p, the EB1 homolog Mal3, and the CLIP-170 homolog Tip1p (Chang and Peter 2003).

One of the factors in the process of cell polarization is a cell-end marker protein Tea1p. Tea1p is located on the growing plus ends of microtubules (Mata and Nurse 1997), and its localization is dependent on the CLIP-170 Tip1p and the Kip2-like kinesin Tea2p (Browning et al. 2000; Brunner and Nurse 2000). When microtubules reach cell tips, Tea1p is deposited at the cell cortex, establishing its specific bipolar localization (Mata and Nurse 1997) in a process that requires the cortical anchor Mod5p (Snaith and Sawin 2003) (Figure 11). If Tea1p is mutated, mutant cells cannot grow in a bipolar fashion and very often show T-shaped morphology (Mata and Nurse 1997).

Recently, a new factor Tea4p, that binds directly to Tea1p and to formin For3p, was identified (Martin et al. 2005). Thus, Tea4p has a linking role connecting microtubule plus end polarity factors with the formin For3p, an actin nucleating factor (Wallar and Alberts 2003).

In a simplified model (Figure 11), Tip1p, Tea1p and Tea4p form a protein complex (which is sometimes called polarizome) at the plus end of microtubules. This complex is transported down the microtubules, where it meets up with Mod5p at the cell tip and interacts and activates For3p. This might be a key event in initiating actin cable assembly and setting off positive feedback mechanisms that establish and maintain polarized cell growth (Martin et al. 2005).

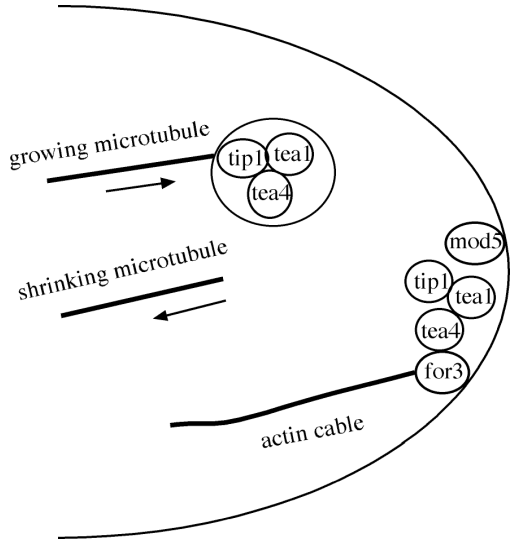

Figure 11. Establishment of cell polarity at the new end of the fission yeast cell. (see explanation in the text) Adapted from Martin et al., 2005

In multicellular organisms, cell polarity is determined primarily by external stimuli. Contact receptors such as integrins and cadherins, as well as receptors for soluble ligands such as chemokines, allow individual cells to sense their environment and organize polarity accordingly. This is controlled by Cdc42 and, as in yeast, the localized recruitment and activation of Cdc42 is likely to be a key signaling event leading to cell polarization (Etienne-Manneville and Hall 2002).

One good example of cell polarization is cell migration. Cells migrate by coordinating cytoskeletal-mediated extensions and contractions with making and breaking contacts to an underlying substratum. To coordinate directional movements, cells must activate specific sites at the membrane periphery in response to a polarized external cue. A particular location then becomes a 'cortical platform' for the transmission of converging internal signals that are necessary to elicit subsequent cytoskeletal responses. The outcome is dependent upon the cell type and the precise signaling pathways that are engaged, and can range from the polymerization and/or reorganization of actin to the polarized capture and stabilization of microtubules and their associated microtubule organizing center (MTOC).

Localized activation of small GTPases appears to be a unifying and early step in orchestrating the downstream rearrangements in cytoskeleton necessary to polarize cell motility. Downstream GTPase-activated effector proteins, including actin binding proteins and +TIPs, are then recruited to these activated sites. This starts a molecular cascade of events that culminates in the polarization and polymerization of actin and capturing of the growing ends of microtubules. Polarized rearrangement of actin-based structures provides the driving force for motility, resulting in the GTPase-dependent induction of filopodia, lamellipodia, and stress fibers (Hall 1998).

However, without the concurrent polarization of the microtubule cytoskeleton, cells cannot sustain the directionality of their movements. Microtubules 'search' cytoplasmic space by continuously growing and shrinking from their plus ends (Kirschner and Mitchison 1986). Microtubules are then 'captured' and transiently stabilized at specific membrane target sites through plus end-interacting proteins (+TIPs), such as EB1 and CLIP-170 (Schuyler and Pellman 2001; Gundersen et al. 2004). +TIPs are thought to act in part by protecting the growing ends of microtubules from catastrophe proteins that might otherwise bind to and initiate the depolymerization of the microtubule (Komarova et al. 2002; Tirnauer et al. 2002), and by targeting microtubules to specific locales. +TIPs can also interact with members of protein complexes at cortical platforms. One such protein is APC, which through independent binding domains has the capacity to bind to both EB1 and cortical proteins (Barth et al. 2002).

A particularly powerful system for dissecting the sequence of molecular events involved in cellular polarization is the introduction of scratches or wounds into a monolayer of adherent mammalian cells in culture. In wounded astrocyte cultures, for instance, the small GTPase Cdc42 is activated at the leading edge, a process that triggers the binding of a polarizing protein Par6, which in turn activates PKCζ, which then phosphorylates and inactivates GSK3β (Etienne-Manneville and Hall 2001; Etienne-Manneville and Hall 2003). This cascade has been proposed to enable APC to then associate with microtubule tips and allow the selective capturing and stabilization of microtubules at the leading edge of the migrating front. In one report the downstream effector was IQGAP, which is also a direct binding partner for activated Cdc42 at the leading edge (Fukata et al. 2002a). Additional direct interactions between IQGAP and the +TIP CLIP-170 then appeared to link the temporal capture of the microtubule plus ends to this activated cortical platform. Expression of mutant IQGAP that could not bind activated GTPases resulted in multiple protrusion sites. This provides further evidence that coupling microtubule stabilization to a cortical platform is required for sustaining polarity. Additional direct GTPase targets such as mDia have also surfaced as binding partners or regulators of the +TIP EB1 (Wen et al. 2004). Other proteins that localize to and are likely to be involved in these types of F-actin-microtubule connections include the minus end-directed microtubule motor protein dynein, the CLASPs, and the gigantic spectraplakin protein ACF7 (Leung et al. 1999; Karakesisoglou et al. 2000; Kodama et al. 2003; Gundersen et al. 2004). Many cells also often polarize their MTOC in the direction of migration. In wounded astrocyte cultures, dominant-negative disruption of dynein function abrogates the MTOC reorientation process (Etienne-Manneville and Hall 2001), and this and other reports implicate dynein/dynactin in the signaling pathway that

leads to MTOC positioning (Burakov et al. 2003). Although a direct connection between dynein/dynactin and the Cdc42/Par6/PKCζ/GSK3β pathway has not yet surfaced, increasing evidence points to the view that the cortical platform that develops at a wound edge can act as a scaffolding complex. This concept sets the scene for multiple +TIPs to encounter many different receptor proteins that may converge at this platform.

Since in CLASP2 knock out mice the hematopoietic system and specially megakaryocytes are affected, a short overview of hematopoiesis and megakaryocytopoiesis is given in the second part of this chapter.

References

Abraha, A., Ghoshal, N., Gamblin, T.C., Cryns, V., Berry, R.W., Kuret, J., and Binder, L.I. 2000. C-terminal inhibition of tau assembly in vitro and in Alzheimer's disease. J Cell Sci 113 Pt 21: 3737-3745.

Adames, N.R. and Cooper, J.A. 2000. Microtubule interactions with the cell cortex causing nuclear movements in Saccharomyces cerevisiae. J Cell Biol 149(4): 863-874.

Aizawa, H., Emori, Y., Murofushi, H., Kawasaki, H., Sakai, H., and Suzuki, K. 1990. Molecular cloning of a ubiquitously distributed microtubule-associated protein with Mr 190,000. J Biol Chem 265(23): 13849-13855.

Aizawa, H., Kawasaki, H., Murofushi, H., Kotani, S., Suzuki, K., and Sakai, H. 1989. A common amino acid sequence in 190-kDa microtubule-associated protein and tau for the promotion of microtubule assembly. J Biol Chem 264(10): 5885-5890.

Akhmanova, A. and Hoogenraad, C.C. 2005. Microtubule plus-end-tracking proteins: mechanisms and functions. Curr Opin Cell Biol 17(1): 47-54.

Akhmanova, A., Hoogenraad, C.C., Drabek, K., Stepanova, T., Dortland, B., Verkerk, T., Vermeulen, W., Burgering, B.M., De Zeeuw, C.I., Grosveld, F., and Galjart, N. 2001. Clasps are CLIP-115 and -170 associating proteins involved in the regional regulation of microtubule dynamics in motile fibroblasts. Cell 104(6): 923-935.

Alberts, B. 1994. Molecular biology of the cell. Garland Pub, New York.

Arimura, N., Inagaki, N., Chihara, K., Menager, C., Nakamura, N., Amano, M., Iwamatsu, A., Goshima, Y., and Kaibuchi, K. 2000. Phosphorylation of collapsin response mediator protein-2 by Rho-kinase. Evidence for two separate signaling pathways for growth cone collapse. J Biol Chem 275(31): 23973-23980.

Arimura, N., Menager, C., Fukata, Y., and Kaibuchi, K. 2004. Role of CRMP-2 in neuronal polarity. J Neurobiol 58(1): 34-47.

Askham, J.M., Moncur, P., Markham, A.F., and Morrison, E.E. 2000. Regulation and function of the interaction between the APC tumour suppressor protein and EB1. Oncogene 19(15): 1950-1958.

Barth, A.I., Siemers, K.A., and Nelson, W.J. 2002. Dissecting interactions between EB1, microtubules and APC in cortical clusters at the plasma membrane. J Cell Sci 115(Pt 8): 1583-1590.

Beilharz, E.J., Zhukovsky, E., Lanahan, A.A., Worley, P.F., Nikolich, K., and Goodman, L.J. 1998. Neuronal activity induction of the stathmin-like gene RB3 in the rat hippocampus: possible role in neuronal plasticity. J Neurosci 18(23): 9780-9789.

Beinhauer, J.D., Hagan, I.M., Hegemann, J.H., and Fleig, U. 1997. Mal3, the fission yeast homologue of the human APC-interacting protein EB-1 is required for microtubule integrity and the maintenance of cell form. J Cell Biol 139(3): 717-728.

Belmont, L.D., Hyman, A.A., Sawin, K.E., and Mitchison, T.J. 1990. Real-time visualization of cell cycle-dependent changes in microtubule dynamics in cytoplasmic extracts. Cell 62(3): 579-589.

Belmont, L.D. and Mitchison, T.J. 1996. Identification of a protein that interacts with tubulin dimers and increases the catastrophe rate of microtubules. Cell 84(4): 623-631.

Benson, D.A., Karsch-Mizrachi, I., Lipman, D.J., Ostell, J., Rapp, B.A., and Wheeler, D.L. 2000. GenBank. Nucleic Acids Res 28(1): 15-18.

Berrueta, L., Kraeft, S.K., Tirnauer, J.S., Schuyler, S.C., Chen, L.B., Hill, D.E., Pellman, D., and Bierer, B.E. 1998. The adenomatous polyposis coli-binding protein EB1 is associated with cytoplasmic and spindle microtubules. Proc Natl Acad Sci U S A 95(18): 10596-10601.

Bhat, R.V., Baraban, J.M., Johnson, R.C., Eipper, B.A., and Mains, R.E. 1994. High levels of expression of the tumor suppressor gene APC during development of the rat central nervous system. J Neurosci 14(5 Pt 2): 3059-3071.

Bloom, G.S. and Endow, S.A. 1995. Motor proteins 1: kinesins. Protein Profile 2(10): 1105-1171.

Borisy, G.G. and Olmsted, J.B. 1972. Nucleated assembly of microtubules in porcine brain extracts. Science 177(55): 1196-1197.

Brakeman, J.S., Gu, S.H., Wang, X.B., Dolin, G., and Baraban, J.M. 1999. Neuronal localization of the Adenomatous polyposis coli tumor suppressor protein. Neuroscience 91(2): 661-672.

Brattsand, G. 2000. Correlation of oncoprotein 18/stathmin expression in human breast cancer with established prognostic factors. Br J Cancer 83(3): 311-318.

Browning, H., Hayles, J., Mata, J., Aveline, L., Nurse, P., and McIntosh, J.R. 2000. Tea2p is a kinesin-like protein required to generate polarized growth in fission yeast. J Cell Biol 151(1): 15-28.

Brugg, B. and Matus, A. 1991. Phosphorylation determines the binding of microtubule-associated protein 2 (MAP2) to microtubules in living cells. J Cell Biol 114(4): 735-743.

Brunner, D. and Nurse, P. 2000. CLIP170-like tip1p spatially organizes microtubular dynamics in fission yeast. Cell 102(5): 695-704.

Bu, W. and Su, L.K. 2001. Regulation of microtubule assembly by human EB1 family proteins. Oncogene 20(25): 3185-3192.

Burakov, A., Nadezhdina, E., Slepchenko, B., and Rodionov, V. 2003. Centrosome positioning in interphase cells. J Cell Biol 162(6): 963-969.

Burns, R.G. 1991. Alpha-, beta-, and gamma-tubulins: sequence comparisons and structural constraints. Cell Motil Cytoskeleton 20(3): 181-189.

Busch, K.E., Hayles, J., Nurse, P., and Brunner, D. 2004. Tea2p kinesin is involved in spatial microtubule organization by transporting tip1p on microtubules. Dev Cell 6(6): 831-843.

Capote, C. and Maccioni, R.B. 1998. The association of tau-like proteins with vimentin filaments in cultured cells. Exp Cell Res 239(2): 202-213.

Carvalho, P., Gupta, M.L., Jr., Hoyt, M.A., and Pellman, D. 2004. Cell cycle control of kinesin-mediated transport of Bik1 (CLIP-170) regulates microtubule stability and dynein activation. Dev Cell 6(6): 815-829.

Carvalho, P., Tirnauer, J.S., and Pellman, D. 2003. Surfing on microtubule ends. Trends Cell Biol 13(5): 229-237.

Chang, F. 2001. Establishment of a cellular axis in fission yeast. Trends Genet 17(5): 273-278.

Chang, F. and Peter, M. 2003. Yeasts make their mark. Nat Cell Biol 5(4): 294-299.

Chapin, S.J. and Bulinski, J.C. 1992. Microtubule stabilization by assembly-promoting microtubule-associated proteins: a repeat performance. Cell Motil Cytoskeleton 23(4): 236-243.

Chen, J., Kanai, Y., Cowan, N.J., and Hirokawa, N. 1992. Projection domains of MAP2 and tau determine spacings between microtubules in dendrites and axons. Nature 360(6405): 674-677.

Chretien, D. and Wade, R.H. 1991. New data on the microtubule surface lattice. Biol Cell 71(1-2): 161-174.

Coquelle, F.M., Caspi, M., Cordelieres, F.P., Dompierre, J.P., Dujardin, D.L., Koifman, C., Martin, P., Hoogenraad, C.C., Akhmanova, A., Galjart, N., De Mey, J.R., and Reiner, O. 2002. LIS1, CLIP-170's key to the dynein/dynactin pathway. Mol Cell Biol 22(9): 3089-3102.

Cross, D., Vial, C., and Maccioni, R.B. 1993. A tau-like protein interacts with stress fibers and microtubules in human and rodent cultured cell lines. J Cell Sci 105 (Pt 1): 51-60.

Curmi, P.A., Andersen, S.S., Lachkar, S., Gavet, O., Karsenti, E., Knossow, M., and Sobel, A. 1997. The stathmin/tubulin interaction in vitro. J Biol Chem 272(40): 25029-25036.

De La Cruz, E.M., Mandinova, A., Steinmetz, M.O., Stoffler, D., Aebi, U., and Pollard, T.D. 2000. Polymerization and structure of nucleotide-free actin filaments. J Mol Biol 295(3): 517-526.

De Zeeuw, C.I., Hoogenraad, C.C., Goedknegt, E., Hertzberg, E., Neubauer, A., Grosveld, F., and Galjart, N. 1997. CLIP-115, a novel brain-specific cytoplasmic linker protein, mediates the localization of dendritic lamellar bodies. Neuron 19(6): 1187-1199.

Derry, J.M., Ochs, H.D., and Francke, U. 1994. Isolation of a novel gene mutated in Wiskott-Aldrich syndrome. Cell 79(5): following 922.

Desai, A. and Mitchison, T.J. 1997. Microtubule polymerization dynamics. Annu Rev Cell Dev Biol 13: 83-117.

Dhamodharan, R. and Wadsworth, P. 1995. Modulation of microtubule dynamic instability in vivo by brain microtubule associated proteins. J Cell Sci 108 (Pt 4): 1679-1689.

Diamantopoulos, G.S., Perez, F., Goodson, H.V., Batelier, G., Melki, R., Kreis, T.E., and Rickard, J.E. 1999. Dynamic localization of CLIP-170 to microtubule plus ends is coupled to microtubule assembly. J Cell Biol 144(1): 99-112.

Domann, E., Wehland, J., Rohde, M., Pistor, S., Hartl, M., Goebel, W., Leimeister-Wachter, M., Wuenscher, M., and Chakraborty, T. 1992. A novel bacterial virulence gene in Listeria monocytogenes required for host cell microfilament interaction with homology to the proline-rich region of vinculin. Embo J 11(5): 1981-1990.

Dujardin, D., Wacker, U.I., Moreau, A., Schroer, T.A., Rickard, J.E., and De Mey, J.R. 1998. Evidence for a role of CLIP-170 in the establishment of metaphase chromosome alignment. J Cell Biol 141(4): 849-862.

Edelmann, W., Zervas, M., Costello, P., Roback, L., Fischer, I., Hammarback, J.A., Cowan, N., Davies, P., Wainer, B., and Kucherlapati, R. 1996. Neuronal abnormalities in microtubule-associated protein 1B mutant mice. Proc Natl Acad Sci U S A 93(3): 1270-1275.

Endow, S.A. 1999. Microtubule motors in spindle and chromosome motility. Eur J Biochem 262(1): 12-18.

Erickson, H.P. and Stoffler, D. 1996. Protofilaments and rings, two conformations of the tubulin family conserved from bacterial FtsZ to alpha/beta and gamma tubulin. J Cell Biol 135(1): 5-8.

Etienne-Manneville, S. 2004. Cdc42--the centre of polarity. J Cell Sci 117(Pt 8): 1291-1300.

Etienne-Manneville, S. and Hall, A. 2001. Integrin-mediated activation of Cdc42 controls cell polarity in migrating astrocytes through PKCzeta. Cell 106(4): 489-498.

-. 2002. Rho GTPases in cell biology. Nature 420(6916): 629-635.

-. 2003. Cdc42 regulates GSK-3beta and adenomatous polyposis coli to control cell polarity. Nature 421(6924): 753-756.

Feldner, J.C. and Brandt, B.H. 2002. Cancer cell motility--on the road from c-erbB-2 receptor steered signaling to actin reorganization. Exp Cell Res 272(2): 93-108.

Fuchs, E. 1995. Keratins and the skin. Annu Rev Cell Dev Biol 11: 123-153.

Fujiwara, I., Takahashi, S., Tadakuma, H., Funatsu, T., and Ishiwata, S. 2002. Microscopic analysis of polymerization dynamics with individual actin filaments. Nat Cell Biol 4(9): 666-673.

Fukata, M., Watanabe, T., Noritake, J., Nakagawa, M., Yamaga, M., Kuroda, S., Matsuura, Y., Iwamatsu, A., Perez, F., and Kaibuchi, K. 2002a. Rac1 and Cdc42 capture microtubules through IQGAP1 and CLIP-170. Cell 109(7): 873-885.

Fukata, Y., Itoh, T.J., Kimura, T., Menager, C., Nishimura, T., Shiromizu, T., Watanabe, H., Inagaki, N., Iwamatsu, A., Hotani, H., and Kaibuchi, K. 2002b. CRMP-2 binds to tubulin heterodimers to promote microtubule assembly. Nat Cell Biol 4(8): 583-591.

Galjart, N. and Perez, F. 2003. A plus-end raft to control microtubule dynamics and function. Curr Opin Cell Biol 15(1): 48-53.

Ghosh, P.K., Anderson, J., Cohen, N., Takeshita, K., Atweh, G.F., and Lebowitz, P. 1993. Expression of the leukemia-associated gene, p18, in normal and malignant tissues; inactivation of expression in a patient with cleaved B cell lymphoma/leukemia. Oncogene 8(10): 2869-2872.

Gonczy, P., Echeverri, C., Oegema, K., Coulson, A., Jones, S.J., Copley, R.R., Duperon, J., Oegema, J., Brehm, M., Cassin, E., Hannak, E., Kirkham, M., Pichler, S., Flohrs, K., Goessen, A., Leidel, S., Alleaume, A.M., Martin, C., Ozlu, N., Bork, P., and Hyman, A.A. 2000. Functional genomic analysis of cell division in C. elegans using RNAi of genes on chromosome III. Nature 408(6810): 331-336.

Gonzalez-Billault, C., Demandt, E., Wandosell, F., Torres, M., Bonaldo, P., Stoykova, A., Chowdhury, K., Gruss, P., Avila, J., and Sanchez, M.P. 2000. Perinatal lethality of microtubule-associated protein 1B-deficient mice expressing alternative isoforms of the protein at low levels. Mol Cell Neurosci 16(4): 408-421.

Goode, B.L., Drubin, D.G., and Barnes, G. 2000. Functional cooperation between the microtubule and actin cytoskeletons. Curr Opin Cell Biol 12(1): 63-71.

Gottlieb, T.A., Ivanov, I.E., Adesnik, M., and Sabatini, D.D. 1993. Actin microfilaments play a critical role in endocytosis at the apical but not the basolateral surface of polarized epithelial cells. J Cell Biol 120(3): 695-710.

Gundersen, G.G., Gomes, E.R., and Wen, Y. 2004. Cortical control of microtubule stability and polarization. Curr Opin Cell Biol 16(1): 106-112.

Hall, A. 1998. Rho GTPases and the actin cytoskeleton. Science 279(5350): 509-514.

Harada, A., Oguchi, K., Okabe, S., Kuno, J., Terada, S., Ohshima, T., Sato-Yoshitake, R., Takei, Y., Noda, T., and Hirokawa, N. 1994. Altered microtubule organization in small-calibre axons of mice lacking tau protein. Nature 369(6480): 488-491.

Heidemann, S.R. 1996. Cytoplasmic mechanisms of axonal and dendritic growth in neurons. Int Rev Cytol 165: 235-296.

Helfand, B.T., Mikami, A., Vallee, R.B., and Goldman, R.D. 2002. A requirement for cytoplasmic dynein and dynactin in intermediate filament network assembly and organization. J Cell Biol 157(5): 795-806.

Hirata, D., Nakano, K., Fukui, M., Takenaka, H., Miyakawa, T., and Mabuchi, I. 1998. Genes that cause aberrant cell morphology by overexpression in fission yeast: a role of a small GTP-binding protein Rho2 in cell morphogenesis. J Cell Sci 111 (Pt 2): 149-159.

Hirokawa, N. 1994. Microtubule organization and dynamics dependent on microtubule-associated proteins. Curr Opin Cell Biol 6(1): 74-81.

Hirokawa, N., Pfister, K.K., Yorifuji, H., Wagner, M.C., Brady, S.T., and Bloom, G.S. 1989. Submolecular domains of bovine brain kinesin identified by electron microscopy and monoclonal antibody decoration. Cell 56(5): 867-878.

Hirotsune, S., Fleck, M.W., Gambello, M.J., Bix, G.J., Chen, A., Clark, G.D., Ledbetter, D.H., McBain, C.J., and Wynshaw-Boris, A. 1998. Graded reduction of Pafah1b1 (Lis1) activity results in neuronal migration defects and early embryonic lethality. Nat Genet 19(4): 333-339.

Holleran, E.A., Tokito, M.K., Karki, S., and Holzbaur, E.L. 1996. Centractin (ARP1) associates with spectrin revealing a potential mechanism to link dynactin to intracellular organelles. J Cell Biol 135(6 Pt 2): 1815-1829.

Hoogenraad, C.C., Koekkoek, B., Akhmanova, A., Krugers, H., Dortland, B., Miedema, M., van Alphen, A., Kistler, W.M., Jaegle, M., Koutsourakis, M., Van Camp, N., Verhoye, M., van der Linden, A., Kaverina, I., Grosveld, F., De Zeeuw, C.I., and Galjart, N. 2002. Targeted mutation of Cyln2 in the Williams syndrome critical region links CLIP-115 haploinsufficiency to neurodevelopmental abnormalities in mice. Nat Genet 32(1): 116-127.

Horwitz, S.B., Shen, H.J., He, L., Dittmar, P., Neef, R., Chen, J., and Schubart, U.K. 1997. The microtubule-destabilizing activity of metablastin (p19) is controlled by phosphorylation. J Biol Chem 272(13): 8129-8132.

Hotani, H. and Horio, T. 1988. Dynamics of microtubules visualized by darkfield microscopy: treadmilling and dynamic instability. Cell Motil Cytoskeleton 10(1-2): 229-236.

Howard, J. and Hyman, A.A. 2003. Dynamics and mechanics of the microtubule plus end. Nature 422(6933): 753-758.

Howell, B., Larsson, N., Gullberg, M., and Cassimeris, L. 1999. Dissociation of the tubulin-sequestering and microtubule catastrophe-promoting activities of oncoprotein 18/stathmin. Mol Biol Cell 10(1): 105-118.

Huff, T., Muller, C.S., Otto, A.M., Netzker, R., and Hannappel, E. 2001. beta-Thymosins, small acidic peptides with multiple functions. Int J Biochem Cell Biol 33(3): 205-220.

Hyman, A.A. and Karsenti, E. 1996. Morphogenetic properties of microtubules and mitotic spindle assembly. Cell 84(3): 401-410.

Inagaki, N., Chihara, K., Arimura, N., Menager, C., Kawano, Y., Matsuo, N., Nishimura, T., Amano, M., and Kaibuchi, K. 2001. CRMP-2 induces axons in cultured hippocampal neurons. Nat Neurosci 4(8): 781-782.

Inoue, Y.H., do Carmo Avides, M., Shiraki, M., Deak, P., Yamaguchi, M., Nishimoto, Y., Matsukage, A., and Glover, D.M. 2000. Orbit, a novel microtubule-associated protein essential for mitosis in Drosophila melanogaster. J Cell Biol 149(1): 153-166.

Joshi, H.C. 1994. Microtubule organizing centers and gamma-tubulin. Curr Opin Cell Biol 6(1): 54-62.

Jourdain, L., Curmi, P., Sobel, A., Pantaloni, D., and Carlier, M.F. 1997. Stathmin: a tubulin-sequestering protein which forms a ternary T2S complex with two tubulin molecules. Biochemistry 36(36): 10817-10821.

Juwana, J.P., Henderikx, P., Mischo, A., Wadle, A., Fadle, N., Gerlach, K., Arends, J.W., Hoogenboom, H., Pfreundschuh, M., and Renner, C. 1999. EB/RP gene family encodes tubulin binding proteins. Int J Cancer 81(2): 275-284.

Karakesisoglou, I., Yang, Y., and Fuchs, E. 2000. An epidermal plakin that integrates actin and microtubule networks at cellular junctions. J Cell Biol 149(1): 195-208.

Kasai, M., Asakura, S., and Oosawa, F. 1962. The cooperative nature of G-F transformation of actin. Biochim Biophys Acta 57: 22-31.

Katsuki, M., Tokuraku, K., Murofushi, H., and Kotani, S. 1999. Functional analysis of microtubule-binding domain of bovine MAP4. Cell Struct Funct 24(5): 337-344.

Kirschner, M. and Mitchison, T. 1986. Beyond self-assembly: from microtubules to morphogenesis. Cell 45(3): 329-342.

Kirschner, M.W. 1980. Implications of treadmilling for the stability and polarity of actin and tubulin polymers in vivo. J Cell Biol 86(1): 330-334.

Kodama, A., Karakesisoglou, I., Wong, E., Vaezi, A., and Fuchs, E. 2003. ACF7: an essential integrator of microtubule dynamics. Cell 115(3): 343-354.

Komarova, Y.A., Akhmanova, A.S., Kojima, S., Galjart, N., and Borisy, G.G. 2002. Cytoplasmic linker proteins promote microtubule rescue in vivo. J Cell Biol 159(4): 589-599.

Korinek, W.S., Copeland, M.J., Chaudhuri, A., and Chant, J. 2000. Molecular linkage underlying microtubule orientation toward cortical sites in yeast. Science 287(5461): 2257-2259.

Kosik, K.S. 1993. The molecular and cellular biology of tau. Brain Pathol 3(1): 39-43.

Kosik, K.S., Joachim, C.L., and Selkoe, D.J. 1986. Microtubule-associated protein tau (tau) is a major antigenic component of paired helical filaments in Alzheimer disease. Proc Natl Acad Sci U S A 83(11): 4044-4048.

Lamaze, C., Fujimoto, L.M., Yin, H.L., and Schmid, S.L. 1997. The actin cytoskeleton is required for receptor-mediated endocytosis in mammalian cells. J Biol Chem 272(33): 20332-20335.

Lane, J. and Allan, V. 1998. Microtubule-based membrane movement. Biochim Biophys Acta 1376(1): 27-55.

Lee, G. and Brandt, R. 1992. Microtubule-bundling studies revisited: is there a role for MAPs? Trends Cell Biol 2(10): 286-289.

Lee, H., Engel, U., Rusch, J., Scherrer, S., Sheard, K., and Van Vactor, D. 2004. The microtubule plus end tracking protein Orbit/MAST/CLASP acts downstream of the tyrosine kinase Abl in mediating axon guidance. Neuron 42(6): 913-926.

Lee, M.K., Tuttle, J.B., Rebhun, L.I., Cleveland, D.W., and Frankfurter, A. 1990. The expression and posttranslational modification of a neuron-specific beta-tubulin isotype during chick embryogenesis. Cell Motil Cytoskeleton 17(2): 118-132.

Lee, W.L., Oberle, J.R., and Cooper, J.A. 2003. The role of the lissencephaly protein Pac1 during nuclear migration in budding yeast. J Cell Biol 160(3): 355-364.

Lemos, C.L., Sampaio, P., Maiato, H., Costa, M., Omel'yanchuk, L.V., Liberal, V., and Sunkel, C.E. 2000. Mast, a conserved microtubule-associated protein required for bipolar mitotic spindle organization. Embo J 19(14): 3668-3682.

Leung, C.L., Sun, D., Zheng, M., Knowles, D.R., and Liem, R.K. 1999. Microtubule actin cross-linking factor (MACF): a hybrid of dystonin and dystrophin that can interact with the actin and microtubule cytoskeletons. J Cell Biol 147(6): 1275-1286.

Liao, G., Nagasaki, T., and Gundersen, G.G. 1995. Low concentrations of nocodazole interfere with fibroblast locomotion without significantly affecting microtubule level: implications for the role of dynamic microtubules in cell locomotion. J Cell Sci 108 (Pt 11): 3473-3483.

Lin, H., de Carvalho, P., Kho, D., Tai, C.Y., Pierre, P., Fink, G.R., and Pellman, D. 2001. Polyploids require Bik1 for kinetochore-microtubule attachment. J Cell Biol 155(7): 1173-1184.

Liu, Q., Xie, F., Siedlak, S.L., Nunomura, A., Honda, K., Moreira, P.I., Zhua, X., Smith, M.A., and Perry, G. 2004. Neurofilament proteins in neurodegenerative diseases. Cell Mol Life Sci 61(24): 3057-3075.

Lopata, M.A. and Cleveland, D.W. 1987. In vivo microtubules are copolymers of available beta-tubulin isotypes: localization of each of six vertebrate beta-tubulin isotypes using polyclonal antibodies elicited by synthetic peptide antigens. J Cell Biol 105(4): 1707-1720.

Luduena, R.F. 1998. Multiple forms of tubulin: different gene products and covalent modifications. Int Rev Cytol 178: 207-275.

Maccioni, R.B. and Cambiazo, V. 1995. Role of microtubule-associated proteins in the control of microtubule assembly. Physiol Rev 75(4): 835-864.

Machesky, L.M., Atkinson, S.J., Ampe, C., Vandekerckhove, J., and Pollard, T.D. 1994. Purification of a cortical complex containing two unconventional actins from Acanthamoeba by affinity chromatography on profilin-agarose. J Cell Biol 127(1): 107-115.

Machesky, L.M., Mullins, R.D., Higgs, H.N., Kaiser, D.A., Blanchoin, L., May, R.C., Hall, M.E., and Pollard, T.D. 1999. Scar, a WASp-related protein, activates nucleation of actin filaments by the Arp2/3 complex. Proc Natl Acad Sci U S A 96(7): 3739-3744.

Maiato, H., Sampaio, P., Lemos, C.L., Findlay, J., Carmena, M., Earnshaw, W.C., and Sunkel, C.E. 2002. MAST/Orbit has a role in microtubule-kinetochore attachment and is essential for chromosome alignment and maintenance of spindle bipolarity. J Cell Biol 157(5): 749-760.

Mandelkow, E. and Mandelkow, E.M. 1995. Microtubules and microtubule-associated proteins. Curr Opin Cell Biol 7(1): 72-81.

Mandelkow, E.M. and Mandelkow, E. 1993. Tau as a marker for Alzheimer's disease. Trends Biochem Sci 18(12): 480-483.

Margolis, R.L. and Wilson, L. 1998. Microtubule treadmilling: what goes around comes around. Bioessays 20(10): 830-836.

Marsden, K.M., Doll, T., Ferralli, J., Botteri, F., and Matus, A. 1996. Transgenic expression of embryonic MAP2 in adult mouse brain: implications for neuronal polarization. J Neurosci 16(10): 3265-3273.

Martin, S.G., McDonald, W.H., Yates, J.R., 3rd, and Chang, F. 2005. Tea4p links microtubule plus ends with the formin for3p in the establishment of cell polarity. Dev Cell 8(4): 479-491.

Mata, J. and Nurse, P. 1997. tea1 and the microtubular cytoskeleton are important for generating global spatial order within the fission yeast cell. Cell 89(6): 939-949.

-. 1998. Discovering the poles in yeast. Trends Cell Biol 8(4): 163-167.

Matus, A. 1991. Microtubule-associated proteins and neuronal morphogenesis. J Cell Sci Suppl 15: 61-67.

Maucuer, A., Doye, V., and Sobel, A. 1990. A single amino acid difference distinguishes the human and the rat sequences of stathmin, a ubiquitous intracellular phosphoprotein associated with cell regulations. FEBS Lett 264(2): 275-278.

Meixner, A., Haverkamp, S., Wassle, H., Fuhrer, S., Thalhammer, J., Kropf, N., Bittner, R.E., Lassmann, H., Wiche, G., and Propst, F. 2000. MAP1B is required for axon guidance and Is involved in the development of the central and peripheral nervous system. J Cell Biol 151(6): 1169-1178.

Melhem, R.F., Zhu, X.X., Hailat, N., Strahler, J.R., and Hanash, S.M. 1991. Characterization of the gene for a proliferation-related phosphoprotein (oncoprotein 18) expressed in high amounts in acute leukemia. J Biol Chem 266(27): 17747-17753.

Mimori-Kiyosue, Y., Grigoriev, I., Lansbergen, G., Sasaki, H., Matsui, C., Severin, F., Galjart, N., Grosveld, F., Vorobjev, I., Tsukita, S., and Akhmanova, A. 2005. CLASP1 and CLASP2 bind to EB1 and regulate microtubule plus-end dynamics at the cell cortex. J Cell Biol 168(1): 141-153.

Mimori-Kiyosue, Y., Shiina, N., and Tsukita, S. 2000. The dynamic behavior of the APC-binding protein EB1 on the distal ends of microtubules. Curr Biol 10(14): 865-868.

Mitchison, J.M. and Nurse, P. 1985. Growth in cell length in the fission yeast Schizosaccharomyces pombe. J Cell Sci 75: 357-376.

Mitchison, T. and Kirschner, M. 1984. Dynamic instability of microtubule growth. Nature 312(5991): 237-242.

Mitchison, T.J. and Salmon, E.D. 1992. Poleward kinetochore fiber movement occurs during both metaphase and anaphase-A in newt lung cell mitosis. J Cell Biol 119(3): 569-582.

Morrison, E.E., Wardleworth, B.N., Askham, J.M., Markham, A.F., and Meredith, D.M. 1998. EB1, a protein which interacts with the APC tumour suppressor, is associated with the microtubule cytoskeleton throughout the cell cycle. Oncogene 17(26): 3471-3477.

Mullins, R.D., Heuser, J.A., and Pollard, T.D. 1998. The interaction of Arp2/3 complex with actin: nucleation, high affinity pointed end capping, and formation of branching networks of filaments. Proc Natl Acad Sci U S A 95(11): 6181-6186.

Munemitsu, S., Souza, B., Muller, O., Albert, I., Rubinfeld, B., and Polakis, P. 1994. The APC gene product associates with microtubules in vivo and promotes their assembly in vitro. Cancer Res 54(14): 3676-3681.

Nakagawa, H., Koyama, K., Murata, Y., Morito, M., Akiyama, T., and Nakamura, Y. 2000. EB3, a novel member of the EB1 family preferentially expressed in the central nervous system, binds to a CNS-specific APC homologue. Oncogene 19(2): 210-216.

Nurse, P. 1994. Fission yeast morphogenesis--posing the problems. Mol Biol Cell 5(6): 613-616.

Olmsted, J.B. 1991. Non-motor microtubule-associated proteins. Curr Opin Cell Biol 3(1): 52-58.

Ozon, S., Byk, T., and Sobel, A. 1998. SCLIP: a novel SCG10-like protein of the stathmin family expressed in the nervous system. J Neurochem 70(6): 2386-2396.

Ozon, S., Maucuer, A., and Sobel, A. 1997. The stathmin family -- molecular and biological characterization of novel mammalian proteins expressed in the nervous system. Eur J Biochem 248(3): 794-806.

Perez, F., Diamantopoulos, G.S., Stalder, R., and Kreis, T.E. 1999. CLIP-170 highlights growing microtubule ends in vivo. Cell 96(4): 517-527.

Pierre, P., Scheel, J., Rickard, J.E., and Kreis, T.E. 1992. CLIP-170 links endocytic vesicles to microtubules. Cell 70(6): 887-900.

Pollard, T.D. 1986. Rate constants for the reactions of ATP- and ADP-actin with the ends of actin filaments. J Cell Biol 103(6 Pt 2): 2747-2754.

Pollard, T.D., Blanchoin, L., and Mullins, R.D. 2000. Molecular mechanisms controlling actin filament dynamics in nonmuscle cells. Annu Rev Biophys Biomol Struct 29: 545-576.

-. 2001. Actin dynamics. J Cell Sci 114(Pt 1): 3-4.

Prahlad, V., Yoon, M., Moir, R.D., Vale, R.D., and Goldman, R.D. 1998. Rapid movements of vimentin on microtubule tracks: kinesin-dependent assembly of intermediate filament networks. J Cell Biol 143(1): 159-170.

Radcliffe, P., Hirata, D., Childs, D., Vardy, L., and Toda, T. 1998. Identification of novel temperature-sensitive lethal alleles in essential beta-tubulin and nonessential alpha 2-tubulin genes as fission yeast polarity mutants. Mol Biol Cell 9(7): 1757-1771.

Reiner, O. 2000. LIS1. let's interact sometimes. (part 1). Neuron 28(3): 633-636.

Renner, C., Pfitzenmeier, J.P., Gerlach, K., Held, G., Ohnesorge, S., Sahin, U., Bauer, S., and Pfreundschuh, M. 1997. RP1, a new member of the adenomatous polyposis coli-binding EB1-like gene family, is differentially expressed in activated T cells. J Immunol 159(3): 1276-1283.

Rickard, J.E. and Kreis, T.E. 1990. Identification of a novel nucleotide-sensitive microtubule-binding protein in HeLa cells. J Cell Biol 110(5): 1623-1633.

Rogers, S.L., Rogers, G.C., Sharp, D.J., and Vale, R.D. 2002. Drosophila EB1 is important for proper assembly, dynamics, and positioning of the mitotic spindle. J Cell Biol 158(5): 873-884.

Sawin, K.E. and Nurse, P. 1998. Regulation of cell polarity by microtubules in fission yeast. J Cell Biol 142(2): 457-471.

Schafer, D.A., Gill, S.R., Cooper, J.A., Heuser, J.E., and Schroer, T.A. 1994. Ultrastructural analysis of the dynactin complex: an actin-related protein is a component of a filament that resembles F-actin. J Cell Biol 126(2): 403-412.

Schiebel, E. 2000. Two new tubulins differ in a split decision. Nat Cell Biol 2(1): E3-4.

Schoenfeld, T.A., McKerracher, L., Obar, R., and Vallee, R.B. 1989. MAP 1A and MAP 1B are structurally related microtubule associated proteins with distinct developmental patterns in the CNS. J Neurosci 9(5): 1712-1730.

Schroer, T.A., Bingham, J.B., and Gill, S.R. 1996. Actin-related protein 1 and cytoplasmic dynein-based motility - what's the connection? Trends Cell Biol 6(6): 212-215.

Schuyler, S.C. and Pellman, D. 2001. Microtubule "plus-end-tracking proteins": The end is just the beginning. Cell 105(4): 421-424.

Schwartz, K., Richards, K., and Botstein, D. 1997. BIM1 encodes a microtubule-binding protein in yeast. Mol Biol Cell 8(12): 2677-2691.

Sheetz, M.P. 1999. Motor and cargo interactions. Eur J Biochem 262(1): 19-25.

Sisson, J.C., Field, C., Ventura, R., Royou, A., and Sullivan, W. 2000. Lava lamp, a novel peripheral golgi protein, is required for Drosophila melanogaster cellularization. J Cell Biol 151(4): 905-918.

Sloboda, R.D. and Rosenbaum, J.L. 1979. Decoration and stabilization of intact, smooth-walled microtubules with microtubule-associated proteins. Biochemistry 18(1): 48-55.

Snaith, H.A. and Sawin, K.E. 2003. Fission yeast mod5p regulates polarized growth through anchoring of tea1p at cell tips. Nature 423(6940): 647-651.

Sobel, A. 1991. Stathmin: a relay phosphoprotein for multiple signal transduction? Trends Biochem Sci 16(8): 301-305.

Stearns, T., Evans, L., and Kirschner, M. 1991. Gamma-tubulin is a highly conserved component of the centrosome. Cell 65(5): 825-836.

Steinert, P.M. 1991. Organization of coiled-coil molecules in native mouse keratin 1/keratin 10 intermediate filaments: evidence for alternating rows of antiparallel in-register and antiparallel staggered molecules. J Struct Biol 107(2): 157-174.

Steinert, P.M. and Liem, R.K. 1990. Intermediate filament dynamics. Cell 60(4): 521-523.

Steinmetz, M.O., Kammerer, R.A., Jahnke, W., Goldie, K.N., Lustig, A., and van Oostrum, J. 2000. Op18/stathmin caps a kinked protofilament-like tubulin tetramer. Embo J 19(4): 572-580.

Su, L.K., Burrell, M., Hill, D.E., Gyuris, J., Brent, R., Wiltshire, R., Trent, J., Vogelstein, B., and Kinzler, K.W. 1995. APC binds to the novel protein EB1. Cancer Res 55(14): 2972-2977.

Tai, C.Y., Dujardin, D.L., Faulkner, N.E., and Vallee, R.B. 2002. Role of dynein, dynactin, and CLIP-170 interactions in LIS1 kinetochore function. J Cell Biol 156(6): 959-968.

Tanaka, E., Ho, T., and Kirschner, M.W. 1995. The role of microtubule dynamics in growth cone motility and axonal growth. J Cell Biol 128(1-2): 139-155.

Teng, J., Takei, Y., Harada, A., Nakata, T., Chen, J., and Hirokawa, N. 2001. Synergistic effects of MAP2 and MAP1B knockout in neuronal migration, dendritic outgrowth, and microtubule organization. J Cell Biol 155(1): 65-76.

Theodorakis, N.G. and Cleveland, D.W. 1992. Physical evidence for cotranslational regulation of beta-tubulin mRNA degradation. Mol Cell Biol 12(2): 791-799.

Tirnauer, J.S., Grego, S., Salmon, E.D., and Mitchison, T.J. 2002. EB1-microtubule interactions in Xenopus egg extracts: role of EB1 in microtubule stabilization and mechanisms of targeting to microtubules. Mol Biol Cell 13(10): 3614-3626.

Tirnauer, J.S., O'Toole, E., Berrueta, L., Bierer, B.E., and Pellman, D. 1999. Yeast Bim1p promotes the G1-specific dynamics of microtubules. J Cell Biol 145(5): 993-1007.

Vale, R.D., Reese, T.S., and Sheetz, M.P. 1985. Identification of a novel force-generating protein, kinesin, involved in microtubule-based motility. Cell 42(1): 39-50.

Vallee, R.B. and Sheetz, M.P. 1996. Targeting of motor proteins. Science 271(5255): 1539-1544.

Verde, F., Mata, J., and Nurse, P. 1995. Fission yeast cell morphogenesis: identification of new genes and analysis of their role during the cell cycle. J Cell Biol 131(6 Pt 1): 1529-1538.

Wade, R.H. and Hyman, A.A. 1997. Microtubule structure and dynamics. Curr Opin Cell Biol 9(1): 12-17.

Walker, R.A., O'Brien, E.T., Pryer, N.K., Soboeiro, M.F., Voter, W.A., Erickson, H.P., and Salmon, E.D. 1988. Dynamic instability of individual microtubules analyzed by video light microscopy: rate constants and transition frequencies. J Cell Biol 107(4): 1437-1448.

Wallar, B.J. and Alberts, A.S. 2003. The formins: active scaffolds that remodel the cytoskeleton. Trends Cell Biol 13(8): 435-446.

Wegner, A. 1976. Head to tail polymerization of actin. J Mol Biol 108(1): 139-150.

Wen, Y., Eng, C.H., Schmoranzer, J., Cabrera-Poch, N., Morris, E.J., Chen, M., Wallar, B.J., Alberts, A.S., and Gundersen, G.G. 2004. EB1 and APC bind to mDia to stabilize microtubules downstream of Rho and promote cell migration. Nat Cell Biol 6(9): 820-830.

Wiche, G., Oberkanins, C., and Himmler, A. 1991. Molecular structure and function of microtubule-associated proteins. Int Rev Cytol 124: 217-273.

Windoffer, R. and Leube, R.E. 1999. Detection of cytokeratin dynamics by time-lapse fluorescence microscopy in living cells. J Cell Sci 112 (Pt 24): 4521-4534.

Xiang, X. 2003. LIS1 at the microtubule plus end and its role in dynein-mediated nuclear migration. J Cell Biol 160(3): 289-290.

Yoon, M., Moir, R.D., Prahlad, V., and Goldman, R.D. 1998. Motile properties of vimentin intermediate filament networks in living cells. J Cell Biol 143(1): 147-157.

Yoshimura, T., Kawano, Y., Arimura, N., Kawabata, S., Kikuchi, A., and Kaibuchi, K. 2005. GSK-3beta regulates phosphorylation of CRMP-2 and neuronal polarity. Cell 120(1): 137-149.

Zheng, Y., Jung, M.K., and Oakley, B.R. 1991. Gamma-tubulin is present in Drosophila melanogaster and Homo sapiens and is associated with the centrosome. Cell 65(5): 817-823.

Zheng, Y., Wong, M.L., Alberts, B., and Mitchison, T. 1995. Nucleation of microtubule assembly by a gamma-tubulin-containing ring complex. Nature 378(6557): 578-583.

Zigmond, S.H. 1998. Actin cytoskeleton: the Arp2/3 complex gets to the point. Curr Biol 8(18): R654-657.

2. Hematopoiesis

General introduction

Blood consists of several differentiated, highly specialized cell types, such as erythrocytes, granulocytes, monocytes, platelets and lymphocytes. These cells perform diverse cellular functions, ranging from oxygen and carbon dioxide transport, to mediation of processes of inflammation and phagocytosis, hemostasis and immunity. Despite the broad range of their structural and functional differences, all blood cell types develop from the same multipotential hematopoietic stem cell in a process called hematopoiesis (Jordan and Lemischka 1990; Keller and Snodgrass 1990; Godin et al. 1995).

The hematopoietic stem cell (HSC) has the capacity of self-renewal. It can divide to give rise either to more self-renewing cells, or to the committed progenitors of different cell lineages that have more limited proliferation and differentiation potential (Figure 1) (Dexter 1990; Metcalf 1999). Finally, committed progenitors will give rise to a more mature set of precursor cells, that constitutes the majority of bone marrow cells and has unique identifiable features by light microscopy. Rapid divisions and subsequent differentiation of precursor cells culminate in the production of mature blood cells (Figure 1).

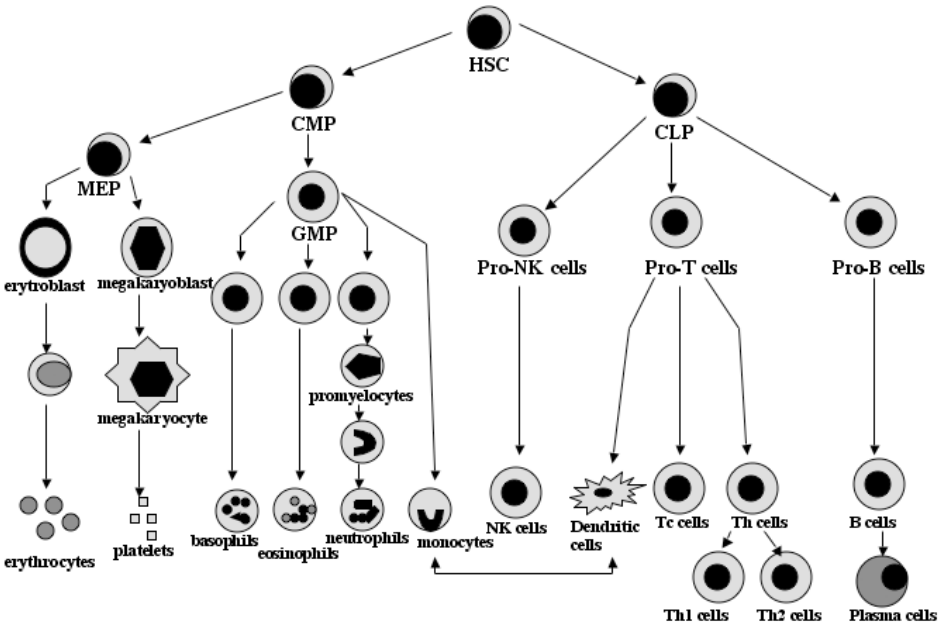

Figure 1. Schematic representation of the process of hematopoiesis. CMPs-common myeloid precursors, CLPs-common lymphoid precursors, MEPs-megakaryotic/erythroid progenitors; GMPs-granulocyte/monocyte common progeniotors
Adapted from Kluger et al., 2004

The first lineage decision step taken by HSCs is to form either common lymphoid precursors (CLPs) or common myeloid precursors (CMPs). CLPs can differentiate into T, B and natural killer cells (Kondo et al. 1997). On the other hand, CMPs give rise to all myeloid lineages. CMPs can give rise to either megakaryocyte/erythroid progenitors (MEPs), which will differentiate into erythrocytes and platelets, or granulocyte/monocyte common progenitors (GMCs), which will then produce granulocytes and monocytes (see Figure 1).

Hematopoiesis begins early during embryogenesis, and continues throughout adult life. The cells of the blood have finite life spans, which vary depending on the cell type. In humans, it can range from several days in the case of blood platelets, up to several months in the case of lymphocytes. After this period cells are degraded and replaced by newly formed cells. The number of cells in the blood is kept more or less in a constant range, thus production of new cells is tightly regulated.

The regulation of the process of hematopoiesis is complex. The fate of the HSC is directed by the coordinated actions of hematopoietic cytokines (via their specific receptors) and lineage-restricted transcription factors. For example, the nuclear proteins GATA-1, Myb, Rbtn2, Tal-1/SCL, Ikaros, E2A, Pax5/BSAP and PU.1 are essential for normal erythroid, lymphoid, or myeloid differentiation (Calabretta and Skorski 1997; Nielsen et al. 2002). Hematopoiesis is governed by a number of cytokines that promote the survival, proliferation and differentiation of hematopoietic stem cells and progenitor cells (Metcalf 1993).

2.1. Megakaryocytes

Megakaryocytes represent only a small fraction (0.02% to 0.05%) of total bone marrow cells. They are easily recognizable due to their large size and lobulated nuclei (Hoffman 1989). Almost a century ago, it was discovered that cytoplasmic pseudopodia of the megakaryocytes had the same staining characteristics as platelets. Therefore it was concluded that platelets were derived from megakaryocytes. Since that time, progress has been made in this field of research. Development of in vitro culture systems and the application of specific immunological markers have facilitated the isolation and purification of megakaryocytes. However, the real break-through was the identification, purification and cloning of thrombopoietin (TPO), the primary regulator of megakaryocyte and platelet production. TPO has allowed the preparation of large numbers of megakaryocytes (Kaushansky 1995) for many of the current and ongoing studies.

Endomitosis

One of the most remarkable features of megakaryocytes is their polyploidy. Mature megakaryocytes contain from 2 (4N) to 32 (64N) times the normal diploid amount of DNA (Kuter et al. 1989). This high level of polyploidy is achieved by a process called endomitosis (Odell and Jackson 1968) (Figure 2). Although the occurrence of endomitosis in maturing megakaryocytes has been known for a long time, the molecular mechanisms that underlie this process are still not completely clarified. Endomitosis is a peculiar process in which DNA replication occurs without corresponding nuclear and cytoplasmic separation, and is

essential for platelet production because the size and the ploidy of megakaryocytes respond to platelet demand (Kaushansky 1999; Ravid et al. 2002). The purpose of polyploidization of megakaryocytes might be to enable megakaryocytes to obtain the large cytoplasmic volume necessary for efficient platelet production.

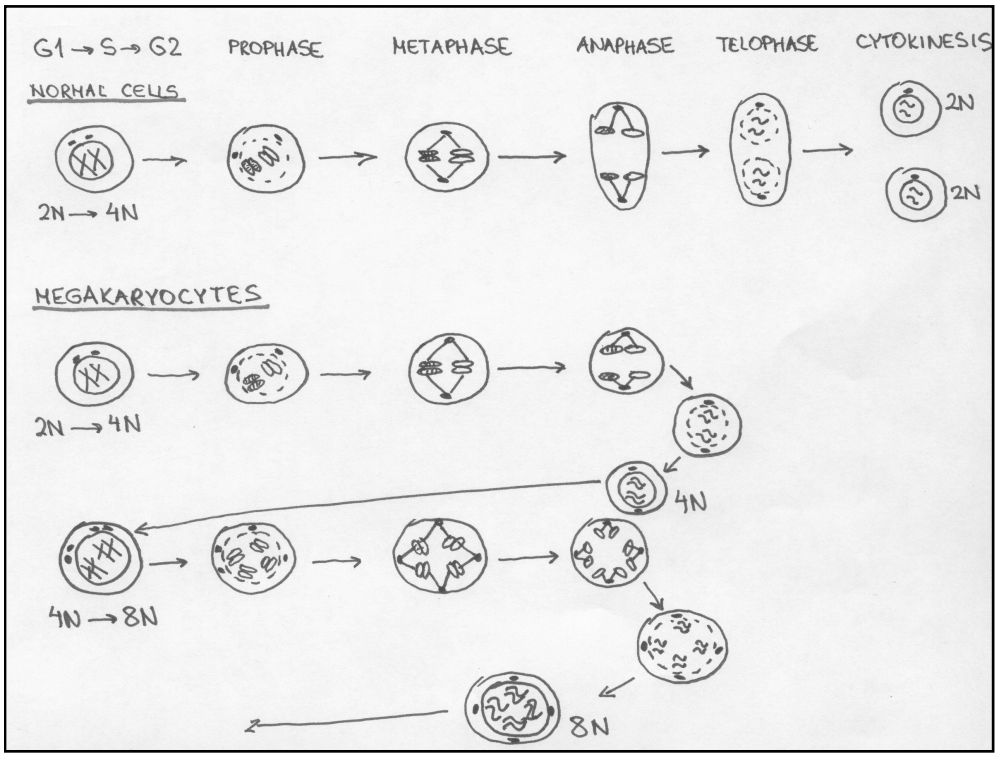

Figure 2. Polyploidization mechanism. During megakaryocyte polyploidization, multiple spindle poles are formed as the polyploid megakaryocyte enters mitosis. Nuclear membrane breaks down during prophase. The sister chromatids are aligned on a multifaced plate, and the centrosomes are symmetrically located on either side of each face of the plate in metaphase. A set of sister chromatides moves into the multiple centrosomes during anaphase A. Spindle poles are located in close proximity during anaphase, so reassembling the nuclear envelope may enclose all the sister chromatids in a single nucleus at anaphase, and than skip telophase and cytokinesis (Nagata et al., 1997).

It is now generally accepted that the endomitotic cell cycle in megakaryocytes consists of a DNA replication S-phase, an M-phase with multiple pole spindles, but aborted anaphase B and cytokinesis, and a Gap-phase that allows re-entry to the next round of S-phase (Ravid et al. 2002) (for schematic overview see Figure 2).

Megakaryocytes must have a unique regulatory mechanism in anaphase, in order to continue to live and cycle. Different cyclins and mitotic checkpoint proteins have been checked for their involvement in the process of megakaryocyte polyploidization. So far, the results are quite controversial, and are probably depending on wheather primary mouse/

human megakaryocytes were used, or different megakaryocyte-like cell lines (Zimmet and Ravid 2000). For example, there are different findings about cyclin B and cdc2 kinase activity. According to some studies their activity is reduced during polyploidization (Zhang et al. 1996; Zhang et al. 1998), while in other studies their level was found to be normal (Vitrat et al. 1998).

There are some suggestions about involvement of the aurora kinase and polo kinase pathways. For instance, AIM-1 kinase (also known as aurora-B), one of the important regulators of mitosis and cytokinesis, has been shown to be down-regulated in the megakaryocytes, and its overexpression prevents ploidy promotion in cell lines treated with phorbol ester (Kawasaki et al. 2001). AIM-1 is properly expressed and localized during early mitosis in polyploidizing bone marrow megakaryocytes, but it is either absent or difused throughout the nucleus at late anaphase of the endomitotic cycle (Zhang et al. 2004).

Cytoplasmic differentiation

Another remarkable feature of the megakaryocyte is manifested in its cytoplasm. Here a system of membranes, known as the demarcation membrane system (DMS), appears to be involved in delineating areas believed to represent platelet territories or platelet fields (Radley and Haller 1982). DMS begins as invaginations of the plasma membrane, and develops into a highly branched interconnected system of channels throughout the cytoplasm, that is in open communication with the extracellular space (Behnke 1968). In the final stage of megakaryocyte maturation, individual platelets are formed by fragmentation of the cytoplasm (Zucker-Franklin and Petursson 1984). Each megakaryocyte can give rise to 1000 to 5000 platelets (Stenberg and Levin 1989) before it is eliminated by bone marrow macrophages (Radley and Haller 1983). Recent studies showed that exvaginations of megakaryocytes, and formation of so-called proplatelet processes (by using DMS surface), give rise to fragmentation to mature platelets (Italiano et al. 1999). Microtubules play a major role in organization of the DMS, and may affect the subdivision of megakaryocyte cytoplasm into platelets (Stenberg et al. 1995). The question concerning where megakaryocyte fragmentation occurs has not yet been answered definitively. There is a data that support the concept that the majority of megakaryocytes exit from the bone marrow compartment intact, and that most platelets are released in the capillary bed of the lungs (Levine et al. 1993). It is also possible that platelets can be released in both the bone marrow and lung capillaries.

In parallel with plasma membrane invaginations, two major types of secretion granules are formed: α-granules and dense granules. The most important and numerous are the α-granules. They appear early during megakaryocyte maturation, at the same time as the DMS (Heijnen et al. 1998). Some proteins in these granules, like αIIbβ3 integrin, von Willebrand factor (vWF), P-selectin, β-thromboglobulin and platelet-derived growth factor (PDGF), arise from de novo megakaryocyte synthesis, some from nonspecific pinocytosis of environmental proteins (albumin and IgG), and some, like fibrinogen, fibronectin and factor V, by cell-surface membrane receptor-mediated uptake from the environment (Harrison et al. 1990; Camire et al. 1998).

Dense granules are compacted in their appearance, and are detected quite late during megakaryocyte maturation (Youssefian et al. 1997). Major constituent of dense granules is serotonin (5-hydroxytryptamine, 5-HT), ADP, ATP and calcium (Rendu and Brohard-Bohn 2001). Both granules greatly contribute to the hemostatic function of platelets.

2.2. Megakaryocytopoiesis

The process of bone marrow megakaryocytopoiesis that leads to platelet formation involves a lineage-specific differentiation of bone marrow stem cells. Through a series of cell types mature megakaryocytes are produced which then fragment into functional platelets (Avraham and Price 1999). The initial stage of megakaryocyte differentiation involves sequential proliferation of CD34+ haematopoietic stem cells into proliferating progenitor megakaryocyte cells (Kaushansky et al. 1994). The second phase involves nuclear polyploidization of precursor cells, increase in cell size, formation of a demarcation membrane system in the cytoplasm, and expression of lineage-specific surface markers (Figure 3) (Gewirtz 1995). The terminal differentiation process involves the shedding of proplatelet fragments, which become functional platelets (Leven 1995).

Long before its identification, it has been predicted that megakaryocytes and erythroid cells share the same common progenitor, because both lineages display many common features. They share number of transcription factors (SCL, GATA-1, GATA-2, NF-E2), cell-surface molecules (Ter119), and cytokine receptors (for IL-3, EPO and TPO). Furthermore, EPO and TPO are somewhat related cytokines (de Sauvage et al. 1994) and they display synergy in stimulating progenitor growth of both lineages (Kieran et al. 1996; Birkmann et al. 1997).

A bipotent erythroid/megakaryocytic cell precursor has been identified and isolated from bone marrow and spleen of mice (Vannucchi et al. 2000). This precursor expresses both erythroid (Ter-119) and megakaryocyte (4A5) markers, and is able to differentiate within 24-48 hours in the presence of EPO or TPO into both erythroid and megakaryocytic cells (Vannucchi et al. 2000).

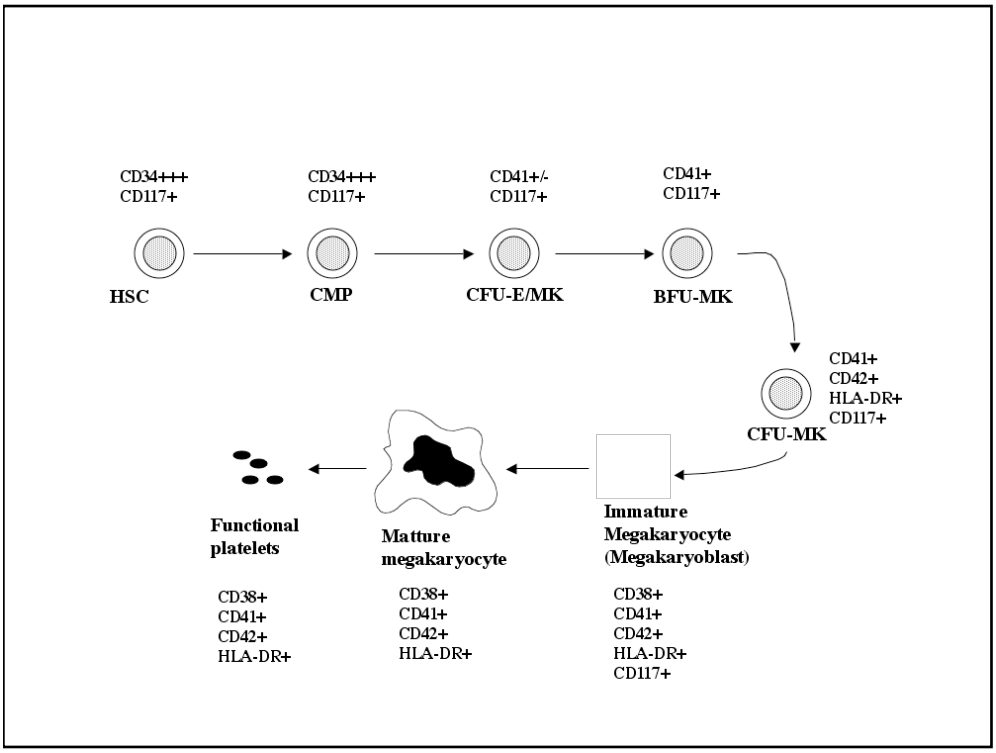

3. Megakaryocytopoiesis. Schematic representation of the process of megakaryocytopoiesis, with antigenic profile of developing megakaryocytes. Note: + to +++ indicate relative levels of antigen expression (see text for details)

The most primitive progenitor cell committed to the MK lineage, that can be assayed from different adult hematopoietic tissues, is the burst forming unit-MK (BFU-MK) (Briddell et al. 1989). The colony forming unit-MK (CFU-MK) is the most differentiated MK progenitor cell capable of forming pure MK colonies in vitro (Figure 3). BFU-MK and CFU-MK can be distinguished by a variety of characteristics. BFU-MK give rise to clusters of megakaryocytes (100 cells or more), is fully developed at 21 days following initiation of culture, they are resistant to 5-fluorouracil (5-FU) treatment, express the hematopoietic stem cell marker CD34, and are HLA-DR-negative (Figure 3) (Briddell et al. 1989; Hoffman 1989). A later progenitor, CFU-MK, gives rise to colonies composed of smaller numbers of megakaryocytes developed after 12 days in culture, they are sensitive to 5-FU, express membrane CD42 (Miyazaki et al. 1992) and HLA-DR antigens (Hoffman 1998). Eventually CFU-MK stops mitosis and enter endomitosis in which polyploid precursors with negligible amount of cytoplasm are formed. After completion of endomitosis, immature megakaryocytes develop a mature cytoplasm, and eventually release platelets.

2.2.1. Cytokine regulation of megakaryocytopoiesis and TPO signaling

Megakaryocytopoiesis is dependent on a variety of specific growth factors and cytokines. Most of these factors are acting in a pleiotropic fashion, such as stem cell factor (SCF), the interleukins IL-3, IL-6, IL-11, and leukemia inhibitory factor (LIF) (Yonemura et al. 1992; Debili et al. 1993; Sitnicka et al. 1996). However, thrombopoietin (TPO) is the major physiological regulator of megakaryocytopoiesis and thrombopoiesis (Kaushansky 1995; Kaushansky 1998). TPO alone can promote normal megakaryocyte development and platelet formation in vitro from CD34+ stem cells (Guerriero et al. 1995).

Thrombopoietin was cloned independently by several groups in 1994 (Bartley et al. 1994; de Sauvage et al. 1994; Lok et al. 1994; Sohma et al. 1994). It binds to its receptor c-Mpl, that is present on platelets, megakaryocytes and a few earlier hematopoietic precursor cells (Kaushansky 1995; Kaushansky 2003). The name Mpl comes from the initial finding that a truncated form of this receptor, v-Mpl, is part of the transforming gene in a murine myeloproliferative leukemia retrovirus (MPLV) (Wendling et al. 1986).

Thrombopoietin is the major regulator of megakaryocyte proliferation, differentiation, and platelet production. It also induces platelet-specific proteins and ultrastructural features, and increases endomitosis (Kaushansky 1995). In vitro, TPO stimulates proliferation of megakaryocyte progenitor cells, and this activity may be increased by the combination of TPO with other cytokines, in particular interleukin-3 (IL-3), stem cell factor (SCF), IL-11, and erythropoietin (EPO) (Broudy et al. 1995).

Besides influencing the megakaryocytic lineage, TPO can act on other hematopoietic lineages, and is a major regulator of primitive multilineage stem cells (Sitnicka et al. 1996; Kaushansky 2002). Administration of TPO to normal or myelosuppressed mice increased progenitor cells of all hematopoietic lineages and speeds up hematopoietic recovery (Kaushansky et al. 1996).

The importance of TPO in megakaryocytopoiesis and thrombopoiesis was confirmed by generation of mice deficient in the Mpl receptor (Gurney et al. 1994; Alexander et al. 1996) or TPO (Carver-Moore et al. 1996). Both TPO and Mpl KO mice are severely thrombocytopenic, with only 10-15% of the normal platelet levels (Gurney et al. 1994; de Sauvage et al. 1996) and both KO mice exhibit markedly reduced megakaryocyte and CFU-MK progenitor numbers, as well as decreased megakaryocyte ploidy (Alexander et al. 1996).

Mice lacking Mpl are deficient not only in committed proliferative precursors for the megakaryocytic lineage, but also erythroid and myeloid lineage cells and HSCs (Kimura et al. 1998). Interestingly, megakaryocytes and platelets that are still formed in these mice are structurally and functionally normal (Bunting et al. 1997).

TPO is produced constitutively and predominantly by the hepatocytes in liver (Qian et al. 1998), with lesser contributions from the kidney, spleen and bone marrow (Sungaran et al. 1997; Wolber et al. 1999). After binding and activating c-Mpl receptors on platelets and megakaryocytes, TPO is internalized and degraded (Fielder et al. 1997; Li et al. 1999).

It has been hypothesized that serum TPO concentration is regulated by circulating platelet numbers (Kojima et al. 1997; Hou et al. 1998). There are several lines of evidence that support this hypothesis. Several studies showed an inverse correlation of TPO plasma levels and platelets counts in patients with marrow failure (Nichol 1998). Furthermore, in the experiments where both thrombocytopenic patients and thrombocytopenic animals were given platelet transfusions, TPO plasma levels rapidly decreased and then increased after the platelet counts dropped again (Kuter and Rosenberg 1995; Shinjo et al. 1998; Folman et al. 2001).

Many of the effects of TPO on cell survival and proliferation have been ascribed to activation of the Jak/STAT and Ras/Raf/MAPK pathways (Drachman et al. 1999). Activation of Jak2 leads to tyrosine phosphorylation of Mpl as well as STAT3 and STAT5, and the phosphorylated STATs dimerize and translocate to the nucleus, where they stimulate transcription (Bacon et al. 1995; Drachman et al. 1995). There are other pathways that are likely to contribute to the cellular response to TPO. One such pathway that may contribute to Mpl signaling is phosphatidylinositol 3-kinase (PI3K) (Geddis et al. 2001). Although the evidence is strong for each of these pathways participating in megakaryocytopoiesis, it is unclear what molecular mechanism is switching a proliferative precursor cell towards endomitotic divisions and production of a polyploid megakaryocyte.

2.2.2. Molecular regulation of megakaryocytopoiesis

In addition to cytokines, different transcription factors are also involved in the regulation of megakaryocyte development. It appears that particularly important transcription factors for the process of megakaryocytopoiesis are GATA-1, FOG-1 and NF-E2 (Orkin 1992; Shivdasani et al. 1995; Shivdasani et al. 1997; Tsang et al. 1997; Tsang et al. 1998).

GATA-1 is expressed in the erythroid, megakaryocyte, eosinophil, and mast cell lineages (Martin et al. 1990). A number of megakaryocyte-specific genes contain GATA binding sequences in their promotor regions, suggesting a role for GATA-1 in megakaryocyte commitment and differentiation (Hashimoto and Ware 1995; Ludlow et al. 1996; Holmes et al. 2002; Eisbacher et al. 2003). The best evidence for the importance of GATA-1 was obtained from GATA-1 mutant mice. GATA-1 homozygous mice in which the gene is selectively lost in the megakaryocytic lineage (Shivdasani et al. 1997), are highly thrombocytopenic with a platelet count of only 15%. These mice display deregulated megakaryocyte maturation and proliferation, increased mean platelet volume, abnormal platelet and megakaryocyte ultrastructure with marked heterogeneity in number and distribution of granules and organelles (Shivdasani et al. 1997; Vyas et al. 1999).

Thrombocytopenia and defective platelets are the result of a unique megakaryocyte differentiation arrest. As a result of that, concomitant expansion of immature megakaryocytes is taking place in the bone marrow. These megakaryocytes are smaller and with reduced ploidy (Shivdasani et al. 1997; Vyas et al. 1999).

Definitive evidence for the requirement of GATA-1 for the process of megakaryocytopoiesis was obtained from studies involving human patients with megakaryocytic disorders. It has been shown that at the base of some of these disorders there is a mutation in the

GATA-1 gene, resulting in the disruption of the interaction between GATA-1 and FOG-1 (Crispino 2005).

The erythroid/megakaryocytic transcription factor NF-E2 is vital for terminal megakaryocyte maturation and platelet release. NF-E2 is a heterodimer that consists of a 45 kDa subunit restricted to hematopoietic cells, and a ubiquitously expressed 18 kDa subunit (Shivdasani et al. 1995). The p45 subunit is co-expressed with GATA-1 in erythrocytes, megakaryocytes and mast cells. Mice lacking the p45 subunit of NF-E2 have a complete and sustained absence of circulating platelets, and die of haemorrhages (Shivdasani et al. 1995). Thus, thrombocytopenia in these mice results from a primary failure of platelet development. Ultrastructural analysis of mutant megakaryocytes has shown a deficit in the number of granules and absence of platelet territories.

2.3. Thrombocytopenias

Thrombocytopenia, or lack of platelets, represents a significant medical problem, since it can lead to hemorrhagic disorder and bleeding. In humans, thrombocytopenia is defined as a platelet count of less than 150 000/µl (150 x 10^9/l).
Different mechanisms can contribute to the development of thrombocytopenia, such as decreased platelet production, increased platelet destruction, or abnormal sequestration of platelets in the spleen. Regardless of the mechanism involved, thrombocytopenias can be categorized into two main categories: acquired and inherited thrombocytopenias.

Frequent causes of acquired thrombocytopenias are drug treatments, such as chemotherapy (MacDonald et al. 1980; Murgo 1987), and bone marrow transplantation (Pettitt and Clark 1994; Schriber and Herzig 1997). Acquired thrombocytopenias can develop also as a consequence of a variety of infections. For instance, HIV infection commonly results in thrombocytopenia through multiple mechanisms (Glatt and Anand 1995; Moses et al. 1998). Other factors that can also cause development of thrombocytopenia are alcohol ingestion (Sullivan et al. 1977) and nutritional deficiencies (Stabler et al. 1990).

Hereditary thrombocytopenias include a variety of disorders such as Congenital Amegakaryocytic Thrombocytopenia (CAMT), Amegakaryocytic Thrombocytopenia with Radio-Ulnar Synostosis (ATRUS), Familial Platelet Syndrome with predisposition to Acute Myelogenous Leukemia (FPS/AML), X-linked thrombocytopenia with dyserythropoiesis, Paris-Trousseau syndrome, Thrombocytopenia with Absent Radii (TAR), Bernard Soulier syndrome and Wiskott-Aldrich Syndrome (WAS).

Inherited thrombocytopenias may be relatively rare disorders, but progress made in uncovering the molecular basis of these disorders has contributed greatly to our present understanding and knowledge about the genesis of megakaryocytes and platelets. Classification of hereditary thrombocytopenias can be made from the inheritance pattern, platelet function, platelet morphology and the presence of additional phenotypic abnormalities. Classification according to these criteria and description of the most important features of the disorders are presented in Table 2.

Disease	Gene	Clinical and laboratory features
Small platelets		
Wiskott-Aldrich Syndrome	WAS (Xp11)	Thrombocytopenia usually severe. Severe immunodeficiency. Defective WAS protein.
X-linked Thrombocytopenia		Thrombocytopenia usually severe. Possible mild immunodeficiency. Defective WAS protein.
Normal-sized platelets		
Congenital Amegakaryocytic Thrombocytopenia (CAMT)	c-mpl (1p34)	Thrombocytopenia usually severe. Hypomegakaryocytic thrombocytopenia evolving into bone marrow aplasia.
Thrombocytopenia with Absent Radii (TAR)	nd	Thrombocytopenia usually severe in the first years of life. Reduced megakaryocytes. Bilateral radial aplasia plus other malformations.
Amegakaryocytic Thrombocytopenia with Radio-Ulnar Synostosis (CTRUS)	HOXA11 (7p15-14)	Thrombocytopenia usually severe. Reduced-absent megakaryocytes. Possible aplastic anemia. Radio-ulnar synostosis, plus other malformations.
Large platelets		
Bernard-Soulier Syndrome (BSS)	GPIbα(17p13) GPIbβ(22q11) GPIX(3q21)	Defective GPIb/IX/V. Homozygous: thrombocytopenia usually severe. Giant platelets and defective ristocetin-induced platelet agglutination.
MYH9-related disease May-Hegglin Anomaly Sebastian Syndrome Fechtner Syndrome Epstein Syndrome	MYH9 (22q12-13)	Giant platelets, neutrophil inclusions, plus hearing loss, plus cataract, plus renal defect.
Gray Platelet Syndrome (GPS)	nd	Pale, ghost-like platelets on blood films due to reduced-absent alfa granules.
Dyserythropoietic anemia with thrombocytopenia	GATA1 (Xp11)	Thrombocytopenia usually severe. Anemia from milde to severe, red cell anisopoikilocytosis, reduced expression of GPIb in a subpopulation of large platelets, dysmegakaryocytopoiesis.

Table 2. Classification of thrombocytopenias. Main features of inherited thrombocytopenias classified according to platelet size.
Adapted from Balduini et al., 2003

As the table already describes, inherited thrombocytopenias are caused by mutations in different genes, on different chromosomes. Symptoms in affected patients can range from mild to severe thrombocytopenic disorders. The example of the inherited thrombocytopenia that can be linked to the cytoskeleton is Wiskott-Aldrich Syndrome (WAS), a rare X-linked immunodeficiency disorder that affects T-lymphocytes and platelets (Burns et al. 2004). At the base of this disorder is the mutation in the Wiskott-Aldrich Syndrome protein (WASp), a multi-domain protein involved in cytoskeletal organization of the hematopoietic

cells. WASp is a key activator of the Arp2/3 complex and activates actin filament assembly in response to upstream intracellular signals (Snapper and Rosen 1999). As outlined in the following chapters, mutations in the gene encoding the cytoskeletal associated protein CLASP2 might underlie forms of human thrombocytopenias that have not yet been characterized at the molecular level.

References

Alexander, W.S., Roberts, A.W., Nicola, N.A., Li, R., and Metcalf, D. 1996. Deficiencies in progenitor cells of multiple hematopoietic lineages and defective megakaryocytopoiesis in mice lacking the thrombopoietic receptor c-Mpl. Blood 87(6): 2162-2170.

Avraham, H. and Price, D.J. 1999. Regulation of megakaryocytopoiesis and platelet production by tyrosine kinases and tyrosine phosphatases. Methods 17(3): 250-264.

Bacon, C.M., Tortolani, P.J., Shimosaka, A., Rees, R.C., Longo, D.L., and O'Shea, J.J. 1995. Thrombopoietin (TPO) induces tyrosine phosphorylation and activation of STAT5 and STAT3. FEBS Lett 370(1-2): 63-68.

Bartley, T.D., Bogenberger, J., Hunt, P., Li, Y.S., Lu, H.S., Martin, F., Chang, M.S., Samal, B., Nichol, J.L., Swift, S., and et al. 1994. Identification and cloning of a megakaryocyte growth and development factor that is a ligand for the cytokine receptor Mpl. Cell 77(7): 1117-1124.

Behnke, O. 1968. An electron microscope study of the megacaryocyte of the rat bone marrow. I. The development of the demarcation membrane system and the platelet surface coat. J Ultrastruct Res 24(5): 412-433.

Birkmann, J., Oez, S., Smetak, M., Kaiser, G., Kappauf, H., and Gallmeier, W.M. 1997. Effects of recombinant human thrombopoietin alone and in combination with erythropoietin and early-acting cytokines on human mobilized purified CD34+ progenitor cells cultured in serum-depleted medium. Stem Cells 15(1): 18-32.

Briddell, R.A., Brandt, J.E., Straneva, J.E., Srour, E.F., and Hoffman, R. 1989. Characterization of the human burst-forming unit-megakaryocyte. Blood 74(1): 145-151.

Broudy, V.C., Lin, N.L., and Kaushansky, K. 1995. Thrombopoietin (c-mpl ligand) acts synergistically with erythropoietin, stem cell factor, and interleukin-11 to enhance murine megakaryocyte colony growth and increases megakaryocyte ploidy in vitro. Blood 85(7): 1719-1726.

Bunting, S., Widmer, R., Lipari, T., Rangell, L., Steinmetz, H., Carver-Moore, K., Moore, M.W., Keller, G.A., and de Sauvage, F.J. 1997. Normal platelets and megakaryocytes are produced in vivo in the absence of thrombopoietin. Blood 90(9): 3423-3429.

Burns, S., Cory, G.O., Vainchenker, W., and Thrasher, A.J. 2004. Mechanisms of WASp-mediated hematologic and immunologic disease. Blood 104(12): 3454-3462.

Calabretta, B. and Skorski, T. 1997. Gene regulatory mechanisms operative on hematopoietic cells: proliferation, differentiation, and neoplasia. Crit Rev Eukaryot Gene Expr 7(1-2): 117-124.

Camire, R.M., Pollak, E.S., Kaushansky, K., and Tracy, P.B. 1998. Secretable human platelet-derived factor V originates from the plasma pool. Blood 92(9): 3035-3041.

Carver-Moore, K., Broxmeyer, H.E., Luoh, S.M., Cooper, S., Peng, J., Burstein, S.A., Moore, M.W., and de Sauvage, F.J. 1996. Low levels of erythroid and myeloid progenitors in thrombopoietin-and c-mpl-deficient mice. Blood 88(3): 803-808.

Crispino, J.D. 2005. GATA1 in normal and malignant hematopoiesis. Semin Cell Dev Biol 16(1): 137-147.

de Sauvage, F.J., Carver-Moore, K., Luoh, S.M., Ryan, A., Dowd, M., Eaton, D.L., and Moore, M.W. 1996. Physiological regulation of early and late stages of megakaryocytopoiesis by thrombopoietin. J Exp Med 183(2): 651-656.

de Sauvage, F.J., Hass, P.E., Spencer, S.D., Malloy, B.E., Gurney, A.L., Spencer, S.A., Darbonne, W.C., Henzel, W.J., Wong, S.C., Kuang, W.J., and et al. 1994. Stimulation of megakaryocytopoiesis and thrombopoiesis by the c-Mpl ligand. Nature 369(6481): 533-538.

Debili, N., Masse, J.M., Katz, A., Guichard, J., Breton-Gorius, J., and Vainchenker, W. 1993. Effects of the recombinant hematopoietic growth factors interleukin-3, interleukin-6, stem cell factor, and leukemia inhibitory factor on the megakaryocytic differentiation of CD34+ cells. Blood 82(1): 84-95.

Dexter, T.M. 1990. Introduction to the haemopoietic system. Cancer Surv 9(1): 1-5.

Drachman, J.G., Griffin, J.D., and Kaushansky, K. 1995. The c-Mpl ligand (thrombopoietin) stimulates tyrosine phosphorylation of Jak2, Shc, and c-Mpl. J Biol Chem 270(10): 4979-4982.

Drachman, J.G., Rojnuckarin, P., and Kaushansky, K. 1999. Thrombopoietin signal transduction: studies from cell lines and primary cells. Methods 17(3): 238-249.

Eisbacher, M., Holmes, M.L., Newton, A., Hogg, P.J., Khachigian, L.M., Crossley, M., and Chong, B.H. 2003. Protein-protein interaction between Fli-1 and GATA-1 mediates synergistic expression of megakaryocyte-specific genes through cooperative DNA binding. Mol Cell Biol 23(10): 3427-3441.

Fielder, P.J., Hass, P., Nagel, M., Stefanich, E., Widmer, R., Bennett, G.L., Keller, G.A., de Sauvage, F.J., and Eaton, D. 1997. Human platelets as a model for the binding and degradation of thrombopoietin. Blood 89(8): 2782-2788.

Folman, C.C., de Jong, S.M., de Haas, M., and von dem Borne, A.E. 2001. Analysis of the kinetics of TPO uptake during platelet transfusion. Transfusion 41(4): 517-521.

Geddis, A.E., Fox, N.E., and Kaushansky, K. 2001. Phosphatidylinositol 3-kinase is necessary but not sufficient for thrombopoietin-induced proliferation in engineered Mpl-bearing cell lines as well as in primary megakaryocytic progenitors. J Biol Chem 276(37): 34473-34479.

Gewirtz, A.M. 1995. Megakaryocytopoiesis: the state of the art. Thromb Haemost 74(1): 204-209.

Glatt, A.E. and Anand, A. 1995. Thrombocytopenia in patients infected with human immunodeficiency virus: treatment update. Clin Infect Dis 21(2): 415-423.

Godin, I., Dieterlen-Lievre, F., and Cumano, A. 1995. Emergence of multipotent hemopoietic cells in the yolk sac and paraaortic splanchnopleura in mouse embryos, beginning at 8.5 days postcoitus. Proc Natl Acad Sci U S A 92(3): 773-777.

Guerriero, R., Testa, U., Gabbianelli, M., Mattia, G., Montesoro, E., Macioce, G., Pace, A., Ziegler, B., Hassan, H.J., and Peschle, C. 1995. Unilineage megakaryocytic proliferation and differentiation of purified hematopoietic progenitors in serum-free liquid culture. Blood 86(10): 3725-3736.

Gurney, A.L., Carver-Moore, K., de Sauvage, F.J., and Moore, M.W. 1994. Thrombocytopenia in c-mpl-deficient mice. Science 265(5177): 1445-1447.

Harrison, P., Savidge, G.F., and Cramer, E.M. 1990. The origin and physiological relevance of alpha-granule adhesive proteins. Br J Haematol 74(2): 125-130.

Hashimoto, Y. and Ware, J. 1995. Identification of essential GATA and Ets binding motifs within the promoter of the platelet glycoprotein Ib alpha gene. J Biol Chem 270(41): 24532-24539.

Heijnen, H.F., Debili, N., Vainchencker, W., Breton-Gorius, J., Geuze, H.J., and Sixma, J.J. 1998. Multivesicular bodies are an intermediate stage in the formation of platelet alpha-granules. Blood 91(7): 2313-2325.

Hoffman, R. 1989. Regulation of megakaryocytopoiesis. Blood 74(4): 1196-1212.

Holmes, M.L., Bartle, N., Eisbacher, M., and Chong, B.H. 2002. Cloning and analysis of the thrombopoietin-induced megakaryocyte-specific glycoprotein VI promoter and its regulation by GATA-1, Fli-1, and Sp1. J Biol Chem 277(50): 48333-48341.

Hou, M., Andersson, P.O., Stockelberg, D., Mellqvist, U.H., Ridell, B., and Wadenvik, H. 1998. Plasma thrombopoietin levels in thrombocytopenic states: implication for a regulatory role of bone marrow megakaryocytes. Br J Haematol 101(3): 420-424.

Italiano, J.E., Jr., Lecine, P., Shivdasani, R.A., and Hartwig, J.H. 1999. Blood platelets are assembled principally at the ends of proplatelet processes produced by differentiated megakaryocytes. J Cell Biol 147(6): 1299-1312.

Jordan, C.T. and Lemischka, I.R. 1990. Clonal and systemic analysis of long-term hematopoiesis in the mouse. Genes Dev 4(2): 220-232.

Kaushansky, K. 1995. Thrombopoietin: the primary regulator of platelet production. Blood 86(2): 419-431.

-. 1998. Thrombopoietin. N Engl J Med 339(11): 746-754.

-. 1999. The enigmatic megakaryocyte gradually reveals its secrets. Bioessays 21(4): 353-360.

-. 2002. Mpl and the hematopoietic stem cell. Leukemia 16(4): 738-739.

-. 2003. Thrombopoietin: a tool for understanding thrombopoiesis. J Thromb Haemost 1(7): 1587-1592.

Kaushansky, K., Lin, N., Grossmann, A., Humes, J., Sprugel, K.H., and Broudy, V.C. 1996. Thrombopoietin expands erythroid, granulocyte-macrophage, and megakaryocytic progenitor cells in normal and myelosuppressed mice. Exp Hematol 24(2): 265-269.

Kaushansky, K., Lok, S., Holly, R.D., Broudy, V.C., Lin, N., Bailey, M.C., Forstrom, J.W., Buddle, M.M., Oort, P.J., Hagen, F.S., and et al. 1994. Promotion of megakaryocyte progenitor expansion and differentiation by the c-Mpl ligand thrombopoietin. Nature 369(6481): 568-571.

Kawasaki, A., Matsumura, I., Miyagawa, J., Ezoe, S., Tanaka, H., Terada, Y., Tatsuka, M., Machii, T., Miyazaki, H., Furukawa, Y., and Kanakura, Y. 2001. Downregulation of an AIM-1 kinase couples with megakaryocytic polyploidization of human hematopoietic cells. J Cell Biol 152(2): 275-287.

Keller, G. and Snodgrass, R. 1990. Life span of multipotential hematopoietic stem cells in vivo. J Exp Med 171(5): 1407-1418.

Kieran, M.W., Perkins, A.C., Orkin, S.H., and Zon, L.I. 1996. Thrombopoietin rescues in vitro erythroid colony formation from mouse embryos lacking the erythropoietin receptor. Proc Natl Acad Sci U S A 93(17): 9126-9131.

Kimura, S., Roberts, A.W., Metcalf, D., and Alexander, W.S. 1998. Hematopoietic stem cell deficiencies in mice lacking c-Mpl, the receptor for thrombopoietin. Proc Natl Acad Sci U S A 95(3): 1195-1200.

Kojima, S., Matsuyama, T., Kodera, Y., Tahara, T., and Kato, T. 1997. Measurement of endogenous plasma thrombopoietin in patients with acquired aplastic anaemia by a sensitive enzyme-linked immunosorbent assay. Br J Haematol 97(3): 538-543.

Kondo, M., Weissman, I.L., and Akashi, K. 1997. Identification of clonogenic common lymphoid progenitors in mouse bone marrow. Cell 91(5): 661-672.

Kuter, D.J., Greenberg, S.M., and Rosenberg, R.D. 1989. Analysis of megakaryocyte ploidy in rat bone marrow cultures. Blood 74(6): 1952-1962.

Kuter, D.J. and Rosenberg, R.D. 1995. The reciprocal relationship of thrombopoietin (c-Mpl ligand) to changes in the platelet mass during busulfan-induced thrombocytopenia in the rabbit. Blood 85(10): 2720-2730.

Leven, R.M. 1995. Differential regulation of integrin-mediated proplatelet formation and megakaryocyte spreading. J Cell Physiol 163(3): 597-607.

Levine, R.F., Eldor, A., Shoff, P.K., Kirwin, S., Tenza, D., and Cramer, E.M. 1993. Circulating megakaryocytes: delivery of large numbers of intact, mature megakaryocytes to the lungs. Eur J Haematol 51(4): 233-246.

Li, J., Xia, Y., and Kuter, D.J. 1999. Interaction of thrombopoietin with the platelet c-mpl receptor in plasma: binding, internalization, stability and pharmacokinetics. Br J Haematol 106(2): 345-356.

Lok, S., Kaushansky, K., Holly, R.D., Kuijper, J.L., Lofton-Day, C.E., Oort, P.J., Grant, F.J., Heipel, M.D., Burkhead, S.K., Kramer, J.M., and et al. 1994. Cloning and expression of murine thrombopoietin cDNA and stimulation of platelet production in vivo. Nature 369(6481): 565-568.

Ludlow, L.B., Schick, B.P., Budarf, M.L., Driscoll, D.A., Zackai, E.H., Cohen, A., and Konkle, B.A. 1996. Identification of a mutation in a GATA binding site of the platelet glycoprotein Ibbeta promoter resulting in the Bernard-Soulier syndrome. J Biol Chem 271(36): 22076-22080.

MacDonald, J.S., Schein, P.S., Woolley, P.V., Smythe, T., Ueno, W., Hoth, D., Smith, F., Boiron, M., Gisselbrecht, C., Brunet, R., and Lagarde, C. 1980. 5-Fluorouracil, doxorubicin, and mitomycin (FAM) combination chemotherapy for advanced gastric cancer. Ann Intern Med 93(4): 533-536.

Martin, D.I., Zon, L.I., Mutter, G., and Orkin, S.H. 1990. Expression of an erythroid transcription factor in megakaryocytic and mast cell lineages. Nature 344(6265): 444-447.

Metcalf, D. 1993. Hematopoietic regulators: redundancy or subtlety? Blood 82(12): 3515-3523.

-. 1999. Stem cells, pre-progenitor cells and lineage-committed cells: are our dogmas correct? Ann N Y Acad Sci 872: 289-303; discussion 303-284.

Miyazaki, H., Inoue, H., Yanagida, M., Horie, K., Mikayama, T., Ohashi, H., Nishikawa, M., Suzuki, T., and Sudo, T. 1992. Purification of rat megakaryocyte colony-forming cells using a monoclonal antibody against rat platelet glycoprotein IIb/IIIa. Exp Hematol 20(7): 855-861.

Moses, A., Nelson, J., and Bagby, G.C., Jr. 1998. The influence of human immunodeficiency virus-1 on hematopoiesis. Blood 91(5): 1479-1495.

Murgo, A.J. 1987. Thrombotic microangiopathy in the cancer patient including those induced by chemotherapeutic agents. Semin Hematol 24(3): 161-177.

Nichol, J.L. 1998. Thrombopoietin levels after chemotherapy and in naturally occurring human diseases. Curr Opin Hematol 5(3): 203-208.

Nielsen, J.S., Doyonnas, R., and McNagny, K.M. 2002. Avian models to study the transcriptional control of hematopoietic lineage commitment and to identify lineage-specific genes. Cells Tissues Organs 171(1): 44-63.

Odell, T.T., Jr. and Jackson, C.W. 1968. Polyploidy and maturation of rat megakaryocytes. Blood 32(1): 102-110.

Orkin, S.H. 1992. GATA-binding transcription factors in hematopoietic cells. Blood 80(3): 575-581.
Pettitt, A.R. and Clark, R.E. 1994. Thrombotic microangiopathy following bone marrow transplantation. Bone Marrow Transplant 14(4): 495-504.
Qian, S., Fu, F., Li, W., Chen, Q., and de Sauvage, F.J. 1998. Primary role of the liver in thrombopoietin production shown by tissue-specific knockout. Blood 92(6): 2189-2191.
Radley, J.M. and Haller, C.J. 1982. The demarcation membrane system of the megakaryocyte: a misnomer? Blood 60(1): 213-219.
-. 1983. Fate of senescent megakaryocytes in the bone marrow. Br J Haematol 53(2): 277-287.
Ravid, K., Lu, J., Zimmet, J.M., and Jones, M.R. 2002. Roads to polyploidy: the megakaryocyte example. J Cell Physiol 190(1): 7-20.
Rendu, F. and Brohard-Bohn, B. 2001. The platelet release reaction: granules' constituents, secretion and functions. Platelets 12(5): 261-273.
Schriber, J.R. and Herzig, G.P. 1997. Transplantation-associated thrombotic thrombocytopenic purpura and hemolytic uremic syndrome. Semin Hematol 34(2): 126-133.
Shinjo, K., Takeshita, A., Nakamura, S., Naitoh, K., Yanagi, M., Tobita, T., Ohnishi, K., and Ohno, R. 1998. Serum thrombopoietin levels in patients correlate inversely with platelet counts during chemotherapy-induced thrombocytopenia. Leukemia 12(3): 295-300.
Shivdasani, R.A., Fujiwara, Y., McDevitt, M.A., and Orkin, S.H. 1997. A lineage-selective knockout establishes the critical role of transcription factor GATA-1 in megakaryocyte growth and platelet development. Embo J 16(13): 3965-3973.
Shivdasani, R.A., Rosenblatt, M.F., Zucker-Franklin, D., Jackson, C.W., Hunt, P., Saris, C.J., and Orkin, S.H. 1995. Transcription factor NF-E2 is required for platelet formation independent of the actions of thrombopoietin/MGDF in megakaryocyte development. Cell 81(5): 695-704.
Sitnicka, E., Lin, N., Priestley, G.V., Fox, N., Broudy, V.C., Wolf, N.S., and Kaushansky, K. 1996. The effect of thrombopoietin on the proliferation and differentiation of murine hematopoietic stem cells. Blood 87(12): 4998-5005.
Snapper, S.B. and Rosen, F.S. 1999. The Wiskott-Aldrich syndrome protein (WASP): roles in signaling and cytoskeletal organization. Annu Rev Immunol 17: 905-929.
Sohma, Y., Akahori, H., Seki, N., Hori, T., Ogami, K., Kato, T., Shimada, Y., Kawamura, K., and Miyazaki, H. 1994. Molecular cloning and chromosomal localization of the human thrombopoietin gene. FEBS Lett 353(1): 57-61.
Stabler, S.P., Allen, R.H., Savage, D.G., and Lindenbaum, J. 1990. Clinical spectrum and diagnosis of cobalamin deficiency. Blood 76(5): 871-881.
Stenberg, P.E. and Levin, J. 1989. Mechanisms of platelet production. Blood Cells 15(1): 23-47.
Stenberg, P.E., McDonald, T.P., and Jackson, C.W. 1995. Disruption of microtubules in vivo by vincristine induces large membrane complexes and other cytoplasmic abnormalities in megakaryocytes and platelets of normal rats like those in human and Wistar Furth rat hereditary macrothrombocytopenias. J Cell Physiol 162(1): 86-102.
Sullivan, L.W., Adams, W.H., and Liu, Y.K. 1977. Induction of thrombocytopenia by thrombopheresis in man: patterns of recovery in normal subjects during ethanol ingestion and abstinence. Blood 49(2): 197-207.
Sungaran, R., Markovic, B., and Chong, B.H. 1997. Localization and regulation of thrombopoietin mRNa expression in human kidney, liver, bone marrow, and spleen using in situ hybridization. Blood 89(1): 101-107.
Tsang, A.P., Fujiwara, Y., Hom, D.B., and Orkin, S.H. 1998. Failure of megakaryopoiesis and arrested erythropoiesis in mice lacking the GATA-1 transcriptional cofactor FOG. Genes Dev 12(8): 1176-1188.
Tsang, A.P., Visvader, J.E., Turner, C.A., Fujiwara, Y., Yu, C., Weiss, M.J., Crossley, M., and Orkin, S.H. 1997. FOG, a multitype zinc finger protein, acts as a cofactor for transcription factor GATA-1 in erythroid and megakaryocytic differentiation. Cell 90(1): 109-119.
Vannucchi, A.M., Paoletti, F., Linari, S., Cellai, C., Caporale, R., Ferrini, P.R., Sanchez, M., Migliaccio, G., and Migliaccio, A.R. 2000. Identification and characterization of a bipotent (erythroid and megakaryocytic) cell precursor from the spleen of phenylhydrazine-treated mice. Blood 95(8): 2559-2568.
Vitrat, N., Cohen-Solal, K., Pique, C., Le Couedic, J.P., Norol, F., Larsen, A.K., Katz, A., Vainchenker, W., and Debili, N. 1998. Endomitosis of human megakaryocytes are due to abortive mitosis. Blood 91(10): 3711-3723.
Vyas, P., Ault, K., Jackson, C.W., Orkin, S.H., and Shivdasani, R.A. 1999. Consequences of GATA-1 deficiency in megakaryocytes and platelets. Blood 93(9): 2867-2875.

Wendling, F., Varlet, P., Charon, M., and Tambourin, P. 1986. MPLV: a retrovirus complex inducing an acute myeloproliferative leukemic disorder in adult mice. Virology 149(2): 242-246.

Wolber, E.M., Dame, C., Fahnenstich, H., Hofmann, D., Bartmann, P., Jelkmann, W., and Fandrey, J. 1999. Expression of the thrombopoietin gene in human fetal and neonatal tissues. Blood 94(1): 97-105.

Yonemura, Y., Kawakita, M., Masuda, T., Fujimoto, K., Kato, K., and Takatsuki, K. 1992. Synergistic effects of interleukin 3 and interleukin 11 on murine megakaryopoiesis in serum-free culture. Exp Hematol 20(8): 1011-1016.

Youssefian, T., Masse, J.M., Rendu, F., Guichard, J., and Cramer, E.M. 1997. Platelet and megakaryocyte dense granules contain glycoproteins Ib and IIb-IIIa. Blood 89(11): 4047-4057.

Zhang, Y., Nagata, Y., Yu, G., Nguyen, H.G., Jones, M.R., Toselli, P., Jackson, C.W., Tatsuka, M., Todokoro, K., and Ravid, K. 2004. Aberrant quantity and localization of Aurora-B/AIM-1 and survivin during megakaryocyte polyploidization and the consequences of Aurora-B/AIM-1-deregulated expression. Blood 103(10): 3717-3726.

Zhang, Y., Wang, Z., Liu, D.X., Pagano, M., and Ravid, K. 1998. Ubiquitin-dependent degradation of cyclin B is accelerated in polyploid megakaryocytes. J Biol Chem 273(3): 1387-1392.

Zhang, Y., Wang, Z., and Ravid, K. 1996. The cell cycle in polyploid megakaryocytes is associated with reduced activity of cyclin B1-dependent cdc2 kinase. J Biol Chem 271(8): 4266-4272.

Zimmet, J. and Ravid, K. 2000. Polyploidy: occurrence in nature, mechanisms, and significance for the megakaryocyte-platelet system. Exp Hematol 28(1): 3-16.

Zucker-Franklin, D. and Petursson, S. 1984. Thrombocytopoiesis--analysis by membrane tracer and freeze-fracture studies on fresh human and cultured mouse megakaryocytes. J Cell Biol 99(2): 390-402.

Chapter 2

CLASPS are CLIP-115 and -170 associating proteins involved in the regional regulation of microtubule dynamics in motile fibroblasts

Cell 2001 104(6):923-35

CLASPs Are CLIP-115 and -170 Associating Proteins Involved in the Regional Regulation of Microtubule Dynamics in Motile Fibroblasts

Anna Akhmanova,*‖ Casper C. Hoogenraad,*†‖ Ksenija Drabek,* Tatiana Stepanova,* Bjorn Dortland,* Ton Verkerk,* Wim Vermeulen,* Boudewijn M. Burgering,‡ Chris I. De Zeeuw,† Frank Grosveld,* and Niels Galjart*§

*MGC Department of Cell Biology and Genetics and
†MGC Department of Anatomy
Erasmus University
P.O. Box 1738
3000 DR Rotterdam
The Netherlands
‡Laboratory for Physiological Chemistry and Centre for Biomedical Genetics
University of Utrecht
Universiteitsweg 100
3584 CG Utrecht
The Netherlands

Summary

CLIP-170 and CLIP-115 are cytoplasmic linker proteins that associate specifically with the ends of growing microtubules and may act as anti-catastrophe factors. Here, we have isolated two *CL*IP-*a*ssociated *p*roteins (CLASPs), which are homologous to the *Drosophila* Orbit/Mast microtubule-associated protein. CLASPs bind CLIPs and microtubules, colocalize with the CLIPs at microtubule distal ends, and have microtubule-stabilizing effects in transfected cells. After serum induction, CLASPs relocalize to distal segments of microtubules at the leading edge of motile fibroblasts. We provide evidence that this asymmetric CLASP distribution is mediated by PI3-kinase and GSK-3β. Antibody injections suggest that CLASP2 is required for the orientation of stabilized microtubules toward the leading edge. We propose that CLASPs are involved in the local regulation of microtubule dynamics in response to positional cues.

Introduction

Microtubules (MTs) constitute an important part of the cellular cytoskeleton. They are essential for chromosome segregation in mitosis and for organelle movement and positioning in interphase cells. MTs are inherently polarized structures, with a fast-growing end (the plus end) and a slow growing end (the minus end). In fibroblasts, the majority of MTs is attached with the minus end to the MT organizing center (MTOC), while the plus ends are directed to the cell periphery. Both in vitro and in vivo, the MT plus ends alternate between phases of elongation and shrinkage. This phenomenon is called dynamic instability (reviewed by Desai and Mitchison, 1997).

MT dynamics in living cells is regulated by a variety of protein factors. These include MT destabilizing proteins, such as stathmin/Op18 and XKCM1, as well as factors that promote MT elongation, such as XMAP215/TOG1 (for review, see Wittmann et al., 2001). Some of the proteins involved in regulating MT growth, depolymerization, and/or MT interaction with the cellular cortex are localized specifically at the MT plus end. For example, the yeast protein BIM1p, which increases MT dynamicity, localizes to dots at the distal ends of cytoplasmic MTs (Tirnauer et al., 1999), as does its mammalian homolog EB1 (Mimori-Kiyosue et al., 2000). Another protein demonstrated to be present at the plus ends is mammalian CLIP-170. Using a fusion of CLIP-170 to the green fluorescent protein (GFP), it was shown that CLIP-170 moves together with the tips of growing MTs in living cells (Perez et al., 1999). However, CLIP-170 was previously also implicated in the attachment of endosomes to MTs (Pierre et al., 1992) and, in addition, it was found at the kinetochores of the prometaphase chromosomes (Dujardin et al., 1998). In fibroblasts, CLIP-170 colocalizes with cytoplasmic dynein and dynactin at the distal ends of MTs (Valetti et al., 1999; Vaughan et al., 1999). It was suggested, therefore, that these regions represent the cargo-loading sites for the minus end directed organelle movement by dynein, and that CLIP-170 might be involved in this process. However, no association of CLIP-170 with dynein and dynactin has been demonstrated. To resolve CLIP-170 function at MT plus ends, it is essential to define with what proteins it interacts directly.

The closest homolog of CLIP-170 in mammals is CLIP-115 (De Zeeuw et al., 1997). Both CLIP-170 and CLIP-115 contain two MT binding (MTB) domains at their N termini, surrounded by positively charged, serine rich regions. One such MTB motif, together with one serine rich region, is sufficient for MT binding (Hoogenraad et al., 2000). The middle part of both proteins contains a long region of heptad repeats, which form a coiled-coil and mediate homodimerization of these proteins (Scheel et al., 1999; Hoogenraad et al., 2000). While CLIP-170 is expressed in many different cell lines and tissues, CLIP-115 appears to be predominantly present in neurons, where it is localized in dendrites (De Zeeuw et al., 1997). When expressed in fibroblasts at low levels, CLIP-115 localizes at the MT plus ends, similar to CLIP-170 (Hoogenraad et al., 2000). This suggests that in neurons, the function of CLIP-115 might be related to some aspect of MT dynamics.

Given the common properties of the two CLIPs, we hypothesized that they might have overlapping functions and, therefore, common protein partners. We searched for such partners (*CL*IP-*a*ssociating *p*roteins, or CLASPs) with the aid of a yeast two-hybrid system, using a conserved part of the coiled-coil region of CLIP-115 as bait. We identified two mammalian proteins, CLASP1 and CLASP2, with similarity to regulators of MT dynamics. CLASPs bind both to CLIPs and to MTs and

§To whom correspondence should be addressed (e-mail: galjart@ch1.fgg.eur.nl).
‖These authors contributed equally to the results described in this paper.

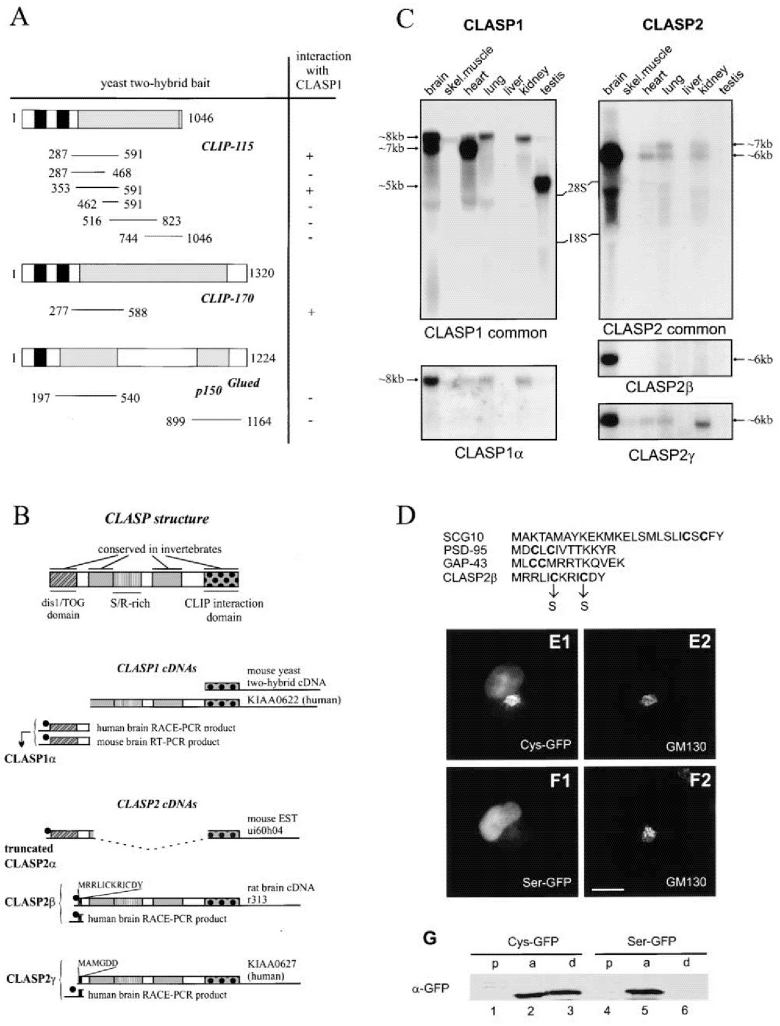

Figure 1. CLASP Isolation and Structure

(A) The region spanning amino acids 287–591 of CLIP-115 was used in a yeast two-hybrid screen of an E14.5 day mouse cDNA library. Mouse *CLASP1* cDNA, isolated in this screen, was next tested in yeast two-hybrid assays with protein fragments from CLIP-115, CLIP-170, and p150^{Glued}. The domain structure of these three proteins, with MT binding motifs (black bars) and coiled-coil regions (gray bars), is represented. The amino acids covered by each fragment are indicated; their interaction with mCLASP1 is shown to the right (+: positive interaction, −: no interaction).

(B) Schematic representation of CLASP structure and the CLASP-encoding cDNAs. Protein-coding regions are represented by bars and untranslated regions by lines. The top bar represents the largest CLASP ORF, encoded by CLASP1/2α cDNAs. Above the CLASP2β and -γ cDNAs, the sequence of the alternatively spliced, N-terminal domain is shown. A vertical line with a filled circle on top indicates a stop codon upstream and in-frame with the translational start codon, suggesting the presence of a full-length ORF. The stippled line in the mouse EST clone ui60h04 indicates the position of a deletion, which is probably an artifact, because it could not be confirmed by Northern blotting or RT-PCR.

(C) *CLASP* expression profile. Northern blots with total RNA from different mouse tissues (~20 μg per lane) were hybridized with probes, encompassing the CLIP binding domain of CLASP1 and -2 ("common" probes), or with 5′ probes, specific for particular CLASP variants. Approximate sizes of the different CLASP transcripts and positions of the 18S and 28S rRNAs are indicated.

(D) Comparison of the N terminus of CLASP2β with known palmitoylation motifs. Fatty acylated cysteine residues are in bold. Amino acid substitutions are indicated.

(E and F) Intracellular distribution of GFP, fused either to the first 40 amino acids of wild-type CLASP2β (Cys-GFP) or to the sequence with two serine substitutions (Ser-GFP). Transfected COS-1 cells were fixed and stained with antibodies to the *cis*-Golgi marker GM130. GFP

have a MT stabilizing effect in transfected cells. Using motile fibroblasts as a model system, we find that CLASPs specifically mark the distal ends of MTs at the leading edge of the cell and are involved in organizing stabilized MTs. Thus, CLASPs may play a role in local MT stabilization in response to positional cues.

Results

Characterization of CLIP-Associating Proteins (CLASPs)

Within the coiled-coil region of CLIP-115 and -170, the N-terminal portion is best conserved. This part of CLIP-115 (amino acids 287–591; Figure 1A) was therefore used as bait in a yeast two-hybrid screen to identify common *CL*IP-*as*sociating *p*roteins (CLASPs). We found one clone, which interacted both with CLIP-115 and with the corresponding region of CLIP-170 and which was therefore named CLASP1. This clone did not interact with vector alone, with other portions of CLIP-115, or with the coiled-coil domains of $p150^{Glued}$, a dynactin subunit that structurally resembles CLIP-170 (Pierre et al., 1992). Deletion analysis demonstrated that the whole coiled-coil part of the CLIP-115 bait construct is necessary and sufficient for binding to CLASP1 (Figure 1A).

Mouse *CLASP1* cDNA (*mCLASP1*) contains a 5′ truncated open reading frame (ORF) with very high similarity to the C termini of the proteins encoded by the incomplete human brain cDNAs KIAA0622 (98% identity, hCLASP1) and KIAA0627 (75% identity, hCLASP2). We searched for complete ORFs of CLASP1 and -2 by cDNA library screening, RACE-PCR, and EST database analysis. This yielded several cDNAs, named *CLASP1/2*α, *-2*β, and *-2*γ, which encode different protein isoforms (Figure 1B). Northern blot analysis with probes to the common C-terminal domains of *CLASP1* and *-2* shows that differently sized *CLASP* mRNAs are present in various tissues (Figure 1C), indicating that *CLASP* transcripts undergo alternative splicing. *CLASP1* shows highest expression in brain, heart, and testis, while *CLASP2* mRNAs are enriched in the brain. Interestingly, the *CLASP2*β transcript appears to be brain specific (Figure 1C). Using probes, specific for *CLASP1*α (Figure 1C) or *CLASP2*α (data not shown), we only detect hybridization to the longest transcript of each *CLASP* ($\sim$8 kb for *CLASP1*α and $\sim$7 kb for *CLASP2*α, respectively). The presence of 5 and 7 kb *CLASP1* transcripts indicates that there are additional N-terminal variants of CLASP1, similar to CLASP2.

The different *CLASP1* and *-2* cDNAs encode proteins with a predicted molecular mass of $\sim$170 kDa (α isoforms) and $\sim$140 kDa (β/γ isoforms). A database search revealed a striking similarity of the CLASPs to a protein called either Orbit or Mast, which is an essential MT-associated protein (MAP) from *D. melanogaster*, involved in the regulation of MT behavior during mitosis (Inoue et al., 2000; Lemos et al., 2000). Three putative CLASPs are also present in *C. elegans* (ZC84.3, R107.6, and C07h6.3). The domains of CLASP that are conserved in invertebrates are schematically indicated in Figure 1B. Interestingly, our 5′ RACE analysis demonstrates that an N-terminal $\sim$200 amino acid domain in Mast, which is similar to a repeated motif in the dis1/TOG family of vertebrate MT stabilizing proteins (Lemos et al., 2000), is also present in CLASP1α and -2α. These observations indicate that CLASPs might bind MTs.

CLASP2β is represented by the rat hippocampus cDNA clone r313 (Figure 1B). Instead of the dis1/TOG-homologous domain, this isoform contains a short N-terminal motif, which is conserved in humans (Figure 1B). It is characterized by two cysteines, surrounded by positively charged and hydrophobic residues (Figures 1B and 1D). Similar motifs in other proteins were shown to cause membrane anchoring, due to palmitoylation of the cysteine residues (Resh, 1999). Fusion of the N terminus of CLASP2β to GFP gives rise to a protein that accumulates in the region of the Golgi complex in transfected COS-1 cells (Figure 1E1, compare to the Golgi marker GM130 in Figure 1E2). Substitution of cysteine residues for serines (Figure 1F) or alanines (not shown) abolishes targeting to the Golgi, supporting the idea that fatty acylation of the cysteines within the N-terminal peptide stretch of CLASP2β causes membrane targeting. Triton-X114 partitioning experiments (Hancock et al., 1989), in which the cysteine-containing, but not the serine-containing, GFP fusion is partially retained in the detergent enriched (i.e., the membranous) phase (Figure 1G, compare lanes 1–3 and 4–6, respectively), further support this notion. Subsequent shortening of the CLASP2β N terminus within the fusion construct demonstrated that the first 14 amino acids of this CLASP isoform are sufficient for membrane association (data not shown).

In contrast to the α- and β-isoforms, CLASP2γ, represented by KIAA0627 cDNA, contains an inconspicuous peptide (MAMGDD) at its N terminus (Figure 1B). In conclusion, CLASPs appear to be the mammalian counterparts of the *D. melanogaster* protein Orbit/Mast. They exist as a family of widely distributed isoforms, each with a CLIP interaction domain but with variable N termini, and are likely to have MT binding properties.

CLASPs Colocalize with CLIPs at MT Distal Ends

We raised antibodies against the conserved C-terminal domain of hCLASP2 (antiserum #2358) in order to investigate the intracellular distribution of different CLASP isoforms. These studies were carried out both in COS-1 cells and in 3T3 fibroblasts, to compare results in different systems and to take advantage of the fact that COS-1 cells are easily transfected, whereas in 3T3 cells MT dynamics have been extensively studied. Interestingly, COS-1 cells express only CLIP-170, while in 3T3 fibroblasts, both CLIP-115 and CLIP-170 are present at MT distal ends. The specificity of antiserum #2358 was

fluorescence is shown in (E1) and (F1), and the antibody labeling of the same cells in (E2) and (F2). Bar, 10 μm.

(G) COS-1 cells, transfected with Cys-GFP or Ser-GFP, were lysed using Triton X-114. After pelleting of the insoluble fraction (lanes marked "p"), the lysate was partitioned into an aqueous phase ("a") and a detergent-enriched phase ("d"). The volumes of the three fractions were equalized before loading on gel and proteins were analyzed by Western blotting with anti-GFP serum.

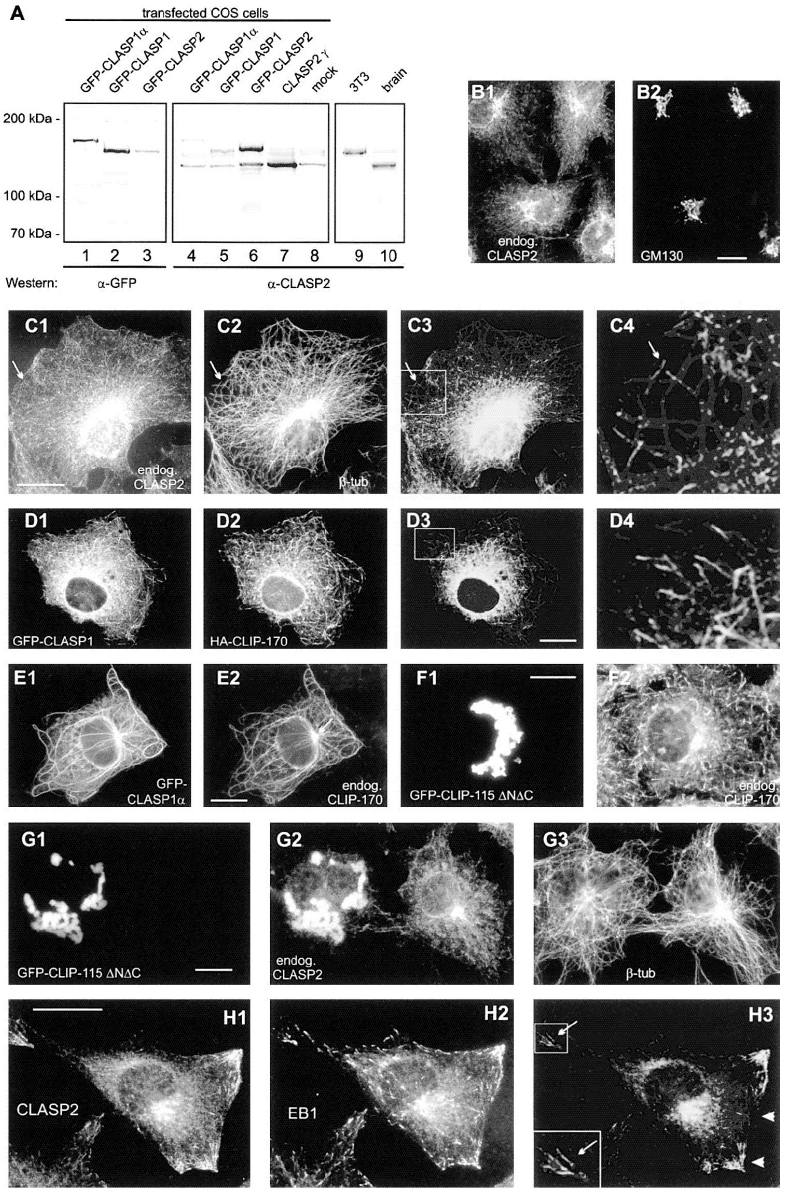

Figure 2. Localization of CLASPs in Cultured Cells

(A) Specificity of #2358 antibodies. Protein extracts from COS-1 cells, transiently transfected with the indicated CLASP expression constructs (lanes 1–7) or mock transfected (lane 8), and from 3T3 cells (lane 9) or mouse brain (lane 10) were analyzed by Western blotting, using antibodies against GFP (lanes1–3, α-GFP) or with the #2358 antiserum (lanes 4–10, α-CLASP2). Notice that GFP-CLASP1 fusions are more abundantly expressed than GFP-CLASP2 (lanes 1–3), but less well recognized by #2358 antibodies (lanes 4–6).

(B and C) Untransfected COS-1 cells, immunostained with #2358 antiserum and anti-GM130 (B) or anti-β-tubulin (C). In (C3) and (C4), signals of (C1) (green) and (C2) (red) are merged. (C4) is an enlargement of the indicated area in (C3) to demonstrate the MT plus end labeling of CLASP2 (indicated by an arrow). Bar, 10 μm.

(D–G) COS-1 cells, transfected with different cDNA constructs, fixed 24 hr after transfection and immunostained using specific antisera. Bar, 10 μm.

first analyzed by Western blotting in transfected COS-1 cells using different GFP-CLASP1 and -2 fusion proteins or untagged CLASP2γ (Figure 2A). In these cells, the #2358 antibodies react strongly with GFP-CLASP2 and with untagged CLASP2γ (Figure 2A, lanes 6 and 7, respectively). Weak cross-reactivity with GFP-CLASP1 proteins is also observed (Figure 2A, lanes 4 and 5). In agreement with these Western blot data, immunofluorescence experiments in transfected COS-1 cells with #2358 antibodies show very strong reaction with GFP-CLASP2 proteins and a weak reaction with GFP-CLASP1 fusions (data not shown). Based on these observations, we conclude that antiserum #2358 recognizes CLASPs specifically, but that use of these antibodies predominantly reflects the distribution of CLASP2 isoforms. Thus, the #2358 antiserum is also named anti-CLASP2 antiserum.

In mock transfected COS-1 cells, #2358 antibodies detect proteins of ~170 and ~140 kDa (Figure 2A, lane 8), which are the expected lengths for CLASP2α and -β/γ, respectively. Surprisingly, Western blot analysis of 3T3 cell lysates with antiserum #2358 reveals only a protein of ~170 kDa (Figure 2A, lane 9), whereas in mouse brain, the tissue with highest expression of CLASP2, proteins of ~140 and ~170 kDa are detected (Figure 2A, lane 10). These Western blots results with antiserum #2358 were verified by Northern blot analysis (data not shown). Together, the data demonstrate that CLASP2β and -γ are not highly expressed in 3T3 cells, whereas in brain they are more abundant than CLASP2α.

CLASP2 distribution was next examined using immunofluorescence microscopy. In COS-1 cells, prominent labeling is detected in the perinuclear region, corresponding to the Golgi apparatus (Figure 2B). In addition, anti-CLASP2 antibodies stain MT plus ends (Figure 2C) in a pattern similar to that described previously for CLIP-170 (Pierre et al., 1992; Perez et al., 1999). Both types of CLASP staining are completely inhibited by preincubation of the antibodies with the antigen used for their generation, while affinity-purified antibodies produce the same signal as the crude serum (data not shown). Thus, CLASP2 distribution in COS-1 cells overlaps with that of CLIP-170 at the distal ends of MTs.

Using GFP-CLASP1 (containing the 5′ truncated ORF from KIAA0622), GFP-CLASP1α, and GFP-CLASP2 (derived from KIAA0627), we next investigated the distribution of individual, overexpressed CLASP1 and -2 isoforms and the effect of coexpression with the CLIPs. At low expression levels, all three GFP-CLASP fusions colocalize with CLIP-170 or CLIP-115 at MT plus ends (Figure 2D and data not shown). When GFP-CLASPs are highly overexpressed, they accumulate along the whole length of MTs, causing MT rearrangement and bundling and CLIP-170 relocalization to these MT bundles (Figure 2E). At low expression levels in live transfected cells, GFP-CLASP2 behaves very similar to GFP-CLIP-170 (see Supplemental Information for live GFP-CLASP2 and GFP-CLIP-170 behavior in COS-1 cells at http://www.cell.com/cgi/content/full/104/6/923/DC1), which was shown to move with the growing ends of MTs (Perez et al., 1999). Taken together, these data verify the distribution of endogenous CLASP2, as detected with #2358 antibodies and establish CLASPs as a novel family of proteins that bind to the distal ends of interphase MTs.

A GFP fusion protein, containing the CLASP-interacting region of CLIP-115 (GFP-CLIP-115ΔNΔC, including amino acids 353–756 of CLIP-115), is unable to bind MTs, since it lacks the MTB domains. Instead, it forms cytoplasmic aggregates, which contain no significant amount of tubulin (Figures 2G1 and 2G3). Strikingly, in cells overexpressing this mutant protein, endogenous CLASP is titrated away from the Golgi complex as well as from MT distal ends and is detected in the aggregates (Figure 2G2). In contrast, both CLIP-170 (Figure 2F) and EB1 (data not shown) remain bound to MT distal ends. These results validate the yeast two-hybrid interaction between CLIPs and CLASPs. In addition, they indicate that CLIP-170 and EB1 are able to associate with MT distal ends in the absence of CLASP.

In 3T3 cells, CLASP2 distribution is similar to that in COS-1 cells. However, we noted that in cells with a shape characteristic of motile fibroblasts, intense labeling of MT distal segments is detected at the leading edge, but not in the cell body (Figures 2H1 and 2H3). This asymmetric distribution is particularly apparent when CLASP2 localization is compared to that of EB1, which marks MT tips throughout 3T3 cells (Figures 2H2 and 2H3). When a distal segment of an MT appears positive for both CLASP2 and EB1, the highest concentration of EB1 is often observed at the tip, while a more proximal portion of the MT is strongly stained with anti-CLASP2 antibodies (see insets in Figure 2H3). Thus, the MT labeling by CLASP2 at the periphery of subconfluent 3T3 cells is often nonuniform.

CLASPs Bind to CLIPs and MTs

To verify the CLIP–CLASP interactions, we tested their association in vitro. Radioactively labeled hCLASP1 and hCLASP2, generated by in vitro transcription-translation, bind to bacterially produced GST fusions of full-length CLIP-115 and the yeast two-hybrid fragment (CLIP-115-TH), but not to control GST fusion proteins (Figure 3C). Alternatively, in vitro translated CLIP-115 specifically binds to the GST fusion of the mCLASP1 C terminus (GST-CLASP1-C; Figure 3D). A GST pulldown assay with mouse brain extracts shows that both CLIP-115 and CLIP-170 are retained by GST-CLASP1-C, but not by GST alone (Figure 3E). Since all GST fusion pro-

(D) Cotransfection of GFP-CLASP1 (low level of expression) and HA-tagged CLIP-170, staining with antibody against the HA tag. (D4) is an enlargement of the indicated area in (D3).
(E) Transfection with GFP-CLASP1α, staining with antibodies against CLIP-170. The MTOC is indicated by an arrow.
(F and G) Transfections with GFP-CLIP-115ΔNΔC, staining with antibodies against CLASP2 (G2) and tubulin (G3), or with antibodies against CLIP-170 (F2).
(H) Intracellular distribution of CLASP2 in Swiss 3T3 fibroblasts. Cells were stained with anti-CLASP2 (H1) and anti-EB1 (H2) antisera. The overlay is shown in (H3) (CLASP2 is green, EB1 red). The arrow in (H3) indicates an example of MT distal ends with a high concentration of EB1 at the tip and CLASP2 at a more proximal segment. Arrowheads indicate the leading edge.

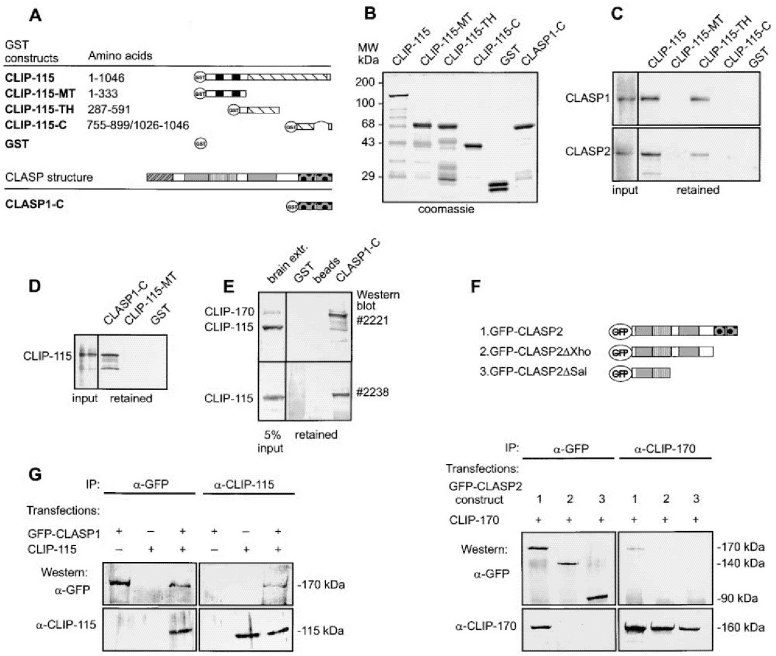

Figure 3. Analysis of CLIP–CLASP Interactions

(A) Schematic representation of bacterial GST fusion proteins of CLIP-115 and mCLASP1.

(B) SDS-PAGE analysis of purified GST fusions. All proteins are soluble and have the expected size. Molecular weight markers are indicated on the left.

(C) In vitro binding of ^{35}S-methionine-labeled CLASP1 and CLASP2 (see lanes, marked "input") to the GST fusion proteins, depicted in (A) and (B). Radioactive proteins were visualized by X-ray film exposure of dried gels.

(D) In vitro binding of ^{35}S-methionine-labeled CLIP-115 to GST fusion proteins. The experiment was performed as in (C).

(E) GST pulldown assay using mouse brain extract. Proteins, retained by glutathione-sepharose beads alone, beads decorated with GST, or with GST-mCLASP1-C, were analyzed by Western blotting, using antibody #2221, which recognizes both CLIP-115 and CLIP-170, or antibody #2238, which is specific for CLIP-115.

(F) Immunoprecipitations (IP) from COS-1 cells, transiently expressing rat brain CLIP-170, together with GFP-CLASP2, or C-terminal deletion mutants of CLASP2 (see scheme above the Western). Precipitated proteins were analyzed by Western blotting with antibodies against GFP or CLIP-170.

(G) Immunoprecipitations (IP) from COS-1 cells, transiently expressing GFP-CLASP1, CLIP-115, or both proteins. Precipitated proteins were analyzed by Western blotting with antibodies against GFP or CLIP-115.

teins (Figure 3A) are soluble and produced in comparable quantities (Figure 3B), these data suggest that the retention of CLASP1 and -2 by GST-CLIP-115 and GST-CLIP-115-TH and that of CLIP-115 and -170 by GST-CLASP1-C is specific.

We next immunoprecipitated different transfected GFP-CLASP fusion proteins from COS-1 cells, cotransfected with the CLIPs. Both full-length GFP-CLASP1 and -2 coprecipitate with CLIP-115 and -170 (Figures 3F and 3G and data not shown). These immunoprecipitates of CLIPs and CLASPs contain neither tubulin nor EB1 or dynactin (data not shown), indicating that these proteins do not mediate the CLIP–CLASP interaction. In addition, truncated GFP-CLASP2 proteins, where the C-terminal CLIP binding domain (GFP-CLASP2ΔXho) or the whole C-terminal half of the protein (GFP-CLASP2ΔSal) is deleted (Figure 3F), do not coprecipitate with CLIP-170 (Figure 3F) or CLIP-115 (data not shown) while being present in similar quantities as full-length GFP-CLASP2 (Figure 3F). Since these mutants still bind MTs (see below) but fail to bind CLIPs, these data strongly suggest that the CLIP–CLASP interaction is not mediated via tubulin, but occurs directly through the C-terminal CLIP-interacting domain of the CLASPs.

A sedimentation assay, whereby in vitro translated CLASPs were tested for their ability to cosediment with purified, taxol-stabilized MTs, reveals that only a small proportion of the CLASPs comes down with MTs (Figure 4A, left panels). This could be partially due to phosphorylation of CLASPs in the translation mix since this has been shown to inhibit MT binding of CLIP-115 and CLIP-170 (Pierre et al., 1992; Hoogenraad et al., 2000). To reduce the extent of phosphorylation of the CLASPs, after translation the system was depleted of ATP with apyrase. This caused a considerable increase in the proportion of CLASPs pelleted with MTs (Figure 4A,

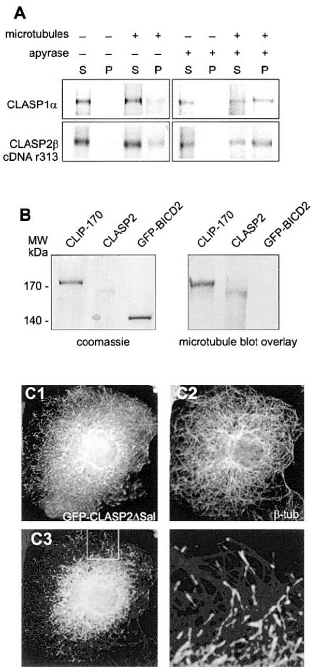

Figure 4. CLASPs Bind MTs Directly and Independently of CLIPs

(A) In vitro binding of CLASPs to MTs. ^{35}S-methionine-labeled CLASP1 and -2 were pelleted in the absence or in the presence of MTs, and the supernatants (lanes marked "S") and pellets (lanes marked "P") were analyzed by SDS-PAGE and autoradiography. In some cases, translation products were incubated with apyrase prior to the addition of MTs.

(B) MT blot overlay. CLIP-170, immunoprecipitated with antibodies #2221 from HeLa cells (500 ng), CLASP2, immunoprecipitated with antibodies #2358 from 3T3 cells (100 ng), and GFP-BICD2, immunoprecipitated from transfected COS-1 cells with GFP-specific antibodies (500 ng) were analyzed by SDS-PAGE or transferred to a Western blot, which was incubated with taxol-stabilized MTs (50 mg/ml). MTs, retained on the blot, were detected with anti-tubulin antibodies.

(C) COS-1 cells, transfected with GFP-CLASP2ΔSal (GFP signal shown in [C1]) were stained with anti-tubulin antibodies (C2). In (C3) and (C4), signals of (C1) (green) and (C2) (red) are merged. In (C4), an enlargement of the area indicated in (C3) is shown to demonstrate MT plus end labeling. Bar, 10 μm.

right panels). In MT blot overlays, immunoprecipitated CLASP2 and CLIP-170 bind MTs, whereas a Golgi-associated GFP fusion protein of similar size and quantity (GFP-BICD2; C. Hoogenraad et al., submitted) does not (Figure 4B). Thus, these results suggest that CLASPs bind MTs directly and this binding may be influenced by phosphorylation.

The GFP-CLASP2ΔSal mutant binds neither CLIP-115 nor CLIP-170 (Figure 3F) due to the absence of the C-terminal CLIP interaction domain. However, this protein does contain a presumptive MT binding domain (Inoue et al., 2000; Lemos et al., 2000). At low expression levels in transfected cells, this fusion protein localizes to the distal ends of MTs (Figure 4C) and colocalizes with CLIP-170 and EB1, while at high expression levels, GFP-CLASP2ΔSal is detected along the MTs (data not shown). These results suggest that CLASPs can accumulate on distal ends of MTs independently of their binding to CLIPs.

CLASP2 Localization in 3T3 Fibroblasts Correlates with the Orientation of Stabilized MTs

Since we observed that CLASP2 distribution in 3T3 cells with a representative motile shape is asymmetric, we investigated CLASP2 function further using the in vitro wound healing model (Liao et al., 1999). Swiss 3T3 fibroblasts were grown to confluence and a stripe of cells was scraped off, creating a "wound" in the monolayer. Cells at the edge of the wound polarize in such a way that their leading edges face the cell-free area. A subset of MTs, oriented in the direction of the wound along the polarization axis, becomes stabilized (Liao et al., 1999) and accumulates posttranslationally modified forms of tubulin, such as detyrosinated (Glu) tubulin and acetylated (Ac) tubulin, which can be visualized using specific antibodies (Bulinski and Gundersen, 1991).

Selective stabilization of MTs, oriented toward the leading edge, does not occur in serum-starved 3T3 cells, but can be quickly induced by the addition of serum (Cook et al., 1998). In agreement with these data, we find that after 24–48 hr of serum starvation, fibroblasts contain very few detyrosinated and acetylated MTs, which are concentrated in the region occupied by the Golgi complex (Figure 5A). Under these conditions, CLASP2 is mainly detected in the region of the Golgi complex, although weak staining with anti-CLASP2 antibodies is observed at the MT tips, which are also positive for EB1 (Figure 5B). Addition of serum induces formation of detyrosinated and acetylated MTs directed toward the edge of the wound (Figure 5C). The distribution of the two different posttranslationally modified forms of tubulin shows a strong correlation (but not a complete colocalization). MT tips at the leading edge and in the cell body are still stained with anti-EB1 antiserum as well as with anti-CLIP antibodies, which produce a highly similar staining pattern (Figure 5D).

In contrast to the MT distribution of EB1 and CLIP, anti-CLASP2 antibodies mainly stain the distal segments of MTs at the leading edge of the cell (Figure 5E). Very little MT bound CLASP2 is observed in the cell body and at the lateral edges of the cells, in areas of intercellular contacts (compare Figure 5E5 to 5E4). When CLASP2 localization is compared to that of acetylated tubulin, it becomes clear that many stabilized, acetylated MT bundles display a high accumulation of CLASP2 at their distal ends (Figure 5F).

MT stabilization at the leading edge of fibroblasts is induced rapidly (~5 min) in response to serum factors, although it takes about 30 min before posttranslationally modified tubulin isoforms have accumulated (Cook et al., 1998). Redistribution of CLASP2 in response to serum addition can be observed already after 5 min (data not shown), although all cells at the edge of the monolayer acquire a highly polarized CLASP2 staining pattern only after 15–20 min. Taken together, these data suggest that serum addition to wounded monolayers of 3T3 cells causes the rapid and asymmetric redistribution of CLASP2 to a subset of MT distal ends.

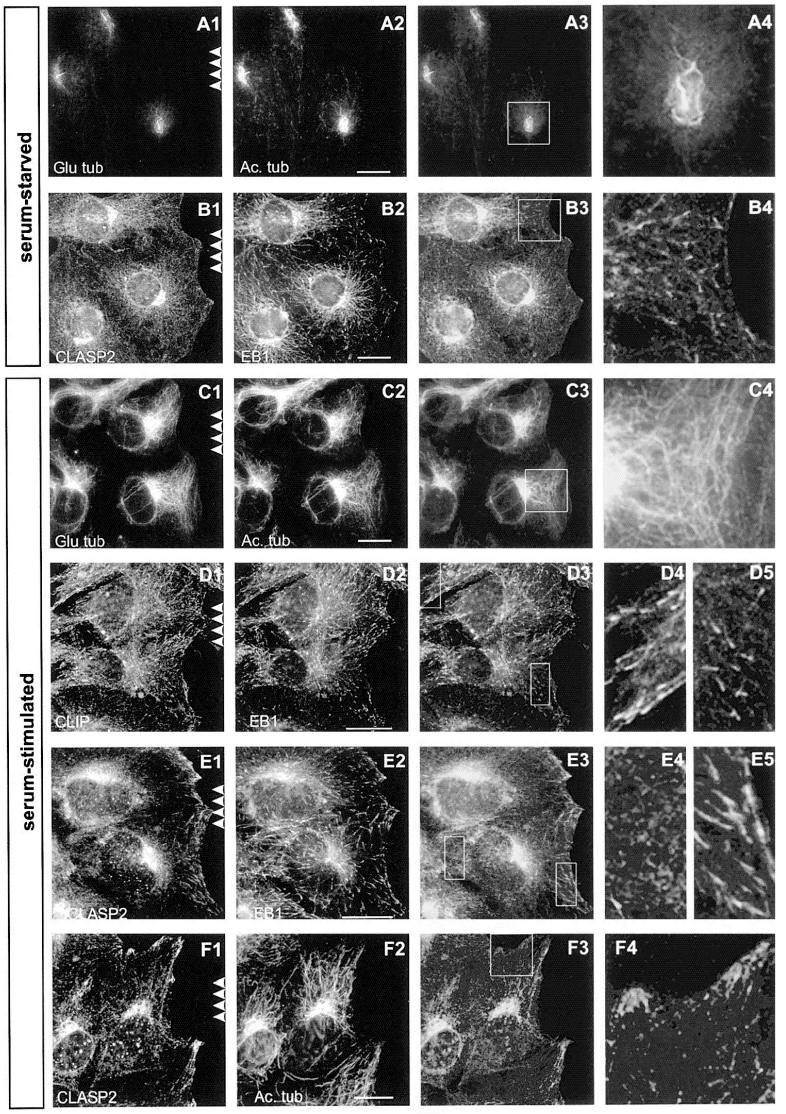

Figure 5. Localization of CLASP2 at the Leading Edge of Serum-Stimulated 3T3 Cells

3T3 cells were grown to 95% confluence in serum-containing medium and then incubated with serum-free medium for 30 hr. Narrow stripes of cells were removed by scraping, and after incubating for 2 more hr without serum, cells were fed either serum-free (A and B) or serum-containing medium (C–F) for an additional 30 min. Cells were fixed and costained with antibodies against Glu tubulin and acetylated tubulin (A and C), CLASP2 and EB1 (B and E), CLIP-115/CLIP-170 (#2221) and EB1 (D), and CLASP2 and acetylated tubulin (F). Images (A3)–(F3) represent overlays of images (A1)–(F1) (green) with images (A2)–(F2) (red). Panels on the right show an enlargement of part of the overlays (indicated by white rectangles). MT tips from the trailing part of the cell are shown in (D4) and (E4), MT tips from the leading edge in (D5) and (E5). The position of the wound is indicated (arrowheads; in [F], the leading edge also extends towards the top). Bar, 10 μm.

CLASPs Stabilize MTs

The similarity of CLASPs to Orbit/Mast and their asymmetric distribution in motile fibroblasts suggests that these proteins might be involved in the regulation of MT dynamics. We examined the MT-stabilizing effect of CLASPs first in COS-1 cells, which normally have few stabilized MTs, as determined by Glu tubulin antibody staining (Figure 6B). Overexpression of GFP-CLASP fu-

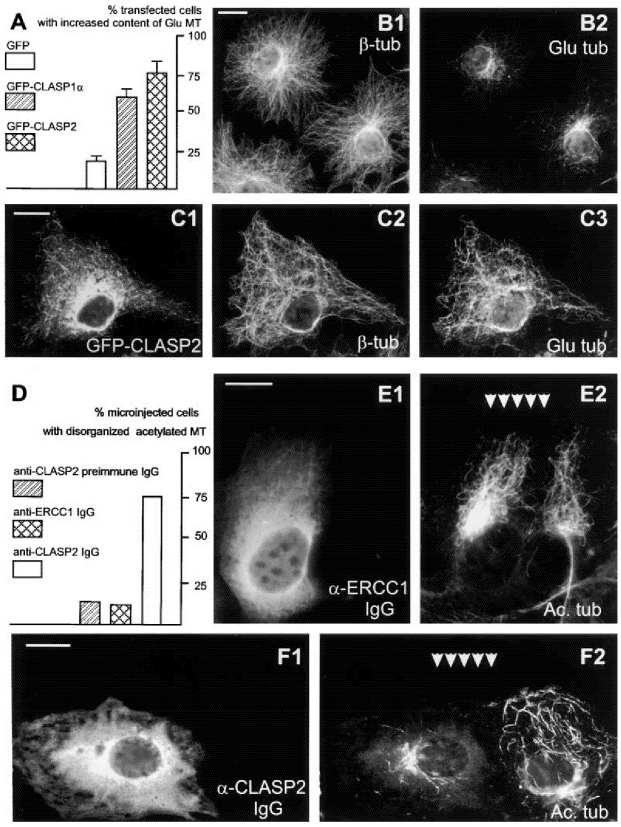

Figure 6. CLASPs Have an MT-Stabilizing Effect

(A) COS-1 cells were transfected with constructs, expressing GFP, GFP-CLASP1α, or GFP-CLASP2, and stained with Glu tubulin antibodies to detect stabilized MTs. The percentage of transfected cells, displaying a significant amount of Glu tubulin at the cell periphery, is shown in (A) (three experiments performed per construct, 100 cells counted per experiment, standard deviation indicated). Cells with very low GFP levels (not visible at data collection times below 600 ms, see Experimental Procedures) or high expression levels (visible at data collection times of 150 ms) were excluded from the analysis.

(B and C) Examples of tubulin (β-tub) and Glu tubulin (Glu tub) staining in untransfected COS-1 cells (B), or in cells expressing moderate levels of GFP-CLASP2 (C). The data collection time was 600 ms in (C1). Bar, 10 μm.

(D–F) Serum-starved 3T3 fibroblasts were injected with anti-CLASP2 or control antibodies, induced with serum for 2 hr, and stained for rabbit IgG (E1 and F1) and acetylated tubulin (E2 and F2). Position of the wound is indicated (arrowheads).

(D) The percentage of injected cells, displaying few or disorganized acetylated MTs, was determined for cells injected with control (#2358 preimmune and anti-ERCC1) antibodies or with anti-CLASP2 antibodies.

(E) 3T3 fibroblast injected with control antibodies.

(F) 3T3 fibroblast injected with anti-CLASP2 antibodies. Bar, 10 μm.

sions induces highly increased levels of detyrosinated MTs (Figures 6A and 6C). In the GFP-CLASP transfected cells, almost all cells contain many stabilized MTs outside the Golgi region, while in a control transfection, GFP alone does not have this effect. Importantly, MT stabilization occurs already at moderate levels of CLASP overexpression, when the distal segments of MTs are decorated by CLASPs (Figure 6C).

In the MT stabilizing assay, GFP-CLASP1α and GFP-CLASP2 fusions show comparable induction of detyrosinated MTs (Figure 6A), indicating that both CLASP1 and -2 have MT-stabilizing properties. In cells displaying an increased number of detyrosinated MTs, also the level of acetylated MTs is increased (data not shown). Such accumulation of two independent posttranslationally modified forms of tubulin argues in favor of an effect of GFP-CLASP overexpression on MT longevity rather than on the tubulin modification machinery itself. In agreement with a stabilizing function of CLASPs, the whole MT cytoskeleton becomes much more dense and entangled in GFP-CLASP-expressing cells (compare Figure 6B1 to Figure 6C2).

In a second experiment, we examined the effect of injected anti-CLASP2 antibodies on the orientation of stabilized MTs at the leading edge. A very high proportion of cells, injected with purified anti-CLASP2 antibodies, show reduced and disorganized stabilized MTs (Figures 6D and 6F) as compared to cells injected with control antibodies (Figures 6D and 6E). The fact that not all cells are affected by anti-CLASP2 injection might be due to variations in the amount of antibody injected, to variations in the state of polarization of motile fibroblasts that were injected, and/or to differences in the expression levels of CLASP1 and -2 within individual cells. Taken together, both the overexpression and antibody inhibition analyses point to a crucial role for CLASPs in the regulation of MT dynamics, in particular in the stabilization of MTs in polarized fibroblasts.

Regulation of CLASP-MT Association by Phosphorylation

The relocalization of CLASP2 upon serum stimulation suggests that CLASPs associate with MTs in a spatially regulated manner. Recently, it was documented that spatial sensing in fibroblasts is mediated by 3′ phosphoinositides (Haugh et al., 2000), implying the involvement of phosphoinositide (PI)-3 kinase at the leading edge. We therefore tested whether inhibition of PI-3 kinase activity affects polarized localization of CLASP2. Serum stimulation in the presence of the PI-3 kinase inhibitors

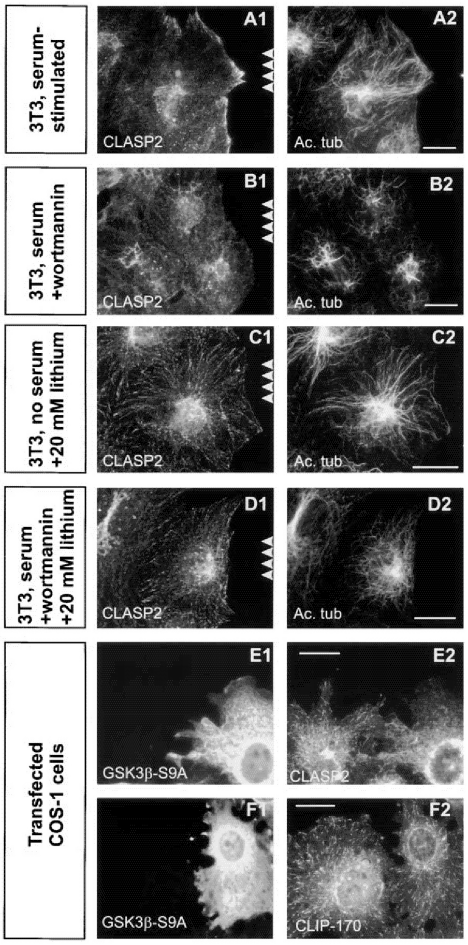

Figure 7. Regulation of Asymmetric CLASP2 Distribution

(A–D) A wounded monolayer of 3T3 cells (see Figure 5) was serum stimulated (A, B, and D) or kept on serum-free medium (C). To inhibit PI-3 kinase or GSK3β, either wortmannin (B and D) or LiCl (C and D) were added, respectively. Cells were fixed and costained with antibodies against CLASP2 and acetylated tubulin. White arrowheads mark the position of the wound in the monolayer.

(E and F) COS-1 cells, transfected with constitutively active, HA-tagged GSK3β-S9A, were fixed and costained with anti-HA antibodies (E1 and F1) and antibodies against CLASP2 (E2) or CLIP-170 (F2). Bar, 10 μm.

wortmannin or LY294002 indeed reduces the normal serum-induced accumulation of CLASP2 at the leading edge (compare Figure 7B to Figure 7A, or 5E). Absence of CLASP accumulation correlates with lack of polarized arrays of acetylated MTs (Figure 7B2). We next tested if glycogen synthase kinase (GSK)-3β, one of the downstream targets of PI-3 kinase, plays a role in regulating CLASP-MT distal end association. Treatment of serum-starved 3T3 cells (which normally do not contain much MT bound CLASP, Figure 5B) with lithium chloride, a direct inhibitor of GSK-3β, results in a significant increase in CLASP2 signal at distal MT ends (Figure 7C1) and in the appearance of extended acetylated MTs (Figure 7C2), which, like CLASP2, are localized throughout the cell. A similar result is observed in lithium-treated cells, which are serum stimulated in the presence of wortmannin (Figure 7D), indicating that GSK-3β inhibition is critical in regulating CLASP–MT interactions. This idea is supported by the observation that overexpression of a constutively active form (GSK-3β-S9A, where serine 9 is replaced by alanine) significantly inhibits CLASP2 localization to MT plus ends in transfected COS-1 cells (Figure 7E), but not that of CLIP-170 (Figure 7F).

Discussion

CLASPs Induce Local Stabilization of MTs

The MT network is a highly dynamic structure that is capable of quick rearrangements in response to environmental cues (Kirschner and Mitchison, 1986). Proteins, which bind to MT tips are of particular interest, since they are likely to be involved in regulation of MT dynamics and/or the interaction of MTs with the cellular cortex. CLIP-170 and CLIP-115 are such plus end binding proteins (Perez et al., 1999; Hoogenraad et al., 2000). Recently, a CLIP-170-like protein from fission yeast, tip1p, was shown to function as an anti-catastrophe factor (Brunner and Nurse, 2000), indicating that CLIP-115 and -170 might have a similar role in mammals. In this study, we identified CLASP1 and -2 as common protein partners of CLIP-115 and -170, which, similar to CLIPs, localize to MT tips. CLASPs are homologous along their entire length to the *Drosophila* MAP Orbit/Mast (Inoue et al., 2000; Lemos et al., 2000). Like Orbit/Mast, CLASPs directly bind MTs. Overexpression of CLASPs in COS-1 cells induces MT stabilization, while inhibition of CLASP2 function by antibody injections prevents the formation of aligned and stabilized MTs in motile fibroblasts. CLASP2 is predominantly bound to MTs at the leading edge of 3T3 cells, where they tend to grow or become stabilized, and not in the cell body, where MTs are unstable and often depolymerize. Taken together, this evidence strongly suggests that CLASPs are MAPs that regulate MT dynamics in polarized cells.

Potential Role of CLASP Isoform Variability

CLASPs exist as a family of isoforms, distinguished by their N-terminal sequences. The domain present in the long CLASP1/2α isoforms (and in Orbit/Mast) is similar to protein sequences in the MT stabilizing proteins of the dis1/TOG family. Although this suggests a function for the dis1/TOG domain of CLASPα in MT stabilization, deletion of the domain did not make a difference in the MT stabilization assay in transfected COS-1 cells. Interestingly, the dis1/TOG members ZYG-9 and Mini Spindles associated with spindle poles and centrosomes (Matthews et al., 1998; Cullen et al., 1999) and transfected GFP-CLASP1α preferentially accumulated in centrosomally originating MT bundles, while the other isoforms did not. It is therefore possible that the N-terminal domain of CLASPα plays a role in centrosomal MT nucleation.

The N terminus of CLASP2β is a membrane-targeting domain, similar to the dual palmitoylation module identified in several other proteins (Resh, 1999). Palmitoylation plays an essential role in protein sorting; for example, it is required to target the membrane-associated guanylate kinase PSD-95 to the postsynaptic density (El-Husseini et al., 2000). The existence of a brain-specific CLASP isoform with a membrane-targeting signal, together with more widely expressed isoforms lacking such a signal, is reminiscent of a situation described for the stathmin protein family. Stathmin is a small cytosolic phosphoprotein, which destabilizes MTs and which is the prototype member of a family, that includes the nervous system proteins SCG10, SCLIP, and RB3 (Gavet et al., 1998). These proteins can associate with membranes through their dually palmitoylated N termini and at least one of them, SCG10, is specifically localized to neuronal growth cones (Di Paolo et al., 1997). The existence of both stabilizing (CLASP) and destabilizing (stathmin) factors with similar targeting properties could provide a mechanism for the fine regulation of MT dynamics in particular neuronal compartments.

Regulation of CLASP–MT Interactions at Distal Ends

Different from other MT-stabilizing factors, such as XMAP215, which bind along the whole length of MTs, CLASPs can induce MT stabilization when present only at the distal ends of MTs. Both in CLASP-overexpressing COS-1 cells and at the leading edge of 3T3 fibroblasts, this stabilization is associated with the presence of a "coat" of CLASP at distal segments. Our findings indicate that PI-3 kinase signaling through GSK3β is an important mediator of the asymmetric CLASP2–MT interactions in 3T3 fibroblasts. These results are consistent with the observation that PI-3 kinase plays an essential role in the polarization of fibroblasts (Haugh et al., 2000) and that one of the biological responses of PI-3 kinase activation is the inactivation of GSK3β (van Weeren et al., 1998). The latter actually fulfills all the requirements for being a negative regulator of CLASP2–MT interactions. First, our in vitro studies suggest that MT binding by CLASPs is negatively influenced by phosphorylation. Second, unlike many other kinases, GSK3β is constitutively active in resting cells (such as serum-starved cells) and is inhibited when cells are stimulated by a number of growth factors. These results are in line with the fact that CLASP binding to distal ends is reduced in serum-starved cells (or in cells overexpressing a constitutively active form of GSK3β) and stimulated by serum (or by inactivation of GSK3β with lithium chloride). Thus, the polarized accumulation of CLASPs is subject to regulation by positional cues and by serum, which distinguishes CLASPs from other MT plus end binding proteins, such as CLIPs and EB1.

Functional Significance of the CLIP–CLASP Interaction

We have shown that the C-terminal domain of CLASPs specifically binds to a portion of the coiled-coil domain of CLIP-115 and -170. In vivo, this CLIP–CLASP interaction might be transient since the distribution of CLIPs and CLASPs shows only partial overlap in interphase fibroblasts. There is a substantial Golgi-associated pool of CLASPs, while CLIP-170 and CLIP-115 do not accumulate significantly in the Golgi. Also, in serum-stimulated 3T3 cells, only a subset of EB1/CLIP-positive MT tips are labeled strongly with anti-CLASP2 antibodies. In serum-grown 3T3 cells, CLIPs and EB1 are most concentrated at the very tip of an MT, while longer and more proximal MT segments are stained by anti-CLASP2 antibodies. A transient CLIP–CLASP interaction would account for previous failures to copurify CLASPs (or any other protein) with CLIP-170 (Scheel et al., 1999). Also, in our hands, no significant amounts of CLIP-170 could be coprecipitated with CLASP from untransfected COS-1 cells.

The affinity of CLASPs for MT tips is not solely dependent on interaction with CLIPs since a CLASP2 mutant, lacking the CLIP binding domain, is still targeted to MT plus ends. In spite of this fact and the putative transient nature of the CLIP–CLASP interaction, these proteins are highly likely to influence the affinity of each other for MTs and thereby affect the fate of MTs. For example, CLIPs could stimulate the loading of (membrane bound) CLASPs onto the MT plus ends. Conversely, accumulation of CLASPs on distal segments of a subset of MTs might serve to attract CLIP-170 (or CLIP-115) to the tips of MTs, even under conditions of MT shrinkage and/or pausing, conditions that normally cause dissociation of CLIP-170 from the distal ends (Perez et al., 1999). Attraction of the CLIPs by a CLASP-positive segment may rescue pausing/retracting MTs and revert them to a state of growth and may be one of the mechanisms by which CLASPs stabilize MTs. This model is both in line with the proposed anti-catastrophe role of tip1p (Brunner and Nurse, 2000) and with the observation that CLIP-170 treadmills on the growing ends of MTs by copolymerization with tubulin and could thus be an inherent part of the MT polymerization machinery (Diamantopoulos et al., 1999; Perez et al., 1999). It also would explain the increased longevity of a subset of MTs at the leading edge (Cook et al., 1998) and why these MTs still have their tips decorated with EB1/CLIP. In conclusion, we propose that CLIP–CLASP interactions constitute part of a regulatory device on the distal ends of MTs that is needed to target or modulate MT dynamics in polarized cells. The partnership between CLIPs and CLASPs bears a striking resemblance to that of APC and EB1, two proteins which bind to each other, accumulate at MT plus ends, and regulate MT dynamics in polarized cells (for review, see Tirnauer and Bierer, 2000). It will be interesting to investigate to what extent CLIP-CLASP and APC-EB1 pathways interact.

Experimental Procedures

Yeast Two-Hybrid Screen

A mouse E14.5 day embryonic cDNA library (Chevray and Nathans, 1992) was screened by the yeast two-hybrid assay (Wolthuis et al., 1996). Fragments of rat CLIP-115, rat brain CLIP-170, and chicken $p150^{Glued}$ were cloned into the pPC97 yeast two-hybrid vector (see Figure 1A). Production of yeast proteins was verified by Western blotting using monoclonal antibodies against GAL4 DNA binding and activation domains (Clontech). Mouse CLASP1 cDNA, derived from the yeast two-hybrid screen, corresponds to the 3′ portion of KIAA0622, starting from position 3010 (see Figure 1B). Interaction of mCLASP1 with CLIP-115 was verified by exchanging the inserts of bait and fish vectors.

cDNA Isolation and Northern Blotting

The CLIP-170 clone used here is a rat brain cDNA encoding a CLIP-170 isoform with a 115 amino acid deletion in the C-terminal portion of the coiled-coil region (accession number AJ237670). Human KIAA0622 (CLASP1) and KIAA0627 (CLASP2) cDNAs (Ishikawa et al., 1998) were obtained from the Kazuza DNA Research Institute. To complete the 5′ ends of these cDNAs, we used RACE-PCR with human adult brain poly(A)$^+$ RNA (Clontech) or mouse brain RNA as a template. Mouse EST ui60h04 (truncated CLASP2α) is an IMAGE clone. Rat cDNA clone r313 (CLASP2β) was isolated by screening of a rat hippocampus cDNA library (De Zeeuw et al., 1997). Accession numbers are: AJ288057 (human brain 5′ end CLASP1α), AJ288058, and AJ288059 (human brain 5′ end CLASP2γ and -β, respectively); AJ288060 (clone r313); AJ288061 (mouse yeast two-hybrid CLASP1); AJ276961 (ui60h04), and AJ276962 (mouse brain 5′ end CLASP1α). Northern blots were prepared and hybridized using standard protocols (Sambrook et al., 1989).

GST Fusion Constructs and Generation of CLASP Antisera

Glutathione S-transferase (GST) fusions were generated using plasmids pGEX-2T and pGEX-3X (Pharmacia). GST-mCLASP1-C contains the whole coding part of the mouse yeast two-hybrid CLASP1 cDNA. GST-hCLASP2 contains the corresponding C terminus of human CLASP2 (nucleotide positions 3074–3976 of the KIAA0627 cDNA). The GST-CLIP fusion proteins are explained in Figure 3A. Purification of GST fusion proteins and immunization of rabbits were performed as described (Hoogenraad et al., 2000). Antiserum #2358 is against GST-hCLASP2.

Western Blot Analysis and Immunoprecipitations

Protein extract preparation, Western blotting, and CLIP antisera have been described (Hoogenraad et al., 2000). Proteins were detected using rabbit polyclonal anti-GFP (1:2500; Clontech) or anti-CLIP and CLASP antibodies (all used at 1:2500). The Triton-X114 partitioning assay was performed as published (Hancock et al., 1989).

In the immunoprecipitation experiments, transfected COS-1 cells were lysed in buffer containing 30 mM HEPES (pH 7.4), 100 mM KCl, 1% NP-40, supplemented with protease inhibitors (Boehringer Mannheim), and incubated at 4°C for 30 min to depolymerize MTs. All subsequent steps were carried out as described (Hoogenraad et al., 2000).

GST Pulldown and MT Binding Assays

KIAA0622, KIAA0627, and CLIP-115 cDNAs were transcribed and translated in vitro using the TnT-coupled transcription-translation system (Promega) and ^{35}S-methionine (Trans35S label, ICN). Aliquots of radiolabeled proteins were incubated with different GST fusion proteins in NETT buffer (100 mM NaCl, 50 mM Tris (pH 7.5), 5 mM EDTA, 0.5% Triton X-100) for 2 hr at room temperature. Afterwards, samples were washed five times in NETT buffer. Proteins were eluted by boiling in sample buffer and analyzed by SDS-PAGE. Dried gels were exposed to film.

Mouse brains were homogenized in NETT buffer containing protease inhibitors. After removing insoluble material by centrifugation for 10 min at 10,000 × g, protein extract was used for the GST pulldown assay, as described above. Bound proteins were detected by Western blotting.

For the MT binding assays (Hoogenraad et al., 2000), CLASP1α and r313 plasmids were transcribed and translated. Some samples were treated for 15 min at 30°C with apyrase (1 U, Sigma) immediately after translation. The MT blot overlay was performed as described (Brunner and Nurse, 2000).

Expression Constructs

GFP-CLASP1 contains the whole open reading frame of KIAA0622, subcloned in-frame into pEGFP-C1 (Clontech). CLASP1α was constructed from KIAA0622 and an overlapping human brain RACE product, encoding the XMAP215-homologous domain, by using a unique AvrII site at position 580 in KIAA0622. Fusing the CLASP1α insert into pEGFP-C1 produced GFP-CLASP1α. Untagged CLASP2γ consists of the whole insert of KIAA0627, cloned into pCI-neo (Promega). GFP-CLASP2 was made by inserting KIAA0627 cDNA from the BspEI site at position 184 into pEGFP-C1; it therefore lacks the first 29 amino acids encoded by KIAA0627. In the GFP-CLASP2 C-terminal deletion constructs, the CLASP2 coding sequence was abrogated at nucleotide positions 1830 (GFP-CLASP2ΔSal) and 3138 (GFP-CLASP2ΔXho) of the KIAA0627 sequence. The GSK-3β (S9A) construct has been described (van Weeren et al., 1998).

Cell Culture Manipulations and Immunofluorescence

COS-1 cells were cultured and transfected as described (Hoogenraad et al., 2000). Swiss 3T3 fibroblasts were cultured in DMEM medium with 8% fetal calf serum. Serum starvation and monolayer wounding were as reported (Gundersen et al., 1994). For PI3-kinase inhibition, 100 nM wortmannin or 300 μM LY294002 (Sigma) was used. For GSK-3β inhibition, 10–20 mM LiCl was added to the culture medium. Antibody injections into fibroblasts on the edge of the stripes were performed as published previously (van Vuuren et al., 1994). Injections were done 2 hr prior to serum induction using IgG-purified antibodies at 5 mg/ml. Injected cells were detected using fluorescently labeled rabbit secondary antibodies. The percentage of cells with reduced or disorganized stabilized MTs was determined by staining with antibodies against acetylated tubulin. Stabilized MTs were scored as disorganized if their amount was highly reduced (see example in Figure 6F) and/or if they displayed random orientation with respect to the leading edge. Percentages were determined by counting 79 cells injected with control #2358 preimmune IgG (16% disorganized), 86 cells injected with control anti-ERCC1 antibodies (van Vuuren et al., 1994; 14% disorganized), and 233 cells injected with anti-CLASP2 antibodies (results from the two independent experiments with the different control antibodies; 76% disorganized).

Immunofluorescence experiments (Hoogenraad et al., 2000) were performed using rabbit anti-CLASP2 antiserum, antiserum #2221, which recognizes both CLIP-115 and CLIP-170 and antiserum #2238, which is specific for CLIP-115 (Hoogenraad et al., 2000), in a dilution of 1:300. Rabbit antibodies against Glu tubulin (a gift from Dr. J. C. Bulinski) were diluted at 1:500. Mouse monoclonal antibodies against the HA tag (BAbCO), β-tubulin, acetylated tubulin and vinculin (Sigma), EB1, and GM130 (Transduction Laboratories) were diluted 1:100. Secondary antibodies used were rhodamine-conjugated sheep anti-mouse (1:25, Boehringer Mannheim), Alexa 594-conjugated goat anti-rabbit (1:500, Molecular Probes), FITC-conjugated goat anti-rabbit (1:100, Nordic Laboratories), and Alexa 350-conjugated sheep anti-mouse (1:250, Molecular Probes).

Signals were captured with a Leica DMRBE fluorescence microscope equipped with a Hamamatsu C4880 DCC camera. To quantify the GFP fluorescence, cells were imaged using fixed data collection times: 150 ms for highly expressing cells, 600 ms for moderately expressing cells, and 1200 ms for cells expressing low levels of GFP fusion protein.

Acknowledgments

We are grateful to Dr. T. A. Schroer for sending the chicken p150^{Glued} cDNA, to Dr. J. C. Bulinski for sending anti-Glu tubulin antiserum, and to Dr. T. Nagase for providing KIAA0622 and KIAA0627 cDNAs. This research was supported by grants from the Netherlands Organization for Scientific Research (NWO; GB-MW 903-68-361), the Life Sciences Foundation (SLW; 805.33.310; 803.33.311), and the Royal Dutch Academy of Sciences (KNAW).

Received June 23, 2000; revised January 25, 2001.

References

Brunner, D., and Nurse, P. (2000). CLIP170-like tip1p spatially organizes microtubular dynamics in fission yeast. Cell *102*, 695–704.

Bulinski, J.C., and Gundersen, G.G. (1991). Stabilization of post-translational modification of microtubules during cellular morphogenesis. Bioessays *13*, 285–293.

Chevray, P.M., and Nathans, D. (1992). Protein interaction cloning in yeast: identification of mammalian proteins that react with the leucine zipper of Jun. Proc. Natl. Acad. Sci. USA *89*, 5789–5793.

Cook, T.A., Nagasaki, T., and Gundersen, G.G. (1998). Rho guano-

sine triphosphatase mediates the selective stabilization of microtubules induced by lysophosphatidic acid. J. Cell Biol. *141*, 175–185.

Cullen, C.F., Deak, P., Glover, D.M., and Ohkura, H. (1999). Mini spindles: a gene encoding a conserved microtubule-associated protein required for the integrity of the mitotic spindle in Drosophila. J. Cell Biol. *146*, 1005–1018.

Desai, A., and Mitchison, T.J. (1997). Microtubule polymerization dynamics. Annu. Rev. Cell Dev. Biol. *13*, 83–117.

De Zeeuw, C.I., Hoogenraad, C.C., Goedknegt, E., Hertzberg, E., Neubauer, A., Grosveld, F., and Galjart, N. (1997). CLIP-115, a novel brain-specific cytoplasmic linker protein, mediates the localization of dendritic lamellar bodies. Neuron *19*, 1187–1199.

Di Paolo, G., Lutjens, R., Pellier, V., Stimpson, S.A., Beuchat, M.H., Catsicas, S., and Grenningloh, G. (1997). Targeting of SCG10 to the area of the Golgi complex is mediated by its NH2-terminal region. J. Biol. Chem. *272*, 5175–5182.

Diamantopoulos, G.S., Perez, F., Goodson, H.V., Batelier, G., Melki, R., Kreis, T.E., and Rickard, J.E. (1999). Dynamic localization of CLIP-170 to microtubule plus ends is coupled to microtubule assembly. J. Cell Biol. *144*, 99–112.

Dujardin, D., Wacker, U.I., Moreau, A., Schroer, T.A., Rickard, J.E., and De Mey, J.R. (1998). Evidence for a role of CLIP-170 in the establishment of metaphase chromosome alignment. J. Cell Biol. *141*, 849–862.

El-Husseini, A.E., Craven, S.E., Chetkovich, D.M., Firestein, B.L., Schnell, E., Aoki, C., and Bredt, D.S. (2000). Dual palmitoylation of PSD-95 mediates its vesiculotubular sorting, postsynaptic targeting, and ion channel clustering. J. Cell Biol. *148*, 159–172.

Gavet, O., Ozon, S., Manceau, V., Lawler, S., Curmi, P., and Sobel, A. (1998). The stathmin phosphoprotein family: intracellular localization and effects on the microtubule network. J. Cell Sci. *111*, 3333–3346.

Gundersen, G.G., Kim, I., and Chapin, C.J. (1994). Induction of stable microtubules in 3T3 fibroblasts by TGF-beta and serum. J. Cell Sci. *107*, 645–659.

Hancock, J.F., Magee, A.I., Childs, J.E., and Marshall, C.J. (1989). All ras proteins are polyisoprenylated but only some are palmitoylated. Cell *57*, 1167–1177.

Haugh, J.M., Codazzi, F., Teruel, M., and Meyer, T. (2000). Spatial sensing in fibroblasts mediated by 3′ phosphoinositides. J. Cell Biol. *151*, 1269–1280.

Hoogenraad, C.C., Akhmanova, A., Grosveld, F., De Zeeuw, C.I., and Galjart, N. (2000). Functional analysis of CLIP-115 and its binding to microtubules. J. Cell Sci. *113*, 2285–2297.

Inoue, Y.H., do Carmo Avides, M., Shiraki, M., Deak, P., Yamaguchi, M., Nishimoto, Y., Matsukage, A., and Glover, D.M. (2000). Orbit, a novel microtubule-associated protein essential for mitosis in Drosophila melanogaster. J. Cell Biol. *149*, 153–166.

Ishikawa, K., Nagase, T., Suyama, M., Miyajima, N., Tanaka, A., Kotani, H., Nomura, N., and Ohara, O. (1998). Prediction of the coding sequences of unidentified human genes. X. The complete sequences of 100 new cDNA clones from brain which can code for large proteins in vitro. DNA Res. *5*, 169–176.

Kirschner, M., and Mitchison, T. (1986). Beyond self-assembly: from microtubules to morphogenesis. Cell *45*, 329–342.

Lemos, C.L., Sampaio, P., Maiato, H., Costa, M., Omel'yanchuk, L.V., Liberal, V., and Sunkel, C.E. (2000). Mast, a conserved microtubule-associated protein required for bipolar mitotic spindle organization. EMBO J. *19*, 3668–3682.

Liao, G., Kreitzer, G., Cook, T.A., and Gundersen, G.G. (1999). A signal transduction pathway involved in microtubule-mediated cell polarization. Faseb. J. *13*, S257–S260.

Matthews, L.R., Carter, P., Thierry-Mieg, D., and Kemphues, K. (1998). ZYG-9, a Caenorhabditis elegans protein required for microtubule organization and function, is a component of meiotic and mitotic spindle poles. J. Cell Biol. *141*, 1159–1168.

Mimori-Kiyosue, Y., Shiina, N., and Tsukita, S. (2000). The dynamic behavior of the APC-binding protein EB1 on the distal ends of microtubules. Curr. Biol. *10*, 865–868.

Perez, F., Diamantopoulos, G.S., Stalder, R., and Kreis, T.E. (1999). CLIP-170 highlights growing microtubule ends in vivo. Cell *96*, 517–527.

Pierre, P., Scheel, J., Rickard, J.E., and Kreis, T.E. (1992). CLIP-170 links endocytic vesicles to microtubules. Cell *70*, 887–900.

Resh, M.D. (1999). Fatty acylation of proteins: new insights into membrane targeting of myristoylated and palmitoylated proteins. Biochim. Biophys. Acta *1451*, 1–16.

Sambrook, J., Fritsch, E.F., and Maniatis, T. (1989). Molecular Cloning: A Laboratory Manual, 2nd Edition (New York: Cold Spring Harbor Laboratory Press).

Scheel, J., Pierre, P., Rickard, J.E., Diamantopoulos, G.S., Valetti, C., van der Goot, F.G., Haner, M., Aebi, U., and Kreis, T.E. (1999). Purification and analysis of authentic CLIP-170 and recombinant fragments. J. Biol. Chem. *274*, 25883–25891.

Tirnauer, J.S., and Bierer, B.E. (2000). EB1 proteins regulate microtubule dynamics, cell polarity, and chromosome stability. J. Cell Biol. *149*, 761–766.

Tirnauer, J.S., O'Toole, E., Berrueta, L., Bierer, B.E., and Pellman, D. (1999). Yeast Bim1p promotes the G1-specific dynamics of microtubules. J. Cell Biol. *145*, 993–1007.

Valetti, C., Wetzel, D.M., Schrader, M., Hasbani, M.J., Gill, S.R., Kreis, T.E., and Schroer, T.A. (1999). Role of dynactin in endocytic traffic: effects of dynamitin overexpression and colocalization with CLIP-170. Mol. Biol. Cell *10*, 4107–4120.

van Vuuren, A.J., Vermeulen, W., Ma, L., Weeda, G., Appeldoorn, E., Jaspers, N.G., van der Eb, A.J., Bootsma, D., Hoeijmakers, J.H., Humbert, S., et al. (1994). Correction of xeroderma pigmentosum repair defect by basal transcription factor BTF2 (TFIIH). EMBO J. *13*, 1645–1653.

van Weeren, P.C., de Bruyn, K.M., de Vries-Smits, A.M., van Lint, J., and Burgering, B.M. (1998). Essential role for protein kinase B (PKB) in insulin-induced glycogen synthase kinase 3 inactivation. Characterization of dominant-negative mutant of PKB. J. Biol. Chem. *273*, 13150–13156.

Vaughan, K.T., Tynan, S.H., Faulkner, N.E., Echeverri, C.J., and Vallee, R.B. (1999). Colocalization of cytoplasmic dynein with dynactin and CLIP-170 at microtubule distal ends. J. Cell Sci. *112*, 1437–1447.

Wittmann, T., Hyman, A., and Desai, A. (2001). The spindle: a dynamic assembly of microtubules and motors. Nat. Cell Biol. *3*, E28–E34.

Wolthuis, R.M., Bauer, B., van't Veer, L.J., de Vries-Smits, A.M., Cool, R.H., Spaargaren, M., Wittinghofer, A., Burgering, B.M., and Bos, J.L. (1996). RalGDS-like factor (Rlf) is a novel Ras and Rap 1A-associating protein. Oncogene *13*, 353–362.

GenBank Accession Numbers

The GenBank accession numbers for the eight sequences reported in this paper are: AJ237670 (rat brain CLIP-170); AJ288057 (human brain 5′ end CLASP1α); AJ288058 and AJ288059 (human brain 5′ end CLASP2γ and -β, respectively); AJ288060 (clone r313); AJ288061 (mouse yeast two-hybrid CLASP1); AJ276961 (ui60h04) and AJ276962 (mouse brain 5′ end CLASP1α).

Chapter 3

CLASP2 targets to focal adhesions and regulates cell polarity in fibroblasts in response to fibronectin signalling

Manuscript in preparation

CLASP2 targets to focal adhesions and regulates cell polarity in fibroblasts in response to fibronectin signalling

Ksenija Drabek[1], Marco van Ham[1], Tatiana Stepanova[1*], Remco van Horssen[2], Katharina Draegestein[1], Michael van der Reijden[1], Anna Akhmanova[1], Timo ten Hagen[2], Adriaan Houtsmuller[3], Frank Grosveld[1] and Niels Galjart[1*]

1: Department of Cell Biology and Genetics
2: Department of Surgical Oncology
3: Department of Pathology, Josephine Nefkens Institute

Erasmus MC, P.O. Box 1738, 3000 DR Rotterdam, The Netherlands

Abstract
CLASPs are conserved microtubule plus end tracking proteins involved in the local control of microtubule stabilisation in interphase and mitosis. Here we show that in 3T3 cells stably expressing GFP-CLASP2, serum addition results in the rapid targeting of fusion protein to microtubule ends near focal adhesions and the leading edge. Bleaching studies indicate that at these sites GFP-CLASP2 is less mobile than elsewhere in the cytoplasm. We further show that CLASP2 knock out fibroblasts do not form stable microtubules efficiently after adherence to fibronectin. In motile, CLASP2-deficient fibroblasts, microtubule dynamics is affected, which leads to altered cell polarity and motility features. We propose that CLASP2 forms part of a signalling loop: its enhanced association with microtubule ends in response to specific cues causes their stabilisation, which in turn enables CLASP2 to organise domains at microtubule ends that sustain cell polarity.

Introduction

Cell migration is initiated by local, actin-rich membrane protrusions and the asymmetric positioning of intracellular structures (Ridley et al., 2003). Actin polymerisation enables the advance of lamellipodia and/or filopodia and is achieved by the specific activation of members of the small Rho GTPase family, Cdc42 and Rac (Etienne-Manneville and Hall, 2002; Wittmann and Waterman-Storer, 2001). Polarity is sustained by the redistribution of other key factors, for example PI3 kinases and the phosphatase PTEN, but also non-enzymatic components are important for this process (Meili and Firtel, 2003). To maintain a polarized phenotype, a positive feedback loop signalling has been invoked, i.e. the amplification and/or maintenance of initial regulatory signals by locally confined mechanisms.

Migrating cells have a leading edge at the front of the cell and a trailing edge at the back. In fast moving cells reorganization of the actin network appears to be the predominant requirement for migration. Disassembly of the MT cytoskeleton in neutrophils actually causes cell polarity and migration (Niggli, 2003), yet affects the efficiency of migration (Xu et al., 2005). In fibroblasts, removal of the microtubule (MT) cytoskeleton with nocodazole, in combination with local application of the contractility inhibitor ML-7, induces polarisation and migration (Kaverina et al., 2000). These data indicate that MTs play a role in certain aspects of migration. These aspects may gain importance in slow moving cells, such as fibroblasts and astrocytes, which are dependent on MTs for reorientation of the microtubule organising centre (MTOC) and for the formation of cell protrusions (Etienne-Manneville and Hall, 2001; Palazzo et al., 2001b). In both cell types signalling pathways have been defined that regulate these processes (Etienne-Manneville and Hall, 2003; Palazzo et al., 2001a; Wen et al., 2004).

Cell orientation and migration require cell adhesion to the extracellular matrix and the exertion of force against the matrix. Cell-matrix interactions are mediated, among others, by integrins, which accumulate in focal adhesions where they assemble, through complex pathways, the machinery required for controlled force generation (Galbraith et al., 2002; Schwartz and Ginsberg, 2002). MTs are targeted with great accuracy towards focal adhesions (Krylyshkina et al., 2003), they can be stabilised there (Kaverina et al., 1998) and have been suggested to deliver regulatory components for turnover of these sites (Kaverina et al., 1999). Thus, MTs appear to be involved in aspects of cell polarity and migration at multiple levels.

MTs are synthesised by the linear polymerisation of alpha- and beta-tubulin dimers into polar, hollow fibres. In fibroblasts most MTs originate at the MTOC and growth occurs at one end (the plus end) of the fibre. A remarkable feature of the MT cytoskeleton is called dynamic instability, i.e. the switch of MTs from growth to shrinkage and vice versa (Desai and Mitchison, 1997). In cultured fibroblasts most MTs are dynamic and the shrinking ones actually provide tubulin subunits for incorporation into growing MTs. In spite of the intrinsic dynamic nature of MTs, a subset of MT fibres is stable and does not appear to undergo net growth or shrinkage. Such MTs become posttranslationally modified and are specifically stained by antibodies (Bulinski and Gundersen, 1991). In motile fibroblasts and astrocytes, stable MTs are asymmetrically distributed towards the leading edge of the cell, upon signalling with specific factors (Cook et al., 1998; Etienne-Manneville and Hall, 2001). These

MTs have been suggested to form an important component of cell polarity (Gundersen et al., 2004).

Regulation of MT dynamic behaviour in cells occurs by a large group of structurally different MT- or tubulin-associated proteins. Recently, "MT plus-end tracking proteins", or +TIPs (Schuyler and Pellman, 2001) have attracted a lot of attention, because these proteins localise specifically at the distal ends of MTs and regulate MT dynamics from this position (for review, see Akhmanova and Hoogenraad, 2005). +TIPs also appear to act as part of a MT capture device, that enables prolonged contact between the cell cortex and MTs. Among the +TIPs are CLIPs (cytoplasmic linker proteins) and CLASPs (CLIP-associating proteins), EB1 (end binding protein 1) and related proteins, and APC (adenomatous polyposis coli). Mammalian CLIPs and their yeast counterparts are positive regulators of MT growth (for review, see Galjart, 2005). EB1 has a cell type specific and cell cycle dependent influence on MTs, perhaps because this protein has many interaction partners, including APC , CLIPs and CLASPs. Mammalian CLIPs and EB1-related proteins are detected on all growing MTs, indicating that their action is in principle not restricted to a particular site in the cell or a subset of MTs. By contrast, CLASP2 and APC can distribute asymmetrically and both proteins play a role in the local stabilisation of MTs at the leading edge of motile cells (Akhmanova et al., 2001; Etienne-Manneville and Hall, 2003; Nathke et al., 1996).

In fixed 3T3 fibroblasts, redistribution of CLASP2 to the leading edge is observed after serum induction and depends on the local activation of PI3 kinase and inactivation of GSK3-beta (Akhmanova et al., 2001). Recent data indicate that Rac is an upstream spatial regulator of GSK3beta and CLASP (Wittmann and Waterman-Storer, 2005). Studies in neurons suggest that CLASP is controlled by the Abl kinase, which acts downstream of the signalling molecule Slit (Lee et al., 2004). RNA interference (RNAi) studies in HeLa cells have shown that CLASPs stabilise MTs by acting as local rescue factors and that they may bridge interactions between MTs and the cell cortex (Mimori-Kiyosue et al., 2005). These data have established a role for CLASPs in the local stabilisation of MTs and have started to reveal the upstream factors which act on CLASPs. Several studies have also documented a role for APC in the local stabilisation of MTs in astrocytes, neurons and fibroblasts (Etienne-Manneville and Hall, 2003; Wen et al., 2004; Zhou et al., 2004). APC function in DRG neurons and astrocytes is regulated by GSK3beta (Etienne-Manneville and Hall, 2003; Zhou et al., 2004), whereas in 3T3 fibroblasts a complex of APC, EB1 and mDia1 was suggested to control the formation of stabilised, leading edge MTs (Wen et al., 2004).

Given the apparently overlapping roles of APC and CLASPs, we were interested in analyzing the mechanism of CLASP2 action in more detail. Here, we provide evidence for the targeting of CLASP2 to focal adhesions and the increased immobilisation of GFP-CLASP2 on distal ends of MTs, that are directed towards focal adhesions and the leading edge. Using CLASP2-deficient mouse embryonic fibroblasts (MEFs) we show that CLASP2 plays a role in the serum- and fibronectin-induced stabilisation of MTs in fibroblasts. Our data indicate that CLASP2 is part of a positive feedback loop at the ends of stable MTs, thus sustaining cell polarity in response to highly specific signalling cues.

Results

Characterisation of GFP-CLASP2 in a stably expressing 3T3 cell line

To analyse the dynamic behaviour of CLASP2 during cell migration, we generated a stable GFP-CLASP2 expressing 3T3 cell line using the tetracycline-controlled transcription system (Tet-on system, Baron and Bujard, 2000); for details, see Materials and Methods). With this system the expression levels of GFP-CLASP2 can be regulated, which is important because abundant overexpression of this protein may have consequences for the MT network. Using the same approach, we also generated 3T3 cell lines expressing GFP-CLIP170 (data not shown). The latter served as control for GFP-CLASP2 behaviour and will be described elsewhere in more detail.

We analyzed protein extracts of GFP-CLASP2 expressing cell lines, either treated with doxicyclin, or not treated (Supplementary Fig. 1A). In one cell line (clone 86) GFP-CLASP2 expression is induced after treatment with doxicyclin, hence this clone was chosen for further analysis. Western blot analysis demonstrates a correct size of GFP-CLASP2 (Supplementary Fig. 1A). Immunofluorescence analysis shows that in nonmigratory 3T3 cells GFP-CLASP2 is localised near the Golgi apparatus and on MT ends (Supplementary Fig. 1B-D). The application of lithium chloride, an inhibitor of GSK3beta, on nonmigratory cells caused a significant increase of GFP-CLASP2 signal at distal ends of MTs (data not shown).

In the wound healing model confluent MEFs are deprived of serum for 24-48 hours. Subsequently, a cell free area is generated by scratching the confluent cell layer and removing several layers of cells (generating the “wound”). Immediately afterwards, cells are incubated in medium with serum, which induces their migration into the cell-free area (“wound healing”). Under these conditions we detected GFP-CLASP2 at the distal ends of stable MTs, which were mostly directed towards the leading edge of clone 86 cells (Supplementary Fig. 1E-G).

Time-lapse analysis (Supplemental information, movies 1 and 2 and data not shown) demonstrated the presence of comet-like GFP-CLASP2 dashes, which moved with an average velocity of 0,48 +/- 0,09 micrometres per second (63 dashes analysed in 11 cells, standard deviation indicated). These values are consistent with the speed of movement of other GFP-tagged +TIPs (Stepanova et al., 2003) and are similar to the movement of GFP-CLASP2 in transiently transfected COS-1 cells (Akhmanova et al., 2001). Combined, these data strongly suggest that GFP-CLASP2 recapitulates the behaviour of endogenous CLASP2 in 3T3 cells, including regulation of its MT binding capacity by by GSK3beta.

GFP-CLASP2 is targeted to the leading edge of motile cells and to focal adhesions

Wound healing on GFP-CLASP2 expressing cells was performed to investigate (re)localisation of GFP-CLASP2 after serum induction. We first imaged live cells at the wound at low resolution, with a time interval of 20 seconds between consecutive images. GFP-CLASP2 redistributed towards the leading edge within 3-5 minutes after serum addition and after about 15-20 minutes we observed a complete accumulation of polarized GFP-CLASP2 at the wound edge (Supplementary information, movie 3). These data are consistent with the behaviour of CLASP2 in fixed 3T3 cells (Akhmanova et al., 2001).

We analysed whether cell migration into a wound influences the velocity of GFP-CLASP2 displacements in cytoplasmic areas (Supplemental Information movie 4 and data not shown). After the addition of serum, we measured an average speed of fluorescent dashes of 0,44 +/- 0,05 micrometres per second (standard deviation indicated, 57 dashes analyzed in 9 cells). This is similar to movement of GFP-CLASP2 dashes in non-motile clone 86 cells (see above), suggesting that the relocalisation of GFP-CLASP2 during cell migration does not affect MT growth velocities in the cytoplasm of cells.

We noted that GFP-CLASP2 also accumulated at specific intracellular sites. Co-staining with anti-paxillin and anti-vincullin antibodies showed that GFP-CLASP2 targets to focal adhesions (Fig. 1A-F). Co-staining of endogenous CLASP2 and focal adhesion markers in 3T3 cells confirmed the GFP staining pattern (data not shown). An exact colocalisation GFP-CLASP2 with vincullin or paxillin was not observed. Some focal adhesions, mostly oriented in the interior of the cell, were actually devoid of GFP-CLASP2. Conversely, some GFP-CLASP2 accumulations inside cells were not stained by vincullin or paxillin, indicating that GFP-CLASP2 is targeted towards focal adhesions with different kinetics compared to vinculin or paxillin.

Imaging of motile clone 86 cells suggested that the accumulations of GFP-CLASP2 in areas near the cell edge and at focal adhesions are static compared to the "comet-like" dashes. However, fluorescent dashes of GFP-CLASP2, which represent growing MTs, often entered (and exited) areas of "static" GFP-CLASP2 accumulation. Each accumulation had its distinct pattern of behaviour and was able to change size, becoming larger or smaller, even within the time frame of a movie (data not shown). These data indicate that GFP-CLASP2 is targeted to focal adhesions and the leading edge in a highly regulated manner.

GFP-CLASP2 mobility and conformation

We used fluorescent recovery after photobleaching (FRAP) and fluorescence loss in photobleaching (FLIP) to analyze the intracellular mobility of GFP-CLASP2. Relatively large areas of the cell were bleached (Fig. 1 and Supplementary Fig. 2, see also Supplemental Information movies 5-7) that often included focal adhesions and/or the leading edge. We then selected small rectangles (regions of interest, or ROIs) inside and outside of the bleached areas to compare fluorescent recovery (or loss) in ROIs that contained an accumulation of GFP-CLASP2 and in cytoplasmic areas next to these sites.

In Fig. 1G-I (corresponding to Supplemental Information movie 5) an experiment is shown in which an area (ROI 1) near the leading edge of a motile cell was bleached. ROI 6, which is in part of the leading edge that was not bleached, maintains roughly equal fluorescence intensity throughout the experiment (Fig. 1I). Recovery of fluorescence in ROIs 4 and 5, which are inside ROI 1 and next to the area of local GFP-CLASP2 accumulation, takes approximately 50 seconds. Fluorescence recovery in areas within the zone of GFP-CLASP2 accumulation (ROIs 2, 3) is slower. In addition, a significant fraction of GFP-CLASP2 in ROIs 2 and 3 appears to be immobile, as it does not recover within the time frame of the experiment. These data indicate that leading edge accumulations of GFP-CLASP2 are relatively immobile. In Supplementary Fig. 2A-D (corresponding to Supple-

mental Information movie 6) an area near the leading edge of another GFP-CLASP2 expressing cell was bleached, with similar results.

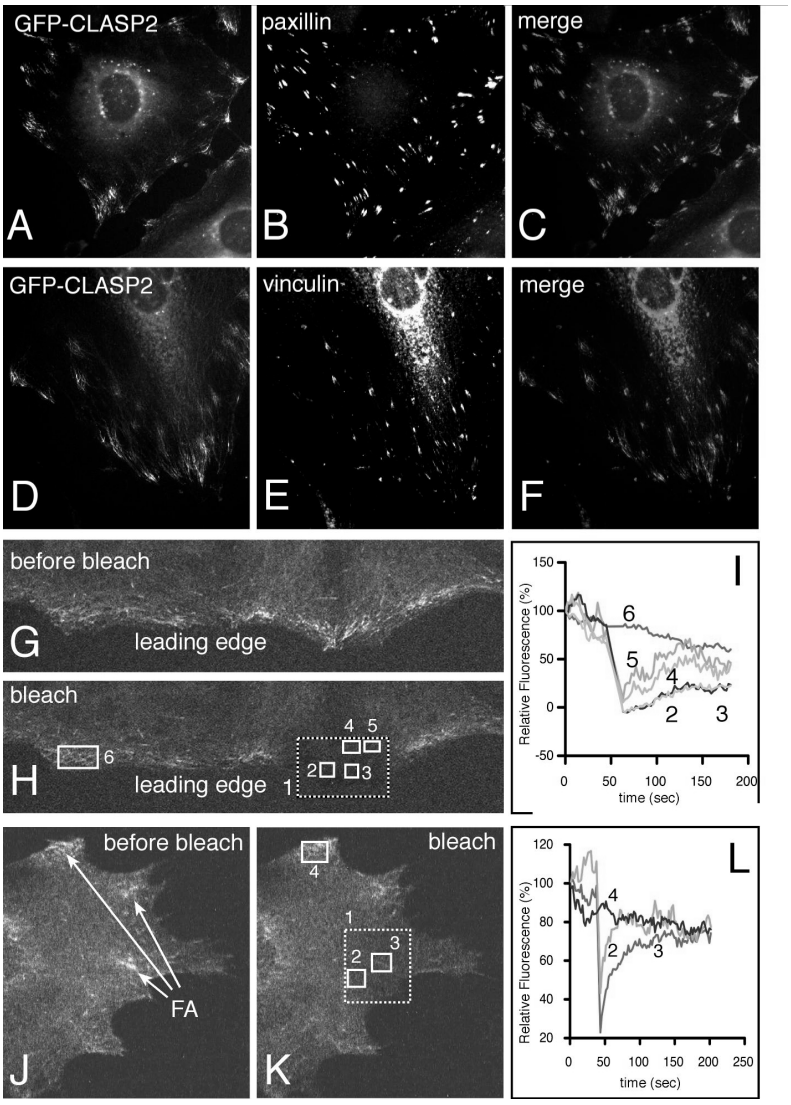

Figure 1. GFP-CLASP2 behaviour in 3T3 cells.
A-F) Clone 86 cells, expressing GFP-CLASP2 were fixed and stained with anti-paxillin (B, C) or anti-vinculin (E, F) antibodies. Notice the colocalisation of GFP-CLASP2 with these markers of focal adhesions. The colocalisation is not complete.
G-L) Migrating clone 86 cells, expressing GFP-CLASP2, were bleached (ROI 1, indicated by stippled rectangles in H and K). Fluorescence loss or recovery was measured in the indicated ROIs. In panels G, J still images are shown prior to bleaching, which was done during 5 seconds. In panels H, K still images are shown immediately after bleaching. In panels I, L fluorescence intensities are plotted of the different ROIs. FA: focal adhesion. Notice that GFP-CLASP2 fluorescence recovers more slowly in regions that contain accumulations of the protein.

In Fig. 1J-L (corresponding to Supplementary Information movie 7) a region of a GFP-CLASP2 expressing cell, including a focal adhesion, was bleached. Recovery of GFP-CLASP2 in the focal adhesion (ROI 3) is complete approximately 100 seconds after the bleach. Strikingly, a similarly sized rectangle next to this focal adhesion (ROI 2) reveals recovery after approximately 30 seconds, which is 3 times faster and indicates that GFP-CLASP2 in focal adhesions near the leading edge is more immobile than in regions next to these sites.

Pronounced differences in GFP-CLASP2 recovery were not detected in ROIs that were placed inside bleached areas that contained neither focal adhesions nor leading edges; we also did not detect significant differences in a similar FRAP analysis in 3T3 cells stably expressing GFP-CLIP170 (data not shown). Combined, the data suggest that GFP-CLASP2 is relatvely immobile in focal adhesions and at the leading edge, compared to other areas of the cell.

We next examined whether GFP-CLASP2 is delivered to focal adhesions by virtue of its association with MT ends. In Supplemental Information movie 8 most, if not all, cytoplasmic GFP-CLASP2 comets move in one direction only (i.e. downward, see also the still image in Supplemental Fig. 2A). Accumulation of GFP-CLASP2 is observed both above (ROI 2) and below (ROI 3) the bleach zone. After bleaching both accumulations show significant fluorescence loss (Supplementary Fig. 2G), indicating that they have exchanged fluorescent for non-fluorescent GFP-CLASP2. In ROI2, the latter must have arrived by a mechanism other than delivery via MT ends, since comets move 'downwards' and non-fluorescent GFP-CLASP2 has moved 'upwards'.

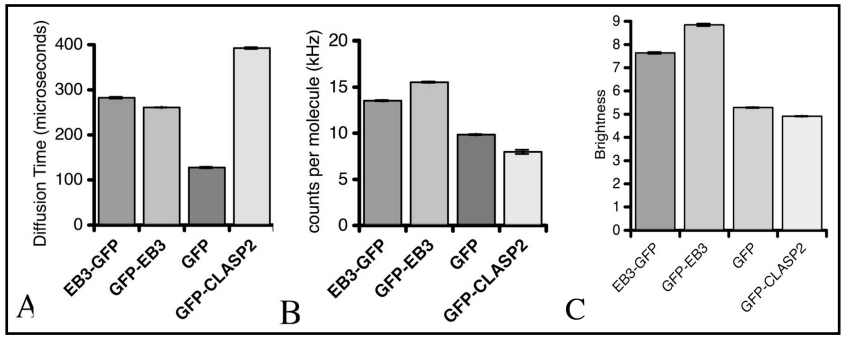

Figure 2. FCS and PCH analysis of GFP-CLASP2.
A, B) FCS analysis of GFP-CLASP2, EB3-GFP, GFP-EB3 and GFP in extracts of transfected COS-1 cells. In panel A diffusion times are indicated, in panel B the counts per molecule.
C) PCH analysis of GFP-CLASP2, EB3-GFP, GFP-EB3 and GFP in extracts of transfected COS-1 cells. Combined the analyses suggest that GFP-CLASP2 is monomeric.

It is unknown whether CLASPs are monomeric or multimeric in solution. We used fluorescence correlation spectroscopy (FCS) and Photon Counting Histogram (PCH) approaches to examine the diffusion characteristics and the conformation of soluble GFP-

CLASP2 in lysates from transfected COS-7 cells, as compared to GFP, EB3-GFP and GFP-EB3. The FCS analysis indicates that in cell extracts GFP-CLASP2 diffuses approximately 4 times more slowly than GFP (Fig. 2A). The diffusion time of GFP-CLASP2 is, however, only marginally less than that of EB3-GFP and GFP-EB3, in spite of the fact that the M_r of GFP-CLASP2, which is approximately 170 kDa, is three times that of monomeric EB3-GFP. In addition, the counts per molecule (cpm) value is lower for GFP-CLASP2 than for EB3-GFP or GFP-EB3 (fig. 2B). We therefore performed a PCH analysis to examine molecular brightness of these molecules. The PCH results show that GFP-CLASP2 has a molecular brightness that is comparable to that of monomeric GFP and lower than that of dimeric EB3-GFP, or GFP-EB3 (Fig. 2C). Combined, these data strongly suggest that soluble GFP-CLASP2 is monomeric. The local retardation of GFP-CLASP2 in focal adhesions and at the leading edge is therefore best explained by interactions of monomeric CLASP molecules with MTs, other proteins and/or membranes.

Characterisation of CLASP2 knock out MEFs.

To analyze the behaviour of CLASP2-deficient cells during cell migration and adhesion, we generated a knock out allele. For this purpose, a GFP-loxP-pMC1neo-loxP cassette was inserted in an exon that is common to all known *Clasp2* mRNAs (Fig. 3A), using homologous recombination in embryonic stem (ES) cells (K. Drabek and N. Galjart, manuscript in preparation). In this modified CLASP2 allele expression of CLASP2 is interrupted by the GFP open reading frame and the transcription of the neomycin resistance gene (neo) is antisense with respect to the CLASP2 gene (Fig. 3A).

ES cells were used to generate CLASP2 knock out mice (K. Drabek and N. Galjart, manuscript in preparation). We derived mouse embryonic fibroblasts (MEFs) from E13.5 day CLASP2 knock out embryos and wild type littermates. Western blot analysis on confluent fibroblasts, derived from two wild type and two knock out cell lines and using different anti-CLASP2 antisera, demonstrates that CLASP2 (~160 kDa in wild type cells) is not present in the knock out cells (Fig. 3B). The levels of tubulin, actin and CLASP1 (Fig. 3C, D), CLIP-115, CLIP-170, p150Glued, EB1 and EB3, focal adhesion markers and beta-catenin (Supplemental Fig. 3) are not significantly affected by a lack of CLASP2. Surprisingly, the levels of acetylated alpha-tubulin, which is a marker for stable MTs, are similar in confluent CLASP2 knock out and wild type MEFs (Fig. 3D). Since the RNAi approach in HeLa cells suggested that CLASPs play redundant roles in the stabilisation of MTs (Mimori-Kiyosue et al., 2005), we assume that in confluent cells CLASP1 levels are sufficient to maintain stable MTs.

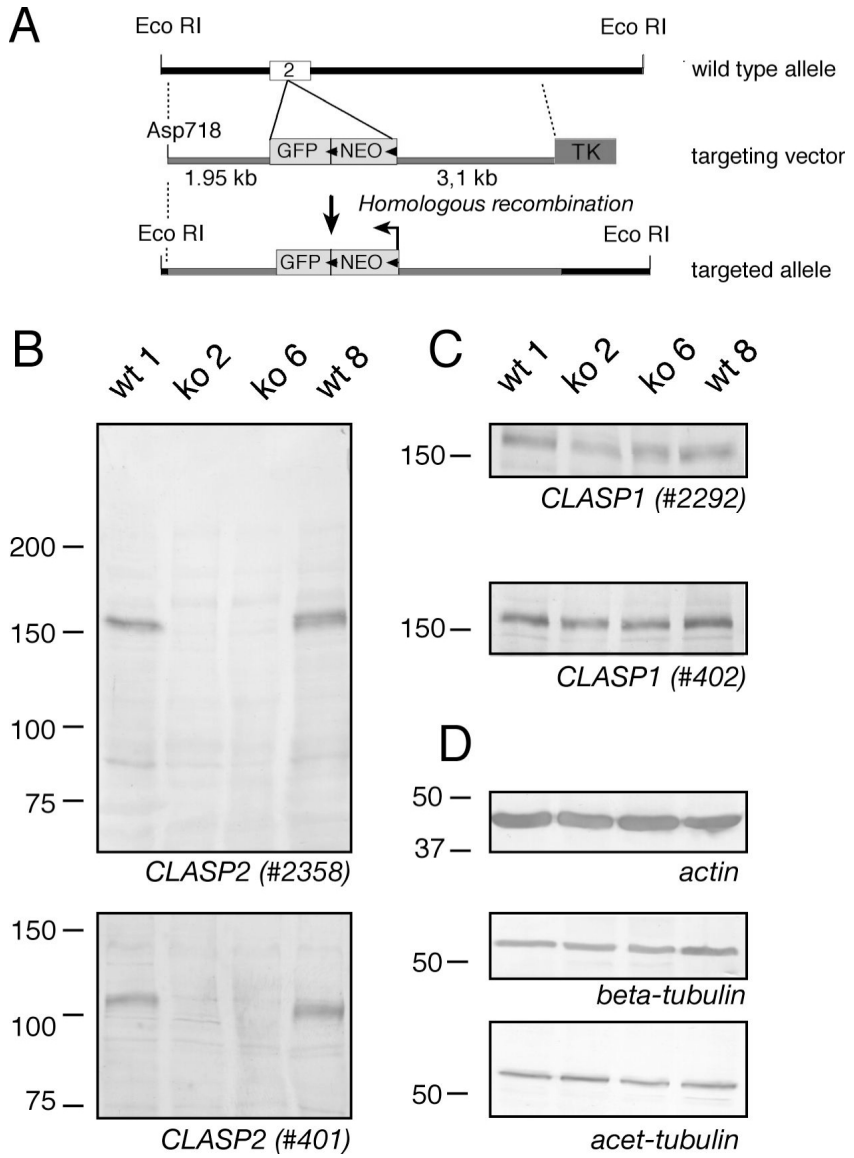

Figure 3. Generation of CLASP2 knock out fibroblasts.
A) Targeting strategy. The murine CLASP2 gene was targeted by inserting a casette (GFP-lox-neo-lox, where "neo" is the neomycin resistance gene) into a common exon used by all known splice variants (common exon 2). The neo gene is transcribed antisense with respect to the CLASP2 gene. Selected restriction enzyme sites are shown. TK: the thymidine kinase negative selection marker.
B-D) Western blot analysis. Cell extracts were made of two wild type (lines 1 and 8) and two CLASP2-deficient (lines 2 and 6) MEF lines. Western blots were incubated with antibodies against CLASP2 (#2358, #401), CLASP1 (#2292, #402), beta-tubulin, acetylated tubulin and actin.

To investigate whether deletion of CLASP2 influences MT dynamics, we transfected EB3-GFP into CLASP2 knock out and wild type MEFs and measured speed of movement of the fusion protein, which reflects the rate of MT polymerisation and is an indirect measure of the ratio of tubulin versus MTs. The average velocity of EB3-GFP in CLASP2 knock out MEFs (0.44 +/- 0.11 micrometres per second, 58 dashes analysed in 5 cells, standard deviation indicated) is somewhat lower than in wild type cells (0.55 +/- 0.23 micrometres per second, 26 dashes analysed in 3 cells, standard deviation indicated), whereas the average length of EB3-GFP displacements is similar (1.48 +/- 0.50 micrometre in CLASP2 knock out MEFs (66 dahses analysed +/- standard deviation) and 1.39 +/- 0.52 micrometre in wild type MEFs (106 dashes analysed +/- standard deviation)).

We examined MT growth rates also by measuring the average rate of GFP-CLIP170 movement, instead of EB3-GFP. For this analysis, we chose to use adult dermal fibroblasts that carried a GFP-CLIP170 knock in allele (Akhmanova et al., 2005) in the wild type or CLASP2 knock out background. Thus, these cells do not require transfection to visualise MT growth rates. MT growth rates were similar in GFP-CLIP170 expressing cells, i.e. 0.44 +/- 0.06 micrometres per second in CLASP2 knock out cells (30 dashes analysed in 6 cells, standard deviation indicated), versus 0.45 +/- 0.04 micrometres per second in wild type cells (24 dashes analysed in 4 cells, standard deviation indicated). Thus, deletion of CLASP2 has no significant influence on MT growth rates under normal culture conditions.

Effects of a CLASP2 deficiency on parameters of cell polarity

Because confluent CLASP2 deficient cells have normal levels of stabilised MTs, we examined whether CLASP2-deficient cells could form stable MTs in a wound healing assay. Cells were fixed at different time points after serum induction and stained with antibodies recognising stable MTs and other antisera (Fig. 4). The results show that a MT array is present after serum induction, that is directed towards the leading edge in wild type and CLASP2 knock out fibroblasts (Fig. 4A-D). Furthermore, both EB1 and -3 (Fig. 4M-P and data not shown) and CLIP-115 and -170 (Fig. 4Q-T and data not shown) are detected at MT ends of motile CLASP2 knock out and wild type MEFs. However, in wild type cells the formation of stable MTs, as measured with antisera against acetylated alpha-tubulin (acet-tub) and detyrosinated (glu-tub) alpha-tubulin, is significantly more obvous than in knock out cells (Fig. 4E-L).

To examine the quantitative effect of a CLASP2 deficiency on MT stabilisation during wound healing, we performed western blot analysis. This revealed that the formation of stable MTs is particularly affected in the first hours of wound healing in CLASP2 knock out cells (Fig. 4U). At later time points stable MTs do form, which might explain why there is no obvious reduction in confluent, serum-fed fibroblasts. We conclude that in motile, serum-induced MEFs CLASP2 is important for the formation of a subset of stabilised MTs and that under such conditions CLASP1 can not rescue this function fully.

Centrosome reorientation in fibroblasts is dependent on Cdc42 and the dynein-dynactin motor complex, but not on stable MTs (Palazzo et al., 2001b). In line with this hypothesis CLASP2-deficient cells are able to reorient their centrosomes, 2-6 hr after serum induction in the wound healing paradigm (Fig. 5A). However, we noted an increased number

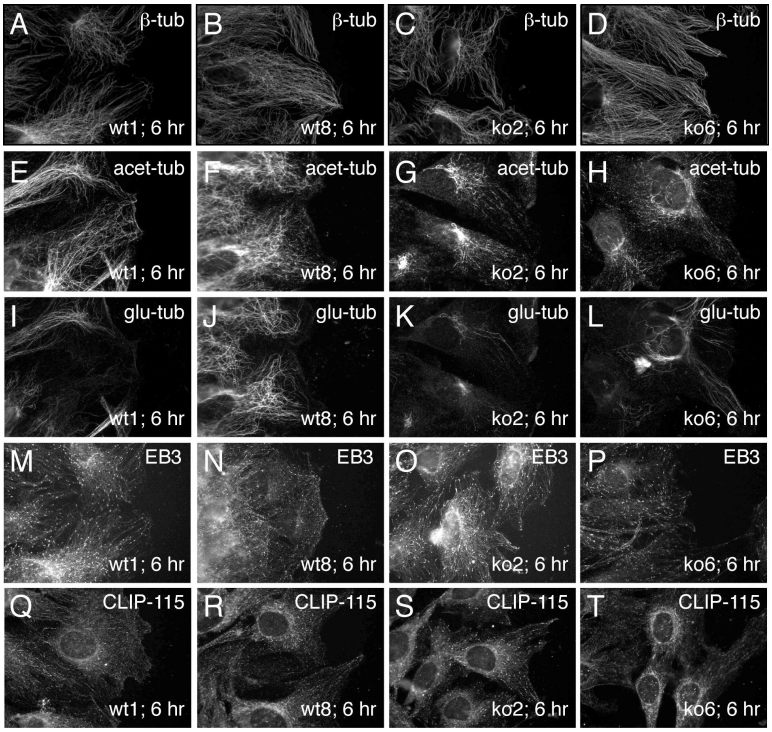

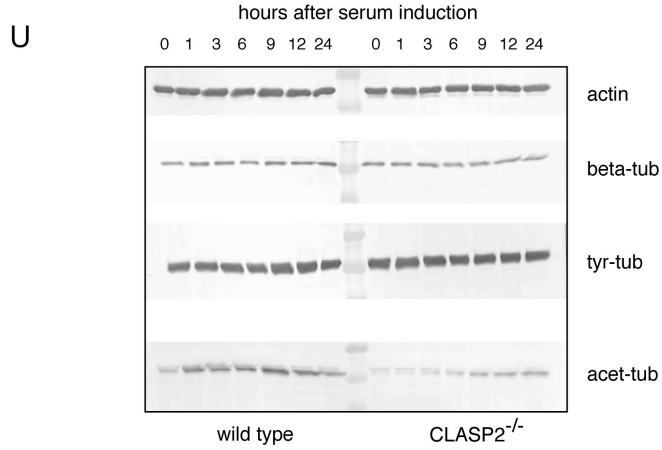

Figure 4. CLASP2 regulates microtubule stabilisation in fibroblasts.
A-T) Immunofluorescent analysis of wild type (lines 1 and 8) and CLASP2 knock out (lines 2 and 6) MEFs. Fibroblasts were examined in the wound healing assay, shown are migrating cells 6 hours after serum induction. Antibodies: acetylated and glu-tubulin, beta-tubulin, EB -3 and CLIP-115.
U) Western blot analysis of proteins after serum starvation and induction. Antibodies against actin, beta-tubulin, tyrosinated tubulin and acetylated tubulin were used.

of cells from the CLASP2 knock out background in which centrosomes were separated (data not shown). These results indicate that CLASP2-mediated stabilisation of MTs is not required for centrosome reorientation. However, CLASP2 is required for maintaining mother and daughter centrioles in close proximity.

One obvious phenotype of CLASP2 deficient fibroblasts is the formation of thin and long, phalloidin-positive cell protrusions (Fig. 5B-E). In the wound healing assay these extensions are mostly located at the rear of the CLASP2 knock out cells, but we also observed increased numbers of extensions in normal cultured cells. Moreover, CLASP2 knock out fibroblasts that migrate into the wound are more often randomly oriented in comparison to wild type cells (Fig. 5D, E). These results indicate that deletion of CLASP2 causes both polarity and motility defects in MEFs. It is noteworthy that CLASP2 is mainly targeted to the leading edge of motile cells, yet one of the obvious phentotypes that we observe during migration is actually located at the back of the cell.

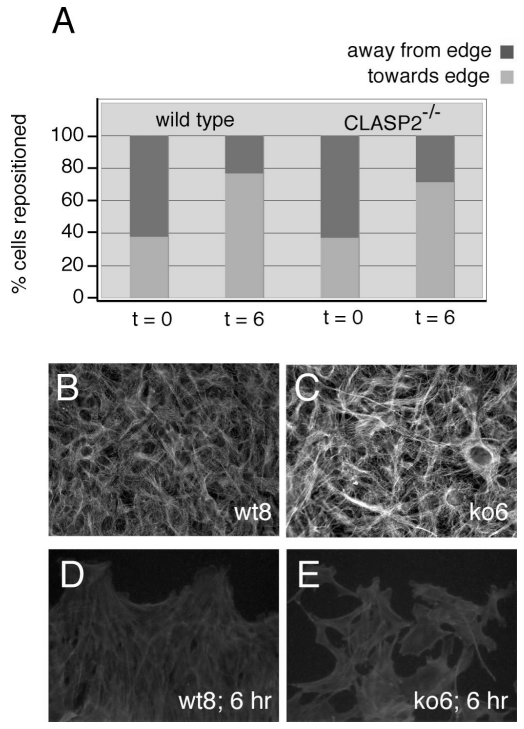

Figure 5. Effect of CLASP2 knock out on cell behaviour.

A) Centrosome repositioning in wild type and CLASP2 knock out MEFs. Two independent cell lines were measured for each genotype. Cells were fixed and stained with antibodies against gamma-tubulin, a centrosomal marker. In four independent experiments 100 cells at the leading edge were scored whether their centrosome was oriented towards the leading edge. We plotted the average values, notice that both types of cells reorient their centrosomes after serum induction.

B-E) Phalloiding staining in wild type and CLASP2 knock out MEFs. In B, C confluent cells were stained, whereas in D, E migrating cells were stained. Notice trailing end extensions in the CLASP2 knock out fibroblasts. CLASP2-deficient cells do not migrate as a sheet of cells into the wound.

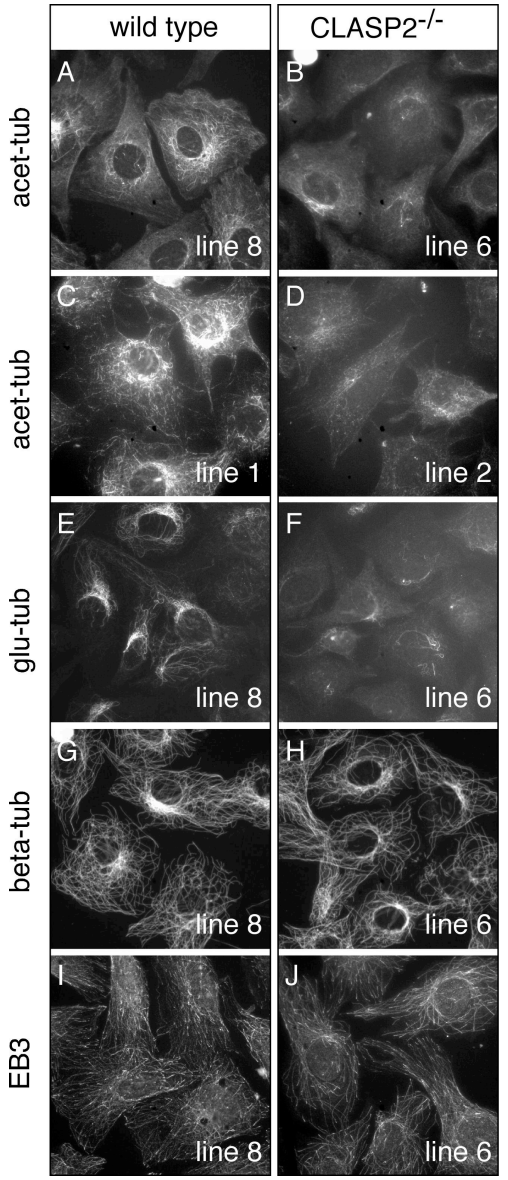

Figure 6. Fibronectin induced microtubule stabilisation is inhibited in CLASP2 knock out MEFs.
Immunofluorescent analysis of wild type (lines 1 and 8) and CLASP2 knock out (lines 2 and 6) fibroblasts, after adherence for 90 minutes to fibronectin.
A-F) CLASP2 knock out MEFS do not form stable MTs as efficiently as wild type cells, as measured with two different antibodies (anti-acetylated tubulin and anti-detyrosinated tubulin).
G, H) CLASP2 knock out fibroblasts form a normal MT array.
I, J) EB3 is normally localised at the ends of MTs in CLASP2 knock out fibroblasts.

CLASP2 is involved in fibronectin-induced microtubule stabilisation

The finding that GFP-CLASP2 targets to focal adhesions and that CLASP2 mediates MT stabilisation in motile cells, prompted us to investigate whether this protein is involved in local MT stabilisation after adherence of fibroblasts to fibronectin, since this involves integrins and focal adhesions (Palazzo et al., 2004). We plated serum-starved wild type and CLASP2 knock out MEF lines, that had been maintained in suspension for 30 minutes, on fibronectin- (or on poly-L-ornithine-)coated glass coverslips. We then examined the appearance of focal adhesions and stabilised MTs 90 minutes after plating, by immunofluorescence analysis (Fig. 6). After adherence to fibronectin, wild type MEFs form stable MTs, as detected with anti-acetylated and anti-detyrosinated alpha-tubulin antisera (Fig. 6A, C, E). By contrast, the CLASP2-deficient cells fail to form such arrays, independent of the antibody used (Fig. 6B, D, F). A MT array is present in both cell types (Fig. 6G, H) and EB3 is localized to MT ends (Fig. 6I, J). MT stabilisation is rescued in cells expressing GFP-CLASP2 (data not shown). In the case of adherence to poly-L-ornithine hardly any stable MT could be detected in wild type or CLASP2-deficient cells (data not shown). These data indicate that CLASP2 is involved in fibronectin-mediated signalling that leads to formation of stable MTs.

Upon adherence to fibronectin, both wild type cells and CLASP2 knock out cells form focal adhesions, as detected with an antibody against phosphorylated focal adhesion kinase (FAK-pY397, data not shown). These data indicate that in CLASP2 knock out fibroblasts, the fibronectin and integrin-mediated signalling pathway to generate focal adhesions is intact. In line with these results we find that during wound healing FAK-pY397 levels are not significantly different in CLASP2 knock out cells compared to wild type fibroblasts (data not shown).

Discussion

Using CLASP2-deficient MEFs, we show here that CLASP2 mediates the stabilisation of a subset of MTs in motile and fibronectin-adherent cells. A role for CLASP2 in MT stabilisation in motile MEFs is consistent with our previous studies in 3T3 cells (Akhmanova et al., 2001). Our RNAi knock down analysis in non-motile HeLa cells suggested that CLASP1 and -2 may have redundant functions in MT stabilisation (Mimori-Kiyosue et al., 2005). The present data indicate that CLASP1 indeed may compensate for CLASP2 in confluent MEFs, as we do not detect a deficiency in stable MTs in such cells. However, after stimulation of migration with serum, or adherence to fibronectin, the CLASP2 deficiency does become visible. Either the levels of CLASP1 are not sufficient to compensate under these conditions, or there are protein-specific functions for CLASP1 and -2.

The present data implicate CLASP2 in a specific signalling pathway that responds to fibronectin and that leads to the stabilisation of MTs. It has been shown that this signalling cascade is organised by integrins in focal adhesions and also involves Rho and mDia (Palazzo et al., 2004). The block in signal transduction in CLASP2-deficient MEFs occurs after FAK phosphorylation, indicating that initial signalling events are intact. Using GFP-CLASP2 in 3T3 cells, we show that CLASP2 is targeted to focal adhesions. Thus, unlike Rho and mDia (Palazzo et al., 2004), CLASP2 is present at the right place and at the right

time to perform a MT stabilising role. Interestingly, in Drosophila neurons, CLASP is a target of the tyrosine kinase Abl (Lee et al., 2004). The activities of Abl and the tyrosine kinase Abl-related gene (Arg) are similar (for review, see (Hernandez et al., 2004) and Arg has been shown to be important for the adhesion of fibroblasts to fibronectin (Miller et al., 2004). It will therefore be interesting to see if CLASP2 is a target of Arg in fibroblasts. If so, we predict that Arg phosphorylates CLASP2 to increase its affinity for MTs.

We found that after serum-induction, motile and CLASP2-deficient MEFs had problems in increasing their content of stable MTs, directed towards the leading edge. Instead, we detected long cytoplasmic extensions at the rear of a subset of migrating CLASP2$^{-/-}$ cells. Cells did migrate into the wound but not as a "sheet", like wild type cells, making a quantitative measurement of migration velocity difficult. We further found that the longitudinal axis of migrating CLASP2-deficient cells was less uniformly oriented with respect to the wound edge. Taken together, these data suggest that lack of CLASP2 at the leading edge results in defects in the overall maintenance, but not the initiation, of polarity. The extensions at the rear of some of the cells could indicate a deregulated Rho activity. Further studies are required to determine whether CLASP2 regulates Rho and/or targets of this small GTPase directly or indirectly.

In 3T3 cells a complex of APC, mDia and EB1 has been implicated downstream of Rho in the control of stable, leading edge-oriented MTs (Wen et al., 2004). How can this result be reconciled with our data, both in 3T3 cells (Akhmanova et al., 2001) and in MEFs (our present data), that it is CLASP2 that is mainly responsible for local MT stabilisation? One explanation is that a single pathway exists that leads to the local stabilisation of MTs. In this view, CLASPs, APC and other MT regulatory factors such as the spectraplakin ACF7 (Kodama et al., 2003) would each have essential, sequential roles in regulating MT dynamics. Indeed all three proteins bind EB1 (for review, see Galjart, 2005). However, CLASP2$^{-/-}$ cells do migrate, albeit in a perturbed manner, whereas 3T3 cells in which APC-mDia-EB1 function is perturbed, do not (Wen et al., 2004). Moreover, recent data indicate that in migrating epithelial cells APC and CLASP2 are targeted to completely different subsets of MTs (Wittmann and Waterman-Storer, 2005), making it unlikely that these proteins have significant redundancy in vivo. Thus, a second and more likely possibility is that the complex of APC-mDia-EB1 would be specifically required for lysophosphatidic acid-mediated MT stabilisation, whereas CLASP2 is involved in other signalling pathways, for example, the one which leads to fibronectin-mediated MT stabilisation. In addition, a different protein composition in different cell lines may determine which factor plays a role in MT stabilisation. For example, in our MEFs, as well as in our 3T3 cell cultures, both EB1 and EB3 are expressed, whereas in the report of Wen and colleagues an RNAi knock down of EB1 was sufficient to see an effect, indicating that EB3 is not expressed in the 3T3 cells used in that study (Wen et al., 2004). In addition, our MEFs do not express clearly detectable levels of APC (M. van Ham and N. Galjart, unpublished observations). This leads us to propose a third possibility, which is that CLASPs are required for MT stabilisation in specific cell types while APC is required in other cell types.

A rapid CLASP polarisation towards the leading edge of motile fibroblasts has been described in fixed 3T3 cells (Akhmanova et al., 2001). We generated a stable line of GFP-

CLASP2 expressing 3T3 cells to study how this protein behaves dynamically, particularly during cell migration. Consistent with the previous study, we find that GFP-CLASP2 redistributes within 3-5 minutes after serum induction to the leading edge of 3T3 cells. Furthermore, using the inducible clone 86 cell line, we observed, for the first time, GFP-CLASP2 accumulation at focal adhesions. This was corroborated by immunocytochemical staining with antibodies against endogenous CLASP2 in 3T3 cells. Focal adhesions are dynamic structures that constantly undergo assembly and disassembly during cell migration. It was proposed that the MT cytoskeleton modulates focal adhesion turnover via specific targeting interactions (Small et al., 2002). Our data in fixed cells indicate that GFP-CLASP2 is more favourably targeted to focal adhesions that are positioned near the leading edge. In live studies, we visualised MTs with GFP-CLASP2 at their plus ends to grow over and into immobile GFP-CLASP2 accumulations, which we presume to be at adhesion complexes. Interestingly, we observed that the GFP-CLASP2 dashes entering focal adhesions were often following the same tracks. This observation corresponds to and can be explained by an earlier suggestion, that MTs polymerise along another cytoskeletal element (most likely, actin) that terminates in adhesion complexes (Salmon et al., 2002). Recently, we could show that CLASP2 actually interacts with actin filaments (Andrey S. Tsvetkov, Andrey Samsonov, Anna Akhmanova, Niels Galjart, Sergey V. Popov, manuscript submitted for publication). Thus, it is tempting to speculate that the interaction between CLASP2 and actin filaments actually causes MTs to follow the same track.

We visualised size changes and sometimes even the complete disassembly of particular GFP-CLASP2 accumulations, while growing MTs, decorated with GFP-CLASP2, targeted these sites. These observations are consistent with previous reports that focal adhesion targeting by MTs correlates with adhesion complex turnover (Kaverina et al., 1999) and are supported by observations that MTs are able to target very precisely into adhesion foci (Krylyshkina et al., 2003). The question to address is whether the attachment of stable MTs and the repeated targeting of dynamic MTs have the same or different effects on focal adhesions. After all, a different subset of proteins is associated with the ends of dynamic, growing MTs, as compared to static, stable MTs.

The accumulation of GFP-CLASP2 in focal adhesions, or at the leading edge is highly likely to depend on parameters such as type, size and location of the focal adhesion and the state of the leading edge. This individuality precluded a quantitative FRAP analysis of GFP-CLASP2 in these sites. However, we consistently noticed that GFP-CLASP2 is less mobile when localised at focal adhesions or at the leading edge, compared to adjacent sites. Such a qualitative observation does allow us to conclude that at the ends of stable MTs, CLASP2-positive domains are present, where the protein is relatively immobile.

Our previous data in 3T3 cells suggested that CLASP2 is a target of GSK3beta, whose activity is, in turn, regulated by PI3 kinase (Akhmanova et al., 2001). In migrating epithelial Ptk1 cells it is Rac1 that is upstream of GSK3beta and CLASP2 (Wittmann and Waterman-Storer, 2005). In Ptk1 cells, Rac1 inhibits GSK3beta in the broad lamellipodium into which “pioneering” MTs penetrate and this event leads to the association of CLASP2 with the MT lattice instead of the MT end. As a result, pioneering MTs that enter the big lamellipodium at the leading edge, are entirely labelled by CLASP2. However, these MTs

do not become stabilized (Wittmann and Waterman-Storer, 2005), whereas MTs in motile fibroblasts, that are labelled with CLASP2 at distal segments and that are directed towards the leading edge, do become stabilised (Akhmanova et al., 2001). These data indicate that although the regulation of CLASP2 behaviour by GSK3beta is similar in epithelial and fibroblastic cells, epithelial cells lack certain components in their lamellipodium that can "crosslink" CLASP2, render it more immobile and thereby cause MT stabilisation. This is consistent with the idea that the migration of epithelial cells is different from that of fibroblastic cells (Wittmann et al., 2003).

One mechanism proposed for MT tip association is called "treadmilling" (Perez et al., 1999). It involves the specific association of +TIPs with a freshly synthesized MT tip, followed by dissociation from the MT lattice somewhat later. Treadmilling explains CLASP2 association with MT plus ends in the cytoplasm. Our data suggest that soluble GFP-CLASP2 is a monomeric protein. This would partially explain why tip association of GFP-CLASP2 is more difficult to detect than that of dimeric EB3-GFP and GFP-CLIP-170. However, GFP-CLASP2 does not accumulate solely at focal adhesions by MT tip delivery. We hypothesise that a positive feedback loop involving CLASP2 exists: extracellular signalling (for example via fibronectin) causes the local activation of PI3 kinase (for example via integrins and/or focal adhesions). This in turn causes the inactivation of GSK3beta at specific cellular sites, which enables the CLASP2-mediated stabilisation of a subset of MTs. By as yet unknown mechanisms CLASP2 is rendered more immobile and is able to organise domains at the ends of stable MTs. This, in turn, maintains cell polarity. The proteins that mediate feedback loop signalling of CLASP2 are unknown, but one possibility is that CLASP2 acts to keep PI3-kinase localised and active.

Methods

Molecular biology

The rtTA2-M2 (pUHrT 62-1) regulator plasmid DNA (Baron and Bujard, 2000) was a kind gift of H. Bujard. The neomycin resistance plasmid (pHA178neo, vector pSP72), is a derivative of pMC1-NeopolyA. In the puromycin resistance plasmid (which is also pSP72 based), the selection gene is under control of the PGK promoter. pTRE-GFP-CLASP2 was generated using a short isoform of CLASP2 (CLASP2gamma, accession number AJ276961, see (Akhmanova et al., 2001)). To enhance splicing, we added a beta-globin intron just after GFPCLASP2 in the pTRE vector. Constructs for targeting of the murine *Clasp2* gene will be described elsewhere in more detail (K. Drabek and N. Galjart, manuscript in preparation).

For western blotting 3T3 cell cultures were harvested 24 hours after doxicycline induction (see below), and total protein extracts were prepared. Western blotting was performed as described earlier (Hoogenraad et al., 2000). Proteins were detected with the rabbit polyclonal antibodies against CLIPs and CLASP2 (see below) in a 1:2000 dilution, or anti-GFP (Clontech) in a 1:2500 dilution. Secondary goat anti-rabbit antibodies, coupled to alkaline phosphatase (Sigma) were used at 1:7000.

Cell culture and transfection

Swiss 3T3 fibroblasts were cultured in (1:1) DMEM/F10 medium with 8 % fetal calf serum. Cell lines, stably expressing GFP fusion proteins under doxicyclin control, were generated according to the instructions of the supplier (Clontech). Briefly, 3T3 cells were grown to 80% confluence and subsequently transfected with two linearized DNA plasmids (rtTA2-M2 and pHA178neo), using lipofectamine 2000 (Invitrogen). Cotransfection yielded 33 rtTA-positive clones from 100 resistant ones (data not shown). Selected, neomycin positive clones were transfected with linearized pTRE-GFP-CLASP2 DNA, together with a PGK-puromycin DNA, using lipofectamine 2000. Clone selection for GFP fusion protein was done by fluorescent microscopy, i.e. clones that contained fluorescent cells after doxicyclin induction were considered as positive. Positive clones after neomycin and puromycin selection represent stable cell lines containing GFP-CLASP2 fusions under control of rtTA. Different amounts of doxicyclin were added to induce variable expression levels of GFP-fusion proteins. This procedure yielded 9 GFP-CLASP2-positive clones out of 100 puromycin resistant clones (data not shown).

Targeting of the murine *Clasp2* gene in embryonic stem (ES) cells and the generation of CLASP2 knock out mice will be described elsewhere (K. Drabek and N. Galjart, manuscript in preparation). The generation of wild type and CLASP2 knock out MEF lines and of adult dermal fibroblasts, carrying a GFP-CLIP170 knock in allele in the CLASP2 knock out or wild type background, was performed as published (Akhmanova et al., 2005).

Immunofluorescent analysis

Cells were fixed and immunocytochemistry was performed as described earlier (Akhmanova et al., 2001; Akhmanova et al., 2005). Cells were stained with monoclonal antisera against actin, beta-tubulin, acetylated alpha-tubulin, vincullin, paxillin (all from Sigma) and GM130 (Transduction Laboratories) and with polyclonal antisera against detyrosinated alpha-tubulin (a kind gift of C. Bulinski) in a 1:100 dilution. Polyclonal rabbit antisera against CLASP1 (#2292, #402), CLASP2 (#2358, #401), CLIP-170 (2260) and CLIP-115 (2238) have been described (Akhmanova et al., 2001; Coquelle et al., 2002; Hoogenraad et al., 2000; Mimori-Kiyosue et al., 2005) and were used in a dilution of 1:300. Alexa 594- conjugated goat anti-mouse or anti-rabbit (Molecular Probes,1:500) and Alexa 350 sheep antimouse (Molecular Probes,1:300) were used as secondary antibodies.

Images were acquired as published (Akhmanova et al., 2005; Stepanova et al., 2003). Immunofluorescent analysis of 3T3 cells stably expressing GFP-CLIP170 or GFP-CLASP2 was performed before and after induction with doxicyclin, treatment with this compound was for 6-15 hours. The centrosome repositioning assay was performed as described (Etienne-Manneville and Hall, 2003), using antibodies against gamma-tubulin as marker for the centrosomes.

Cell migration

For cell migration experiments, we used a wound healing model as described previously (Akhmanova et al., 2001), which is based on the method described by Gundersen and co-workers (Liao et al., 1995). Briefly, cells were grown to confluence, after which serum was

removed for 24-48 hours. Subsequently, a stripe of cells was scratched off, creating a "wound" in the monolayer. Then serum was added to the culture medium again. Cells were analysed live, or after fixation at specific time points, followed by incubation with antibodies.

Live imaging

For fluorescent analysis of migration, cells were analyzed at 37 ^{0}C on a Zeiss LSM510 confocal laser scanning microscope. Cells were analyzed for 9-15 hours and image acquisition was started immediately after wounding. For phase-contrast analysis of the migration process, cells were analysed on an inverted microscope (Olympus).

Time-lapse imaging to record the growth speed of MTs was performed as described previously (Stepanova et al., 2003). Bleaching studies a Zeiss LSM510 system was used (488 nm laser set at 2%, image acquisition every 2-3 seconds (approximately 200 images per experiment). Bleaching was performed during the time-lapse assay, mostly after 50 images (several iterations with 488 nm laser set at 100%). The time-lapse imaging was continued for 150-200 seconds after bleaching. The movies were assembled and different parameters (velocities of MT growth, cell migration, fluorescent intensities in the FRAP assay) were estimated using LSM 510 software.

Fluorescence correlation spectroscopy (FCS) and photon counting histogram (PCH)

COS-7 cells were transfected using Polyfect (Quiagen) with GFP, GFP-EB3, EB3-GFP and GFP-CLASP2. Cells were lysed 20 hours after transfection, by collecting on ice in 20 mM Tris-HCl pH 8, 100mM NaCl, 0,5% Triton-X100, with a cocktail of protease inhibitors (Roche). Samples were centrifuged for 10 minutes at 13000 rpm and 4 ^{0}C to remove cell debris and the supernatant was used for further experiments.

FCS measurements were conducted at room temperature with the LSM 510-Confocor II (Zeiss) and the 488nm Ar-laser (tube current 50%, beampath: HFT488-Mirror-BP505-550). Laser power was attenuated to 1% during the 30 second measurement timepoints. A total of 20 measurements per lysate were conducted. To calibrate the system, rhodamine 6G with a known diffusion coefficient was used. The experimentally obtained autocorrelation function was analyzed with the Confocor II software package. The autocorrelation function was fit with

$$G(t) = \frac{1 + \frac{T}{1-T} e^{-t/\tau_T}}{N} \left(\sum_{i=1}^{M} \frac{F_i}{(1 + t/\tau_i)\sqrt{1 + t/(S^2 \tau_i)}} \right) + 1,$$

where $_T$ is the triplet time, set to 9 microseconds, S the structural parameter, obtained from calibration measurements with rhodamine 6G (diffusion coefficient: 28x10^{-10} m^2/s at 20 ^{0}C), N is the number of particles, M the number of components (1 or 2), Fi the fraction of component i, $_1$ the diffusion time of fraction i, and T the fraction of triplet decay.

The molecular brightness of the lysates was analyzed with PCH. The raw data of FCS measurements was converted into PCH data with a home-written program and a binning time of 50 microseconds. The data thus obtained were analyzed using the Globals software package developed at the Laboratory for Fluorescence Dynamics at the University of Illinois at Urbana-Champaign.

Acknowledgements
This research was supported by grants from the Netherlands Organisation for Scientific Research (NWO-ALW, NWO MW investering middelgroot and NWO-MW), the ministry of Economic Afairs (bsik) and the Dutch Cancer Society (KWF).

Supplementary Information

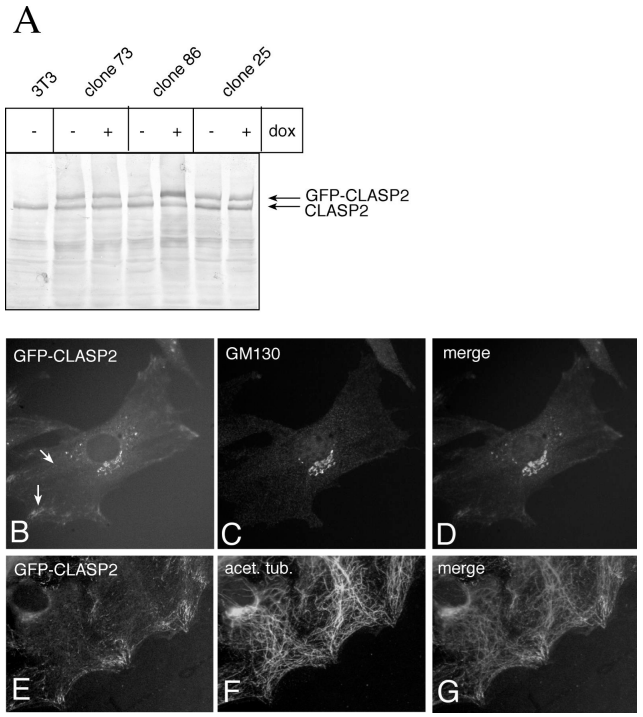

Figure 1. Generation of inducible, GFP-CLASP2 expressing 3T3 cell lines.
A) 3T3 cells stably expressing GFP-CLASP2. Cells were treated for 18 hours with doxicyclin (dox) or not treated. Protein extracts of three different, GFP-CLASP2 expressing cell lines, were analysed by western blot with anti-CLASP antiserum (#2358). Only clone 86 shows inducible GFP-CLASP2 expression.
B-G) Localisation GFP-CLASP2 in stably transfected 3T3 cells. 3T3 cells were fixed and stained with anti-GM130 (B-D), or anti-acetylated tubulin (E-G). For the latter staining cells were first allowed to migrate into a wound so that stable MTs would be generated in a polarised fashion. Notice that GFP-CLASP2 recapitulates behvaiour of the non-tagged protein, indicating its functionality

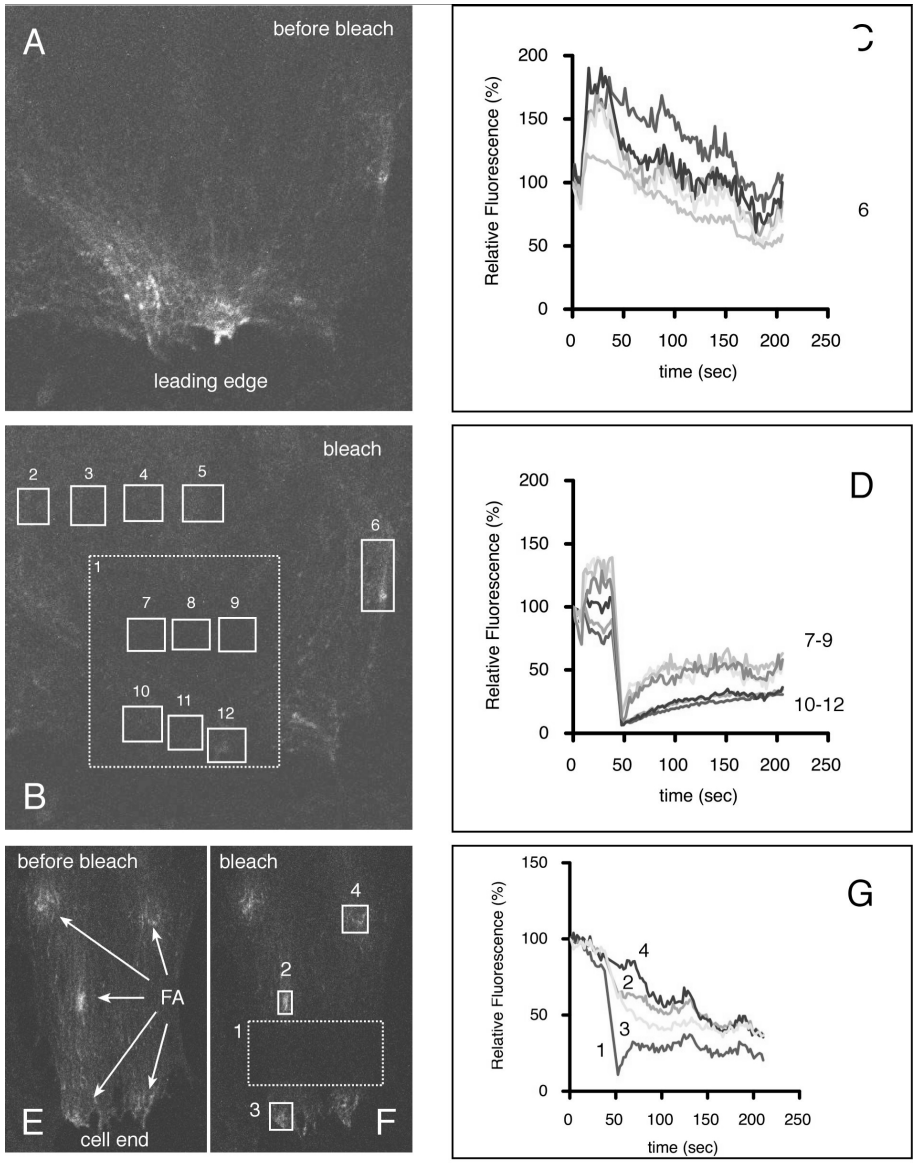

Figure 2. FRAP analysis of GFP-CLASP2 in 3T3 cells.

Migrating clone 86 cells, expressing GFP-CLASP2, were bleached (ROI 1, indicated by stippled rectangles in B and F). Fluorescence loss or recovery was measured in the indicated ROIs. In panels A, E still images are shown prior to bleaching. In panels B, F still images are shown immediately after bleaching. In panels C, D, G fluorescence intensities are plotted of the different ROIs. Because so many ROIs are measured in B, the plots have been split into two: fluorescence loss is visualised in C and recovery in D. FA: focal adhesion.

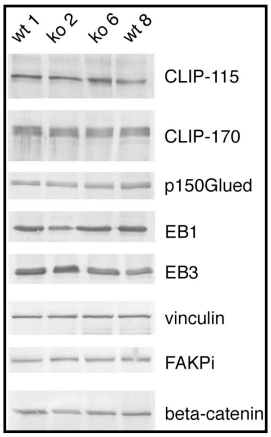

Figure 3. Western blot analysis of CLASP2 knock out fibroblasts.
Cell extracts were made of two wild type (lines 1 and 8) and two CLASP2-deficient (lines 2 and 6) MEF lines. Western blots were incubated with antibodies against CLIP-115, CLIP-170, p150Glued, EB1, EB3, vinculin, phosphorylated focal adhesion kinase (FAKPi) and beta-catenin. None of the teste dproteins is significantly different in knock out cells.

Supplemental Information Movie 1.
GFP-CLASP2 behaviour in stably expressing 3T3 cells (clone 86). No serum induction. GFP-CLASP2 is a +TIP.

Supplemental Information Movie 2
GFP-CLASP2 continuously entering and exiting areas of "static" GFP-CLASP2 accumulation. These areas have their own dynamic behaviour.

Supplemental Information Movie 3.
GFP-CLASP2 behaviour after serum addition. A quick relocalisation towards the leading edges of cells is observed.

Supplemental Information Movie 4.
GFP-CLASP2 displacements in cytoplasmic areas of a cell migrating into a wound. The speed of movement of the comets in the cytoplasm is not altered because of the polarisation of the cell.

Supplemental Information, Movies 5-8
FRAP analysis, for detailed explanation, see results section and Fig. 1 (movies 5 and 7) and Supplementary Fig. 2 (movies 6 and 8).

References

Akhmanova, A., and Hoogenraad, C. C. (2005). Microtubule plus-end-tracking proteins: mechanisms and functions. Curr Opin Cell Biol *17*, 47-54.

Akhmanova, A., Hoogenraad, C. C., Drabek, K., Stepanova, T., Dortland, B., Verkerk, T., Vermeulen, W., Burgering, B. M., De Zeeuw, C. I., Grosveld, F., and Galjart, N. (2001). Clasps are CLIP-115 and -170 associating proteins involved in the regional regulation of microtubule dynamics in motile fibroblasts. Cell *104*, 923-935.

Akhmanova, A., Mausset-Bonnefont, A.-L., Van Cappellen, W., Keijzer, N., Hoogenraad, C. C., Stepanova, T., Drabek, K., van der Wees, J., Mommaas, M., Onderwater, J., van der Meulen, H., Hoogerbrugge, J., Vreeburg, J., Uringa, E.-J., Grootegoed, A., Grosveld, F., and Galjart, N. (2005). The microtuble plus end tracking protein CLIP-170 associates with the spermatid manchette and is essential for spermatogenesis. submitted for publication.

Baron, U., and Bujard, H. (2000). Tet repressor-based system for regulated gene expression in eukaryotic cells: principles and advances. Methods Enzymol *327*, 401-421.

Bulinski, J. C., and Gundersen, G. G. (1991). Stabilization of post-translational modification of microtubules during cellular morphogenesis. Bioessays *13*, 285-293.

Cook, T. A., Nagasaki, T., and Gundersen, G. G. (1998). Rho guanosine triphosphatase mediates the selective stabilization of microtubules induced by lysophosphatidic acid. J Cell Biol *141*, 175-185.

Coquelle, F. M., Caspi, M., Cordelieres, F. P., Dompierre, J. P., Dujardin, D. L., Koifman, C., Martin, P., Hoogenraad, C. C., Akhmanova, A., Galjart, N., De Mey, J. R., and Reiner, O. (2002). LIS1, CLIP-170's key to the dynein/dynactin pathway. Mol Cell Biol *22*, 3089-3102.

Desai, A., and Mitchison, T. J. (1997). Microtubule polymerization dynamics. Annu Rev Cell Dev Biol *13*, 83-117.

Etienne-Manneville, S., and Hall, A. (2001). Integrin-mediated activation of Cdc42 controls cell polarity in migrating astrocytes through PKCzeta. Cell *106*, 489-498.

Etienne-Manneville, S., and Hall, A. (2002). Rho GTPases in cell biology. Nature *420*, 629-635.

Etienne-Manneville, S., and Hall, A. (2003). Cdc42 regulates GSK-3beta and adenomatous polyposis coli to control cell polarity. Nature *421*, 753-756.

Galbraith, C. G., Yamada, K. M., and Sheetz, M. P. (2002). The relationship between force and focal complex development. J Cell Biol *159*, 695-705.

Galjart, N. (2005). CLIPs and CLASPs and cellular dynamics. Nat Rev Mol Cell Biol *6*, 487-498.

Gundersen, G. G., Gomes, E. R., and Wen, Y. (2004). Cortical control of microtubule stability and polarization. Curr Opin Cell Biol *16*, 106-112.

Hernandez, S. E., Krishnaswami, M., Miller, A. L., and Koleske, A. J. (2004). How do Abl family kinases regulate cell shape and movement? Trends Cell Biol *14*, 36-44.

Hoogenraad, C. C., Akhmanova, A., Grosveld, F., De Zeeuw, C. I., and Galjart, N. (2000). Functional analysis of CLIP-115 and its binding to microtubules. J Cell Sci *113*, 2285-2297.

Kaverina, I., Krylyshkina, O., Gimona, M., Beningo, K., Wang, Y. L., and Small, J. V. (2000). Enforced polarisation and locomotion of fibroblasts lacking microtubules. Curr Biol *10*, 739-742.

Kaverina, I., Krylyshkina, O., and Small, J. V. (1999). Microtubule targeting of substrate contacts promotes their relaxation and dissociation. J Cell Biol *146*, 1033-1044.

Kaverina, I., Rottner, K., and Small, J. V. (1998). Targeting, capture, and stabilization of microtubules at early focal adhesions. J Cell Biol *142*, 181-190.

Kodama, A., Karakesisoglou, I., Wong, E., Vaezi, A., and Fuchs, E. (2003). ACF7: an essential integrator of microtubule dynamics. Cell *115*, 343-354.

Krylyshkina, O., Anderson, K. I., Kaverina, I., Upmann, I., Manstein, D. J., Small, J. V., and Toomre, D. K. (2003). Nanometer targeting of microtubules to focal adhesions. J Cell Biol *161*, 853-859.

Lee, H., Engel, U., Rusch, J., Scherrer, S., Sheard, K., and Van Vactor, D. (2004). The microtubule plus end tracking protein Orbit/MAST/CLASP acts downstream of the tyrosine kinase Abl in mediating axon guidance. Neuron *42*, 913-926.

Liao, G., Nagasaki, T., and Gundersen, G. G. (1995). Low concentrations of nocodazole interfere with fibroblast locomotion without significantly affecting microtubule level: implications for the role of dynamic microtubules in cell locomotion. J Cell Sci *108 (Pt 11)*, 3473-3483.

Meili, R., and Firtel, R. A. (2003). Two poles and a compass. Cell *114*, 153-156.

Miller, A. L., Wang, Y., Mooseker, M. S., and Koleske, A. J. (2004). The Abl-related gene (Arg) requires its F-actin-microtubule cross-linking activity to regulate lamellipodial dynamics during fibroblast adhesion. J Cell Biol *165*, 407-419.

Mimori-Kiyosue, Y., Grigoriev, I., Lansbergen, G., Sasaki, H., Matsui, C., Severin, F., Galjart, N., Grosveld, F., Vorobjev, I., Tsukita, S., and Akhmanova, A. (2005). CLASP1 and CLASP2 bind to EB1 and regulate microtubule plus-end dynamics at the cell cortex. J Cell Biol *168*, 141-153.

Nathke, I. S., Adams, C. L., Polakis, P., Sellin, J. H., and Nelson, W. J. (1996). The adenomatous polyposis coli tumor suppressor protein localizes to plasma membrane sites involved in active cell migration. J Cell Biol *134*, 165-179.

Niggli, V. (2003). Microtubule-disruption-induced and chemotactic-peptide-induced migration of human neutrophils: implications for differential sets of signalling pathways. J Cell Sci *116*, 813-822.

Palazzo, A. F., Cook, T. A., Alberts, A. S., and Gundersen, G. G. (2001a). mDia mediates Rho-regulated formation and orientation of stable microtubules. Nat Cell Biol *3*, 723-729.

Palazzo, A. F., Eng, C. H., Schlaepfer, D. D., Marcantonio, E. E., and Gundersen, G. G. (2004). Localized stabilization of microtubules by integrin- and FAK-facilitated Rho signaling. Science *303*, 836-839.

Palazzo, A. F., Joseph, H. L., Chen, Y. J., Dujardin, D. L., Alberts, A. S., Pfister, K. K., Vallee, R. B., and Gundersen, G. G. (2001b). Cdc42, dynein, and dynactin regulate MTOC reorientation independent of Rho-regulated microtubule stabilization. Curr Biol *11*, 1536-1541.

Perez, F., Diamantopoulos, G. S., Stalder, R., and Kreis, T. E. (1999). CLIP-170 highlights growing microtubule ends in vivo. Cell *96*, 517-527.

Ridley, A. J., Schwartz, M. A., Burridge, K., Firtel, R. A., Ginsberg, M. H., Borisy, G., Parsons, J. T., and Horwitz, A. R. (2003). Cell migration: integrating signals from front to back. Science *302*, 1704-1709.

Salmon, W. C., Adams, M. C., and Waterman-Storer, C. M. (2002). Dual-wavelength fluorescent speckle microscopy reveals coupling of microtubule and actin movements in migrating cells. J Cell Biol *158*, 31-37.

Schuyler, S. C., and Pellman, D. (2001). Microtubule "plus-end-tracking proteins": The end is just the beginning. Cell *105*, 421-424.

Schwartz, M. A., and Ginsberg, M. H. (2002). Networks and crosstalk: integrin signalling spreads. Nat Cell Biol *4*, E65-68.

Small, J. V., Geiger, B., Kaverina, I., and Bershadsky, A. (2002). How do microtubules guide migrating cells? Nat Rev Mol Cell Biol *3*, 957-964.

Stepanova, T., Slemmer, J., Hoogenraad, C. C., Lansbergen, G., Dortland, B., De Zeeuw, C. I., Grosveld, F., van Cappellen, G., Akhmanova, A., and Galjart, N. (2003). Visualization of microtubule growth in cultured neurons via the use of EB3-GFP (end-binding protein 3-green fluorescent protein). J Neurosci *23*, 2655-2664.

Wen, Y., Eng, C. H., Schmoranzer, J., Cabrera-Poch, N., Morris, E. J., Chen, M., Wallar, B. J., Alberts, A. S., and Gundersen, G. G. (2004). EB1 and APC bind to mDia to stabilize microtubules downstream of Rho and promote cell migration. Nat Cell Biol *6*, 820-830.

Wittmann, T., Bokoch, G. M., and Waterman-Storer, C. M. (2003). Regulation of leading edge microtubule and actin dynamics downstream of Rac1. J Cell Biol *161*, 845-851.

Wittmann, T., and Waterman-Storer, C. M. (2001). Cell motility: can Rho GTPases and microtubules point the way? J Cell Sci *114*, 3795-3803.

Wittmann, T., and Waterman-Storer, C. M. (2005). Spatial regulation of CLASP affinity for microtubules by Rac1 and GSK3{beta} in migrating epithelial cells. J Cell Biol *169*, 929-939.

Xu, J., Wang, F., Van Keymeulen, A., Rentel, M., and Bourne, H. R. (2005). Neutrophil microtubules suppress polarity and enhance directional migration. Proc Natl Acad Sci U S A *102*, 6884-6889.

Zhou, F. Q., Zhou, J., Dedhar, S., Wu, Y. H., and Snider, W. D. (2004). NGF-induced axon growth is mediated by localized inactivation of GSK-3beta and functions of the microtubule plus end binding protein APC. Neuron *42*, 897-912.

Chapter 4

Murine CLASP2 regulates microtubule levels in vivo and is essential for gametogenesis and hematopoiesis

manuscript in preparation

Murine CLASP2 regulates microtubule levels in vivo and is essential for gametogenesis and hematopoiesis

Ksenija Drabek[1], Marcel Vermeij[2], Wiggert van Cappellen[3], Tanja Nikolic[4], Dubravka Drabek[1], Frank Grosveld[1], Rob Ploemacher[5], Jan Vreeburg[3], J. Anton Grootegoed[3], Joseph E. Italiano[6] and Niels Galjart[1*]

[1]Department of Cell Biology and Genetics, [2]Department of Pathology, [3]Department of Reproduction and Development, [4]Department of Pulmonary Medicine; [5]Department of Hematology; Erasmus MC, P.O.Box 1738, 3000 DR Rotterdam, The Netherlands; [6]Hematology Division, Brigham and Women's Hospital and Harvard Medical School, Boston, MA.

Abstract

Mammalian CLASP1 and -2 are microtubule plus end tracking proteins, involved in the regional regulation of microtubule dynamics. Although an essential role has been established for CLASP homologues in lower organisms, the *in vivo* function of mammalian CLASPs has not yet been addressed. Here, we examine CLASP2-deficient mice, that were generated using homologous recombination in embryonic stem cells. Knock out mice show a weight reduction throughout life, compared to wild type littermates. Both male and female CLASP2 knock out mice have a severely affected germ cell development. Analysis of GFP-CLIP170 expression in dissected testis tubules of the CLASP2 knock out mice strongly suggests a role for CLASP2 in the regulation of microtubule dynamics. Knock out mice also have hematopoietic defects and occasionally succumb to internal bleedings, because of reduced megakaryocyte numbers. We propose that during germ cell development and hematopoiesis CLASP2 is required to stabilize microtubules upon reception of specific signalling cues.

Introduction

Microtubules (MTs) are dynamic polymers assembled from heterodimers of and tubulin polypeptides. They are essential for the maintenance of cell shape, intracellular transport, positioning of cell organelles and formation of the mitotic spindle, on which the chromosomes are segregated to two daughter cells during the process of mitosis. MTs perform many of their cellular tasks by changing their organization and stability in response to the needs of the cell. This process is highly regulated, mainly by heterologous interactions between MTs and specific regulatory proteins. A variety of cellular factors have been identified that can modulate MT dynamics. Some of those regulating proteins, like the cytoplasmic linker protein CLIP-170 (Perez et al. 1999), are localized specifically at MT plus ends and are called "plus end tracking proteins", or +TIPs (Schuyler and Pellman 2001). The group of +TIPs is rapidly expanding and the mechanism by which these proteins recognize the MT plus end has received considerable attention (for recent review, see (Akhmanova and Hoogenraad 2005).

The CLIP-Associating Proteins, CLASP1 and -2, are also +TIPs; their enhanced accumulation at distal MT segments causes MT stabilization (Akhmanova et al. 2001; Mimori-Kiyosue et al. 2005). The affinity of CLASPs for MTs is controlled by GSK3beta, which, in its active form, suppresses CLASP binding to MTs (Akhmanova et al. 2001; Wittmann and Waterman-Storer 2005). These results suggest that CLASPs are involved in the local regulation of MT dynamics in response to positional cues. In the accompanying paper, we test this hypothesis in cultured cells and establish a role for CLASP2 in fibronectin-mediated MT stabilization (Drabek et al. 2005). Functional dissection of CLASP2 reveals that its C terminus is required for interaction with CLIPs and the association with the Golgi and the cell cortex, while a region in the middle of the protein is required for binding to microtubules and the +TIPs EB1 and -3 (Mimori-Kiyosue et al. 2005).

CLASPs are homologous to *D. melanogaster* Orbit/Mast, an essential mitotic protein (Inoue et al. 2000; Lemos et al. 2000). A role in mitosis has also been established for human CLASP1. It is likely that the mitotic roles of mammalian CLASP1 and *D. melanogaster* Orbit/Mast are conserved. In HeLa cells, CLASP1 is an essential outer kinetochore component, which associates near the plus end of growing spindle microtubules and controls microtubule dynamics (Maiato et al. 2003). Recently it was shown that Orbit/Mast is required to maintain the length of the microtubules that connect kinetochores to the spindle pole, by regulating the addition of microtubule subunits onto microtubule plus ends at the kinetochore (Maiato et al. 2004). Orbit/Mast might perform its mitotic function by binding to tubulin. By contrast, it has been hypothesized that CLASP-mediated stabilization of interphase MTs at the cell cortex is carried out by recruitment of the CLIPs (Akhmanova et al. 2001) and/or EB1/3 (Mimori-Kiyosue et al. 2005).

The evidence from cultured cells indicates that CLASPs are regulatable proteins involved in stabilizing a subset of microtubules, whereas CLIPs seem to be part of a more general mechanism that promotes microtubule growth and localizes the dynein–dynactin complex (for review, see (Galjart 2005). What about the *in vivo* function of these interacting proteins? Knock out mouse analysis has revealed that CLIP-115 is important for neuronal development (Hoogenraad et al. 2002), whereas CLIP-170 is essential for spermatogenesis

(Akhmanova et al. 2005). Studies in *D. melanogaster* have shown that Orbit/Mast is required for oogenesis, and associates not only with mitotic spindles and spindle poles but also with other essential cellular structures (Mathe et al. 2003). During embryogenesis, Orbit/Mast is required for chromosome congression, spindle bipolarity and the attachment of microtubules to kinetochores (Maiato et al. 2002). In *D. melanogaster* spermatocytes, Orbit/Mast is required for cytokinesis; it associates with a subset of microtubules, called interior microtubules, that normally form the central spindle (Inoue et al. 2004). To date, nothing is know about the *in vivo* role of mammalian CLASPs.

Both CLASPs exists in several isoforms (Akhmanova et al. 2001). While CLASP1 appears to be ubiquitously expressed, CLASP2 is detected more abundantly in the brain than in other tissues. Thus, we speculated that distinct, cell cycle dependent, roles for CLASP1 and -2 might exist. In order to understand the *in vivo* function of CLASP2, we generated CLASP2 knock-out mice. These mice suffer from central nervous system abnormalities, but defects in the brain appear mild compared to other abnormalities. Here, we provide evidence for an essential role of CLASP2 in gametogenesis and megakaryocytopoiesis. Analysis of live testis tubules strongly suggests that CLASP2 controls MT dynamics *in vivo*. The distribution of CLASP2 indicates a role in mitosis, as well as in interphase. We propose that CLASP2 is involved in MT-mediated signalling pathways that control the proliferation and differentiation of highly specific cell types.

Results

Generation of CLASP2 knock out mice.

We disrupted the murine *Clasp2* gene by insertion of an EGFP-loxPMC1NEOlox cassette (Figure 1A) into the second common exon. With this strategy, GFP fusion proteins should be produced in knock out tissues, which contain only very short, CLASP2-derived N-termini. Targeting efficiency in embryonic stem (ES) cells was low (1/800), due to the presence of a small deletion in the homologous 5'end arm of the targeting construct (data not shown). Homologous recombination was diagnosed using Southern blots with digested genomic ES cell DNA (Figure 1B and data not shown). Recombination was also verified by PCR (Figure 1C and data not shown).

One positive ES cell clone had a correct karyotype and was injected into blastocysts. One of four chimeras was mated into the C57BL/6 background to generate inbred CLASP2 heterozygous and homozygous knock out mice. We derived mouse embryonic fibroblast (MEF) lines from E13.5 day embryos. (Drabek et al. 2005). We removed the neocassette by breeding heterozygous CLASP2 knock out mice with a transgenic mouse line expressing the Cre recombinase under control of the chicken actin promoter (CagCre line). The resulting mouse line is called CLASP2 knock out –neo^r.

In order to show that the CLASP2 gene disruption resulted in the absence of the protein, western blot analysis was performed on protein extracts from brain (Fig. 1) and MEFs (Drabek et al. 2005), where CLASP2 is most abundantly expressed. In wild type brains, major protein(s) of approximately 140 kDa is detected and a minor band of approximately 170 kDa (Fig. 1D). The 140 kDa proteins represent CLASP2beta and -gamma isoforms, whereas

the 170 kDa protein represents CLASP2alpha (Akhmanova et al. 2001). In extracts of homozygous knock out mice no CLASP2 is detectable, while reduced levels are present in heterozygous mice (Fig. 1D). To detect CLASP2-GFP fusion proteins in CLASP2 knock out samples, we incubated Western blots with antibodies against the N-terminus of CLASP2 (#2385) and with anti-GFP antibodies (Fig. 1E). Although the #2385 antiserum crossreacts with a number of aspecific proteins, it detects full length CLASP2 on low percentage polyacrylamide gels (Fig. 1E, left panels) and a CLASP2-GFP fusion protein of approximately 35 kDa in homozygous CLASP2 knock out brain (Fig. 1E, right panels). A similarly sized protein is detected with anti-GFP antiserum, as well as a slightly smaller product. Combined, these data suggest that the targeting strategy generates a CLASP2 knock out allele in mice. The knock out of CLASP2 does not have an influence on the levels of CLASP1 (Fig. 1E) or CLIP-115 and -170 (Fig. 1G).

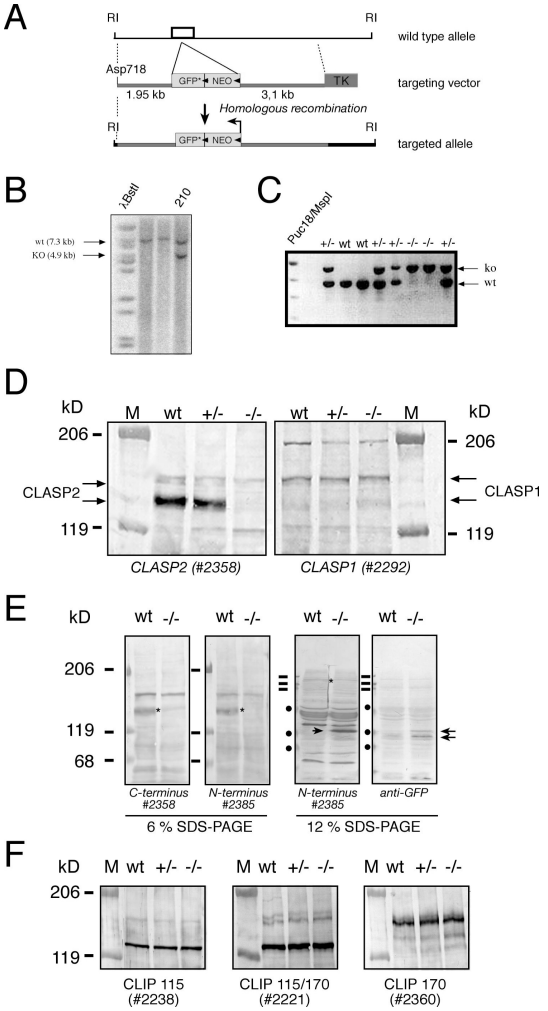

Figure 1 (previous page). Targeted inactivation of CLASP2 gene.
(A) Schematic representation of the targeting strategy. The second common *Clasp2* exon (depicted by a box) is shown. The targeting vector disrupts the *Clasp2* gene by insertion of EGFP-loxPMC1NEOlox (shown in the middle). Neo is transcribed in the opposite direction of *Clasp2* (depicted by arrow). The 3' end of the construct contains a thymidine kinase (TK) gene for counter selection. The targeted allele is presented at the bottom.
B) Southern blot analyses of targeted ES-cell DNA digested with Eco RI, showing clone 210 that was positive for homologous recombination. Wild type and knock out fragments are indicated.
C) Genotyping by PCR. Wild type and knock out fragments are indicated.
D-F) Western blot analyses on brain extracts of wild type (wt), heterozygous (+/-) and homozygous (-/-) *Clasp2* knock out mice, using antibodies against CLASP2 (#2358 and #2385), CLASP1 (#2292), CLIP-115 (#2238, #2221), CLIP-170 (#2221, #2360) and GFP.

Offspring from heterozygous CLASP2 knock out breedings (+neo^r) yielded less homozygous pups than would be expected on the basis of Mendelian segregation (Fig. 2A). Homozygous CLASP2 knock out mice that are born, are viable, but their body weight is significantly lower (approximately 30%) than that of wild-type and heterozygous littermates (Fig. 2B). Interestingly, breedings from heterozygous animals in which the neo^r gene was deleted (- neo^r mice) did yield normal numbers of homozygous offspring (Fig. 2A). In future studies we will addres the expression pattern of different CLASP2 isoforms during this period of development. Here, we focus on the major phenotypes in adult mice. We found similar defects in both types of *Clasp2* knock out mice, irrespective of the neo-casette (data not shown). Thus, insertion of the neo^r gene in an antisense orientation with respect to the *Clasp2* gene has an influence on mouse embryogenesis but not on the functioning of adult animals.

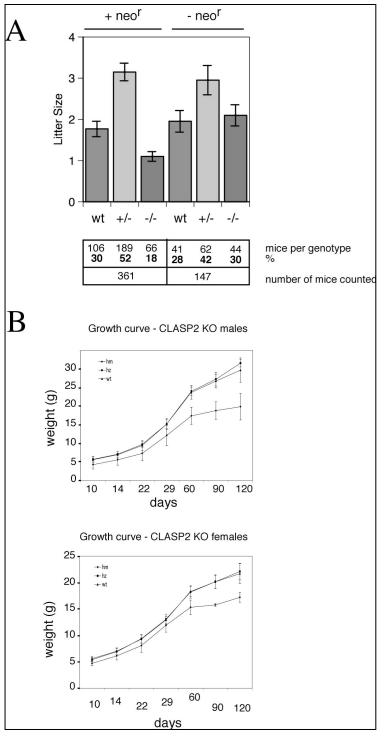

Figure 2. Phenotypic characterization of Clasp2 knock out mice.
A) Average littersize and distribution of genotypes. Live born litters from heterozygous crossings were genotyped.
B) Growth curves. Body weights of the wild type, heterozygous and homozygous mice are shown at different time points (abbreviations: wt-wild type, hz-heterozygous, hm-homozygous). Groups consisted of 4 hm, 14 ht and 9 wt females, and 5 hm, 10 hz and 9 wt males, respectively.

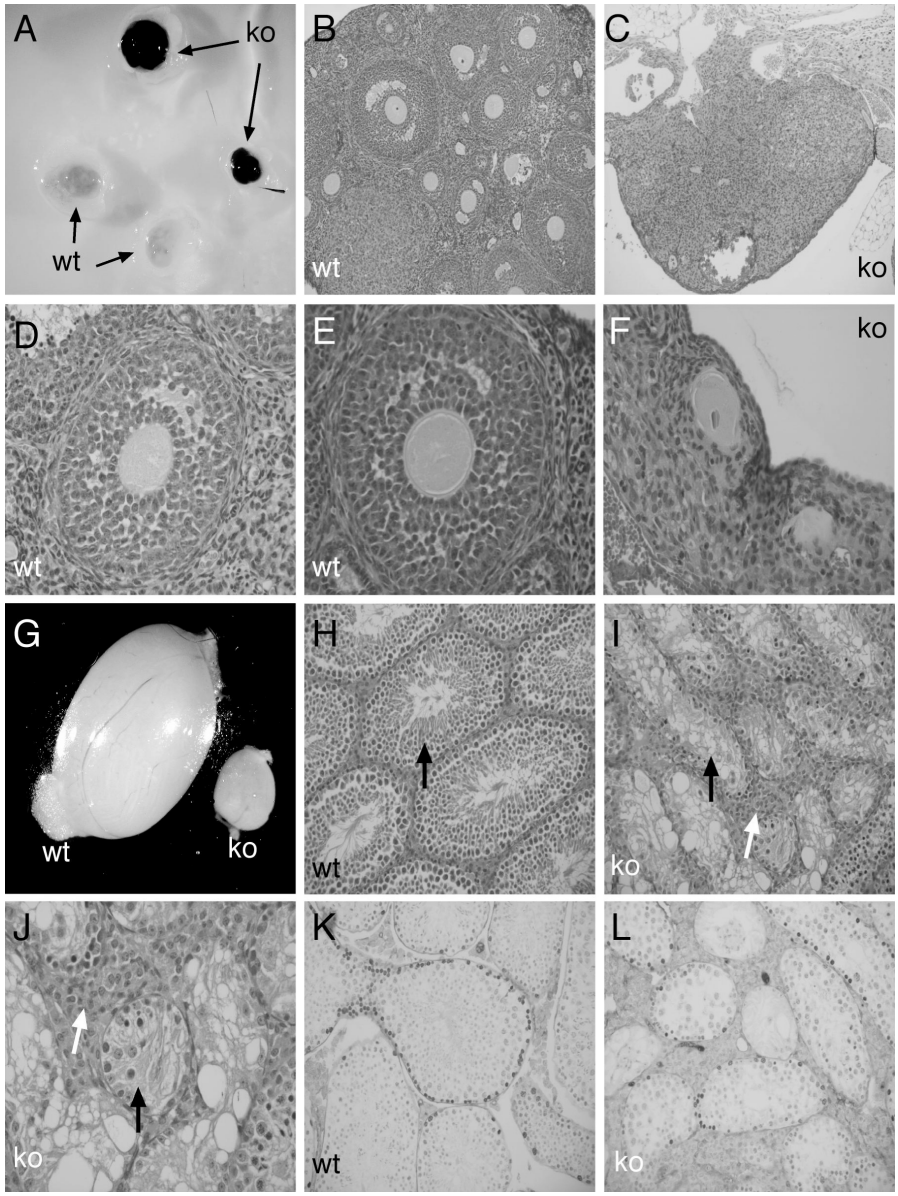

Figre 3. Histological analysis of CLASP2 knock out mouse testis and ovary.
A) Gross morphology of ovaries from a wild type mouse and *Clasp2* knock out littermate.
B-F) Hematoxylin and eosin staining of paraffin-embedded sections of adult ovaries.
G) Gross morphology of a testis from a wild type and a *Clasp2* knock out littermate.
H-J) Hematoxylin and eosin staining of paraffin-embedded sections of adult testis. Seminiferous tubules and interstitium of the wt and *Clasp2* knock out testis are shown.
K, L) Detection of spermatogenic progentior cells. Mice were injected with BrdU 30 minutes before dissection of the testis. Sections were incubated with anti-BrdU antibodies and stained. Despite the morphological aberrations in *Clasp2* knock out testis dividing cells (brown nuclei at abasal lamina of tubules) are present.

CLASP2 is essential for gametogenesis.

Breedings between homozygous CLASP2 knock out animals did not yield any pregnancies, hence we set up separate breedings between homozygous males and heterozygous or wild-type females and vice versa. Since no litters were obtained from any of such breedings either, we hypothesized that both male and female CLASP2$^{-/-}$ mice might be infertile and we investigated ovaries and testes from homozygous knock out mice at the macroscopic level. Examination of ovaries showed no pronounced difference in size, but a difference in coloration, due to hemorrhages (Fig. 3A). By contrast, the testes from CLASP2 knock out mice were severely reduced in size in comparison to wild-type testes (Fig. 3G).

Microscopic analysis of CLASP2 knock out ovaries revealed blood-filled cysts (Fig. 3A, C, F). In these ovaries only very early stages of follicle development could be observed, with many abnormal follicles, as well as small hemorrhages and scar tissue. The granulosa layer surrounding the oocyte was disorganized and the theca layer seemed absent; we could not observe follicles in advanced stages of development (Fig. 3C, F).

Histological analysis of the testes of CLASP2 knock out mice showed severely disorganized seminiferous tubules, with hardly any mature sperm (Fig. 3I, J). The interstitium of the tubule was increased in size and filled with blood vessels. Combined, these data show that in the absence of CLASP2 the development of the seminiferous tubule is severely affected. BrdU incorporation experiments indicated that dividing spermatogenic progenitor cells are present in the testis tubule of CLASP2 knock out mice (Fig. 3L). We conclude that CLASP2 is essential for male and female germ cell development.

CLASP2 regulates MT dynamics in vivo.

We recently generated a GFP-CLIP170 knock in allele in mice and showed that the fusion protein produced by this modified *Restin* gene is fully functional and can be used to visualize MT dynamics in live, dissected testis tubules (Akhmanova et al. 2005). Application of Hoechst to GFP-CLIP170 knock in testis, allows identification of the nuclei of cells and visualization of MT dynamics at the same time in a confocal/multiphoton microscope set up, so that MT patterns can be correlated to different cell types within the testis tubule (Akhmanova et al. 2005). Using this approach, we showed that GFP-CLIP170 is expressed in two waves during spermatogenesis: “plus end tracking” GFP-CLIP-170 is present in spermatogonia, but as spermatogenesis proceeds, GFP-CLIP-170 expression increases and the fusion protein stably marks syncytia of differentiated spermatogonia and early prophase spermatocytes. Subsequently, GFP-CLIP-170 levels drop, but during spermiogenesis GFP-CLIP-170 accumulates again and is present on spermatid manchettes and centrosomes. Surprisingly, GFP-CLIP-170 converts from a mobile “plus end tracking” protein to a relatively immobile protein. GFP-CLIP170 is not present in Sertoli cells (Akhmanova et al. 2005).

We crossed the GFP-CLIP170 knock in allele into the CLASP2 knock out mice. Examination of live dissected testis tubules under a confocal/multiphoton microscope revealed a comparably bright and cytoplasmic GFP staining in wild type and CLASP2 knock out backgrounds, which is due to the expression of GFP-CLIP170 (Fig. 4B, C, E, F). We also observed a diffuse and much weaker nuclear signal in tubule cells of the CLASP2 knock out only; this GFP signal is due to the activity of the CLASP2 promoter, which drives

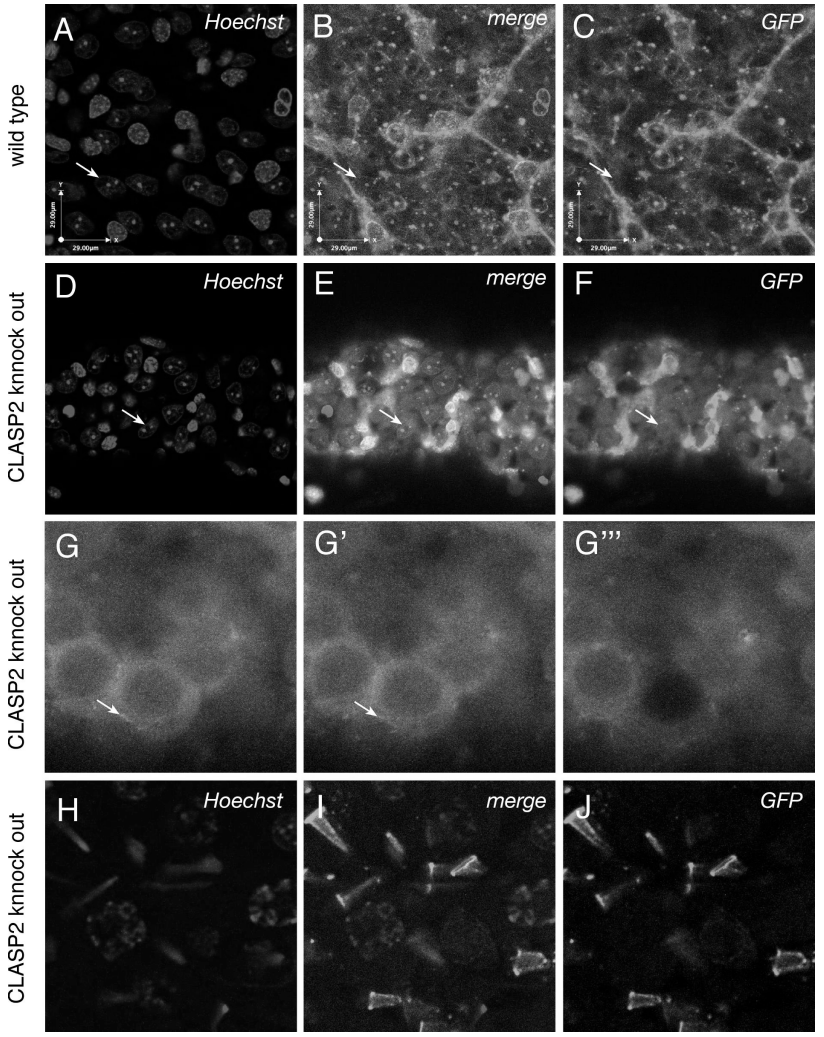

Figure 4. Analysis of live testis tubules

Testis tubules were dissected from GFP-CLIP-170 knock in – Clasp2 knock out mice (in some cases treated with Hoechst) and analyzed with a confocal/multiphoton microscope.

A-C) Low magnification view of GFP-CLIP-170 and Hoechst distribution in wild type testis. Notice the accumulation of GFP-CLIP-170 in syncitia. Sertoli cells are free of GFP labelling.

D-F) Low magnification view of GFP-CLIP-170 and Hoechst distribution in *Clasp2* knock out testis. Notice the smaller size of the tubule. GFP-CLIP170 accumulates in syncitia. Nuclear signal is detected in Sertoli cells.

G-G'') Time lapse analysis of GFP-CLIP-170 in *Clasp2* knock out testis. The panels show images acquired after 0 (G) and 2 seconds (G') and the last image of the series of 60 frames (G''). Arrows indicate GFP-CLIP-170-positive dashes. GFP accumulaiton is observed in the nucleus of cells. During the image analysis a cell in the middle of the syncitium was bleached, hence nuclear GFP signal is lost completely.

H-J) View of GFP-CLIP-170 and Hoechst distribution in elongating *Clasp2* knock out spermatids. Notice the accumulation of GFP-CLIP-170 on manchettes and the manchette ring. Manchettes are, however, deformed and the nucleus of *Clasp2* knock out spermatids does not extrude from the manchette.

the expression of GFP (and/or small CLASP2-GFP fusion proteins), that can enter the nucleus by diffusion.

A combined GFP and Hoechst analysis through testis tubules of wild type and CLASP2 knock out mice showed that tubule diameter in the knock out mice is much smaller (compare Fig. A-C with D-F), in line with the hematoxylin-eosin staining data. Within CLASP2 knock out tubules GFP-CLIP170-positive syncitia are detected near the basal lamina (Fig. 4D-E). The same cells that express GFP-CLIP170 also contain nuclear (and cytoplasmic) GFP, suggesting that the CLASP2 gene is active in spermatogonia. Interestingly, we also detected GFP (and thus CLASP2 expression) in the nuclei of Sertoli cells (Fig. 4E, F), which are easily recognized by the two dots of perinucleolar heterochromatin (Fig. 4D). Compared to wild type Sertoli cells (Fig. 4A, B), the nuclei of the knock out cells are distorted, indicating abnormalities in the Sertoli cell compartment of the CLASP2 knock out mice.

In live imaging experiments, we detected "plus end tracking" GFP-CLIP170 in the CLASP2 knock out tubules (Fig. 4G; see also Supplementary information, Movie 1). The Hoechst staining pattern of CLASP2 knock out spermatogonia expressing "plus end tracking" GFP-CLIP170 was clearly different from wild type cells (data not shown). These data indicate that the differentiation of spermatogonia in CLASP2 knock out testis is affected at an early stage. Whereas the localization of cells expressing "plus end tracking" GFP-CLIP170 was normal (i.e. confined to the outside of the testis tubule) in CLASP2 knock out testis, the localization of other cells expressing GFP-CLIP170 was disorganized and the distribution of GFP-CLIP170 within these CLASP2 knock out cells was abnormal (data not shown). Normal elongating spermatids, for example, have a typical hook-like shape of the nucleus, which forms while the spermatid manchette, an array of regularly spaced and crosslinked MTs, moves over the nucleus (Russell et al. 1991). GFP-CLIP170 abundantly decorates such manchettes (Akhmanova et al. 2005). In CLASP2 knock out testis**,** however, the number of spermatids is greatly reduced and in these cells the nucleus does not extrude from the manchette at all (Fig. 4H-J). Thus, spermatogenesis appears to be affected in multiple cell types in the CLASP2 knock out mouse.

Using GFP-CLIP170 as a marker, we measured MT growht rates in live dissected testis tubules, derived from wild type and CLASP2 knock out mice. In wild type mice we obtained an average growth rate of 0.16 +/- 0.04 micrometre per second (55 dashes analyzed, standard deviation indicated, see (Akhmanova et al. 2005). In CLASP2 knock out mice, we obtained an average growth rate of 0.31 +/- 0.10 micrometre per second (23 dashes analyzed, standard deviation indicated). MT growth rates in CLASP2 knock out testis are two-fold higher than in wild type. ANOVA single factor analysis shows that this difference is highly significant ($P<0.000001$). These data suggest that CLASP2 is involved in the regulation of MT dynamics *in vivo*.

A role for CLASP2 in hematopoiesis.

We noted that many of the CLASP2 knock out mice died prematurely, at different ages. In order to identify a possible defect, we performed histopathological analyses and observed multiple hemorrhages in different organs of the KO mice, including the brain (data not

shown). One of the explanations for such a phenotype is that CLASP2 knock out mice have difficulties in blood clot formation. Indeed, peripheral blood examination showed that KO mice were severely thrombocytopenic (Fig. 5A). Female mice were in this respect more affected than males; whereas the number of thrombocytes in knock out males was approximately 30% of wild type, the number in knock out females was approximately 10% of the values observed in wild type or heterozygous gender and aged matched controls. Circulating red blood cells (RBC) and white blood cells (WBC) were also affected (Figure 5B).

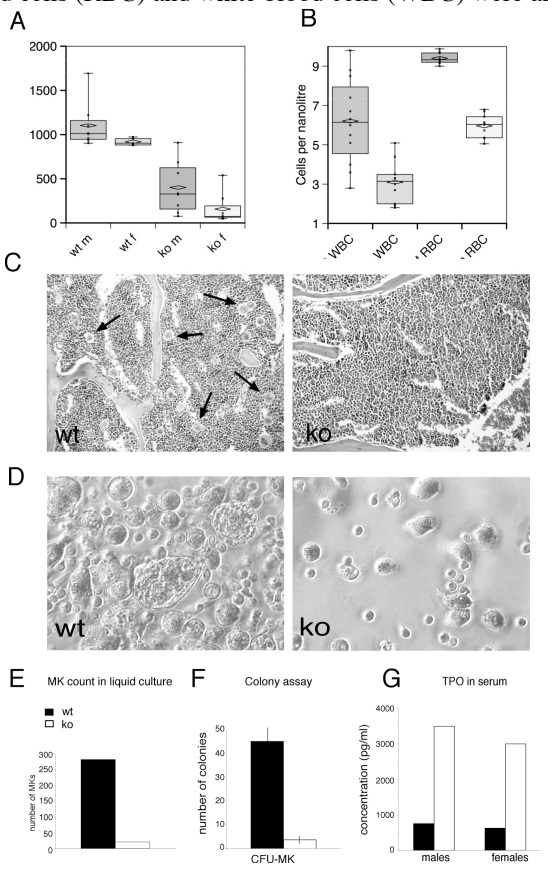

Figure 5. Hematological analysis of CLASP2 KO mouse.

A) Platelets counts in wild-type (wt) and *Clasp2* knock out (ko) mice. Platelets were measured separately in the blood from male (m) and female (f) mice.

B) Red blood cell (RBC) and white blood cell (WBC) counts. Wild type (left), and *Clasp2* knock out mice (right) were measured and values from male and female mice were pooled.

C) Hematoxylin-eosin sections of the bone marrow. Megakaryocytes in wild type bone marrow are indicated with arrows.

D-E) Liquid megakaryocyte cultures. Cells were imaged on day 6 using an inverted microscope. The actual counts are shown in E.

F) CFU-MK progenitor assay. Bone marrow cells were seeded into collagen media containing appropriate cytokine combination. Total number of colonies was counted after 10 days in culture. Cells from bone marrow of each mouse were seeded two times in two-chamber slides. The results are mean values from 2 wild-type and 2 *Clasp2* knock out mice (±SD).

G) TPO assay. Average serum levels of thrombopoetin in wild-type and *Clasp2* knock out male and female mice.

In histological sections of bone marrows, we clearly observed a megakaryocyte deficit. Although the number of megakaryocytes in the knock out bone marrows was variable, it was obviously reduced and in some mice even almost absent (Figure 5C). In such severe cases, bone marrows showed a reduced cellularity as well, resembling the situation observed in aplastic anemia (data not shown). To examine the cellular basis of the megakaryocyte reduction, we cultured megakaryocytes from fetal livers. In knock out cultures far less megakaryocytes developed after 6 days, i.e. cultures from knock out mice produced only 10% of megakaryocytes present in wild-type cultures (Figure 5E). In addition, CLASP2 knock out megakaryocytes were smaller (Fig. 5D), indicating a reduced DNA content.

To further characterize megakaryocytopoiesis in the absence of CLASP2, megakaryocyte progenitor cells were assayed in clonogenic culture. Bone marrow cells from CLASP2 knock out and wild-type littermate mice were seeded into collagen media, containing the appropriate cytokine combination. The total number of colonies was counted after 10 days of in vitro culture (DIV). The CLASP2 knock out samples showed a decreased number of CFU-MK colonies (Figure 5F), which indicates that the development of progenitor megakaryocyte cells from hematopoietic stem cells is affected in the absence of CLASP2. Since thrombopoetin (TPO) is one of the main regulators of the process of megakaryocytopoiesis in vivo (Kaushansky 2002), we next examined plasma TPO levels in the wild-type and CLASP2 knock out mice. TPO values were approximately 4-5 times higher in the plasma of CLASP2 knock out mice (Figure 5G), indicating that a defect in TPO amount is not the underlying cause of thrombocytopenia in the CLASP2 knock out mice.

During their maturation megakaryocytes acquire high DNA ploidy levels by a unique process called endomitosis, which involves replication of the DNA content without subsequent cytokinesis (Kaushansky 1999). To determine whether endomitosis was affected in CLASP2 knock out mice, we performed DNA ploidy analysis on cultured bone marrow megakaryocytes. The results reveal that wild type megakaryocytes showed a higher fraction of cells with a DNA content larger than 8N (Figure 6A). Cells with higher ploidy than 16N were not observed in the KO cultures. These results indicate that CLASP2 has a role in endomitosis. To investigate the cellular distribution of CLASP2, wild-type megakaryocytes from 6 day cultures were stained with anti-CLASP2 antibodies. Immunofluorescent analyis showed that in endomitotic cells CLASP2 co-localizes with the CREST kinetochore marker (Fig. 6B).

Finally, we wanted to check whether megakaryocytes that are present in the CLASP2 knock out mice could form (pro)platelets. Using a megakaryocyte liquid culture system we observed the formation of proplatelets after several days of culture in CLASP2 knock out and wild type mice (Figure 6C). In addition, circulating platelets from CLASP2 knock out mice have a normal shape and size, suggesting normal functionality (Figure 6D).

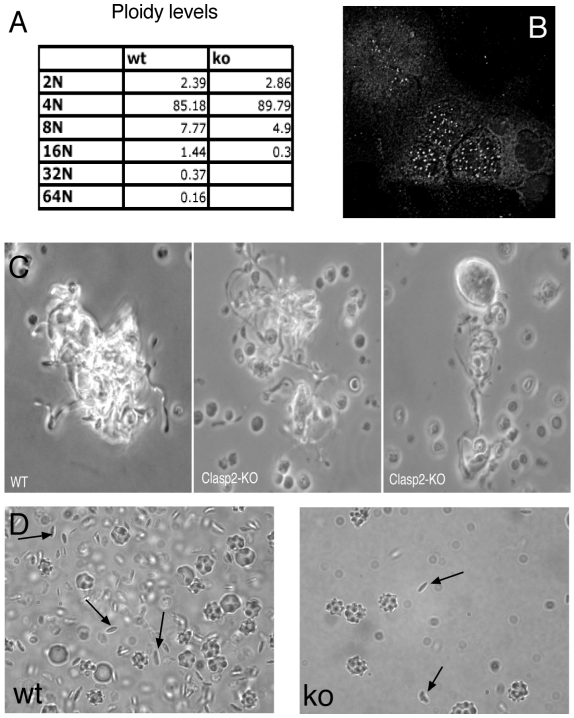

	wt	ko
2N	2.39	2.86
4N	85.18	89.79
8N	7.77	4.9
16N	1.44	0.3
32N	0.37	
64N	0.16	

Figure 6. Megakaryocyte analysis in Clasp2 knock out mice.
A) Ploidy analysis. DNA content from 5 wild-type and 7 *Clasp2* knock out cultured megakaryocytes. Percentages of total cell numbers are shown.
B) Localization of CLASP2 in endomitotic megakaryocytes. Wild-type cells were immunostained with CLASP2 (green) and CREST6 (red) antibodies and with DAPI (blue). Notice kinetochore association of CLASP2.
C) Photomicrographs showing extensive proplatelet networks emanating from wild-type (left) and *Clasp2* knock out (right) megakaryocytes.
D) Phase-contrast representative images of wild-type (left) and *Clasp2* knock out (right) platelets (thrombocytes). Platelets are indicated with arrows.

Discussion

We have generated *Clasp2* knock out mice to characterize the *in vivo* function of CLASP2. In order to interrupt *Clasp2* expression, we inserted a GFP-loxP-neo-loxP casette into the second common exon of the gene. The neomycin resistance gene (neo^r) was placed antisense with respect to the *Clasp2* gene, to interfere with transcription; the GFP open reading frame was followed by a stop codon, to prevent translation of CLASP2 sequences downstream of the integration site. Using anti-GFP antiserum, we detected proteins of approximately 30 and 35 kDa in brain lysates of the *Clasp2* knock out mouse. The size of these proteins correlates well with the size of predicted CLASP2-GFP fusion proteins, in which only the N-terminal, isoform-specific beta- and gamma-sequences of CLASP2 are fused to GFP (Akhmanova et al. 2001). In fibroblasts the alpha-isoform of CLASP2 is more abundantly expressed and in these cells we detected a CLASP2-GFP fusion protein of approximately 60 kDa (data not shown). The alpha-domain of CLASP2 entails approximately 300 residues. This domain does not interact with MTs, EB proteins, CLIPs, or the cell cortex (Mimori-Kiyosue et al. 2005), making it unlikely (but not impossible) that it retains some of the functionality of CLASP2, or that it acts as a dominant negative form.

Alternative splice events that do not include the targeted common exon may occur in the *Clasp2* knock out, but when only this exon is excluded transcripts are made with out-of-frame reading sequences. Our targeting strategy does not prevent the production of CLASP2 isoforms that initiate transcription downstream of the common exon, or that splice

around a few of the common exons to generate in-frame proteins. However, using antibodies against the C-terminus of CLASP2 we did not detect isoforms of CLASP2 other than the 140 and 170 kDa proteins in normal brain lysates and in knock out brain samples no CLASP2-reactive material was detected with these antibodies. We can not exclude the presence of CLASP2 forms below the detection level of the antibodies, or the presence of novel isoforms in other cell types. However, the data suggest that we have generated a valid *Clasp2* knock out mouse model.

Clasp2 knock out mice are characterized by abnormalities in the central nervous system, infertility because of impaired gametogenesis and a severely affected hematopoiesis. The central nervous system defects of *Clasp2* knock out mice will be described elsewhere. Here, we have focussed on the major phenotypes in adult mice. In particular, we have analyzed the mechanism underlying the reduced number of thrombocytes, since our data suggest that thrombocytopenia leads to the development of hemorrhages and the premature death of *Clasp2* knock out mice.

The structure of *Clasp2* knock out testes and ovaries is severely disorganized and includes hemorrhages and scar tissue. The fact that both *Clasp2* knock out female and male mice are infertile and that gametogenesis is affected at very early stages in both sexes, lends credit to the suggestion that CLASP2 has a role in meiosis. Of interest is therefore the detection of CLASP2 in oocytes undergoing meiosis (Moore and Zernicka-Goetz 2005). The role of CLASP during gametogenesis might be conserved since Drosophila Orbit/MAST is essential for oogenesis (Mathe et al. 2003) and spermatogenesis (Inoue et al. 2004). It is striking that CLASP phenotypes are observed in cells that do not complete cytokinesis (this includes megakaryocytes). However, the CLASP2 phenotype in murine spermatogonia and oocytes can also be attributed to defective processes in other, neighbouring, cell types. For example, there is a notable absence of an organized theca cell layer in *Clasp2* knock out follicles, which might contribute to oocyte abnormalities. In the testis CLASP2 is expressed in Sertoli cells which are essential for proper male germ cell development and whose structure appears affected in *Clasp2* knock out mice. A common theme emerging from these studies is that CLASPs might be involved in signalling between neighbouring cells.

Using crosses of *Clasp2* knock out mice with *GFP-Clip170* knock-in mice we could visualize MT plus-ends in live dissected testis tubules (Akhmanova et al. 2005). The average MT growth rate is increased two-fold in CLASP2 knock out cells. The data in spermatogonia are in line with RNAi data in HeLa cells, where a ~70% depletion of both CLASP1 and -2 led to a shift in the balance between free tubulin (up) and MTs (down), with a concomitant increase (~1.5 fold) in MT growth rates (Mimori-Kiyosue et al. 2005). We therefore propose that CLASP2 regulates MT dynamics *in vivo*. We attempted a similar approach in cultured megakaryocytes, but were unable to document dynamic GFP-CLIP170 reliably, because of a low expression of this protein in megakaryocytes and a high interference of GFP, produced from the *Clasp2* knock out allele (data not shown).

The cause of thrombocytopenia in *Clasp2* knock out mice was found to be a reduced number of bone marrow megakaryocytes, which are the direct thrombocyte precursors. Those megakaryocytes that were made produced thrombocytes, that seemed to be of normal size and shape. Under normal circumstances the size and ploidy of megakaryocytes

respond to thrombocyte demand, with higher ploidy (bigger) cells shedding more thrombocytes. Thrombopoietin (TPO) is the major regulator of megakaryocyte proliferation, differentiation, and platelet production (Kaushansky 2002). However, production of TPO is not affected in the CLASP2 knock out mice. Measurements of TPO in the serum of knock out mice even show a significant elevation. This is consistent with the theory of TPO regulation by circulating platelets, which states that a higher number of platelets can sequester more TPO, leading to a reduced signal for platelet production, whereas lower numbers of circulating platelets can not retain TPO efficiently, resulting in a higher serum level of this critical signalling molecule (Kojima et al. 1997; Hou et al. 1998).

We found that lack of CLASP2 already causes a reduction in the number of produced megakaryocyte progenitors, as shown by megakaryocyte clonogenic assays. In addition to the thrombocytopenia, CLASP2 knock out mice are mildly anemic. This could be explained as a secondary effect, that results from bleeding. However, it is possible as well, that CLASP2 is necessary for proliferation of bipotent erythroid/megakaryocytic cell precursor, which was relatively recently identified and isolated from bone marrow (Vannucchi et al. 2000). This would place CLASP2 in the hierarchy of genes necessary for correct hematopoietic differentiation, an interesting hypothesis that merits further investigation.

Megakaryocyte endomitosis is a unique process in which nuclear division occurs without corresponding cytoplasmic separation; it is essential for platelet production because the size and the ploidy of megakaryocytes corresponds to platelet demand (Kaushansky 1999; Ravid et al. 2002). In CLASP2 knock out mice megakaryocytes are produced, albeit in reduced numbers. In addition, megakaryocytes that are present in knock out mice are less polyploid and, consequently, smaller. In wild-type megakaryocytes, CLASP2 is expressed on kinetochores, which implies an involvement of CLASP2 in the process of endomitosis. A localization of CLASP2 at kinetochores is not unexpected, since it has been shown in other cell types and organisms, that CLASP is required at kinetochores to regulate the dynamic behaviour of attached MTs. Thus, partial impairment of the process of endomitosis contributes to the thrombocytopenia observed in CLASP2 knock out mice, by limiting polyploidy levels and thereby size of the megakaryocyte.

The CLASP2 knock out manifests itself at multiple stages during the differentiation of highly specific cell types. What could explain multiple deficits in such specific cell types? First, redundancy of CLASPs has been shown in RNAi knock down experiments in HeLa cells (Mimori-Kiyosue et al. 2005). It is possible that CLASP1 can compensate to a certain extent for a deficiency of CLASP2 *in vivo*. For example, CLASP1 also localizes to megakaryocyte kinetochores (data not shown); a partial rescue by CLASP1 may explain why CLASP2 knock out megakaryocytes proceed through endomitosis to some extent, but these cells can not form highly polyploid cells because of limiting amounts of CLASP1. In other situations, for example during internal bleedings or hemorrhages when a lot of extra megakaryocytes need to be produced from progenitors, the compensation by CLASP1 may also not be sufficient.

Another explanation is that mammalian CLASPs actually have distinct, critical roles in mitosis and in interphase and that CLASP2 depletion affects highly specific aspects of cell division and/or differentiation. CLASP2 is involved in the local stabilization of MTs

in migrating fibroblasts (Akhmanova et al. 2001) and is regulated by different signaling complexes (Akhmanova et al. 2001; Lee et al. 2004; Wittmann and Waterman-Storer 2005). We have recently shown that CLASP2 may be part of an integrin signaling pathway, that responds to fibronectin, and that leads to the stabilization of MTs (Drabek et al. 2005). Similar signaling parthways might be involved in megakaryocyte differentiation, since 1 integrins have been demonstrated to play key roles in hematopoietic cell development, by mediating outside-in signaling (Verfaillie 1998). In mature megakaryocytes, 1 integrins can support attachment and spreading on fibronectin, and focal adhesion formation (Berthier et al. 1998; Schick et al. 1998). CLASP2 could subsequently be required for MT stabilization, which allows further signalling. A detailed microarray analysis of wild type and *Clasp2* knock out hematopoietic precursors should pinpoint the signalling pathways in which CLASP2 is involved.

Materials and methods

Targeting vector construction and generation of CLASP2 deficient mice.

A mouse PAC genomic library RPCI21 (UK HGMP Resource Centre, Hinxton, Cambridge), which was prepared from female 129S6/SvevTac mouse spleen genomic DNA (Osoegawa et al. 2000), was screened for the CLASP2 gene, using human CLASP2 cDNA as a probe. One positive clone (P635-K11), containing a 7.3 kb Eco RI-fragment, which included the second common exon, was chosen to generate the targeting construct. Targeting techniques and the procedures for selection of ES cells and generation of knock out mice have been described (Hoogenraad et al. 2002; Akhmanova et al. 2005). The *Clasp2* knock out mice with neo^r-casette were bred to a home-made transgenic mouse line that expresses the Cre recombinase under control of the chicken beta-actin promoter (kind gift of T. de Wit). This yielded *Clasp2* knock out mice without the neo^r-cassette. Genotyping of animals was performed by PCR.

Molecular biology and antibodies

DNA, RNA and protein isolations were performed according to standard procedures (Sambrook et al. 1989), with modifications (Hoogenraad et al. 2002). Southern, northern and western blot analyses were performed as described (Hoogenraad et al. 2002). For western blot, primary antibodies were used at 1:2000 dilutions, followed by alkaline phosphatase-conjugated goat anti-rabbit IgG (1:2000).

The #2385 anti-CLASP2 antibodies were prepared as described (Hoogenraad et al. 2000), using a GST-fusion protein approach. We also used rabbit polyclonal antibodies #2360 against CLIP-170 (Coquelle et al. 2002), #2221 against CLIP-115 and –170 and #2238 against CLIP-115 (Hoogenraad et al. 2002; Stepanova et al. 2003) and anti-GFP antibodies (Abcam). Mouse monoclonal antibodies were against -tubulin (Sigma), actin (Chemicon) and GFP (Santa Cruz, Roche). Secondary antisera were alkaline phosphatase-labeled anti-rabbit and anti-mouse antibodies (Sigma).

Cell culture and hematological analysis

For megakaryocyte cultures fetal livers from E13.5 day embryos were cultured in Dulbecco's Modified Eagle Medium (DMEM, GIBCO) supplemented with 10% fetal bovine serum, 50 units/ml penicillin, 50 ug/ml streptomycin, 2 mM L-glutamine and 1% tissue culture supernatant from a murine TPO producer cell line (Villeval et al. 1997). After 3 days of culture, megakaryocytes were enriched on a BSA gradient as previously described (Drachman et al. 1997). For quantification purposes, megakaryocytes from three wild-type and three knock out mice, were counted after 6 days of culture. Cells were counted at least in 5 microscopic fields in each culture. For proplatelet formation analysis, cultures were analyzed on day 5 by phase contrast microscopy.

Peripheral blood was collected from the retro-orbital sinus and analyzed in an automated cell counter (ABC-vet blood counter, ABX company). Platelets were separated from whole blood by sequential centrifugation (Schwer et al. 2001). The resulting platelet rich plasma (PRP) was used for further analysis. To examine cell shape, platelets were fixed in 8% PFA for 20 minutes and moved to poly-L-lysine (Sigma) coated coverslips. Images were obtained by using 63x differential interference contrast objective.

For the megakaryocyte progenitor cell assay (CFU-MK assay) bone marrow cells were collected by flushing femurs and tibias of CLASP2 knock out or wild-type mice with Iscove's MDM containing 2% fetal bovine serum. Serum-free collagen assay was performed with a MegaCult TM -C kit (StemCell Technologies Inc.; Vancouver, Canada). As a source of megakaryocyte (MK) colony-stimulating activity, a combination of human recombinant growth factors was used: 1.1 mg/ml collagen, 1% bovine serum albumin (BSA), 10 g/ml bovine pancreatic insulin, 200 g/ml iron-saturated human transferrin, 50 ng/ml thrombopoietin, 10 ng/ml interleukin 6, and 10 ng/ml interleukin 3. Cultures were prepared according to the manufacturer's instructions. The final culture mixture of 1.5 ml was dispensed into the two wells (0.75 ml each) of a chamber slide and incubated in humidified 5% CO_2 incubator at 37°C. After 10 days of incubation, slides were fixed in cold acetone (15 min), stained, and CFU-MK colonies were counted. CFU-MKs were identified by the detection of acetylholinesterase activity of megakaryocytes. A CFU-MK colony was defined as a cluster of three or more MK cells detected under light microscopy.

To measure the DNA content of primary megakaryocytes, individual single-cell suspensions were made from bone marrow harvested from the femurs of five wild-type and seven knock out littermate mice. Cells were cultured using the same conditions as described above. After the second day of culture, megakaryocytes were purified on a BSA gradient, cultured for one more day, and prepared for FACS analysis. In short, harvested cells were fixed in ice-cold 70% ethanol for 48 hours, centrifuged and resuspended in PBS. Cells were subsequently stained with propidium iodide (IP) in a triton/RNase solution for 30 minutes at room temperature, and the DNA content was measured using a FACScan flow cytometer (Becton Dickinson). The proportion of cells in each ploidy class was determined by integrating the area under each peak. Lymphocytes from the spleen were used as 2N/4N control.

TPO immunoassay

Thrombopoietin (TPO) levels were determined in serum by ELISA (Quantikine Mouse TPO Immunoassay; R&D Systems), according to the manufacturer's instructions. TPO levels from five wild-type and two knock out male mice were measured, as well as from 4 wild-type and five knock out female mice. Serum levels from each mouse were measured in duplicate.

Immunohistochemistry and immunofluorescence analysis

For hematoxylin/eosin (H/E) staining, tissues were fixed with buffered formalin, paraffin-embedded, sectioned (7 m), and stained with haematoxylin and eosin. In some cases mice were injected with 5-bromodeoxyuridine (BrdU) 30 minutes prior to dissection of tissue. Sections were incubated with anti-BrdU and processed with peroxidase-conjugated secondary antibodies.

For immunofluorescence megakaryocytes were cultured under the conditions described above. After 6 days of culture cells were cytocentrifuged onto poly-L-lysine-coated coverslips at 400 rpm for 5 minutes, fixed for 15 minutes in ice-cold methanol/1mM EGTA and permeabilized with 0,5% Triton X-100. After blocking with 1% bovine serum albumin (BSA) in PBS, slides were incubated with a 1:300 dilution of rabbit polyclonal antibody against CLASP2 and 1:200 dilution of human anti-CREST6 antibody, for one hour at room temperature. After washing, cells were incubated with FITC-conjugated goat anti-rabbit IgG (1:100) and goat anti-human A594 (1:300) antibodies, for one hour at room temperature. Cells were counterstained with DAPI to visualize nuclear DNA. Controls were processed identically, except for the omission of the primary antibody, and did not give a detectible signal (data not shown). Image acquisition was carried out as descibed previously (Akhmanova et al. 2005).

Imaging of testis tubules was performed as described (Akhmanova et al. 2005). When required, 5 g/ml Hoechst 33342 (Molecular Probes) was either added to the medium or injected through the rete testis with Trypan blue (Sigma). The testis tubules were examined at 33 ^{0}C, using a Zeiss LSM510 confocal/multiphoton set up, to allow simultaneous acquisition of phase-contrast, GFP and Hoechst images. GFP-CLIP-170 movement *ex vivo* was analyzed as published (Stepanova et al. 2003). Values were imported into Aabel (Gigawiz) for graphical representation and statistical analysis.

Acknowledgements

We would like to thank Ton de Wit for generating and donating the Cre transgenic line. This work was supported by the Earth and Life Sciences(ALW) and Medical Sciences (ZonMw) divisions of the Netherlands Organization for Scientific Research (NWO), the Dutch Cancer Society (KWF) and the Dutch Ministry of Economic Affairs (BSIK).

Supplemental Information.

Supplemental Movie 1. Time lapse imaging of GFP-CLIP-170 movement in live testis tubules.

Testis tubules were dissected from the *GFP-Clip-170* knock in – *Clasp2* knock out mice and analyzed with a confocal microscope. A time lapse recording was made (60 images, 1 image every 2 seconds). Notice the comet-like dashes moving through the cytoplasm of two spermatogonia. After 30 images, the cell in the middle of the image was bleached, hence the disappearance of the nuclear GFP signal.

References

Akhmanova, A. and Hoogenraad, C.C. 2005. Microtubule plus-end-tracking proteins: mechanisms and functions. Curr Opin Cell Biol **17**: 47-54.

Akhmanova, A., Hoogenraad, C.C., Drabek, K., Stepanova, T., Dortland, B., Verkerk, T., Vermeulen, W., Burgering, B.M., De Zeeuw, C.I., Grosveld, F., and Galjart, N. 2001. Clasps are CLIP-115 and -170 associating proteins involved in the regional regulation of microtubule dynamics in motile fibroblasts. Cell **104**: 923-935.

Akhmanova, A., Mausset-Bonnefont, A.-L., Van Cappellen, W., Keijzer, N., Hoogenraad, C.C., Stepanova, T., Drabek, K., van der Wees, J., Mommaas, M., Onderwater, J., van der Meulen, H., Hoogerbrugge, J., Vreeburg, J., Uringa, E.-J., Grootegoed, A., Grosveld, F., and Galjart, N. 2005. The microtuble plus end tracking protein CLIP-170 associates with the spermatid manchette and is essential for spermatogenesis. Genes Dev **in press**.

Berthier, R., Jacquier-Sarlin, M., Schweitzer, A., Block, M.R., and Molla, A. 1998. Adhesion of mature polyploid megakaryocytes to fibronectin is mediated by beta 1 integrins and leads to cell damage. Exp Cell Res **242**: 315-327.

Coquelle, F.M., Caspi, M., Cordelieres, F.P., Dompierre, J.P., Dujardin, D.L., Koifman, C., Martin, P., Hoogenraad, C.C., Akhmanova, A., Galjart, N., De Mey, J.R., and Reiner, O. 2002. LIS1, CLIP-170's key to the dynein/dynactin pathway. Mol Cell Biol **22**: 3089-3102.

Drabek, K., van Ham, M., Stepanova, T., van Horssen, R., Van Cappellen, G., Draegestein, K., Akhmanova, A., Houtsmuller, A., ten Hagen, T.L.M., Grosveld, F., and Galjart, N. 2005. CLASP2 localizes to focal adhesions and mediates fibronectin-induced stabilization of microtubules.

Drachman, J.G., Sabath, D.F., Fox, N.E., and Kaushansky, K. 1997. Thrombopoietin signal transduction in purified murine megakaryocytes. Blood **89**: 483-492.

Galjart, N. 2005. CLIPs and CLASPs and cellular dynamics. Nat Rev Mol Cell Biol **6**: 487-498.

Hoogenraad, C.C., Akhmanova, A., Grosveld, F., De Zeeuw, C.I., and Galjart, N. 2000. Functional analysis of CLIP-115 and its binding to microtubules. J Cell Sci **113**: 2285-2297.

Hoogenraad, C.C., Koekkoek, B., Akhmanova, A., Krugers, H., Dortland, B., Miedema, M., van Alphen, A., Kistler, W.M., Jaegle, M., Koutsourakis, M., Van Camp, N., Verhoye, M., van der Linden, A., Kaverina, I., Grosveld, F., De Zeeuw, C.I., and Galjart, N. 2002. Targeted mutation of Cyln2 in the Williams syndrome critical region links CLIP-115 haploinsufficiency to neurodevelopmental abnormalities in mice. Nat Genet **32**: 116-127.

Hou, M., Andersson, P.O., Stockelberg, D., Mellqvist, U.H., Ridell, B., and Wadenvik, H. 1998. Plasma thrombopoietin levels in thrombocytopenic states: implication for a regulatory role of bone marrow megakaryocytes. Br J Haematol **101**: 420-424.

Inoue, Y.H., do Carmo Avides, M., Shiraki, M., Deak, P., Yamaguchi, M., Nishimoto, Y., Matsukage, A., and Glover, D.M. 2000. Orbit, a novel microtubule-associated protein essential for mitosis in Drosophila melanogaster. J Cell Biol **149**: 153-166.

Inoue, Y.H., Savoian, M.S., Suzuki, T., Mathe, E., Yamamoto, M.T., and Glover, D.M. 2004. Mutations in orbit/mast reveal that the central spindle is comprised of two microtubule populations, those that initiate cleavage and those that propagate furrow ingression. J Cell Biol **166**: 49-60.

Kaushansky, K. 1999. The enigmatic megakaryocyte gradually reveals its secrets. Bioessays **21**: 353-360.

Kaushansky, K. 2002. Thrombopoietin: from theory to reality. Int J Hematol **76 Suppl 1**: 343-345.

Kojima, S., Matsuyama, T., Kodera, Y., Tahara, T., and Kato, T. 1997. Measurement of endogenous plasma thrombopoietin in patients with acquired aplastic anaemia by a sensitive enzyme-linked immunosorbent assay. Br J Haematol **97**: 538-543.

Lee, H., Engel, U., Rusch, J., Scherrer, S., Sheard, K., and Van Vactor, D. 2004. The microtubule plus end tracking protein Orbit/MAST/CLASP acts downstream of the tyrosine kinase Abl in mediating axon guidance. Neuron **42**: 913-926.

Lemos, C.L., Sampaio, P., Maiato, H., Costa, M., Omel'yanchuk, L.V., Liberal, V., and Sunkel, C.E. 2000. Mast, a conserved microtubule-associated protein required for bipolar mitotic spindle organization. Embo J **19**: 3668-3682.

Maiato, H., Fairley, E.A., Rieder, C.L., Swedlow, J.R., Sunkel, C.E., and Earnshaw, W.C. 2003. Human CLASP1 is an outer kinetochore component that regulates spindle microtubule dynamics. Cell **113**: 891-904.

Maiato, H., Khodjakov, A., and Rieder, C.L. 2004. Drosophila CLASP is required for the incorporation of microtubule subunits into fluxing kinetochore fibres. Nat Cell Biol.

Maiato, H., Sampaio, P., Lemos, C.L., Findlay, J., Carmena, M., Earnshaw, W.C., and Sunkel, C.E. 2002. MAST/Orbit has a role in microtubule-kinetochore attachment and is essential for chromosome alignment and maintenance of spindle bipolarity. J Cell Biol **157**: 749-760.

Mathe, E., Inoue, Y.H., Palframan, W., Brown, G., and Glover, D.M. 2003. Orbit/Mast, the CLASP orthologue of Drosophila, is required for asymmetric stem cell and cystocyte divisions and development of the polarised microtubule network that interconnects oocyte and nurse cells during oogenesis. Development **130**: 901-915.

Mimori-Kiyosue, Y., Grigoriev, I., Lansbergen, G., Sasaki, H., Matsui, C., Severin, F., Galjart, N., Grosveld, F., Vorobjev, I., Tsukita, S., and Akhmanova, A. 2005. CLASP1 and CLASP2 bind to EB1 and regulate microtubule plus-end dynamics at the cell cortex. J Cell Biol **168**: 141-153.

Moore, C.A. and Zernicka-Goetz, M. 2005. PAR-1 and the microtubule-associated proteins CLASP2 and dynactin-p50 have specific localisation on mouse meiotic and first mitotic spindles. Reproduction **130**: 311-320.

Osoegawa, K., Tateno, M., Woon, P.Y., Frengen, E., Mammoser, A.G., Catanese, J.J., Hayashizaki, Y., and de Jong, P.J. 2000. Bacterial artificial chromosome libraries for mouse sequencing and functional analysis. Genome Res **10**: 116-128.

Perez, F., Diamantopoulos, G.S., Stalder, R., and Kreis, T.E. 1999. CLIP-170 highlights growing microtubule ends in vivo. Cell **96**: 517-527.

Ravid, K., Lu, J., Zimmet, J.M., and Jones, M.R. 2002. Roads to polyploidy: the megakaryocyte example. J Cell Physiol **190**: 7-20.

Russell, L.D., Russell, J.A., MacGregor, G.R., and Meistrich, M.L. 1991. Linkage of manchette microtubules to the nuclear envelope and observations of the role of the manchette in nuclear shaping during spermiogenesis in rodents. Am J Anat **192**: 97-120.

Sambrook, J., Fritsch, E.F., and Maniatis, T. 1989. Molecular cloning: a laboratory manual, 2 Edition. Cold Spring Harbor Laboratory Press, New York.

Schick, P.K., Wojenski, C.M., He, X., Walker, J., Marcinkiewicz, C., and Niewiarowski, S. 1998. Integrins involved in the adhesion of megakaryocytes to fibronectin and fibrinogen. Blood **92**: 2650-2656.

Schuyler, S.C. and Pellman, D. 2001. Microtubule "plus-end-tracking proteins": The end is just the beginning. Cell **105**: 421-424.

Schwer, H.D., Lecine, P., Tiwari, S., Italiano, J.E., Jr., Hartwig, J.H., and Shivdasani, R.A. 2001. A lineage-restricted and divergent beta-tubulin isoform is essential for the biogenesis, structure and function of blood platelets. Curr Biol **11**: 579-586.

Stepanova, T., Slemmer, J., Hoogenraad, C.C., Lansbergen, G., Dortland, B., De Zeeuw, C.I., Grosveld, F., van Cappellen, G., Akhmanova, A., and Galjart, N. 2003. Visualization of microtubule growth in cultured neurons via the use of EB3-GFP (end-binding protein 3-green fluorescent protein). J Neurosci **23**: 2655-2664.

Vannucchi, A.M., Paoletti, F., Linari, S., Cellai, C., Caporale, R., Ferrini, P.R., Sanchez, M., Migliaccio, G., and Migliaccio, A.R. 2000. Identification and characterization of a bipotent (erythroid and megakaryocytic) cell precursor from the spleen of phenylhydrazine-treated mice. Blood **95**: 2559-2568.

Verfaillie, C.M. 1998. Adhesion receptors as regulators of the hematopoietic process. Blood **92**: 2609-2612.

Villeval, J.L., Cohen-Solal, K., Tulliez, M., Giraudier, S., Guichard, J., Burstein, S.A., Cramer, E.M., Vainchenker, W., and Wendling, F. 1997. High thrombopoietin production by hematopoietic cells induces a fatal myeloproliferative syndrome in mice. Blood **90**: 4369-4383.

Wittmann, T. and Waterman-Storer, C.M. 2005. Spatial regulation of CLASP affinity for microtubules by Rac1 and GSK3beta in migrating epithelial cells. J Cell Biol **169**: 929-939.

Chapter 5

Differential roles of microtubule assembly and sliding in pro-platelet formation by megakaryocytes

Blood in press

Differential roles of microtubule assembly and sliding in proplatelet formation by megakaryocytes

Sunita R. Patel[1,3], Jennifer Richardson[1,3], Harald Schulze[2,3], Eden Kahle[1,3], Niels Galjart[4], Ksenija Drabek[4], Ramesh A. Shivdasani[2,3], John H. Hartwig[1,3] , and Joseph E. Italiano Jr.[1,3,5]

[1]Division of Hematology, Brigham and Women's Hospital, [2]Dana Farber Cancer Institute, [3]Department of Medicine, Harvard Medical School, Boston, MA 02115. [4]Department of Cell Biology and Genetics, Erasmus University, 3000 DR Rotterdam, The Netherlands.
[5]Corresponding author:
Division of Hematology, Department of Medicine, Brigham and Women's Hospital, Harvard Medical School, Boston, MA 02115
Phone: (617) 355-9007
Fax: (617) 355-9016
Email: jitaliano@rics.bwh.harvard.edu

Abstract
Megakaryocytes are terminally differentiated cells that, in their final hours, convert their cytoplasm into long, branched proplatelets, which remodel into blood platelets. Proplatelets elongate at an average rate of 0.85 μm/min in a microtubule dependent process. Addition of rhodamine-tubulin to permeabilized proplatelets, immunofluorescence microscopy of the microtubule plus-end marker EB3, and fluorescence time-lapse microscopy of EB3-GFP expressing megakaryocytes reveal that microtubules, organized as bipolar arrays, continuously polymerize throughout the proplatelet. In immature megakaryocytes lacking proplatelets, microtubule plus-ends initiate and grow by centrosomal nucleation at rates of 8.9-12.3 μm/min. In contrast, plus-end growth rates of microtubules within proplatelets are highly variable (1.5-23.5 μm/min) and are both slower and faster than those seen in immature cells. Despite the continuous assembly of microtubules, proplatelets continue to elongate when net microtubule assembly is arrested. One alternative mechanism for force generation is microtubule sliding. Triton X-100 permeabilized proplatelets containing dynein and its regulatory complex, dynactin, but not kinesin, elongate with the addition of ATP at a rate of 0.65 μm/min. Retroviral expression in megakaryocytes of dynamitin (p50), which disrupts dynactin-dynein function, inhibits proplatelet elongation. We conclude that while continuous polymerization of microtubules is necessary to support the enlarging proplatelet mass, the sliding of overlapping microtubules is a vital component of proplatelet elongation.

Introduction

Blood platelets, tiny cells shed by megakaryocytes, circulate throughout blood vessels and survey the integrity of the vascular system. In response to traumatic injuries in which blood vessel continuity is interrupted, platelets bind to exposed collagen, change shape, secrete granule contents, and aggregate with neutrophils to form a hemostatic plug to seal off the damaged blood vessel. The mechanisms by which blood platelets are formed and released from giant precursor cells called megakaryocytes *in situ* remain to be defined. However, the development of megakaryocyte culture systems that produce platelets has provided a means to study the intermediate structures called "proplatelets", long (up to several millimeters), thin extensions of the megakaryocyte cytoplasm that contain multiple platelet-sized beads along their length.[1-7] Based on multiple lines of evidence, we have speculated that platelets are not preassembled in the megakaryocyte cytoplasm but instead are constructed *de novo*, predominantly at the ends of the proplatelets.[8] As predicted, megakaryocytes go to great lengths to amplify the number of proplatelet ends, taking the shaft of each proplatelet and bending it multiple times. Each bend yields a bifurcation in the shaft, generating a new end.

The formation of proplatelets is highly dependent upon a complex network of protein filaments that extends throughout the megakaryocyte cytoplasm. Microtubules, which are formed when thousands of tubulin molecules assemble into linear filaments, are a major component of this cytoskeletal network and function as the primary motor for proplatelet elongation. High concentrations of microtubule poisons prevent proplatelet elongation and cause extended proplatelets to retract.[7,9,10] Deletion of the β1-tubulin gene, which encodes the major β-tubulin isoform expressed in mouse megakaryocytes diminishes the capacity of these cells to assemble microtubules, cripples platelet production and release, and results in aberrant platelet morphologies.[11,12] We have previously described in detail some of the temporal and spatial rearrangements of microtubules that accompany proplatelet formation, which appear to be unique and used only by megakaryocytes to make platelets.[8] The first observable protrusive event in proplatelet elaboration occurs after the bulk movement of microtubules into the cortex of a mature megakaryocyte. Subsequently, broad pseudopodia form and extend from one pole of the megakaryocyte. As proplatelets continue to elongate and narrow, their microtubule bundles align and narrow in the proplatelet shafts. Surprisingly, the arrays of microtubules do not abruptly terminate at the proplatelet tip but instead loop back toward the cell body and re-enter the shaft of the proplatelet. The process of amplifying proplatelet ends by repeatedly bending and bifurcating the proplatelet shaft is dependent on actin-based forces and is inhibited by the cytochalasins, actin toxins.[7,8] These events are highly interrelated, but one can try to dissect their separate mechanisms experimentally. Despite our detailed knowledge of the microtubule architecture within proplatelets, exactly how this cytoskeletal engine reorganizes to power proplatelet elongation is unclear.

In this study, we have focused on how microtubules interact to generate the required forces for proplatelet elongation. Proplatelet elongation occurs as adjacent microtubules slide relative to one another analogous to the way in which a ladder on a fire engine

lengthens by sliding of overlapping sections past each other. Polymerization involves extension through the addition of free tubulin dimers to existing microtubules or the *de novo* formation of new microtubules. We identify the sites of microtubule assembly and directly visualize microtubule dynamics during platelet production using time-lapse video fluorescence microscopy of megakaryocytes directed to express a fluorescent marker of plus-end microtubule growth. Although microtubule plus-ends distribute throughout proplatelets and normally grow both towards and away from the proplatelet tip, we find that microtubule assembly is not required for proplatelet elongation as application of low concentrations of microtubule assembly inhibitors that arrest plus-end growth fail to diminish the rate at which proplatelets are elongated. To dissect apart the contribution of microtubule assembly from that of microtubule sliding in elaborating the proplatelet microtubule array, we studied permeabilized proplatelets. Triton X-100-permeabilized proplatelet shafts remain capable of elongating, and do so in response to the addition of ATP in the absence of microtubule growth. Since dynein and the dynactin complexes are intimately associated with proplatelet microtubules, we show evidence for and favor a mechanism that slides overlapping microtubules relative to one another, within the shafts to lengthen proplatelets.

Materials and Methods

Materials

Nocodazole, vinblastine, and taxol were purchased from Sigma (St. Louis, MO) and prepared as stock solutions in dimethyl sulfoxide.

Megakaryocyte Cultures

Livers were recovered from mouse fetuses and single cell suspensions were generated using methods described previously[8].

DIC Microscopy of Proplatelet Elongation

Megakaryocytes were cultured in DMEM within video chambers as described previously.[8] Samples were imaged with a Nikon TE-200 60X (NA 1.4) DIC objective and captured with an Orca-II ER cooled CCD camera (Hamamatsu, Hamamatsu City, Japan). Illumination was shuttered between exposures. Electronic shutters and image acquisition were under the control of Metamorph software (Universal Imaging Corporation of Molecular Devices, Westchester, PA). Sample temperature was maintained at 37°C using a bipolar temperature controller (Medical Systems Corp., Miami, FL). A stage micrometer was used for measurement of the rate of proplatelet elongation and length measurements were made using the Metamorph image analysis program. The average length of the proplatelet was determined from recordings spaced between 1 and 5 minutes apart over a period of 20-60 min.

Quantitation of Microtubule Polymer Levels

Microtubule polymer fractions in control, nocodazole-, and vinblastine-treated megakaryocytes were analyzed by SDS-PAGE and immunoblot. Control and drugtreated megakaryocytes were rinsed in PEM (100 mM PIPES, 10 mM EGTA, and 2mM MgCl2, pH 7.0) with different doses of drug, and extracted in PEM containing 0.75% Triton X-100 plus Complete protease inhibitor cocktail (Roche) for 5 min. Samples were centrifuged for 30 min at 100,000 g in a centrifuge (model TL-100; Beckman Coulter, Fullerton, CA). The pellet was resuspended with SDS-PAGE sample buffer to the same volume as the supernatant. All samples were incubated at 37°C overnight. An equal volume of each sample was run on SDS-PAGE, transferred to PVDF (Polyvinylidene difluoride), immunoblotted with anti-α-tubulin antibody (Sigma), and the density of the bound antibody was quantitated as described below.

Immunofluorescence Microscopy

Rabbit Anti-EB3 polyclonal antibody was described previously [13]. Mouse anti-p150^{Glued} monoclonal antibody was obtained from Becton Dickinson Biosciences (Franklin Lakes, NJ). Affinity purified rabbit anti-dynactin p50 (UP1097) and anti-dynein intermediate chain (DIC) polyclonal antibodies were a gift from E. Holzbauer (University of Pennsylvania, Philadelphia). Mouse monoclonal anti-kinesin heavy chain antibody (MAB1614) was obtained from Chemicon (Temecula, CA). Rabbit anti-β1 antiserum was a gift from Nick Cowan (New York University Medical Center, New York). Cells were analyzed and photographed on a Zeiss Axivert 200 microscope described below.

Megakaryocytes were fixed on coverslips as described previously. For anti-EB3 immunofluorescence, coverslips were washed with platelet buffer and fixed in freshly prepared -20°C methanol/1 mM EGTA for 10 min at -20°C. Megakaryocytes were permeabilized with 0.5% Triton X-100, then washed with PBS. In experiments where cells were extracted prior to fixation, coverslips were incubated for 5 min in a microtubule-stabilizing buffer (PEM) containing 0.5% Triton X-100, washed with PEM buffer, and fixed with formaldehyde. Specimens were blocked overnight in PBS with 1% BSA, incubated in primary antibody for 2-3 hours, washed, treated with appropriate secondary antibody for 1 hr, and then washed extensively. Primary antibodies were used at 1 μg/ml in PBS containing 1% BSA and secondary antibodies at 1:500 dilution in the same buffer. Controls were processed identically except for omission of the primary antibody.

Reactivation of Elongation in Permeabilized Megakaryocytes

Proplatelet-producing megakaryocytes were attached to coverslips as described above and transferred to the microscope for observation. Cells were treated with microtubule stabilization buffer (PEM buffer plus 30 μm taxol), washed with PEMG buffer (PEM buffer supplemented with 0.1 mM GTP), permeabilized with 0.5% Triton X-100 in PMEG buffer supplemented with 1 mM DTT and Complete protease inhibitor cocktail (Roche),

washed three times with PEM buffer, and then incubated in PEM buffer supplemented with 1 mM DTT. Elongation was initiated by adding 0.1 mM ATP in PEM buffer. All nucleotides were used at concentrations ranging from 0.1-1 mM.

Rhodamine-Tubulin Incorporation in Permeabilized Megakaryocytes

Megakaryocytes were attached to 25 mm coverslips as described above. Cells were briefly washed with platelet buffer, permeabilized with 0.5% Triton X-100 in PMEG buffer with protease inhibitors, and washed with PMEG buffer. Permeabilized proplatelets were incubated for 4 min in 20 μm rhodamine-labeled tubulin (The Cytoskeleton, Denver, CO), 20 μm taxol, 0.1 mM GTP in PMEG solution in the absence of ATP. After incubation, unbound tubulin was removed by washing with PMEG buffer containing 20 μm taxol in PMEG buffer.

Expression of Constructs

Semliki Forest virus (SFV)-mediated gene delivery was used to express EB3-GFP in mouse megakaryocytes.[13] Cultured megakaryocytes were infected by the addition of 1 μl of SFV infectious replicons to 400 μl of Day 2.5 cultures. EB3-GFP movements were visualized by fluorescence microscopy 8-48 hr after infection. A p50 cDNA (Accession no. HIBBF17), kindly obtained from E. Holzbaur (University of Pennsylvania, Philadelphia), was cloned into pWZL plasmids containing the sequence for enhanced green fluorescent protein using previously described methods.[31]

Live Cell Imaging of EB3-GFP Movements

Infected megakaryocytes were pipetted onto video chambers maintained at 37°C. Cells were viewed on a Zeiss Axivert 200 microscope equipped with a 63X objective (NA 1.4) and 1.6X optivar, and a 100-W mercury lamp adjusted to an intensity of 50%. Images of EB3-GFP movements in megakaryocytes were acquired every 2-5 sec with an average image capture time of 500 milliseconds using an Orca II CCD camera (Hamamatsu). The velocity of EB3-GFP comets was determined by dividing the distances traveled by the time elapsed. We included only comets that could be followed for a minimum of 15 seconds.

RESULTS

Proplatelets elongate at an average rate of 0.85 μm/min.

We obtained details of proplatelet elongation using video-enhanced differential-interference-contrast (DIC) microscopy of cultured mouse megakaryocytes (Figure 1, Supplemental Movie 1). Proplatelet formation begins with the extension of a thick cytoplasmic process that elongates from one pole of the megakaryocyte body. The formation of the initial pseudopodia does not require the addition of any “stimulus” to the culture medium and oc-

curs spontaneously on days 4 to 5 in culture. Proplatelets become thinner as they elongate and taper in diameter at their ends (Figure 1, arrow at 9 min). The rate of proplatelet elongation ranged from 0.30 to 1.59 μm/min (mean, 0.85 + 0.24 μm/min, n=77).

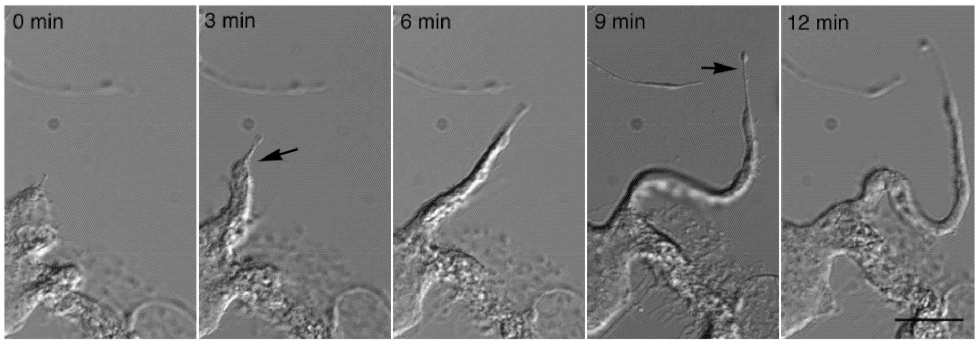

Figure 1. Video-enhanced differential-interference-contrast microscopy showing a representative proplatelet elongating from a mouse megakaryocyte. By 3 min (arrow), the initial broad pseudopodia has converted into a proplatelet process that continues to lengthen and reduce its diameter at the proplatelet tip (arrow at 9 min). Proplatelets elongate at an average rate of 0.85 + 0.24 μm/min, n= 77). Bar, 5 μm. See Supplemental Movie 1.

Visualization of plus-end microtubule growth in megakaryocytes.

Proplatelet morphogenesis depends on the elaboration of a dense and highly organized array of microtubules. Microtubules are polar structures: one end, the plus end, is capable of rapid growth, while the other end, the minus end, tends to lose subunits if not stabilized. Microtubules first collect in the cortex of a mature megakaryocyte, then loop into an initial broad pseudopod. Linear arrays of microtubules align within the shaft as the pseudopod elongates and transforms into a proplatelet. Rather than ending at the proplatelet tip, microtubules instead, loop and reenter the shaft.[8] Given the importance of microtubule-based forces involved in proplatelet extension and the structural constraints imposed by microtubule organization within proplatelets, we first determined the location of growing microtubule plus-ends within proplatelets using two independent approaches. First, proplatelet-producing megakaryocytes were attached to polylysine-coated coverslips, permeabilized with Triton X-100, and incubated with Rhodamine-labeled tubulin. This approach preserves the integrity of the microtubule array in proplatelets. As shown in Figures 2A and 2B, fluorescently-labeled tubulin incorporates into distinct foci along the entire length of proplatelets, indicating that microtubule plus-ends exist along their full length.

Second, the growing ends of microtubules in megakaryocytes were highlighted with antibodies against end-binding protein 3 (EB3), a plus-end-tracking protein (Figure 2CD), [13,14,15] Figure 2C (inset) shows that mouse megakaryocytes express EB3, a 36 kDa protein, when cell lysates are separated by SDS-PAGE and immunoblotted with anti-EB3 antibodies. Immunofluorescence microscopy of proplatelet-producing megakaryocytes with anti-EB3 antibody revealed labeling in both the cell bodies and proplatelets of megakaryo-

cytes (Figure 2C-D). EB3 stained as fluorescent "comets" with bright "fronts" and diffuse "tails" previously described by plus-end markers in other cell types.[13,16-18] Clear staining of comet-like dashes was observed along the total length of the proplatelet and in the cell body, which suggests that plus-ends of microtubules are interspersed across the entire cytoplasm of proplatelet-producing megakaryocytes. We were unable to detect the hallmark "starburst" pattern typical of centrosomal nucleation in the cell bodies of proplatelet-producing megakaryocytes, although it is readily observed in megakaryocytes prior to the proplatelet phase (see below); these results indicate that a centrosomal mode of nucleation is absent during proplatelet formation.

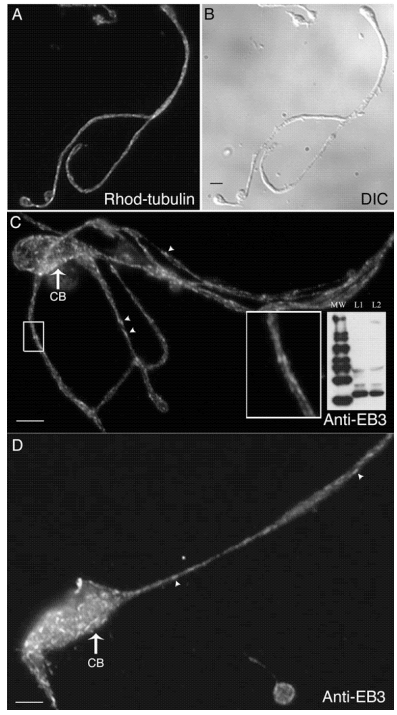

Figure 2. Localization of microtubule plus ends in proplatelets. (A-B) Megakaryocytes extending proplatelets were permeabilized with Triton X-100 and incubated with TRITC-tubulin as described in Materials and Methods. (A) Fluorescence micrograph showing a permeabilized proplatelet after incubation with rhodamine-tubulin for 4 min. TRITC-tubulin incorporates into specific foci along the length of the proplatelet. Bar, 4 μm. (B) Differential interference contrast micrograph of cell labeled in panel (A). (C-D) Anti-EB3 immunofluorescent labeling of a proplatelet-containing megakaryocyte. EB3 staining (arrowheads label comet-like dashes) is dispersed along proplatelets and is abundant in the cell bodies (CB) but is not found in a radial pattern (compare with preproplatelet megakaryocytes in Figure 5). The boxed region in C shows a high magnification view of the comets. Bars, 4 μm. (C, inset) The immunoblot shows that anti-EB3 antibodies recognize a 36 kDa polypeptide in both (L1) preproplatelet megakaryocytes and(L2) proplatelet-containing megakaryocytes.

To gain information on microtubule plus-end dynamics in real time, EB3-GFP was virally expressed in mouse megakaryocytes and movements of the fluorescently tagged protein were visualized 8-48 hr after infection (Figure 3 and 4A-D). The distribution of

EB3-GFP in living cells was similar to that of endogenous EB3 (compare Figure 2C-D and Figure 3A-B). Expression of EB3-GFP had no effect on the rate of proplatelet elongation (0.74 μm/min in EB3-GFP-expressing cells). EB3-GFP appeared as cometlike dashes along the full length of proplatelets, providing direct evidence that microtubule plus-ends are situated throughout the shafts (Figure 3B) and tips (Figure 4B) of proplatelets. Treatment of megakaryocytes with 10 μm nocodazole resulted in a rapid loss of EB3-GFP comets, which indicates that EB3-GFP associates specifically with growing ends of microtubules (data not shown). As observed in the anti-EB3 immunofluorescence experiments, centrosomal nucleation of microtubules was not observed in proplatelet-producing megakaryocytes.

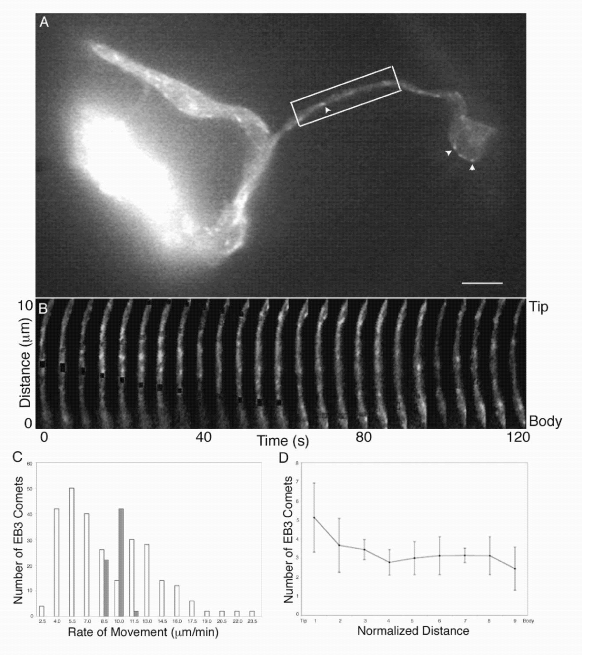

Figure 3. EB3-GFP movements in proplatelet-producing megakaryocytes. (A) First frame from a time-lapse movie of a live megakaryocyte expressing EB3-GFP (see Supplemental Movie 2). The cell body is at the left of the micrograph. EB3-GFP labels growing microtubule plus-ends in a characteristic "comet" staining pattern (arrowheads) that has a bright front and dim tail. Moving comets are found along the proplatelets as well as in the megakaryocyte cell body. The scale bar is 5 μm. (B) Kymograph of the boxed region in panel (A). Images are every 5 seconds. EB3-GFP comets undergo bidirectional movements in proplatelets. Some EB3-GFP comets move tipward and are highlighted in green; others that move towards the cell body are highlighted in red. (C) Comparison of the velocity distribution of comets moving in proplatelets (white bars) with those emanating from the centrosome of pre-proplatelet megakaryocytes (dark bars). The average rate of comet movement in the pre-proplatelet megakaryocytes was 10.2 + 0.77 and the rates of movement were tightly grouped (8.9 – 12.3 μm/min). EB3 movements in proplatelets, however, are apparently bimodal with distinct populations moving slower and faster than those of the pre-proplatelet megakaryocytes. (D) EB3-GFP comets were distributed throughout the proplatelet. Proplatelets were divided into 10 segments (tip =0, cell body = 9) and the number of GFP-EB3 comets in each was determined. The length of the evaluated proplatelet was 28 μm.

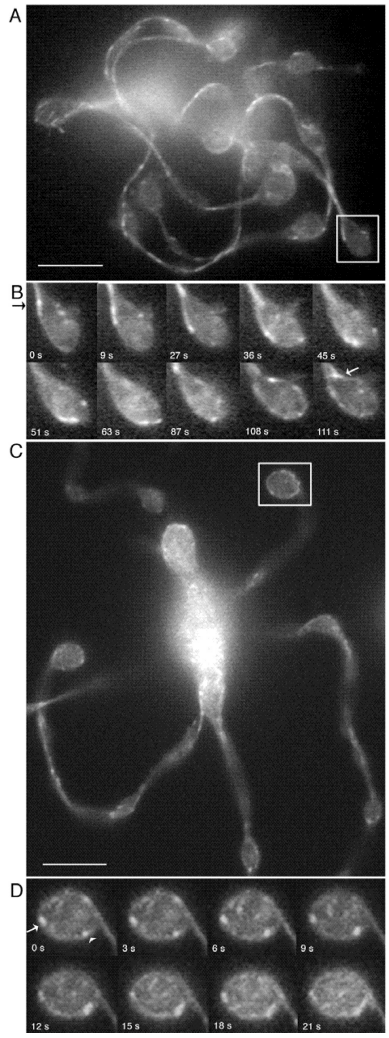

Figure 4. EB3-GFP comet movements in living megakaryocytes. (A-D) EB3-GFP comet movements within the tips of proplatelets. (A) First frame of a time-lapse sequence shown in Supplemental Movie 3. (C) First frame of a time-lapse sequence shown in Supplemental Movie 4. (B, D) Kymograph of EB3 movements around proplatelet tips. In the first example, EB3-comets enter the proplatelet tip, circle its periphery, and then re-enter the shaft of the proplatelet. Images are every 5 seconds. In the second example, EB3-comets move around the periphery of the tip in both directions (arrowhead highlights clockwise movement, arrow highlights counter-clockwise movement). Images are every 2 seconds. Comets also move into the tip on microtubules that end abruptly. The scale bar represents 5 μm. (E-G) Location and dynamics of microtubule plus-ends in representative pre-proplatelet megakaryocytes. (E-F) Anti-EB3 immunofluorescence of pre-proplatelet-megakaryocytes. Cells at this stage of maturation have a radial array of microtubules that emanates from the centrosome. EB3 comets concentrate near the centrosome and are on the plus-ends of microtubules that radiate outward. Bar, 2 μm. (G) Dynamics of EB3-GFP comets in a megakaryocyte lacking proplatelets. This sequence of images shows EB3-GFP to concentrate on the plus-ends of microtubules as they grow from the centrosome (See Supplemental Movie 4). Translocations of EB3-GFP in the cell cortex, parallel to the plasma membrane, are also apparent. Elapsed time is in seconds.

Because the temporal movement of EB3-GFP provides insight into the polarity of individual microtubules within the bundles that line proplatelets, we analyzed the direction and velocities of EB3-GFP comets. Figure 3B and Supplemental Movie 2 demonstrate that EB3-GFP comets move in both directions along proplatelets, and quantitation of the data shows an equal mix of microtubule polarity (51.72 % of the EB3-GFP comets moved toward the tip; 48.28% moved away from the tip, n = 90) in proplatelets. Representative examples of comets moving tipward have been highlighted in green and those moving toward the cell body are highlighted in red (Figure 3B). EB3-GFP comets were also observed to travel around the proplatelet tip and re-enter the shaft (Figure 4B and Supplemental Movie 3). EB3-GFP comets within the microtubule coils at the tips of proplatelets moved bidirectionally (arrowhead, clockwise; arrow, counterclockwise) (Figure 4C-D and Supplemental Movie 4). Although the average rate of comet movement was 8.9 + 3.9 μm/min (mean + SD; data from 133 comets in 12 proplatelet-producing cells), velocity rates were quite broad (Figure 3C, white bars), ranging from 3.75 to 24.77 μm/min. No difference was found in the forward or reverse rate of microtubule growth relative to the proplatelet tips, and the growth rates for individual microtubules were always linear. None of the comets moved at a rate equivalent to proplatelet elongation (0.85 μm/min). Taken together, these results suggest that microtubule assembly is not tightly coupled to proplatelet elongation.

The wide distribution of EB3-GFP comet velocities in proplatelet-producing megakaryocytes could be explained by the superposition of microtubule transport on assembly. To investigate this possibility, we analyzed EB3-GFP comet movements in immature megakaryocytes, which employ centrosomal nucleation and where plus-end growth rates can be ascribed primarily to microtubule assembly. Immunofluorescence staining with anti-EB3 antibody of pre-proplatelet megakaryocytes gave a labeling pattern that was consistent with centrosomal nucleation (Figure 4E-F). At this stage, megakaryocytes elaborate a well-developed, radial microtubule network with readily discernible tips extending toward the cell periphery. Centrosomal nucleation was confirmed in pre-proplatelet megakaryocytes that were virally directed to express EB3-GFP and visualized by fluorescence time-lapse microscopy (Figure 4G, Supplemental Movie 5). The dynamic behavior of EB3-GFP at microtubule plus-ends was displayed by continuous centrifugal movements of the numerous GFP signals. The average rate of EB3-GFP movement during centrosomal nucleation was similar to that observed in proplatelet-producing megakaryocytes (10.2 μm/min +/- 0.77, n=33), but the range of movement was much narrower (8.92-12.28 μm/min), as is expected for a population of microtubules with similar polymerization kinetics. This evidence further supports the idea that the wide distribution of comet velocities observed along proplatelets reflects the process of microtubule sliding superimposed on assembly.

Proplatelets elongate under conditions that arrest net microtubule assembly.

The EB3-GFP expression studies strongly suggest that proplatelet elongation is not coupled directly to microtubule assembly. To further test this hypothesis, we sought methods to tease apart the relative contributions of microtubule sliding and microtubule assembly in elaborating the proplatelet microtubule array. To do so, we studied the outgrowth of pro-

platelets under conditions that arrest microtubule assembly while maintaining substantial levels of pre-existing tubulin polymer available for transport via sliding within proplatelets. We reasoned that if proplatelet elongation is driven entirely by polymerization, inhibition should arrest elongation. However, if microtubule sliding is the predominant mechanism for proplatelet elongation, proplatelets should continue to lengthen even after assembly is inhibited. When microtubule poisons are applied to cells at appropriate concentrations, they can act as kinetic stabilizers of microtubules.[19-21] To investigate the effects of various concentrations of microtubule assembly inhibitors, preproplatelet megakaryocytes were cultured in media containing nocodazole at concentrations of 0, 100, 250, and 1000 nM or vinblastine at concentrations of 0, 16, and 50 nM. Twenty hours after plating, cultures were examined with phase-contrast optics and photographed (Figure 5Ai-xii). Megakaryocytes plated overnight, extended proplatelets in all but the highest drug concentrations (1 μM nocodazole and 50 nM vinblastine). However, the number and length of proplatelets seen in cultures containing 250 nM nocodazole (Figure 5Aiv-v) or 16 nM vinblastine (Figure 5Aix-xi) were diminished.

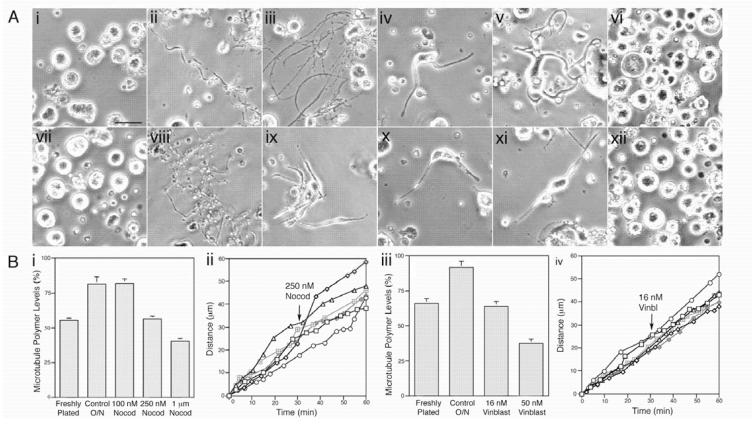

Figure 5. Effect of microtubule assembly inhibitors on proplatelet elaboration. (Aix) Phase-contrast micrographs of mouse megakaryocytes grown for 20 hr in the (ii, viii) absence or (iii-vi, ix-xii) presence of microtubule inhibitors. (i-vii) Freshly plated megakaryocytes lack proplatelet extensions. Megakaryocytes cultured in the presence of (iii) 100 nM, (iv-v) 250 nM, and (vi) 1 μM nocodazole or (ix-xi) 16 nM, and (xii) 50 nM vinblastine. In control cultures, the cells become decorated with long proplatelets in 20 hr. Proplatelets were elaborated normally when the cells were cultured in (iii) 100 nM nocodazole and some proplatelets were found on cells cultured in either (iv-v) 250 nM nocodazole or (ix-xi) 16 nM vinblastine although extensions are shorter and thicker compared to those elaborated in the absence of the inhibitors. Proplatelet formation is completely inhibited by (vi) 1 μM nocodazole or (xii) 50 nM vinblastine. Scale bar, 25 μm. (Bi) Effect of increasing concentrations of nocodazole on tubulin polymer levels in megakaryocytes. The graph compares the percentage of tubulin polymerized into microtubules in freshly plated megakaryocytes lacking proplatelets (~55%) to megakaryocytes plated for 20 hr in the absence (control) or presence of 100 nM, 250 nM, and 1 μM nocodazole. Culturing of megakaryocytes for 20 hr in the absence or presence of 100 nM nocodazole resulted in an increase of total tubulin polymer to ~85% (a 25.9% increase from freshly plated cells). Tubulin polymer levels in megakaryocytes cultured in the presence of 250 nM nocodazole remained stable relative to the initial value, showing that 250 nM nocodazole acts as a kinetic stabilizer of microtubules. The tubulin polymer content of cultured megakarytocytes was decreased to ~40% by 1 μM nocodazole. (Bii) Proplatelet elongation is unaffected by 250 nM nocodazole. The rate of elongation was studied in 6 proplatelets before and after treatment with 250 nM nocodazole. Nocodazole was added after 30 min (arrow). (Biii) Effect of increasing concentrations of vinblastine on tubulin polymer levels in megakaryocytes. The graph compares the percentage of total tubulin polymerized into microtubules in freshly plated megakaryocytes lacking proplatelets (65%) to megakaryocytes plated for 20 hr in the absence (control) or presence of 16 nM and 50 nM vinblastine. Culturing of megakaryocytes for 20 hr increased the total tubulin polymer content of cells to ~90%. Megakaryocytes cultured in the presence of 16 nM and 50 nM vinblastine were unable to increase their polymer content or had diminished tubulin polymer contents, respectively. (Biv) Proplatelet elongation is unaffected by 16 nM vinblastine.. The rate of elongation was studied in 6 proplatelets before and after treatment with 16 nM vinblastine, added at time 30 min (arrow).

To quantify the effects of these drugs on microtubule levels and establish which concentrations block assembly, we compared the levels of polymer in megakaryocytes cultured overnight in the presence of varying concentrations of nocodazole and vinblastine. Figure 5Bi and 5Biii show the effects of increasing concentrations of nocodazole and vinblastine on the microtubule content of proplatelet-producing megakaryocytes. Analysis of tubulin polymer levels in the cytoskeleton (Triton X-100 insoluble fraction) of megakaryocytes, as determined by quantitative immunoblotting, showed that the tubulin polymer level increased from ~55% to 81.3% as megakaryocytes formed proplatelets in culture. Megakaryocytes cultured in 100 nM nocodazole still maintained their capacity to increase microtubule polymer levels. However, when the nocodazole concentration was increased to 250 nM, the polymer level remained at a constant 56.4%. Addition of 1 μM nocodazole to cultures reduced the polymer level to 40.6% of the total. As shown in Figure 5Biii, similar experiments with vinblastine showed 16 nM to prevent the net increase in polymer levels that accompany proplatelet elaboration. The ability of these inhibitor concentrations to block net tubulin assembly was confirmed by the rapid loss of comets in EB3-GFP expressing cells, and similar effects on microtubule levels in megakaryocytes were found after a brief (5 min) treatment with 250 nM and 1 μM nocodazole, which suggests that the effect of the inhibitors rapidly comes to equilibrium (data not shown).

The above experiments delineated the concentrations of inhibitors required to block net assembly of tubulin in megakaryocytes while maintaining an equal fraction of polymer. Next, we studied the immediate influence of 250 nM nocodazole or 16 nM vinblastine on proplatelet elongation. Proplatelet elongation was followed for 30 min prior to and after drug treatment. Figures 5Bii and 5Biv plot the growth of proplatelets over time intervals before and after treatment with 250 nM nocodazole or 16 nM vinblastine. A representative differential-intereference-contrast time-lapse sequence of a proplatelet elongating in the presence of 250 nm nocodazole is shown in Supplemental Movie 6. In all examples studied (n=15 for each microtubule assembly inhibitor), the rate of proplatelet elongation did not change in the continuous presence of the microtubule inhibitors. These experiments demonstrate that proplatelet elongation does not require the polymerization of new microtubules.

Reactivation of elongation in permeabilized proplatelets.

Given that proplatelet elongation is unaffected by inhibitors that block plus-end microtubule assembly, other microtubule-based mechanisms must exist to power proplatelet elongation. Since microtubule sliding is used to drive the motility and extension in a number of cellular processes, we investigated whether proplatelets possess a mechanism to power sliding. Proplatelet-bearing megakaryocytes were permeabilized using 0.5% Triton X-100 in a microtubule-stabilizing buffer, washed, and reactivated by exposure to ATP. Figure 6 shows representative proplatelets before (Figure 6A) and after (Figure 6B) detergent permeabilization. Soluble tubulin was removed by extensive washing with microtubule stabilizing buffer, thus excluding tubulin polymerization as a factor that could contribute to proplatelet elongation. These permeabilized, washed proplatelets were stable for over an hour. Figure 6C and Supplemental Movie 7 show a permeabilized proplatelet that, despite being tethered

at both ends, grew rapidly in length following the addition of 1 mM ATP. In this example, the proplatelet increased its length by ~2.5 μm in 225 sec. In all the examples studied, permeabilized and ATPtreated proplatelets achieved average elongation rates of 0.65 + 0.13 μm/min (n=8) that were sustained for several minutes. In other preparations, immediately after adding ATP, microtubules were rapidly extruded from the ends of proplatelets (Supplemental Figure 1, Supplemental Movie 8). Nonhydrolyzable nucleotide analogues such as adenyl imidodiphosphate (AMPPNP) or adenosine 5'-O-(3-thiotriphosphate) (ATP--S), or the addition of tubulin and GTP, did not permit proplatelet elongation. These findings demonstrate that proplatelet microtubules can slide past one another to power elongation.

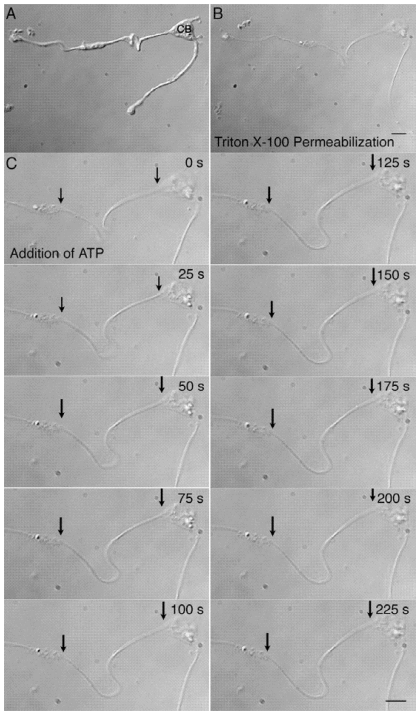

Figure 6. Activation of elongation in a Triton X-100 permeabilized proplatelet by ATP. Changes in proplatelet length after the addition of ATP were monitored by microscopy. (A) A proplatelet viewed with DIC optics just before detergent permeabilization. Two proplatelets can be observed extending from the cell body (CB) of a megakaryocyte. (B) Treatment with 0.5% Triton X-100, followed by washing in a microtubule stabilizing buffer, preserves the general structure of the proplatelet. (C) Time-lapse sequence after the addition of 1 mM ATP. ATP causes the proplatelet residue to increase its contour length and individual microtubules to splay apart from the bundle. Note the increase in distance between the cell body (right arrow) and the swelling that was attached to the substrate (left arrow). The rate of elongation in this example is ~0.7 μm/min. The lengthening of the proplatelet slows after 125 seconds. Scale bar, 5 μm. See Supplemental Movie 6.

The dynein and dynactin complex localize to proplatelet microtubules.

Having demonstrated that proplatelet microtubules can undergo sliding, we addressed the nature of the motors that power such movement. Mouse megakaryocytes at different stages of maturation were stained with antibodies against kinesin, dynein and dynactin, the multi-subunit complex that is required for most, if not all, types of cytoplasmic dynein activity (Figure 7) [22,23]. Figure 7A shows the specificity of antibodies used against mouse megakaryocyte and platelet lysates and rat brain lysate. Anti-kinesin antibody mainly recognizes a 124 kDa band corresponding to kinesin heavy chain in rat brain and mouse megakaryocytes. Anti-dynein intermediate chain antibodies reacted with a 74 kDa band corresponding to dynein intermediate chain. Anti-dynactin p50 antibodies reacted on

immunoblots with the 50 kD dynactin subunit in rat brain and megakaryocytes. Kinesin and dynein localize to different structures in the megakaryocytes; antibodies to kinesin heavy-chain label punctate structures in both the cell body (Figure 7B) and proplatelets (Figure 7D) but do not label proplatelet microtubule bundles, while cytoplasmic dynein or dynactin antibodies strongly stain the microtubule bundles of the proplatelets (Figure 7E, H). The cell bodies stain with a diffuse, cytoplasmic pattern. At high magnfication, the staining pattern of antibodies to dynactin p50 (Figure 7C,G) or dynein intermediate chain reveal linear rows of small foci throughout the proplatelet processes (Fig 7E, inset). Antibodies to dynactin p50 also robustly stain teardrop-shaped structures at the tips of proplatelets that we have shown to correspond to microtubule loops (arrow in Figure 7E), suggesting an intimate association between cytoplasmic dynein and microtubules. The staining signal of the anti-dynein intermediate chain antibody was drastically reduced in mature resting blood platelets compared to proplatelets (Figure 7H-I, arrows), signifying that the dynein motor became delocalized or degraded once the platelet is formed, consistent with a mechanism where the principal role of the motor is during platelet production.

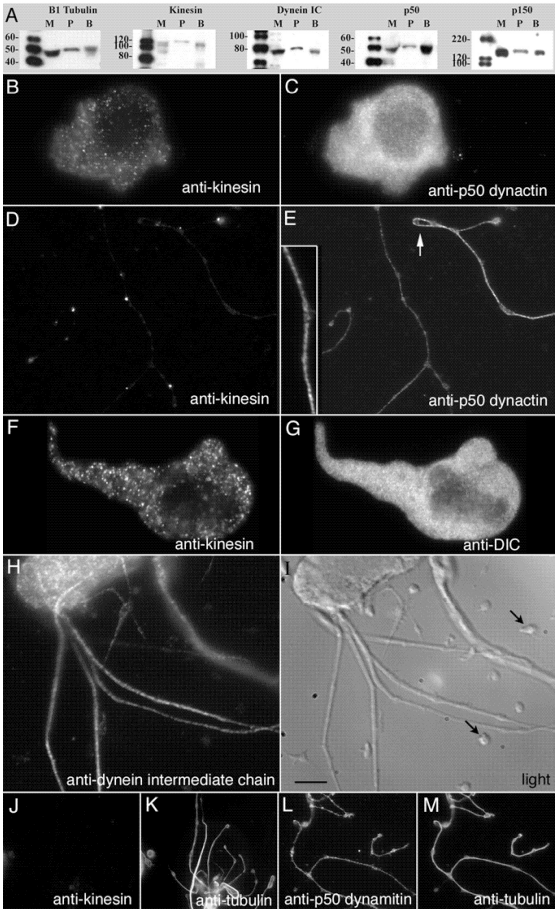

Figure 7 (previous page). Immunolocalization of cytoplasmic dynein, dynactin and kinesin in megakaryocytes. (A) Characterization of antibodies by immunobloting. Whole-cell protein extracts from mouse megakaryocytes (M), mouse platelets (P), and rat brain (B) were displayed by SDS-PAGE, transferred to PVDF, and immunoblotted with antibodies against β1-tubulin, kinesin, dynein-intermediate chain, p50 dynactin, and p150Glued. Double immunofluorescence microscopy of megakaryocytes using antibodies to (B, D, F) anti-kinesin and (C, E) either anti-p50 dynactin or (G) anti-dynein intermediate chain antibodies. Immunofluorescence images of pre-proplatelet megakaryocytes and proplatelet-containing megakaryocytes. (B, F) Kinesin antibodies stain vesicle-like particles within megakaryocytes and (D) along the shafts of proplatelets. (C) p50 dynactin and dynein intermediate chain (DIC) antibodies diffusely stain the megakaryocyte cytoplasm. Proplatelets are intensely stained (E, inset) along their length with anti-p50 dynactin and (H) anti-dynein-intermediate chain antibodies. (H) Comparative immunofluorescent and (I) DIC images of a proplatelet containing megakaryocyte and mouse platelets (arrows) stained with anti-dynein intermediate chain antibodies. Proplatelets stain robustly with anti-dynein intermediate chain antibody. In contrast, staining of platelets seeded onto the coverslip is highly reduced. Scale bar, 5 μm. Dynactin remains associated with the Triton X-100 insoluble megakaryocyte cytoskeleton (J-M). Megakaryocytes were extracted with 0.5 % Triton X-100 in a microtubule-stabilizing buffer before fixation, as described in Materials and Methods. The cells were then immunostained using (J) kinesin and (L) p50 dynamitin and (K, M) counterstained with α-tubulin antibodies to visualize proplatelet microtubules. Kinesin immunoreactivity was removed by the detergent treatment suggesting that kinesin is not associated with the microtubules. In contrast, the p50 dynamitin immunoreactivity is preserved.

In all of the cells we examined, the appearance of the kinesin immunoreactive structures was highly suggestive of vesicle-like, membrane-bounded organelles, while the dynein/dynactin antibodies label along the length of the proplatelet microtubule array. This localization pattern would be consistent with a model in which dynein could be anchored along microtubules and provide the force for sliding. To determine if this is indeed the case, unfixed cultured cells were lysed in a microtubule-stabilizing buffer containing the nonionic detergent Triton X-100 (0.5%), known to dissolve virtually all cytoplasmic, membrane-bounded organelles.[24] After exposure to the detergent, the cells were fixed and double-labeled with motor-specific antibody and anti-tubulin antibody to ensure preservation of the microtubules. Nearly all of the kinesin immunoreactive material detected in unextracted cells (Figure 7D) was removed by the detergent treatment (Figure 7J). This supports their identification as membrane-bounded organelles. In contrast, the anti-dynein intermediate chain immunoreactive structures were still observed in Triton X-100 extracted cells, which implies that they are not localized to membrane-bounded organelles but instead, intimately associated with the microtubule arrays (Figure 7L,M).

Disruption of dynein function by expression of the dynamitin (p50) subunit inhibits proplatelet elongation.

To directly test the hypothesis that dynein contributes to proplatelet elongation, we disrupted dynein function in living megakaryocytes and investigated the effect on proplatelet elongation. To disrupt dynein function, we retrovirally directed megakaryocytes to express the dynamitin (p50) subunit of dynactin fused to GFP. Overexpression of dynamitin (p50), which results in the dissociation of the p150 subunit from the dynactin complex, has previously been demonstrated to disrupt dynein function in a number of cellular processes,[25-29] including axonal outgrowth in cultured cells.[30] When analyzed by fluorescence microscopy, the overexpressed p50-GFP was found diffusely throughout the cyto-

plasm of infected megakaryocytes (Figure 8E-G). Approximately 54% of the megakaryocytes in culture exhibited detectable fluorescence. In nearly all cases, megakaryocytes expressing dynamitin p50-GFP exhibited a striking phenotype of short pseudopodia extending from the cell body that appeared to be arrested in elongation (Figure 8E-G). Normal proplatelets failed to elaborate from infected cells and the typical bulbous end at proplatelet tips was rare. To determine the magnitude of this effect, we compared the morphology of p50-GFP-expressing cells to those of untransfected cells in the same culture or transfected cells overexpressing an unrelated protein, β1-tubulin.[31] Control megakaryocytes directed to express GFP-β1 tubulin using the same retrovirus exhibited normal proplatelet formation (Fig 8H), as did untransfected cells (Fig 8I-J). Nearly all (97%) of the proplatelet-producing megakaryocytes that we observed in the same cultures as p50-GFP expressing cells had no detectable fluorescence, suggesting they were not infected. On the basis of these results, we conclude that cytoplasmic dynein and dynactin contribute to the elongation of proplatelets.

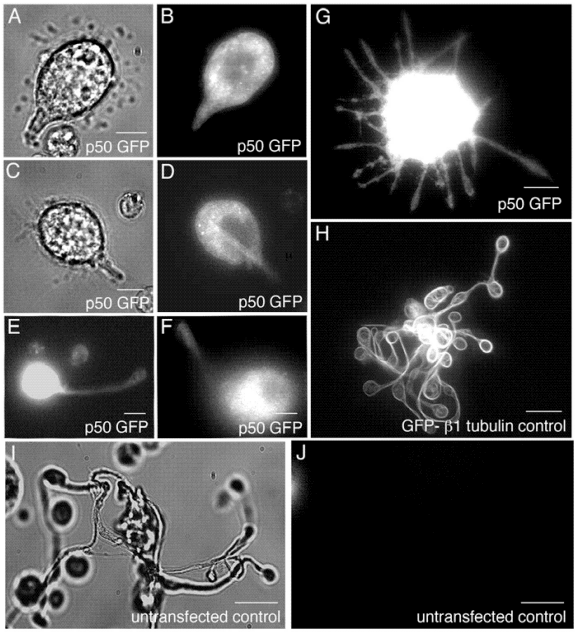

Figure 8. Role of dynactin in proplatelet elongation. (A-J) Effects of p50 dynamitin expression on proplatelet elongation. (A, C) Differential-interference-contrast and (B, DG) fluorescence images of p50-GFP-expressing cells exhibiting a range of elongation distortions, as compared with the unperturbed elongation of representative megakaryocytes (H) retrovirally directed to express GFP-β1-tubulin and (I-J) uninfected, non-expressing cells. All images were acquired by fluorescence and DIC microscopy. Scale bars all represent 10 μm.

DISCUSSION

Platelet formation by megakaryocytes is a complex process that appears to be unique in cell biology. Maturation culminates in an exquisite series of events that ends the megakaryocyte's life as it converts its entire cytoplasm first into proplatelets and then into platelets.[10,32] Proplatelets elongate from the megakaryocyte using bundles of microtubules. The first insights into the cytoskeletal mechanics of platelet formation date from the work of Tablin and Leven, who showed that proplatelet elongation is dependent on microtubules.[7] We now know that microtubules first consolidate in the cortex of the maturing megakaryocyte, and in a mechanism that is poorly understood, cause the cytoplasm to bulge locally. The resulting pseudopod then elongates as its shaft thins into a uniform cylindrical tube characteristic of proplatelets. At the base of the proplatelet, the microtubule bundle is thicker and contains more filaments than at the tip. Since proplatelets can reach a length of several millimeters, it seems unlikely that individual microtubules can span the full distance from cell body to proplatelet tip. Our current experiments support this notion and further demonstrate that microtubule ends are dispersed throughout these bundles. The precise length of individual microtubules is likely to be heterogeneous and remains to be determined. Near the end of the proplatelet, the bundle contains no more than 10-20 microtubules that extend into the bulbous tip before making a U-turn and re-entering the proplatelet shaft. Therefore, the proplatelet end contains cross-polarized portions of the same bundle. Since plus-ends were found in the bulbous tips of the proplatelets and grew in opposing directions, the polarity of microtubules in each bundle is mixed.

Our findings suggest that megakaryocytes employ and superimpose two separate microtubule-based activities to elongate proplatelets. First, as demonstrated by the movement of EB3-GFP comets that mark the growing plus-ends of microtubules, proplatelet microtubules are in a continuous state of growth. This reflects either rapid microtubule turnover, or the need to maintain a steady supply of new microtubules to sustain the increasing mass of elongating proplatelets. If the rate of EB3-GFP comet movement solely reflects the rate of microtubule assembly, then we would expect all elongating microtubules to move at a similar rate. In contrast, microtubule transport driven by sliding of bipolar bundles would lead to variable rates of movement of microtubule plus ends. We find that the rates of microtubule growth in megakaryocytes depend on the maturation state of the cells. Prior to proplatelet morphogenesis, megakaryocytes use centrosomal nucleation to form radiating arrays of microtubules and display microtubule growth rates of ~10.2 μm/min, with tight clustering of all rates around this value. Once proplatelet outgrowth begins, however, measured plus-end growth rates become highly variable and range from 2 to 24 μm/min. Moreover, the distribution of plus-end assembly rates in proplatelets are potentially bimodal, in marked contrast to pre-proplatelet megakaryocytes. Hence, proplatelets house distinct populations of microtubules, which appear to grow 4-5 μm/min slower and 4-5 μm/min faster than those observed in cells that lack proplatelets. These deviations from the norm are best explained by microtubule sliding movements superimposed on plus-end growth.

Indeed, in permeabilized cells, ATP activates a sliding mechanism that elongates proplatelets in the absence of polymer growth. Proplatelet residues in this experimental sys-

tem have the motor protein dynein and its regulator dynactin associated with them, and sliding of growing microtubules relative to one another fully explains the broad range of plus-end assembly rates we record in proplatelets. Our results imply that adjacent microtubules within a bundle may slide toward either the cell body or the proplatelet tip. Furthermore, since microtubules appear to be arranged with mixed polarity, microtubule growth events could similarly occur toward either the cell body or the proplatelet tip. Thus, as we observe, microtubule growth superimposed on microtubule sliding should result in a wide range of plus-end assembly rates; a microtubule polymerizing toward the proplatelet tip but sliding toward the cell body would appear to grow at a diminished rate compared to one that is both polymerizing and sliding in the same direction. This model also explains why proplatelet growth can be uncoupled temporally from microtubule assembly, using a pharmacological regime of plus-end growth inhibitors, without affecting the underlying continuance of proplatelet elongation. We propose that the microtubule-based mechanisms that power extension can also explain many aspects of platelet release and the process of mechanical coiling that produces the marginal microtubule band. In particular, sliding of an uncoiled portion of a microtubule relative to the rigid microtubule bundle in the proplatelet tip would provide a simple mechanism to achieve platelet release.

In previous studies using EB3-GFP, as well as our current studies on young megakaryocytes, rates of plus end microtubule growth appear to be cell-type specific. Growth rates could be controlled by microtubule end-associated proteins that regulate tubulin access and/or by tubulin dimer supply. While this difference could be explained by spatial variations in tubulin supply along the length of the proplatelet, we favor the idea that it is a consequence of plus-end assembly being overlaid on microtubule sliding. There is no relationship between EB3's position in the proplatelet and growth rate, nor is the plus-end growth rate influenced by the directions of microtubule growth, i.e., towards or away from the cell body. Compared to plus-end growth rates during the centrosomal phase, those in proplatelets may slow down or accelerate by ~3-5 μm/min. This finding indicates that individual microtubules slide relative to one another at ~4 μm/min in either direction. The most likely microtubule motor protein candidate to achieve this sliding is dynein, which associates with microtubule bundles in proplatelets, and as supported by our experiments with p50 dynactin expression in megakaryocytes. However, it is possible that other microtubule-based motors contribute to elongation. How might dynein generate outward protrusive movement within the context of microtubule bundles of mixed polarity? The likely explanation is that sliding occurs equally in both directions but translates exclusively into outward protrusive movements because the cell body resists inward sliding forces. Alternatively, positional heterogeneity in microtubule crosslinking could influence the efficiency and direction of net movement if crosslinking between microtubules is greatest near the cell body. However, the sliding of microtubule bundles away from the proplatelet tip is not just an awkward phenomenon that requires explanation. Rather, it may be an integral feature of the process by which proplatelet ends are amplified to enhance the platelet output. Sliding of microtubules away from the cell body may thus fulfill two related needs. First, it could create new points of proplatelet bifurcation. Second, sliding in this direction would serve to meet the steady de-

mand for microtubules from the repeated branching that occurs over the entire length of individual proplatelets.

ACKNOWLEDGMENTS

We thank Dr. T.P. Stossel for his supportive environment, Kurt Barkalow for valuable suggestions, K. Hoffmeister and Jagesh Shah for critical review of the manuscript, and E. Hett for advice with cloning.

REFERENCES

1. Choi ES, Nichol JL, Hokom MM, Hornkohl AC, Hunt P. Platelets generated in vitro from proplatelet-displaying human megakaryocytes are functional. Blood. 1995;85:402-413.
2. Cramer EM, Norol F, Guichard J, et al. Ultrastructure of platelet formation by human megakaryocytes cultured with the Mpl ligand. Blood. 1997;89:2336-2346.
3. Leven RM, Yee MK. Megakaryocyte morphogenesis stimulated in vitro by whole or partially fractionated thrombocytopenic plasma: a model system for the study of platelet formation. Blood. 1987;69.
4. Radley J, Rogerson J, Ellis S, Hasthorpe S. Megakaryocyte maturation in longterm marrow culture. Experimental Hematology. 1991;19:1075-1078.
5. Radley JM, Scurfield G. The mechanism of platelet release. Blood. 1980;56:996-999.
6. Stenberg PE, Levin, J. Mechanisms of platelet production. Blood Cells.
1989;15:23-31.
7. Tablin F, Castro M, Leven RM. Blood platelet formation in vitro: The role of the cytoskeleton in megakaryocyte fragmentation. J Cell Sci. 1990;97:59-70.
8. Italiano JEJ, Lecine P, Shivdasani RA, Hartwig JH. Blood platelets are asembled pricipally at the ends of proplatelet processes produced by differentiated megakaryocytes. J Cell Biol. 1999;147:1299-1312.
9. Handagama PJ, Feldman BF, Jain NC, Farver TB, Kono CS. In vitro platelet release by rat megakaryocytes: effect of metabolic inhibitors and cytoskeletal disrupting agents. Am J of Vet Res. 1987;48:1142-1146.
10. Radley JM, Haller CJ. The demarcation membrane system of the megakaryocyte: a misnomer? Blood. 1982;60:213-219.
11. Italiano JE, Jr., Bergmeier W, Tiwari S, et al. Mechanisms and implications of platelet discoid shape. Blood. 2003;101:4789-4796.
12. Schwer HD, Lecine P, Tiwari S, Italiano JE, Jr., Hartwig JH, Shivdasani RA. A lineage-restricted and divergent beta-tubulin isoform is essential for the biogenesis, structure and function of blood platelets. Curr Biol. 2001;11:579-586.
13. Stepanova T, Slemmer J, Hoogenraad CC, et al. Visualization of microtubule growth in cultured neurons via the use of EB3-GFP (end-binding protein 3-green fluorescent protein). J Neurosci. 2003;23:2655-2664.
14. Akhmanova A, Hoogenraad CC. Microtubule plus-end-tracking proteins: mechanisms and functions. Curr Opin Cell Biol. 2005;17:47-54.
15. Tirnauer JS, Bierer BE. EB1 proteins regulate microtubule dynamics, cell polarity, and chromosome stability. J Cell Biol. 2000;149:761-766.
16. Ma Y, Shakiryanova D, Vardya I, Popov SV. Quantitative analysis of microtubule transport in growing nerve processes. Curr Biol. 2004;14:725-730.
17. Mimori-Kiyosue Y, Shiina N, Tsukita S. The dynamic behavior of the APCbinding protein EB1 on the distal ends of microtubules. Curr Biol. 2000;10:865-868.
18. Schuyler SC, Pellman D. Microtubule "plus-end-tracking proteins": The end is just the beginning. Cell. 2001;105:421-424.
19. Ahmad FJ, Baas PW. Microtubules released from the neuronal centrosome are transported into the axon. J Cell Sci. 1995;108 (Pt 8):2761-2769.
20. Baas PW, Ahmad FJ. The transport properties of axonal microtubules establish their polarity orientation. J Cell Biol. 1993;120:1427-1437.

21. Liao G, Nagasaki T, Gundersen GG. Low concentrations of nocodazole interfere with fibroblast locomotion without significantly affecting microtubule level: implications for the role of dynamic microtubules in cell locomotion. J Cell Sci. 1995;108 (Pt 11):3473-3483.
22. Karki S, Holzbaur EL. Cytoplasmic dynein and dynactin in cell division and intracellular transport. Curr Opin Cell Biol. 1999;11:45-53.
23. Schroer TA. Dynactin. Annu Rev Cell Dev Biol. 2004;20:759-779.
24. Brown S, Lewinson S, Spudich J. Cytoskeletal elements of chick embryo fibroblasts revealed by detergent extraction. J Supramol Struct. 1976;5:119-130.
25. Burkhardt JK, Echeverri CJ, Nilsson T, Vallee RB. Overexpression of the dynamitin (p50) subunit of the dynactin complex disrupts dynein-dependent maintenance of membrane organelle distribution. J Cell Biol. 1997;139:469-484.
26. Echeverri CJ, Paschal BM, Vaughan KT, Vallee RB. Molecular characterization of the 50-kD subunit of dynactin reveals function for the complex in chromosome alignment and spindle organization during mitosis. J Cell Biol. 1996;132:617-633.
27. Eckley DM, Gill SR, Melkonian KA, et al. Analysis of dynactin subcomplexes reveals a novel actin-related protein associated with the arp1 minifilament pointed end. J Cell Biol. 1999;147:307-320.
28. LaMonte BH, Wallace KE, Holloway BA, et al. Disruption of dynein/dynactin inhibits axonal transport in motor neurons causing late-onset progressive degeneration. Neuron. 2002;34:715-727.
29. Presley JF, Cole NB, Schroer TA, Hirschberg K, Zaal KJ, Lippincott-Schwartz J. ER-to-Golgi transport visualized in living cells. Nature. 1997;389:81-85.
30. Ahmad FJ, Echeverri CJ, Vallee RB, Baas PW. Cytoplasmic dynein and dynactin are required for the transport of microtubules into the axon. J Cell Biol. 1998;140:391-401.
31. Schulze H, Korpal M, Bergmeier W, Italiano JE, Jr., Wahl SM, Shivdasani RA. Interactions between the megakaryocyte/platelet-specific beta1 tubulin and the secretory leukocyte protease inhibitor SLPI suggest a role for regulated proteolysis in platelet functions. Blood. 2004;104:3949-3957.
32. Becker RP, DeBruyn PP. The transmural passage of blood cells into myeloid sinusoids and the entry of platelets into the sinusoidal circulation; a scanning electron microscopic investigation. Am J Anat. 1976;145:1046-1052.

Discussion

Discussion

Murine Clasp2 is a member of the so-called "+TIP" group of microtubule binding proteins (Akhmanova and Hoogenraad 2005). This group of proteins specifically binds to the ends of microtubules, in mammalian cells only the growing ones. +TIPs are involved in many processes, including the regulation of microtubule dynamics and cell polarization during migration. CLASP2 is a unique protien in that it binds to specific subsets of microtubules, which is a property not shared by the majority of the other members of +TIPs. We have shown that CLASP2 binds to stabilized microtubules in the leading edge of motile fibroblasts in wound healing experiments (chapter 2). Such microtubules are characterized by acetylated and/or detyrosinated alpha-tubulin subunits and can therefore be recognized by specific antibodies. This result was confirmed with studies on CLASP2 knock out MEFs (chapter 3), where we showed that without CLASP2 the number of stabilized microtubules is reduced.

Our cellular data on CLASP2 knock out MEFs (chapter 3) have established the involvement of CLASP2 in microtubule stabilization through an integrin signaling pathway. Involvement of microtubules and MAPs in different signaling pathways has been suggested before (Gundersen and Cook 1999) and there are examples of +TIPs in such pathways. The best known example to date is the crucial role played by APC (adenomatous polyposis coli, a tumour suppressor protein and a +TIP) in Wnt signaling (Sancho et al. 2004). For the Drosophila CLASP2 homologue (Orbit/MAST) a signalling function in the Robo-Slit pathway, downstream of the non-receptor tyrosine kinase Abl, has been invoked (Lee et al. 2004).

Integrins are heterodimeric transmembrane protein receptors that play a crucial role in the interaction of cells with the extracellular matrix (ECM). They have a profound effect on cell adhesion, migration, proliferation and survival (Hynes 1992; Geiger et al. 2001). An integrin signaling pathway has been implicated in the local stabilization of microtubules in mouse fibroblasts, with EB3 and APC as the downstream effectors (Wen et al. 2004). The issue to be addressed now is what the specific functions are of CLASP2 and APC in microtubule stabilization and signalling. CLASP2 could be involved in more than one signaling pathway, by which different extracellular signals (or cues) can be transduced into the cell. It is possible that in different cell types CLASP2 is involved in different signaling cascades.

Our *in vivo* data in chapter 4 are showing for the first time the importance of CLASP2 in specialized cell types and tissues. The most striking effect is on the process of megakaryocytopoiesis and gametogenesis. Absence of CLASP2 causes reduction in the number of megakaryocyte progenitors and, subsequently, the number of mature megakaryocytes. Since there is also an effect on the number of erythrocytes, it is possible that a common megakaryocyte/erytrocyte progenitor is affected by the CLASP2 deletion. Interestingly, in the absence of CLASP2, the residual megakaryocytes and platelets seem to be morphologically and functionally normal, except for their reduced size and ploidy. Therefore CLASP2 is required for proliferation and/or differentiation of megakaryocyte progenitors, but the protein appears not to be important for megakaryocyte cytoplasmic maturation or platelet formation.

A phenotype similar to that in the CLASP2 knock out is observed in TPO and mpl mutant mice. Those mice are also severely thrombocytopenic with markedly reduced megakaryocytes, megakaryocyte progenitors and decreased megakaryocyte ploidy (Alexander et al. 1996). TPO signaling activates multiple pathways including integrin signaling cascades (Verfaillie 1998). Therefore it is possible that CLASP2 acts downstream of TPO and its mpl receptor. Future studies should determine whether and how CLASP2 is involved in the integrin signaling pathway in the megakaryocytes, and if so, what is the molecular mechanism by which mpl signaling is regulated by CLASP2.

Another hypothesis is that CLASP2 can act downstream from stem cell factor (SCF) and its c-kit receptor. It has been shown that adhesion of human megakaryocytes to the bone marrow stroma could be mediated by c-kit receptor binding to the c-kit receptor of the bone marrow fibroblasts (Avraham et al., 1992). Anchoring megakaryocytes and early hematopoietic progenitors to stroma, and the right positioning of these cells in the bone marrow microenvironment is very important. Only properly positioned cells can adequately respond to different cytokines, and subsequently sufficiently proliferate and differentiate. In the case of the CLASP2 knock out mice, megakaryocyte progenitors without CLASP2 protein would not be able to migrate and anchor properly within the bone marrow, which would affect their ability for sufficient proliferation. The theory about CLASP2 involvement in c-kit signaling becomes even more appealing when we take into account that the c-kit receptor is also expressed on germ cells of testis and ovaries (Hoyer et al. 2005), which are two other compartments severely affected in the CLASP2 knock out mice. Further studies are required to show whether CLASP2 funcitons in the c-kit pathway.

Both spermatogenesis and oogenesis are severely affected in the CLASP2 knock out mice. We have concentrated our efforts on the knock out testis and the process of spermatogenesis, because we have a culture system at hand (developed in the Department of Reproduction and Development) with which we could assay the role of CLASP2 in intact, dissected testis tubules. Such a system does not yet exist for the ovary. Our live studies on the testis from the knock out mouse, that express GFP-CLIP170 from an engineered knock in allele, are showing for the first time that CLASP2 can regulate microtubule dynamics *in vivo*. Microtubule growth rates in spermatogonia of CLASP2 knock out testis are higher than in wild type testis, which could be due to the increased amount of soluble tubulin caused by (for instance) ineffective recycling of microtubules.

Taken all these data together, we propose that CLASP2 is involved in the regional regulation of microtubule dynamics upon reception of specific signaling cues. Because of a potential CLASP1 and CLASP2 redundancy, only certain cell types and tissues might be affected, depending on the ratio between CLASP1 and CLASP2 expression in those cells. A scheme of CLASP2 involvement in different signaling pathways is shown on the next page.

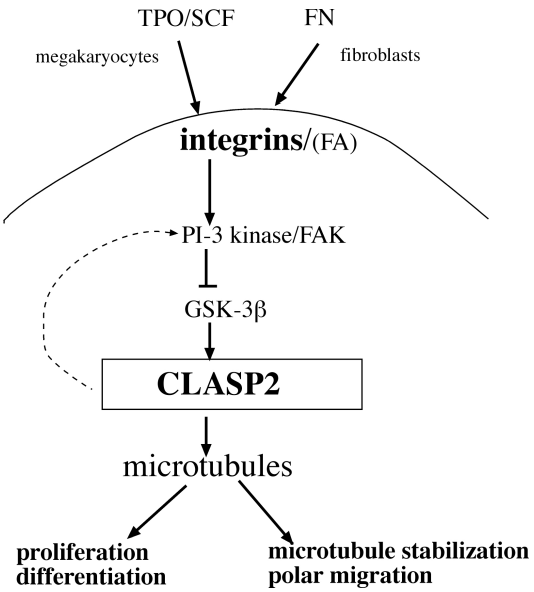

References

Akhmanova, A. and Hoogenraad, C.C. 2005. Microtubule plus-end-tracking proteins: mechanisms and functions. *Curr Opin Cell Biol* 17(1): 47-54.

Alexander, W.S., Roberts, A.W., Nicola, N.A., Li, R., and Metcalf, D. 1996. Deficiencies in progenitor cells of multiple hematopoietic lineages and defective megakaryocytopoiesis in mice lacking the thrombopoietic receptor c-Mpl. *Blood* 87(6): 2162-2170.

Geiger, B., Bershadsky, A., Pankov, R., and Yamada, K.M. 2001. Transmembrane crosstalk between the extracellular matrix--cytoskeleton crosstalk. *Nat Rev Mol Cell Biol* 2(11): 793-805.

Gundersen, G.G. and Cook, T.A. 1999. Microtubules and signal transduction. *Curr Opin Cell Biol* 11(1): 81-94.

Hoyer, P.E., Byskov, A.G., and Mollgard, K. 2005. Stem cell factor and c-Kit in human primordial germ cells and fetal ovaries. *Mol Cell Endocrinol* 234(1-2): 1-10.

Hynes, R.O. 1992. Integrins: versatility, modulation, and signaling in cell adhesion. *Cell* 69(1): 11-25.

Lee, H., Engel, U., Rusch, J., Scherrer, S., Sheard, K., and Van Vactor, D. 2004. The microtubule plus end tracking protein Orbit/MAST/CLASP acts downstream of the tyrosine kinase Abl in mediating axon guidance. *Neuron* 42(6): 913-926.

Sancho, E., Batlle, E., and Clevers, H. 2004. Signaling pathways in intestinal development and cancer. *Annu Rev Cell Dev Biol* 20: 695-723.

Verfaillie, C.M. 1998. Adhesion receptors as regulators of the hematopoietic process. *Blood* 92(8): 2609-2612.

Wen, Y., Eng, C.H., Schmoranzer, J., Cabrera-Poch, N., Morris, E.J., Chen, M., Wallar, B.J., Alberts, A.S., and Gundersen, G.G. 2004. EB1 and APC bind to mDia to stabilize microtubules downstream of Rho and promote cell migration. *Nat Cell Biol* 6(9): 820-830.

Appendix

Generation and characterisation of the CLASP2 specific llama-derived single domain antibody

Generation and characterisation of the CLASP2 specific llama-derived single domain antibody

Ksenija Drabek, Frank Grosveld, Niels Galjart and Dubravka Drabek

Cell Biology Department, Erasmus MC, PO BOX 1738, 3000DR Rotterdam, The Netherlands

Abstract

Screening of an immune llama VHH library yielded one CLASP2 specific single domain antibody (sdAb). The antibody A5 is easily produced and purified by Ni^{+} beads from the periplasm of bacteria. Detection of CLASP2 protein by A5 on Western blots is comparable to that achieved with a rabbit polyclonal antiserum. Our preliminary results also show that A5 can function as an intrabody. Cos cells transiently transfected with A5 express it in the cytoplasm and as a consequence have a reduced amount of acetylated tubulin.

Introduction

The humoral immune response of camels and llamas is based largely on heavy-chain antibodies in which the light chain is totally absent. These unique antibodies interact with the antigen by virtue of only one single variable domain, referred to as VHH (reviewed in (Muyldermans 2001). Antigen specific camelid VHH antibody fragments or single domain antibodies (sdAb) represent the smallest functional antibody format. The affinity of the interaction between monovalent llama VHH antibody fragments and their antigens is close to nanomolar range and similar to bivalent mouse monoclonal antibodies (van der Linden et al. 1999). In contrast to VH domains of conventional antibodies, recombinant VHHs selected from llama libraries are easily expressed and highly soluble in aqueous environments. The latter is due to their unique hydrophilic substitutions in frame work 2, which contribute to the ease of VHH production and high expression yields in bacteria and *Saccharomyces cereavisie* (Frenken et al. 2000).
VHHs appear to be potent enzyme inhibitors by binding active sites in cavities that are not recognized by conventional antibodies (Lauwereys et al. 1998). Another interesting application of VHHs is their intracellular expression and use as intrabodies with the aim to inhibit the *in vivo* function of selected molecules/antigens in different biological systems. The function of several intracellular gene products has been successfully inhibited in the cytoplasm (Dekker et al. 2003), in the nucleus (Zemel et al. 2004) and in the secretory compartments (Paganetti et al. 2005) using appropriate expression vectors for mammalian cells (Persic et al. 1997). The availability of inhibitory, antagonistic or agonistic antibodies would increase the success rate and broaden the applicability of the intrabody technology. Moreover, the mapping of the epitopes engaged will help revealing the specific functions of particular domains. Here we report the isolation and characterization of a llama derived single domain antibody specific for CLASP2, a protein involved in microtubule stabilization. We show that we can inhibit the function of CLASP2 through the use of intrabody technology, thus demonstrating the specific application of this technology.

Results and Discussion

The C terminus of human CLASP2 (nucleotide positions 3074-3976 of the KIAA0627 cDNA) was amplified and the PCR product cloned into the pGEX-3X expression vector (Pharmacia). A purified 65 kD GST-hCLASP2 fusion protein was used for immunisation of a New Zealand rabbit, which yielded in a polyclonal rabbit antiserum **N2358** described in Chapter 2 (Akhmanova et al. 2001). The same protein was used for immunisation of a young adult male *Llama glama*. Specificity of both (rabbit and llama) polyclonal antisera was tested on Western blots. Both sera recognise mouse CLASP2 protein and cross-react with CLASP1, due to the high amino acid similarity at their C termini (data not shown).
Total RNA was isolated from peripheral lymphocytes of the immunised llama. After purification of poly A^+ RNA, cDNA was made using oligo dT. DNA fragments encoding for VHHs and VHs were amplified using the VH1back Sfi I primer in combination with the Lam1 NotI and Lam 3 NotI primers from the CH2 exon. The amplified VHHs (~500bp)

were separated by gel electrophoresis from the VHs of conventional antibodies containing the CH1 exon (~800bp) and gel purified (Figure 1). The isolated DNA was SfiI / NotI digested and cloned into SfiI / NotI of the phagemid vector, derived from pHen-1vector (Hoogenboom et al. 1991). Transformation into TG1 electro-competent cells yielded an immune llama single domain antibody library with an estimated complexity of 10^6 different VHs.

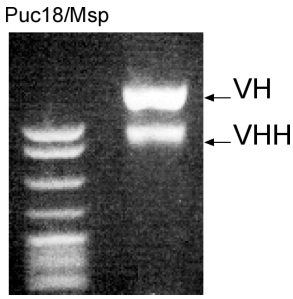

Figure 1. Amplified llama VHs (originating from classical IgGs) and VHHs (originating from heavy chain only IgG2 and IgG3).

Rather than the GST-CLAP2 fusion protein which was used for immunization, a purified his tagged CLASP2 protein was used to screen the library. This was due to the report by Zhang and colleagues (Zhang et al. 2001) that during the selection of specific single chain antibodies with GST fusion proteins many false positives are obtained. Similar observations concerning the background obtained by GST fusion proteins were reported by group of S. Philipsen (personal communication). Two rounds of selection were performed using the panning techniques with his-tagged antigen adsorbed onto plastic (immunotubes coated with 30g/ml and 10g/ml of CLASP2 protein).

All 95 colonies picked from bacterial plates after the second round of selection were positive in the ELISA assay. They were further analysed at the DNA level by Hinf I-fingerprinting. This analysis clearly showed that all the isolated clones represented the same single domain antibody (sdAb) (Figure 2A). The A5 protein sequence is shown in Figure 2C. Thus, we were able to isolate only one llama sdAb that specifically recognizes the CLASP2 protein and originates from a long hinge (IgG2) heavy chain only antibody of *Llama glama*.

For purification and mass production A5 sdAb was shortened at the expense of the hinge region sequence. These modifications made the *his* tag accessible for purification via Ni^+ beads and resulted in the production of satisfactory amounts of sdAbs in the periplasm of bacteria. DNA from the obtained sdAbs was amplified using the same VHback SfiI primer in combination with a LH NotI primer, SfiI / NotI digested and recloned into the same expression vector. The vector contains a pel B leader sequence that directs the expressed VHH towards the periplasm (Skerra 1993). Proteins in this compartment (periplasm) are folded and the oxidising environment stimulates the disulphide bond formation leading to func-

tional VHH sdAb of the expected size (~ 21 kD), detected by anti-myc antibody. (Figure 2B).

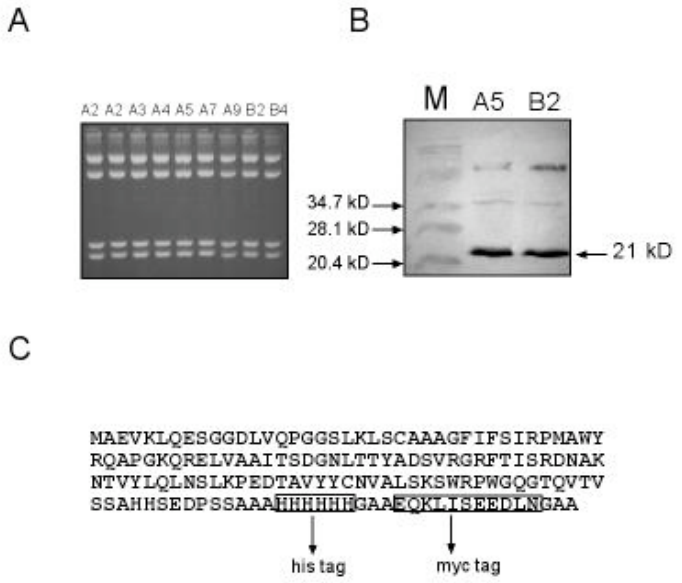

Figure 2: Characterization of clones obtained after screening llama VHH library. A: Example of fingerprinting, showing same patern of Hinf I digested DNA of 9 clones. B: Western blot showing presence of the correct size anti-CLASP2 sdAbs in a bacterial periplasmic fraction, detected via myc tag; C: Amino acid sequence of A5 sdAb .The His and myc tag in frame with the VHH were provided by the phagemid vector.

Next we tested in parallel the performance of the A5 sdAb and the 2358 rabbit antiserum on Western blots. They both specifically recognize GFP-CLASP2 (another fusion protein, different from the one used for immunization and the one used for two rounds of selection), and do not recognize CLIP115, used as a negative control.

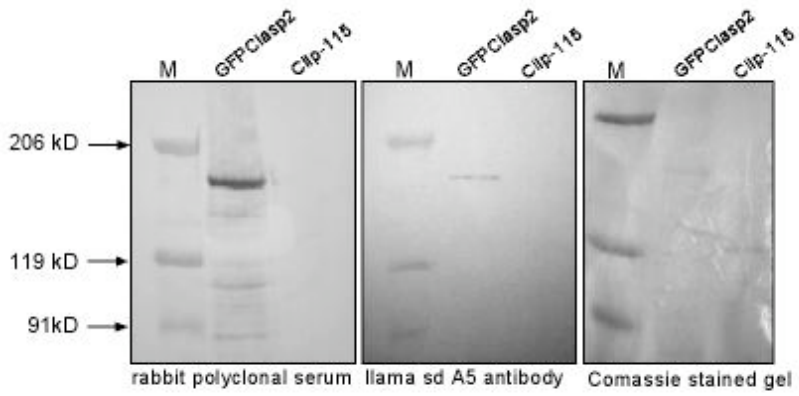

Figure3. Rabbit polyclonal antiserum and A5 sdAb both specifically recognise GFP-CLASP2 purified protein but do not recognise CLIP115 protein used as a negative control.

We then examined if A5 sdAb can be expressed intracellularly and whether its expression influences the function of microtubules. Cos cells were transiently transfected with an A5 expression plasmid and cells expressing A5 sdAb clearly show cytoplasmic staining with the 9E10 anti myc antibody (Figure 4). The cells were simultaneously stained with either an antibody against the plus end binding protein EB1, an antibody against beta tubulin or an antibody against acetylated tubulin. Preliminary results show that the intrabody expression of A5 sdAb reduces the level of acetylated tubulin. This finding is consistent with our previous studies (Akhmanova et al. 2001), where 3T3 fibroblasts injected with rabbit anti-CLASP2 antibody show reduced levels of acetylated tubulin. Analysis of the CLASP2 KO MEFs (Chapter 3) also revealed a reduction in the amount of stabilized (acetylated) microtubules. Further epitope mapping might reveal the amino acid sequences involved in the interactions of CLASP2 with microtubules causing this particular phenotype.

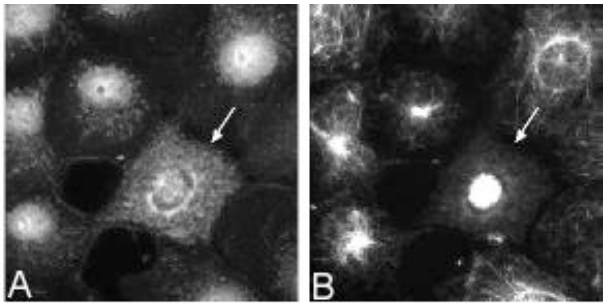

Figure 4. The anti-CLASP2 sdAb used as an intrabody. Cos cells transiently transfected with sdAb expression plasmid were double stained with a polyclonal anti-myc antibody to detect transfected cells that express anti-CLASP2 sdAb, and a monoclonal antibody against acetylated tubulin to detect stabilized microtubules. Panel A: Arrow points at antibody expressing cell. Panel B: Arrow points at the same cell showing lack of acetylated tubulin.

Materials and methods

Construction of expression vectors

The C terminus of human CLASP2 (nucleotide positions 3074-3976 of the KIAA0627 cDNA) was amplified using the following primers: 627 F3g: 5'-gcaggatccaaacagctcttgataataaagc-3' and 627 R3g: 5-gcagaattcactaactttgtccagaaacat-3'. The BamHI / EcoR I digested PCR product was cloned into BamHI / EcoRI sites of the pGEX-3X expression vector (Pharmacia), resulting in the GST-CLASP2 expression vector. The same DNA fragment, was isolated from the GST-CLASP2 expression vector as an EcoRI blunted / BamHI fragment and cloned into the SmaI / BamHI sites of the pQE-32 vector (Qiagen), resulting in the His tagged CLASP2 expression vector. Expression of the his tagged CLASP2 fusion protein was IPTG induced at 30^{o} C in the M15 strain of E. coli and purified on Ni^{+} beads (Qiagen). The GST-CLASP2 fusion protein was IPTG induced at 37^{o}C in strain BL21, purified on glutathione-Sepharose 4B beads (Pharmacia) and concentrated using a Centricon-30 (Amicon) filter before injecting into a rabbit or llama.
The eukaryotic A5 expression vector was constructed by cloning NcoI / Not fragment containing the A5VHH onto NcoI / NotI of the pEF2/myc/cyto vector (Invitrogen).

Immunization

The immunisation schedule was as previously described by van der Linden *et al*. Briefly, injections were performed at days 0, 21 and 35 with 250 g of antigen in water oil emulsion. Blood (~150ml) was collected 7 days after the last immunization.

Construction of llama single domain antibodies (sdAb) library

Total RNA was isolated from peripheral lymphocytes of an immunised llama using the Ultraspec RNA isolation system (Biotecx laboratories, Inc, Houston, Texas, USA) according to the manufacturer's instructions. After purification of poly A^{+} RNA (Oligotex 70022, Qia-

gen), cDNA was made using oligo dT. DNA fragments encoding VHHs and VHs were amplified using VH1back SfiI primer (Hoogenboom et al. 1991) in combination with the Lam1 NotI (5'-cagaaatggagcggccgccttgggttttggdggggaagakgaagacdgatgg –3') and Lam 3 NotI (5'-cctcggggtcgcggccgccacrtccaccaccacrcaygtgacct-3') or LH NotI (5'-ggattgggttgcggccgctggttgtggttgtggttgtggttttggtgtctggggttc-3"), using the following program: 94 ° C for 3', followed by 35 cycles of 94 ° C for 1', 58 ° C for 1' and 72⁰ C for 2'and 10' at 72°C.

The rescuing of the phagemid library, selection of phage-antibody library by panning in immunotubes, ELISA for detection of soluble antibody fragments and preparation of periplasmic proteins from small scale cultures were all done according to CESAME Manual version 2.0: Phage display technology (1996).

Fingerprinting of clones with restriction enzyme Hinf I

The primers used to generate material for fingerprinting were M13 rev in combination with g3prvA: 5' – tagccccttattagcgtttgcca-3'. 3l from the master plate was used as a template in the PCR reaction (30 cycles of 94° C, 1'; 55° C, 1'; 72° C 1.5').
40 l of PCR reaction was digested overnight with HinfI restriction enzyme in the appropriate buffer and digests run on 4% NuSieve agarose gel cast in TBE buffer containing 0.5 g/ml ethidium bromide. The banding pattern of individual clones was visualised on a UV transilluminator.

Western blotting

Western blots were done according to standard procedure, using rabbit polyclonal serum (1: 2000) and A5sdAb (1:500). Secondary steps included alkaline phosphatase conjugated goat anti rabbit IgG (1:2000) from Sigma, or 9E10 anti-myc (1:1000) from Covance followed by HRP conjugated goat anti mouse IgG (1:4000). The substrate for alkaline phosphate was provided by the Sigma Fast BCIP/NBT system while the DAB staining kit from Boehringer was used for HRP detection.

Cell transfections

Transient transfections were performed in simian COS-7 cells with the pEF2/A5myc/cyto plasmid using Superfect reagent (Qiagen), according to the manufacturer's instructions. Cells were grown in Lab-Tek chamber slides (Nunc). Immunofluorescence staining was performed 24h after transfection. Cells were fixed in 100% methanol/1mM EGTA for 10 minutes at -20°C, and permeabilized with 0.15% TritonX-100/PBS. After blocking in 1% BSA/0.05%tween/PBS, the cells were incubated for 1 hour at room temperature with mouse monoclonal antibody against acetylated tubulin (1:100) and polyclonal rabbit anti myc (1:200). Goat anti rabbit-FITC (1:100) was used to detect sdAb and goat anti mouse ALEXA 594 (1:300) to detect acetylated tubulin. All antibodies were purchased from Sigma except polyclonal anti myc, which was from Abcam.

Acknowledgments

We thank Anna Akhmanova for providing a baculovirus lysate used to purify GFP-CLASP2.

References

Akhmanova, A., Hoogenraad, C.C., Drabek, K., Stepanova, T., Dortland, B., Verkerk, T., Vermeulen, W., Burgering, B.M., De Zeeuw, C.I., Grosveld, F., and Galjart, N. 2001. Clasps are CLIP-115 and -170 associating proteins involved in the regional regulation of microtubule dynamics in motile fibroblasts. Cell 104(6): 923-935.

Dekker, S., Toussaint, W., Panayotou, G., de Wit, T., Visser, P., Grosveld, F., and Drabek, D. 2003. Intracellularly expressed single-domain antibody against p15 matrix protein prevents the production of porcine retroviruses. J Virol 77(22): 12132-12139.

Frenken, L.G., van der Linden, R.H., Hermans, P.W., Bos, J.W., Ruuls, R.C., de Geus, B., and Verrips, C.T. 2000. Isolation of antigen specific llama VHH antibody fragments and their high level secretion by Saccharomyces cerevisiae. J Biotechnol 78(1): 11-21.

Hoogenboom, H.R., Griffiths, A.D., Johnson, K.S., Chiswell, D.J., Hudson, P., and Winter, G. 1991. Multi-subunit proteins on the surface of filamentous phage: methodologies for displaying antibody (Fab) heavy and light chains. Nucleic Acids Res 19(15): 4133-4137.

Lauwereys, M., Arbabi Ghahroudi, M., Desmyter, A., Kinne, J., Holzer, W., De Genst, E., Wyns, L., and Muyldermans, S. 1998. Potent enzyme inhibitors derived from dromedary heavy-chain antibodies. Embo J 17(13): 3512-3520.

Muyldermans, S. 2001. Single domain camel antibodies: current status. J Biotechnol 74(4): 277-302.

Paganetti, P., Calanca, V., Galli, C., Stefani, M., and Molinari, M. 2005. beta-site specific intrabodies to decrease and prevent generation of Alzheimer's Abeta peptide. J Cell Biol 168(6): 863-868.

Persic, L., Righi, M., Roberts, A., Hoogenboom, H.R., Cattaneo, A., and Bradbury, A. 1997. Targeting vectors for intracellular immunisation. Gene 187(1): 1-8.

Skerra, A. 1993. Bacterial expression of immunoglobulin fragments. Curr Opin Immunol 5(2): 256-262.

van der Linden, R.H., Frenken, L.G., de Geus, B., Harmsen, M.M., Ruuls, R.C., Stok, W., de Ron, L., Wilson, S., Davis, P., and Verrips, C.T. 1999. Comparison of physical chemical properties of llama VHH antibody fragments and mouse monoclonal antibodies. Biochim Biophys Acta 1431(1): 37-46.

Zemel, R., Berdichevsky, Y., Bachmatov, L., Benhar, I., and Tur-Kaspa, R. 2004. Inhibition of hepatitis C virus NS3-mediated cell transformation by recombinant intracellular antibodies. J Hepatol 40(6): 1000-1007.

Zhang, M.Y., Schillberg, S., Zimmermann, S., Liao, Y.C., Breuer, G., and Fischer, R. 2001. GST fusion proteins cause false positives during selection of viral movement protein specific single chain antibodies. J Virol Methods 91(2): 139-147.

Summary

Summary

The cytoskeleton is composed of three different types of fibers: intermediate filaments, actin, and microtubules. Microtubules are tubular structures, made up of protofilaments of α and β-tubulin heterodimers. They contribute to cell shape and polarity, motility, intracellular transport and signal transduction. They are absolutely essential for mitosis. Two main characteristics of microtubules are their dynamic behaviour and structural polarity. The first is used to adapt cellular shape, the second to enable directional transport and to generate cell polarity.

In vivo, microtubules are often anchored with one end of their fibre (the minus end) to the microtubule organizing centre, or MTOC. As a consequence, the other end (the plus end) continuously alternates between phases of growth, pauze and shrinkage, a behaviour that is termed dynamic instability. Transition from growth to shrinkage is called catastrophe, and transition from shrinkage to growth is called rescue. Dynamic instability is tightly regulated to drive the processes described above. This is achieved by numerous proteins that can stabilize or destabilize microtubules, or that associate with tubulin dimers. The microtubule binding proteins can be divided into microtubule-based motor proteins, and nonmotor microtubule-associated proteins (MAPs).

A subset of MAPs, which accumulate at microtubule plus ends, are central to the spatial control of microtubule dynamics. These proteins have the ability to dynamically track the ends of growing microtubules, and are called +TIPs. The prototype member of this class of proteins is Cytoplasmic Linker Protein of 170 kDa, or CLIP-170. The function of CLIP-170 is to stimulate microtubule growth.

The CLIP-Associating Proteins, CLASP1 and -2, are, among others, also localized at microtubule plus ends, and they therefore belong to the +TIP group of proteins. Both CLASPs exists in several isoforms that differ in their N-terminal sequences. While CLASP1 is ubiquitously expressed, CLASP2 is detected more abundantly in the brain than in other tissues. In interphase cells CLASPs function in the stabilization of microtubules. The unique capacity of these proteins is that they can induce microtubule stabilization at highly specific sites within the cell, for example at the leading edge of a migrating fibroblast. One possibility, that would explain the interaction between CLIPs and CLASPs, is that CLASPs recruit CLIPs to locally stabilize microtubules. However, this hypothesis remains to be proven.

CLASPs are essential mitotic proteins. In HeLa cells CLASP1 is an outer kinetochore component, involved in the regulation of microtubule dynamics during mitosis. In Drosophila, the CLASP homologue Orbit/Mast is required for chromosome congression, spindle bipolarity and the attachment of microtubules to kinetochores. Without Orbit/Mast microtubules actually shorten because they fail to polymerize efficiently at kinetochores, yet continue shrinking at the centrosomes.

We generated CLASP2 knock out mice by using homologous recombination in ES cells, in order to better understand the *in vivo* function of this fascinating protein. CLASP2 knock out mice show a wide range of abnormalities. Our data suggest that CLASP2 is important for mouse development and is essential for hematopoiesis and male and female germ cell development. These roles were unexpected because CLASP2 is most abundantly

expressed in the brain. Analysis of live testis tubules strongly suggests a role of CLASP2 in the regulation of microtubule dynamics. These in vivo data are in line with cellular studies.

CLASP2 knock out mice are severely thrombocytopenic with highly reduced numbers of blood platelets and their precursors, megakaryocytes. A reduced number of megakaryocyte progenitors indicates that CLASP2 is involved in megakaryocytopoiesis, and reduced megakaryocyte ploidy is indicative of a function in the process of endomitosis. Combined the data indicate that CLASP2 might be involved in the control of microtubule dynamics during mitosis, meiosis and interphase. A detailed analysis of CLASP1 and -2 expression in the mouse is now required to address the issue of functional redundancy between these proteins.

CLASP2 accumulates in specific regions of the cell after serum induction. Using FRAP analysis, we show that in these areas GFP-tagged CLASP2 becomes relatively immobile with respect to other regions. We hypothesize that CLASP2 can stabilize microtubules after local immobilization. Analysis of CLASP2 knock out MEFs shows inefficient formation of stable microtubules after adherence to fibronectin, which implicates CLASP2 in an integrin-dependent signaling pathway. According to this hypothesis CLASP2 is part of a pathway in fibroblasts that is involved in transduction of specific positional cues in order to maintain cell polarity. CLASP2 might be involved in the same or in similar pathways in vivo. We hypothesize that this is important for proper megakaryocyte development and that even their progenitors depend on CLASP2 signalling. Similarly, germ cells might require CLASP2 for signalling. Future studies will address this role of CLASP2.

Samenvatting

Het cytoskelet van cellen bestaat uit drie componenten: intermediaire filamenten, actine en microtubuli. Deze moleculen vormen drie verschillende fiberachtige netwerken. Microtubuli zijn holle fibers, gemaakt van alpha- en beta-tubuline, die in lengte richting aan elkaar binden en protofilamenten vormen. Deze lineaire protofilamenten rollen vervolgens via laterale contacten op tot een buis. Microtubuli zijn belangrijk voor vele cellulaire processen, waaronder transport, mitose, signaal transductie en cel beweging. Dit netwerk creert cel polariteit and draagt bij aan de structuur van cellen. De twee belangrijkste eigenschappen van microtubuli zijn de intrinsieke polariteit van de fiber en hun dynamische gedrag.

In veel cellen is een kant van de microtubulus (het min einde) verankerd aan het "microtubule organizing centre", of MTOC. De andere kant (het plus einde) is vrij en daaraan worden tubuline subeenheden vastgezet (polymerisatie of groei) of juist vanaf gehaald (depolymerisatie of krimp). De levensgeschiedenis van veel microtubuli wordt gekarakteriseerd door dit dynamische gedrag. De overgang van groei naar krimp wordt "katastrofe" genoemd, die van krimp naar groei "redding (rescue)" en het gedrag zelf wordt omschreven als "dynamisch instabiel". Het gedrag wordt nauwkeurig gereguleerd en gebruikt om processen te bewerkstelligen. Controle vindt voornamelijk plaats met behulp van eiwitten die aan microtubuli binden (afgekort als "MAPs"), of die aan tubuline dimeren binden. Er zijn met name heel veel verschillende MAPs. Ze worden vaak onderverdeeld naar gelang hun capaciteit om als motor eiwit te fungeren.

Een deel van de MAPs vertoont en heel speciaal gedrag, namelijk binding aan de uiterste eindjes van groeiende microtubuli. Deze groep eiwitten wordt nu +TIPs genoemd; ze spelen een centrale rol in de regulatie van "dynamische instabiliteit". Het eerste eiwit waarvan werd aangetoond dat het dit gedrag had was CLIP-170 ("Cytoplasmic Linker Protein of 170 kDa"). CLIP-170 stimuleert de groei van microtubuli.

Wij hebben CLASP1 en -2 ("CLIP Associating Proteins") ontdekt. Net als de CLIPs zijn deze eiwitten +TIPs, alhoewel ze ook elders in de cel kunnen localiseren. Er bestaan verschillende isovormen van de CLASPs, die elk een specifiek domein aan hun N-terminus hebben. CLASP1 komt in alle geteste weefsels tot expressie, terwijl CLASP2 duidelijk meer voorkomt in de hersenen. In cellen in interfase vervullen CLASPs een rol als stabilisatoren van microtubuli. Het unieke van deze eiwitten is dat ze deze functie uitoefenen op hele specifieke plekken in een cel, bijvoorbeeld aan de voorkant van een migrerende cel, zodat stabiele microtubuli locaal ontstaan. Het is mogelijk dat de CLASPs voor deze rol de CLIPs recruteren. Dit zou verklaren waarom deze eiwitten een interactie aangaan, maar deze hypothese is niet bewezen.

CLASPs zijn essentieel voor mitose. In gekweekte HeLa cellen vormt CLASP1 een onderdeel van de buitenste laag van de kinetochoor, de structuur die microtubuli met centromeren verbindt. In de fruitvlieg is Orbit/Mast het eiwit dat de meeste homologie met CLASPs vertoont. Orbit/Mast is belangrijk voor de congressie van chromosomen, voor het handhaven van de bipolaire mitotische spoel en voor het contact tussen microtubuli en kinetochoren. Zonder dit eiwit krimpen de microtubuli in feite, omdat er bij het kinetochoor geen polymerisatie plaatsvindt.

Wij hebben CLASP2 “knock out” muizen gemaakt door middel van homologe recombinatie in ES cellen. Wij hebben dit gedaan om de rol van CLASP2 te kunnen begrijpen in de muis. CLASP2 “knockout” muizen hebben allerlei aandoeningen. Onze data suggereren dat CLASP2 belangrijk is voor de algehele ontwikkeling van de muis en in het bijzonder voor hematopoiese en de vrouwelijke en mannelijke kiem cel differentiatie. Dit is een enigzins verbazingwekkende vondst omdat CLASP2 juist het meest voorkomt in de hersenen. Een analyse in levende testis buisjes laat zien dat CLASP2 de dynamiek van microtubuli inderdaad controleert. Dit resultaat komt overeen met de cellulaire studies.

CLASP2 “knock out” muizen hebben sterk verminderde hoeveelheden bloedplaatjes. Dat komt omdat de producent van deze plaatjes, de megakaryocyt, ook is aangedaan. We zien in deze cellen met name dat het proces van endomitose (een incomplete celdeling die zorgt voor sterke vermenigvuldiging van het aantal chromosomen) blokkeert. Maar zelfs de aantallen voorloper cellen van megakaryocyten zijn verminderd in de CLASP2 “knock out” muis. De data in de verschillende weefsels suggereren dat CLASP2 betrokken is bij de regulatie van “dynamische instabiliteit” gedurende mitose, meiose en interfase. Nu moeten we uitzoeken in hoeverre de expressie patronen van CLASP1 en -2 overeenkomen. Als het waar is dat CLASP1 en -2 hele overlappende functies hebben, zou zo een analyse kunnen verklaren waarom er in sommige weefsels wel een effect van de CLASP2 deletie is en in andere weefsels niet.

Na toevoegen van serum aan cellen vinden we dat CLASP2 op bepaalde plekken in de cel ophoopt. Met de FRAP techniek konden we laten zien dat de ophoping van fluorescent CLASP2 (waaraan GFP gekoppeld is) komt doordat het eiwit daar minder mobiel is dan in andere gebieden. We veronderstellen dat deze immobilisatie te maken heeft met de functie van CLASP2 in de stabilisatie van microtubuli. Een analyse van CLASP2-deficiente embryonale fibroblasten (MEFs) laat zien dat er minder stabiele microtubuli gevormd worden na het aanhechten van MEFs op fibronectine. Dit plaatst CLASP2 in een signaal transductie cascade, waarin ook integrines zitten, die een interactie aangaan met fibronectine. CLASP2 zou wel eens betrokken kunnen zijn bij het doorgeven van positionele informatie, bij cel polariteit en bij het aanhechten van cellen. Dit zou ook in de muis kunnen gelden. We stellen voor dat de differentiatie van megakaryocyten (en zelfs hun voorlopers) afhangt van een signaal transductie route met functioneel CLASP2. Ook kiemcellen zouden op die manier CLASP2 nodig kunnen hebben. Deze hypothese zal in de toekomst verder getest worden.

Curriculum vitae

Name:	Ksenija Drabek
Born:	17 March 1969, Belgrade, Yugoslavia

1983-1987	Secondary school of science and technology 'Rudjer Boskovic", Belgrade, Yugoslavia Specialized practice in Clinical Medical Center (KBC) 'Bezanijska Kosa", microbiology laboratory, under the supervision of Dr Z. Sokolovski (may-june 1987)
1987-1995	B.S in Molecular Biology and Physiology, University of Belgrade, Yugoslavia 1995 Graduation project and thesis: Supernumerary marker chromosome in human karyotype, under supervision of associate professor Marija Guc-Scekic at Institute for Mother and Child, Belgrade, Yugoslavia
1995-1998	Master in Biology (Molecular Biology and Biochemistry), University of Belgrade, Yugoslavia Project: Antitumor Effect of Tiazofurin on Human Glioma Cell Lines under supervision of Lj. Rakic, MD., PhD, Proffesor of Biochemistry and Neurobiology, member of Serbian Academy of Sciences and Art
1995-1997	Teaching instructor for undergraduate courses in Experimental Physiology and General Physiology with Biophysics, Faculty of Biology, University of Belgrade, Yugoslavia
1997	Junior scientist in the Department of Research and Development, ICN Pharmaceuticals Inc, Costa Mesa, California, USA
1998-1999	Biomedical Research scientist in ICN Yugoslavia Institute, Laboratory for Tumor Biology, Belgrade, Yugoslavia
1999-2003	PhD student Erasmus University Rotterdam, The Netherlands Promoter: Prof. Dr. F.G. grosveld Co-promoter: Dr. Ir. N. Galjart
2003-	until present, wetenschappelijk onderzoeker, Erasmus MC, Rotterdam

List of publications

Pesic M, Drabek K, Esler C, Ruzdijic S, Pejanovic V, Pietrzkowski Z. (2000) Inhibition of cell growth and proliferation in human glioma cells and normal human astrocytes induced by 8-Cl-cAMP and tiazofurin. Nucleosides Nucleotides Nucleic Acids 19 (5-6): 963-75.

Drabek K, Pesic M, Piperski V, Ruzdijic S, Medic-Mijacevic L, Pietrzkowski Z, Rakic L. (2000) 8-Cl-cAMP and tiazofurin affect vascular endothelial growth factor production and glial fibrillary acidic protein expression in human glioblastoma cells. Anticancer Drugs 11(9): 765-70.

Akhmanova A, Hoogenraad C. C, Drabek K, Stepanova T, Dortland B, Verkerk T, Vermeulen W, Burgering B. M, De Zeeuw C. I, Grosveld F, Galjart N. (2001) Clasps are CLIP-115 and -170 associating proteins involved in the regional regulation of microtubule dynamics in motile fibroblasts. Cell 104(6): 923-35.

Patel S. R, Richardson J, Schulze H, Kahle E, Galjart N, Drabek K, Shivdasani R. A, Hartwig J. H, Italiano Jr J. E. (2005) Differential roles of microtubule assembly and sliding in proplatelet formation by megakaryocytes. Blood in press

Akhmanova A, Mausset-Bonnefont A. L, van Cappellen W, Keijzer N, Hoogenraad C. C, Stepanova T, Drabek K, van der Wees J, Mommaas M, Onderwater J, van der Meulen H, Tanenbaum M. E, Medema R. H, Hoogerbrugge J, Vreeburg J, Uringa E.J, Grootegoed J. A, Grosveld F, and Galjart N.
The microtubule plus-end-tracking protein CLIP-170 associates with the spermatid manchette and is essential for spermatogenesis. Gene and Development in press

Dankwoord

I would like to thank my promotor Frank Grosveld for giving me the opportunity to work and to study in an excellent scientific environment, and for all advices and suggestions concerning my project. Thanks for your support during hard times for me and my country, when I was stranded in Rotterdam and practically jobless, with interrupted PhD started back home.

I would also like to thank Artur van de Kamp and Marike van Geest, who went together with me to different police stations on several occasions, which resulted in my "turistic visa" extensions. They were personally involved in sorting all the paper work, which finally allowed me to stay and work at Erasmus University.

Next, I would like to thank my co-promotor Niels Galjart who accepted me as a PhD student in his group, and who gave me an exciting and interesting project to do – make my own knock out mouse! Niels, thanks for the trust and believe that I can run this project and finish my thesis. Thank you for your help with computers (going on-line as well!).

I would like to thank Joseph Italiano for his help with megakaryocytes. Jo, during your visit in Rotterdam, I have learned a lot from you. Thank you for your time and patience.

I would like to thank Manousos Koutsorakis and John Kong-a-San for teaching me how to do blastocyst injections. I could not have wished for better teachers than two of you!

The members of the inner doctoral committee, Elein, Sjaak and Ricardo Fodde, thanks for reading my thesis, and giving me the corrections and useful suggestions.

I would like to thank all of my colleagues and friends for making my PhD time less hard, and Rotterdam nicer place to stay.

I would like to thank Nynke (my paranimf as well!) and Ton for good times during our skiing adventures, wine tasting, dinners etc.

Patrick, Albert and Roy, thanks for badminton games. Sometimes it was really hard to keep up with you!

Jan and Suzanne, thanks for many sailing weekends. Thanks for having me on board! With you I have learned much more about Netherlands, especially the IJsselmeer.

I would also like to thank Ann and Helmut and Karen and Alex for their friendship.

I must not forget present and past members of lab 710/1030: Casper, Bjorn, Filipe, Tatiana, Helen, Anne-Laure, Zjak, Dorota, Anna, Gideon, Daniel, Frank, Marco, Marja, Jeffrey, Suzanne, Nanda, Katharina, Michael and

Laura. Special thanks goes to Filipe and Tatiana my PhD fellow students with whom I have shared a lot of up's and down's, and a very nice time in Prague. Filipe, thanks for being my paranimf!

Thanks to all the personnel from the EDC, in particular Patrick, Danielle and Yvet.

Finally, I would like to thank my mother and father for all the support and love they gave me. I am especially grateful to Dubi, my row model in many things and ways. Without her unconditional support and help, time in Rotterdam wouldn't be the same.